พฤติกรรมของกรรมวิธีทางความร้อนของเหล็กหล่อโครเมียมสูงเพื่อความต้านทานการสึกหรอแบบขัดสี

นาย สุดสาคร อินธิเดช

HEAT TREATMENT BEHAVIOR OF HIGH CHROMIUM CAST IRON FOR ABRASIVE WEAR RESISTANCE

Mr. Sudsakorn Inthidech

Thesis Title	HEAT TREATMENT BEHAVIOR OF HIGH CHROMIUM CAST IRON FOR ABRASIVE WEAR RESISTANCE
By	Mr. Sudsakorn Inthidech
Filed of Study	Metallurgical Engineering
Thesis Advisor	Associate Professor Prasonk Sricharoenchai, D.Eng.
Thesis Co-advisor	Professor Yasuhiro Matsubara, D.Eng.

Accepted by the Faculty of Engineering, Chulalongkorn University in Partial Fulfillment of the Requirements for the Doctor's Degree

....Dean of the Faculty of Engineering
(Professor Direk Lavansiri, Ph.D.)

THESIS COMMITTEE

....Chairman
(Assistant Professor Charkorn Jarupisitthorn, M.E.)

....Thesis Advisor
(Associate Professor Prasonk Sricharoenchai, D.Eng.)

....Thesis Co-advisor
(Professor Yasuhiro Matsubara, D.Eng.)

....Member
(Assistant Professor Sawai Danchaivijit, Ph.D.)

....Member
(Professor Takateru Umeda, D.Eng.)

....Member
(Associate Professor Paritud Bhandhubanyong, D.Eng.)

สุดสาคร อินธิเดช : พฤติกรรมของกรรมวิธีทางความร้อนของเหล็กหล่อโครเมียมสูงเพื่อ
ความต้านทานการสึกหรอแบบขัดสี (HEAT TREATMENT BEHAVIOR OF
HIGH CHROMIUM CAST IRON FOR ABRASIVE WEAR RESISTANCE)
อ. ที่ปรึกษา : รศ.ดร. ประสงค์ ศรีเจริญชัย, อ.ที่ปรึกษาร่วม : Professor Yasuhiro
Matsubara; 284 หน้า. ISBN 974-53-2536-8.

ได้เตรียมเหล็กหล่อที่เป็น ยูเทคติกและไฮโปยูเทคติกที่ไม่เติมธาตุผสม ซึ่งมีปริมาณส่วนผสมโดยประมาณ ของโครเมียมร้อยละ 10, 16, 20 และ 26 โดยมวล และ ยูเทคติกและไฮโปยูเทคติกที่มีส่วนผสมโดยประมาณของโครเมียมร้อยละ 16 และ 26 โดยมวล ที่เติมธาตุผสมเดี่ยว ได้แก่ นิกเกิล ทองแดง โมลิบดินัม และ วานาเดียม เพื่อศึกษาพฤติกรรมของกรรมวิธีทางความร้อนของเหล็กหล่อโครเมียมสูง

ในสภาวะชุบแข็งของเหล็กหล่อโครเมียมสูงที่ไม่เติมธาตุผสม ความแข็งเปลี่ยนไปเล็กน้อยแต่สัดส่วนเชิงปริมาตรของออสเตนไนต์เหลือค้าง (VY) เปลี่ยนแปลงอย่างมากขึ้นกับปริมาณคาร์บอนที่ปริมาณ โครเมียมเท่ากัน สัดส่วนเชิงปริมาตรของออสเตนไนต์เหลือค้างมีค่าสูงใน เหล็กที่อบที่อุณหภูมิการเป็นออสเตนไนต์ที่สูงกว่าและค่อยๆลดลงตามการเพิ่มขึ้นของค่าสัดส่วนโครเมียมต่อคาร์บอนเมื่อมีค่าเพิ่มขึ้นมากกว่า 4.0 กราฟความแข็งของชิ้นงานในสภาพอบคืนตัวแสดงการเกิด Secondary hardening ความแข็งเนื่องจากการตกตะกอนของคาร์ไบด์มีค่าสูงกว่าในเหล็กที่ชุบแข็งจากอุณหภูมิที่อบให้เป็นออสเตนไนต์ที่สูงกว่า อุณหภูมิในการอบคืนตัวเพื่อให้ได้ความแข็งสูงสุด (H_{Tmax}) เพิ่มขึ้นเมื่อเพิ่มอุณหภูมิในการอบชุบ ค่าความแข็งสูงสุดสัมพันธ์กับสัดส่วนเชิงปริมาตรของออสเตนไนต์เหลือค้างในสภาวะชุบแข็งโดยไม่ขึ้นกับอุณหภูมิชุบแข็ง ค่าความแข็งสูงสุดค่อยๆเพิ่มขึ้นจนถึงค่าสูงสุดที่ 800 HV30 ที่ค่าสัดส่วนเชิงปริมาตรของออสเตนไนต์เหลือค้าง 20 % และมีค่าคงที่ถึงแม้ว่าสัดส่วนเชิงปริมาตรของออสเตนไนต์เหลือค้างเพิ่มขึ้นมากกว่า 20%

ในเหล็กหล่อโครเมียมสูงที่เป็นยูเทคติกที่เติมธาตุผสม ความแข็งในสภาพชุบแข็งเปลี่ยนแปลงอย่างมากตามสัดส่วนเชิงปริมาตรของออสเตนไนต์เหลือค้างซึ่งสัมพันธ์กับชนิดและปริมาณของธาตุผสม นิกเกิลและทองแดงลดความแข็ง โมลิบดินัมเพิ่มความแข็ง แต่วานาเดียมเพิ่มความแข็งในเหล็กหล่อที่มีโครเมียมร้อยละ 16 โดยมวล แต่ลดความแข็งในเหล็กหล่อที่มีโครเมียมร้อยละ 26 โดยมวล สัดส่วนเชิงปริมาตรของออสเตนไนต์เหลือค้างเพิ่มขึ้นตามปริมาณของนิกเกิล ทองแดง และโมลิบดินัม แต่ลดลงเมื่อปริมาณของวานาเดียมเพิ่มขึ้น การเพิ่มอุณหภูมิชุบแข็งทำให้สัดส่วนเชิงปริมาตรของออสเตนไนต์เหลือค้างเพิ่มขึ้นในชิ้นงานทดสอบทุกชิ้น กราฟความแข็งในสภาพอบคืนตัวแสดงการเกิด Secondary hardening อย่างชัดเจนเนื่องจากการตกตะกอนของคาร์ไบด์ชนิดพิเศษและการเปลี่ยนเฟสของออสเตนไนต์สลายตัวไปเป็นมาร์เทนไซต์ ดีกรีการเพิ่มความแข็งจากการตกตะกอนมีค่าสูงกว่าในเหล็กหล่อที่เติมธาตุฟอร์มคาร์ไบด์มากกว่าเหล็กหล่อที่ไม่เติมธาตุผสม ยกเว้นเหล็กหล่อที่เติมวานาเดียมเนื่องจากมีสัดส่วนเชิงปริมาตรของออสเตนไนต์เหลือค้างต่ำกว่าและ ดีกรีการเกิด secondary hardening มีค่าสูงในเหล็กหล่อที่ชุบแข็งจากอุณหภูมิที่อบให้เป็นออสเตนไนต์สูงกว่า และมีค่าสูงสุดในเหล็กหล่อโครเมียมสูงที่เติมนิกเกิล และต่ำสุดในเหล็กหล่อโครเมียมสูงที่เติมวานาเดียม

ในเหล็กหล่อที่มีโครเมียมร้อยละ 16 และ 26 โดยมวล ที่เป็นไฮโปยูเทคติก ความแข็งในสภาพชุบแข็งเปลี่ยนแปลงชัดเจนตามสัดส่วนเชิงปริมาตรของออสเตนไนต์เหลือค้าง นิกเกิลและทองแดงลดความแข็ง โมลิบดินัมเพิ่มความแข็ง วานาเดียมเพิ่มความแข็งใน เหล็กหล่อที่มีโครเมียมร้อยละ 16 โดยมวล แต่ลดความแข็งในเหล็กหล่อโครเมียมสูงที่มีโครเมียมร้อยละ 26 โดยมวล สัดส่วนเชิงปริมาตรของออสเตนไนต์เหลือค้างเพิ่มขึ้นตามปริมาณของ นิกเกิล ทองแดง และโมลิบดินัม แต่ลดลงตามปริมาณของวานาเดียมที่เพิ่มขึ้นในเหล็กหล่อที่มีโครเมียมร้อยละ 16 โดยมวล ในเหล็กหล่อที่มีโครเมียมร้อยละ 26 โดยมวล สัดส่วนเชิงปริมาตรของออสเตนไนต์เหลือค้างเพิ่มขึ้นตามปริมาณของ นิกเกิล และโมลิบดินัม แต่ลดลงตามปริมาณของ ทองแดง และ วานาเดียมที่เพิ่มขึ้น อุณหภูมิที่อบให้เป็นออสเตนไนต์ที่สูงกว่าเป็นสาเหตุให้สัดส่วนเชิงปริมาตรของออสเตนไนต์เหลือค้างมากกว่า กราฟความแข็งของชิ้นงานหลังอบคืนตัวแสดงการเกิด Secondary hardening เนื่องจากการตกตะกอนของคาร์ไบด์ชนิดพิเศษและการเปลี่ยนเฟสของออสเตนไนต์เป็นมาร์เทนไซต์ ความแข็งหลังอบคืนตัวสูงในเหล็กหล่อที่มีสัดส่วนเชิงปริมาตรของออสเตนไนต์เหลือค้างในสภาพชุบแข็งสูง ค่าความแข็งสูงสุดหลังอบคืนตัวเกิดขึ้นที่สัดส่วนเชิงปริมาตรของออสเตนไนต์เหลือค้างน้อยกว่า 20% และเพิ่มขึ้นตามการเพิ่มขึ้นของ โมลิบดินัม วานาเดียมเพิ่มความแข็งหลังอบคืนตัวเล็กน้อยในเหล็กหล่อที่มีโครเมียมร้อยละ 16 โดยมวล แต่ลดความแข็งในเหล็กหล่อที่มีโครเมียมร้อยละ 26 โดยมวล นิกเกิลและทองแดงไม่ส่งผลมากนักต่อความแข็งสูงสุดหลังอบคืนตัว ค่าความแข็งสูงสุดหลังอบคืนตัวมีค่าสูงที่สุดในเหล็กหล่อที่เติม โมลิบดินัม

ภาควิชา..........วิศวกรรมโลหการ..............ลายมือชื่อนิสิต...................................

สาขาวิชา..........วิศวกรรมโลหการ.............ลายมือชื่ออาจารย์ที่ปรึกษา.....................

ปีการศึกษา ....2548.................ลายมือชื่ออาจารย์ที่ปรึกษาร่วม.....................

4571842321   : MAJOR METALLURGICAL ENGINEERING
KEY WORD: HEAT TREATMENT / HIGH CHROMIUM CAST IRON/ HARDNESS/ RETAINED AUSTENITE/ ALLOYING ELEMENT

SUDSAKORN INTHIDECH: HEAT TREATMENT BEHAVIOR OF HIGH CHROMIUM CAST IRON FOR ABRASIVE WEAR RESISTANCE. THESIS ADVISOR: ASSOC. PROF. PRASONK SRICHAROENCHAI, THESIS COADVISOR : PROF. YASUHIRO MATSUBARA, 284 pp. ISBN 974-53-2536-8.

Plain high chromium cast irons containing 10 mass%, 16 mass%, 20 mass% and 26 mass% Cr and eutectic and hypoeutectic 16 mass% and 26 mass% Cr cast irons with single addition of Ni, Cu, Mo and V were prepared in order to investigate their heat treatment behaviors.

In plain high chromium cast iron, hardness in as-hardened state does not change much but volume fraction of retained austenite (V_γ) varies greatly at the same chromium level depending on carbon content. The V_γ is high at higher austenitizing temperature, and it gradually decreases with an increase in Cr/C value when the Cr/C value is more than 4.0. Curve of tempered hardness shows a secondary hardening. The precipitation hardening is greater in the iron hardened from higher austenitizing temperature. The tempering temperature to obtain the maximum hardness (H_{Tmax}) shifts to the long time side when the austenitizing temperature rises. The H_{Tmax} can be uniformly related to the V_γ value in as-hardened state irrespective of austenitizing temperature and it increases gradually up to the highest value of around 800 HV30 at 20% V_γ, and the H_{Tmax} is settled even if the V_γ increases over 20%.

In eutectic high chromium cast iron with alloying element, in as-hardened state, hardness is changed remarkably by V_γ which is closely related to kind and amount of alloying element. Ni and Cu decreased and Mo increased the hardness, but V increased it in 16 mass% Cr iron and reduced it in 26 mass% Cr iron. V_γ rose with an increase in Ni, Cu and Mo content but it was reduced by increasing V content. An increase in austenitizing temperature made V_γ more in all the as-hardened specimens. Curve of tempered hardness showed an evident secondary hardening due to both the precipitation of special carbides formed by carbide reaction and the transformation of destabilized austenite into martensite. The degree of the precipitation hardening was much larger in cast irons with carbide forming elements than that in the irons free of them, except for the irons with V which had lower V_γ. The degree of precipitation hardening was greater in the irons hardened from higher austenitizing temperature, and largest in irons with Ni and smallest in the irons with V.

In 16 mass% and 26 mass% Cr hypoeutectic cast irons, in as-hardened state, hardness changed remarkably depending on the V_γ. Ni and Cu decreased hardness and Mo increased it. V increased hardness in 16 mass% Cr cast iron but decreased it in 26 mass% Cr cast iron. The V_γ increased with Ni, Cu and Mo content but diminished with increasing V content in 16 mass% Cr cast iron. In 26 mass% Cr cast iron, the V_γ increased with Ni and Mo content but decreased with increasing Cu and V content. Higher austenitization caused more V_γ. Curves of tempered hardness showed an evident secondary hardening due to precipitation of special carbides and transformation of destabilized austenite into martensite. High tempered hardness was obtained in the specimens with high V_γ in as-hardened state. Maximum tempered hardness (H_{Tmax}) was obtained when V_γ was less than 20% and it increased with an increase in Mo content. The H_{Tmax} slightly increased with V content in 16 mass% Cr cast iron but decreased in 26 mass% Cr cast iron. Ni and Cu did not show significant effects on H_{Tmax}. The highest value of H_{Tmax} was obtained in the cast irons containing Mo.

Department of Metallurgical Engineering …...Student's signature. *Sudsakorn Inthidech*

Field of study Metallurgical Engineering ……Advisor's signature… *Prasonk Sricharoenchai*

Academic year…….. 2005 …………….....Co-advisor's signature *Yasuhiro Matsubara*

ACKNOWLEDGEMENTS

CONTENTS

CHAPTER IV
EXPERIMENTAL RESULTS

CHAPTER V
DISCUSSIONS

CHAPTER I

INTRODUCTION

1.1   Background

Alloyed white cast iron has been researched and developed for a long time as abrasion wear resistant materials. Main purposes of the researches have been for the improvement of wear resistance and toughness under the acceptable cost performance. For the last half century past, the abrasion wear resistant materials changed from low-alloyed cast iron through Ni-hard cast iron to high-alloyed white cast iron. The multi-component white cast iron was developed very recently and it is now getting popular as a new type of abrasion wear resistant material. The high-alloyed cast iron, which is typified by high chromium cast iron, was invented in Europe in late 1970's, and then the low-alloyed white cast iron was replaced by high chromium cast iron.

Chromium cast irons have been used all round in chromium (Cr) content from 2 mass % to 50 mass% (hereafter shown by %). The usages of high chromium cast iron containing Cr over 10% are roughly classified as follows;

(a) 10% to 20 %Cr for abrasion wear resistance
(b) 20% to 30%Cr for abrasion wear resistance and corrosive wear resistance
(c) 30% to 50%Cr for high temperature wear resistance and corrosive wear resistance

The main practical applications are shown in Table 1. As the raw material, it is found that high chromium cast iron which contains chromium from 12% to 28% has been finding so many applications to

Table 1.1 Main practical usage of high chromium cast irons.

Type	Composition (%)				Applications
	C	Ni	Mo	Others	
13% Cr	1.8 – 3.5	0 - 0.3	0.3 – 1.0	0.5 – 1.0 Cu	Ball and liner of tube mill. Blade of short blast.
15% – 17% Cr	2.6 – 3.5	0 – 2.2	1.3 – 3.0	0 - 0.3 V 0 - 1.2 Mn	Roller, segment, ball and liner for mineral pulverizing and tube mills. Hammer of crusher. Impellor (blade) and liner for shot blast machine. Work roll for hot finishing mill. Work roll for roughing mill.
20% Cr	1.5 – 3.5	0 – 1.0	1.0 – 3.0	0 – 1.5 Cu 0 – 1.3 Si	Slurry pump component for impellor and agitator. Roller for briquette machine. Ball, ring and liner for pulverizing mill. Liner of rod mill. Ball for tube mill.
25% - 28% Cr	2.5 – 2.9	0.3 – 1.0	0.5 – 3.0	0 – 3.0 V	Roller and table for cement clinker grinding mill. Roller and table for slag grinding mill. Hammer and liner for impact crusher. Ball and liner for ball mill. Blade and liner for shot blast machine. Slurry pump component. Movable armor in blast furnace.

the parts and the components in the various fields of industries because of superior wear performance and suitable toughness. The industries such as cement, mining, steel-making and thermal power plant have been main users. For pulverizing mills in the cement and mining industries, it is known that balls, liners for tube mill and rollers, tables for vertical mill made by high chromium cast iron show higher performance than those made by Ni-hard cast iron.

With respect to the microstructure, formation of pearlite in matrix is generally considered to deteriorate the abrasion wear resistance and resultantly to reduce the service life. To overcome this problem, an improvement of hardenability and an increase in hardness are considered to be necessary. Alloying elements such as Ni, Mn, Cu, Cr, Mo and V can be added in the same way as alloy steels. In white cast iron, however, Cr, Mo and V that distribute mainly to the carbide can increases the hardness of carbide itself and therefore improve the wear resistance.

Cr is a strong carbide forming element and it is well known that chromium combines with carbon to form chromium carbide of $(CrFe)_7C_3$ (M_7C_3) type or $(CrFe)_{23}C_6$ $(M_{23}C_6)$ type when cast iron contains high level of chromium. The M_7C_3 carbide is harder and eutectic M_7C_3 carbide has discontinuous morphology [1,2] that is, the carbides are interconnected in comparison with the carbide of $(CrFe)_3C$ (M_3C) type that forms in cast iron with low chromium content and has ledeburitic morphology.

In the solidification process of high chromium cast iron, the $(\gamma+M_7C_3)$ eutectic grows with a cellular interface and solidifies as a colony structure [6]. The carbide structure crystallized from melt is varied depending on the combination of contents of carbon (C), Cr and other carbide forming elements. The size of eutectic colony and the coarseness of eutectic carbides can be controlled by the eutectic freezing range and solidification rate or cooling rate [7].

On the other side, the matrix structure can be controlled by the condition of heat treatment. Therefore it can be said that not only

abrasion wear resistance but also mechanical properties must be determined by both of the carbide and matrix structures.

Once high chromium cast iron solidifies, it is very hard to modify the shape of carbide crystallized from the liquid as primary and/or eutectic without using the plastic deformation techniques like rolling, forging and pressing. As for high chromium cast iron, therefore, heat treatment which used to be done at the final stage before machining is the main way and of great importance to improve wear resistance and mechanical properties. It is considered that factors affecting the abrasion wear performance should be hardness and volume fraction of retained austenite in matrix when the carbide structure is similar. Since the quantitative measurement of retained austenite for the high chromium cast iron was already succeeded by X-ray diffraction method [24], it is enabled to connect the wear resistance and other properties with the amount of retained austenite.

Presence of retained austenite in the matrix is beneficial because it has high toughness and gives work hardening on the wear surface by the formation of strain-induced martensite. There is a research report by I.R. Sare [5] that high chromium cast iron which has matensitic matrix with some retained austenite shows the largest wear resistance to spalling. In the practical application of high chromium cast iron, the adequate heat treatment should be given to get the optimal combination of hardness and quantity of retained austenite for abrasion wear resistance and other mechanical properties. The usual heat treatments are homogenizing or annealing, hardening and tempering. These heat treatments seem to be the same as those in general steels, but in high chromium cast irons, there occurs a peculiar phenomena that are the precipitation of carbide during austenitizing (so-called as destabilization of austenite) and even during cooling after austenitizing. The precipitation of secondary carbides in matrix during heat treatment plays very important role for the wear resistance and the mechanical properties[4]. When very high hardness is required in the case of pulverizing mill materials, alloying elements like

Ni, Mn and Cu which will improve the hardenability and Mo and V which will promote the formation of secondary special carbides with higher hardness than chromium carbides, should be added to the high chromium cast iron.

Recently, most of hot work rolls made of high chromium cast iron were replaced by very expensive rolls made of newly developed multi-component white cast iron with higher performance.[5] The applications of this new alloy are gradually expanding in other fields.[5]

When the severe recession took place about 8 years ago, however, an employment of relatively cheaper high chromium cast iron was eyed with fresh interest in place of the high class and costly alloy like the multi-component white cast iron. In these circumstances, further betterment of conventional high chromium cast iron has been in demanded. It is considered for this purpose that more researches on the improvement of solidification structure and matrix structure are needed on the high chromium cast iron. The researches on solidification structure and its quantitative analysis [2,5,6,7], solidification process[1-10], control of microstructure by the addition of other alloying elements[9] have been already reported but systematic researches on the behavior of matrix during heat treating are quite a few [11,15,18].

In order to clarify the heat treatment behavior of high chromium cast irons, chromium content of test specimens ranging from 10% to 28% were determined by considering the abrasion wear resistance. M_3C and M_7C_3 eutectic carbides co-exist in 10% Cr cast iron and then it is assumed that the wear resistance will take up a medium position between the cast irons with only M_3C and M_7C_3 carbides. Because the research work on the heat treatment behavior of 10%Cr cast irons is very limited, it can find more and new applications with cheaper price, if the heat treatment behavior and their characteristics will be clarified. It is well known that the 15% to 17% Cr cast irons have been preferably used for rolling mill rolls in steel industry, and that 25% to 28% Cr cast irons for parts and components of pulverizing mills in mining and cement

industries. Since the superior materials to abrasion wear resistance require more hardness and wider range of mechanical properties, 16% Cr and 26% Cr cast irons should be used for those different types of applications, respectively. At the same time, these 16% and 26% Cr cast irons were employed as the base materials to investigate the effect of alloying elements on the heat treatment behavior. Though it is possible from Fe-Cr-C phase diagram that 20% Cr cast iron is assumed to show the intermediate behavior of heat treatment between 16% Cr and 26% Cr cast irons, this kind of cast iron was also added in the systematic experiment of plain high chromium cast iron.

From the viewpoints mentioned here, it is found that the heat treatment behavior of high chromium cast irons without and with alloying elements must be studied systematically and more in detail by putting the stress on the accurate measurement of volume fraction of retained austenite ($V\gamma$) and that of hardness to connect them to the heat treatment conditions.

In this study, heat treatment conditions are widely varied and effects of Cr and C contents and the third other alloying elements such as Ni, Cu, Mo and V on the heat treatment behaviors are discussed in details.

1.2 Objective of Research

The objective of this research is to clarify the heat treatment behavior of high chromium cast irons without and with alloying elements of Ni, Cu, Mo and V. The employed specimens are 10% Cr, 16% Cr, 20% Cr and 26% Cr alloy free white cast irons with eutectic and hypoeutectic composition, and 16% Cr and 26% Cr alloyed white cast irons with eutectic and hypoeutectic composition. Particularly the investigations are focused on the variation of hardness and the volume fraction of retained austenite ($V\gamma$) and their correlation associated with heat treatment conditions.

1.3 Scopes of Research

The experiments were carried out as follows:

(1) Annealing, hardening and tempering heat treatments of all specimens are conducted.

(2) To measure the macrohardness in as-cast and heat-treated states.

(3) To measure the microhardness of matrix in heat-treated state of hypoeutectic high chromium cast iron.

(4) To measure the volume fraction of retained austenite (Vγ) in as-cast and heat- treated states.

(5) To clarify correlation among hardness, Vγ and condition of heat treatment.

(6) To clarify the effects of alloying elements on the variation of hardness and Vγ.

(7) To observe microstructure by using an optical microscope (OM) and scanning electron microscope (SEM) to discuss the experimental results.

(8) To measure the abrasive wear resistance of high chromium cast iron without alloying element.

1.4   Advantages of Research

(1) This research reveals the quantitative and systematic data of macrohardness and matrix micro-hardness in as-hardened and tempered states of high chromium cast iron without and with alloying element.

(2) This research also reveals the quantitative and systematic data of retained austenite connected with alloy content and condition of heat treatment.

(3) These data are extensively helpful for the commercial heat treatment to improve the properties such as strength, toughness and wear resistance of high chromium cast iron.

CHAPTER II

LITERATURE SURVEY

2.1 Solidification and Microstructure of High Chromium Cast Iron

High chromium cast iron is basically a Fe-Cr-C ternary alloy of which solidification structure consists of carbides precipitated from liquid and matrix. According to the liquidus surface phase diagram of Fe-Cr-C system shown in Fig. 2.1 which was constructed by Thorpe and Chicco [12], the primary phases in the region of high chromium cast iron with practical carbon content of 12 to 30% Cr are austenite (γ) in hypo-eutectic and M_7C_3 carbide in hypereutectic compositions, respectively. Later, Thong and Umeda [13] proposed the convenient equations (2.1 and 2.2) to display the liquidus surface of primary γ and eutectic temperatures. From these equations, the liquidus or primary and eutectic temperatures at various combinations of carbon and chromium contents in hypo-eutectic cast irons can be calculated.

$$T_{liquidus} \ (^oC) \ = \ 1554.5 - 89.2x\%C - 0.77x\%Cr \qquad (2.1)$$

$$T_{Eutectic} \ (^oC) \ = \ 1201.7 - 20.3x\%C + 5.97x\%Cr \qquad (2.2)$$

The paper describes that these formulas are appropriate for industrially used cast irons having the chromium content from 12 and 30%. In the alloy with hypoeutectic composition which is widely and commercially produced, γ solidifies first from the melt and followed by (γ+M_7C_3) binary eutectic solidification. In the alloy with hypereutectic composition, M_7C_3 carbide precipitates first from the melt and solidification of (γ+M_7C_3) eutectic is followed. In the case of alloy with low chromium content (less than 10% Cr), $(Fe,Cr)_3C$ or M_3C carbide precipitates as a eutectic, whereas in the alloy with chromium contents over about 15% [2], only $(CrFe)_7C_3$ or M_7C_3 carbide crystallizes as a eutectic.
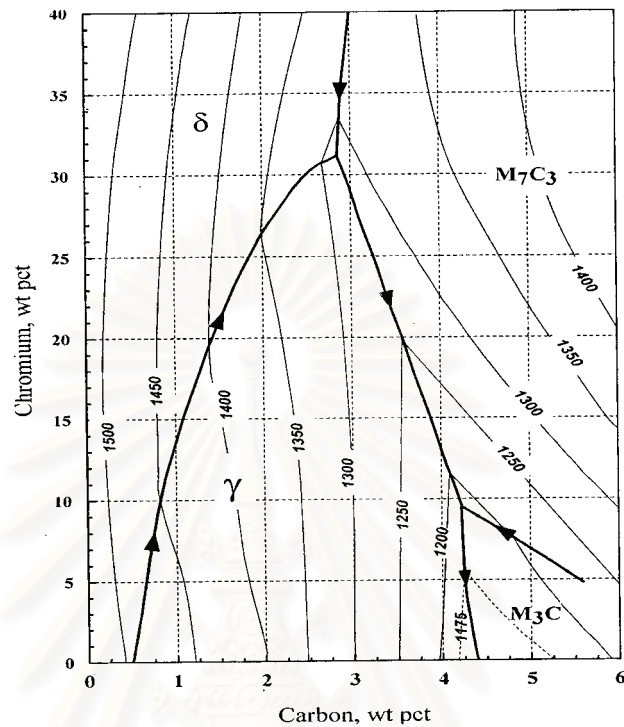
Fig. 2.1   Liquidus surface phase diagram of Fe-Cr-C system. [12]

The M_7C_3 carbide is quite different in morphology from M_3C carbide precipitated in low chromium cast iron. The crystal lattice of M_7C_3 carbide is hexagonal, while the M_3C carbide is orthorhombic.

The hardness of M_7C_3 carbide is 1400-1800 HV and it is much harder than that of M_3C carbide with 800-1100 HV.   Powell[1] observed the carbide morphology of white cast iron by SEM using deep-etched specimen. It is noted that the hexagonal M_7C_3 carbides in the white cast iron with chromium content more than 12% were in rod- and blade-like morphology and they were not completely discontinuous. Matsubara [2] worked widely on the eutectic solidification of high chromium cast iron with chromium content ranging from 10 to 40%. The configurations of $(\gamma+M_7C_3)$ eutectic colony were shown by optical microphotographs and it was pointed out that the eutectic carbides were interconnected and that the interconnectivity decreased with an increase in chromium content up

to 30%.

With respect to the relationship between microstructure and solidification rate, high solidification rate shows a tendency to promote the selective crystallization of M_3C carbide. Irrespective of the solidification rate, the eutectic M_7C_3 carbide precipitates when the chromium content is more than 15%. The as-cast microstructures are shown in Fig. 2.2. The eutectic colony is clearly revealed and the size of colony is found to be changed depending on chemical compositions, carbon and chromium contents. The colony size decreased as the carbon content increases from hypo-eutectic to hypereutectic composition when chromium content is the same. It is also changed by chromium content when compared with those with almost the same eutectic ratio. They also showed a strong relationship between colony diameter and chemical composition as shown graphically in Fig. 2.3 [2], the colony size is smallest in the iron with 30% Cr.

Ogi and Matsubara [7] investigated the growth mechanism of the eutectic cell. The eutectic cell takes a shape of lanky bell and the length of the eutectic cellular projection become larger with an increase in the temperature range of eutectic freezing (ΔT_E). On the other hand, the eutectic colony size can be also connected to the ΔT_E as shown in Fig. 2.4 and it increases with an increase in the ΔT_E. The rate of radial growth (Rr) of eutectic cell is closely related to the size of eutectic carbide particles or carbide spacing in the outside region of the colony, the smaller the Rr, the larger the carbide spacing. Base on thermodynamic principle, alloying elements are distributed to both of phases, austenite dendrite and eutectic carbide during solidification. Therefore, the microstructure of high chromium cast iron is greatly influenced by the addition of alloying elements.

The volume fraction of carbide (Vc) can be estimated from the initial chemical composition of the iron. Maratray [14] demonstrated a following equation that the Vc increases in proportion to the carbon and chromium contents.
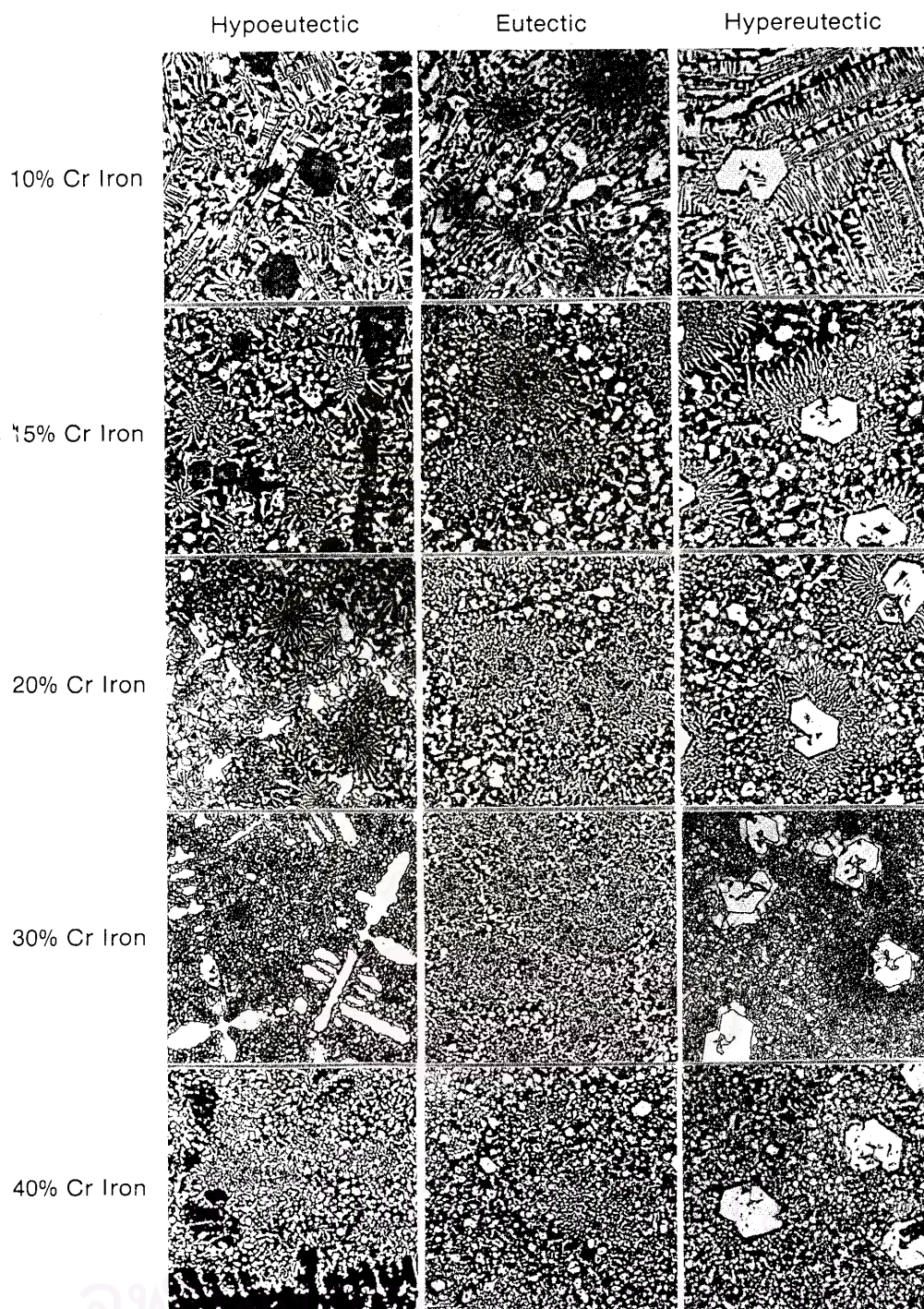
Fig. 2.2 Typical microphotographs of as-cast hypoeutectic, eutectic and hypereutectic high chromium cast irons. [2] (γ+M$_7$C$_3$) eutectic structures show colony morphology and the sizes of eutectic colony and M$_7$C$_3$ carbide particles are smallest in 30% Cr cast iron.
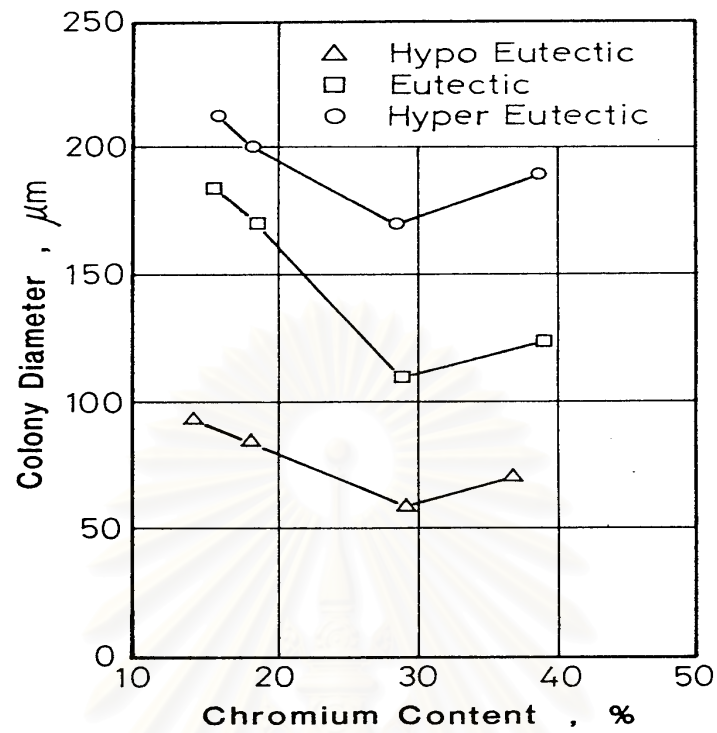
Fig. 2.3 Effect of chromium content on colony diameter at RE (Eutectic solidification rate) : 0.5cm/min. [2]
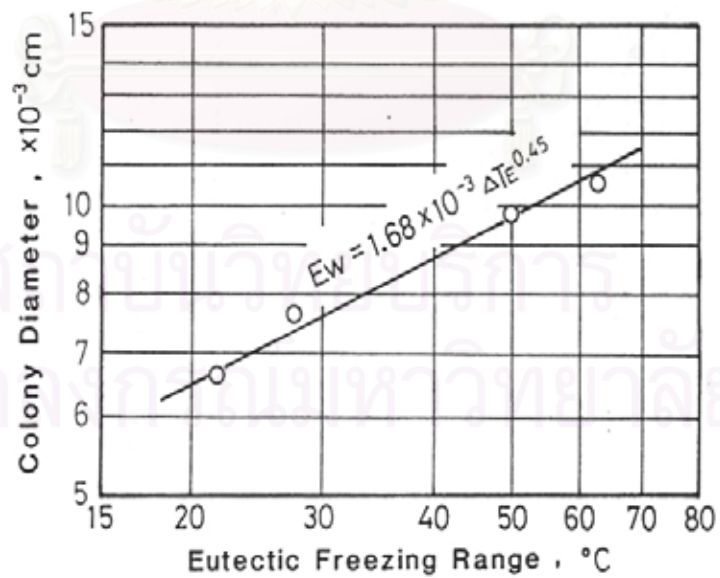
Fig. 2.4 Relationship between colony diameter and eutectic freezing length (ΔT_E). [7]

$$\% \, Vc = 12.33(\%C) + 0.55(\%Cr)-15.2 \qquad\qquad (2.3)$$

High chromium cast irons are sometimes used in as-cast state where some quantity of γ retains in the matrix. As described previously, the hardness is one of very important factors affecting the abrasive wear resistance, and that, the wear resistance increases with an increase in the hardness. The hardness of cast iron is determined by the microstructure consisting of volume fraction of carbide, morphology of carbide and matrix structure.

Matrix hardness in as-cast state varies depending on constitutional phases. Especially the austenite produces due to the supersaturation of chromium and carbon in matrix during solidification. The carbon has more effect on the amount of austenite, the more the carbon content, the more the retained austenite. The influence of chromium on the transformation of austenite in as-cast cooling was investigated by G. Laird II [15]. Chromium retards the transformation from austenite to pearlite as it lowers Ms temperature. Resultantly, a large amount of austenite exists usually in as-cast matrix of high chromium cast iron. The as-cast matrix is composed of plural constituents such as pearlite, bainite, martensite and retained austenite. Martensite appears in the matrix due to the depletion of chromium and carbon around the eutectic carbides. In the case of hardening, the austenite destabilized during austenitization transforms partially into martensite, mixing with retained austenite.

Generally, the alloying element affects the properties of the cast iron in two ways. First, it is partially distributed to the matrix during solidification and determines the matrix structure in both the as-cast and heat-treated states. This can improved the properties of matrix. Second, the element remaining in the melt is consumed by the formation of eutectic carbide. In this case, the element has no longer any effect on the hardenability. There, the distribution coefficient of alloying element should be taken into account.

Austenite tends to reject or to accept a certain alloying element

when it solidifies. The growing austenite dendrite will reject C, Cr, Mo, V and Nb which are ferrite forming elements but accept Si, Cu, Ni and Mn which are austenite forming ones. However, Mn dissolves into austenite and carbide. If a large amount of strong carbide forming elements like Mo and V are added into cast iron, they may possibly form special carbides of Mo_2C and VC which has much higher hardness than chromium carbide (M_7C_3). It is reported that the special carbides form when the content of Mo or V exceeds 2% [33,40]. The formation of such special carbides will bring more decrease of alloying elements in the matrix.

The impure elements of P and S should be also be limited in high chromium cast iron because they remarkably segregate into liquid to solidify as brittle phosphide and sulfide binary or ternary eutectics, and they cause crack or hot shortness.

In order to improve the mechanical properties of high chromium cast irons, the trials to modify the M_7C_3 eutectic carbide were done by controlling the alloy composition. The carbide has been modified by the addition of carbide forming elements, say, Nb, V, and Ti [16, 31-33]. The presence of such elements affects significantly the mechanical property due to the strengthening of the matrix and the separation of carbide phase. Rickard [16] studied the effect of Ti inoculation on ferritic high chromium cast iron with 1.5% C and 30% Cr. The results showed that TiC carbides precipitated first and followed by delta ferrite (δ) in the solidification process and resultantly finer grained microstructure was obtained. This suggests that TiC particles act probably as nucleation sites of the primary δ ferrite during solidification. He also showed the tensile test data which indicating that the grain refinement increased tensile strength from 45 MPa to 54 MPa. The effect of rare earth on the morphology of eutectic carbide was reported by Liang et al. [9]. The mischmetal was added into the low and high chromium cast irons (3.7% Cr and 18% Cr, respectively), and considerable modification of eutectic carbide occurred seen in the low chromium cast iron but little change was

in high chromium cast iron, because eutectic M_7C_3 carbide grew fast to form a characteristic lath or rod-like morphology. However, they suggested that the carbide morphology might be changed by adding a certain element which could hinder the eutectic growth. Powell and Randle [27] observed that the carbide connectivity was reduced when 1.3% Si was added to 18 % Cr cast iron. Laid and Powell [28] followed in their paper that Si inhibited the nucleation of M_7C_3 carbides in 18% Cr iron. However, Shen and Zhou [29] reported an increase in the number of carbide nuclei due to Si addition. It is true that Si can refine the primary dendrite and at the same time shifted the eutectic carbon content to the lower side and resulted in an increase in volume fraction of carbide. However, when the addition is over 3%, transformation of the austenitic matrix to pearlite occurred instated of martensite. B addition to 13% Cr and 28% Cr cast irons [30] changed the carbide morphology from coarse and interconnected state to isolated and parallel distribution. Another way to control the size of eutectic is to make the melt cool fast by using chill mold or permanent mold. Matsubara et al. [17] investigated the influence of alloying element on the eutectic structure of high chromium cast iron and clarified that the sizes of eutectic colony and carbide particle were controlled by the addition of the third alloying elements which could vary the temperature range of eutectic solidification (ΔT_E) being expanded by Mo, Al and reduced by V. The former enlarges both the eutectic colony and carbide particle and the latter refines them. An addition of Ti refined the sizes of eutectic colony and eutectic carbide because of its inoculation effect.

2.2 Heat Treatment

It is known that as–cast high chromium cast iron used to contain some austenite with low hardness. High hardness, good abrasion resistance and resistance to spalling are obtained in martensitic matrix. Generally, the as-cast state does not give the maximum hardness.

However, the high chromium white iron is occasionally used in the as-cast condition leaving some austenite retained. In that case, the transformation of the austenite into martensite can be utilized under a certain wear condition for resulting in higher wear resistance. Under the certain wear circumstances, therefore, not only the martensitic matrix but also matrix with some retained austenite is requested for superior wear performance. In order to get higher hardness, the cast iron has to be heat-treated. The important thing in the heat treatment of alloys is that the phase transformation behaviors of the alloys must be clarified and comprehended. The phase transformation diagram tells us the behavior of alloying elements in the matrix including the formation of secondary carbide.

2.2.1 Destabilization

The hardening process is to increase the hardness by reducing the amount of retained austenite and to allow the martensite transformation for the improvement of wear property. Since the eutectic carbide does not change in the range of temperature up to 1100 ^{o}C, [41,42] the most important factor to understand the kinetic of solid state transformation of high chromium cast iron is the chemical composition of retained austenite because the austenite can transform into various phases depending on alloy concentration in austenite and condition of heat treatment.

The phase transformation in the solid state can be theoretically explained using the isothermal transformation (IT) diagram or continuous cooling transformation (CCT) diagram. Phase transformation diagrams of high chromium cast irons with Mo are reported by Maratray in his book "Atlas Transformation Characteristic and Chromium-Molybdenum White Irons". In each CCT diagram, the start of the precipitation curve for secondary carbide was displayed. When alloy is cooled down after austenitization or during austenitization, carbon and chromium in matrix are combined to precipitate the secondary carbides. This is so-called "destabilization", and it occurs at 1000 ^{o}C to 1050 ^{o}C in the as-cast high

chromium cast iron with considerable amount of austenite.

The effect of destabilization on IT diagram has been explained using a schematic diagram shown in Fig. 2.5. [22] Let's considered that high chromium cast iron cools down after solidification or after austenitization at high temperature. In the case (a), cast iron cools directly below subcritical (A_1) temperature under the condition with more alloy concentration in austenite, and then austenite is more stabilized. When it is held there, the pearlite or bainite transformation begins at the longest time because alloy concentration in the austenite is highest. In the case (b) that the cooling of cast iron is interrupted at about 1000 ^{o}C and held there for a certain time and in another case (c) that cast iron is held at the same temperature for longer time, the precipitation of carbide takes place between the precipitation start (Ps) and precipitation finish (Pf). The volume fraction of precipitated carbides increases as the holding time increases. In the process of (a) and (b), the austenite supersaturated with alloying elements is destabilized partially because the holding does not reach the Pf line. In the case of (a) and (b), therefore, the start of pearlite transformation is determined by the holding time between Ps and Pf. Therefore, the start of pearlite transformation in the case of (b) occurs earlier than that of (a), and in the case (c), the pearlite transformation does earlier than that of the case (b). Maratray [14] has reported that at lower austenitizing temperature, the longer holding time is required to reach equilibrium. When the specimen is austenitized at 1000 ^{o}C to 1050 ^{o}C, two hours have to be taken for reasonable austenitization whereas eight hours are needed for the austenitzation at 1200 K. Pattyn [43] suggested that at minimum, two hours is need for all white cast irons. However, if the holding time is longer than 5 hours, the agglomeration of carbide occurs and the number of secondary carbides, reduced. [44] For austenitization, pearlitic matrix reaches fast an equilibrium carbon content of austenite. It is also noted that if the casting is segregated heavily or very high temperature is used for annealing, longer holding
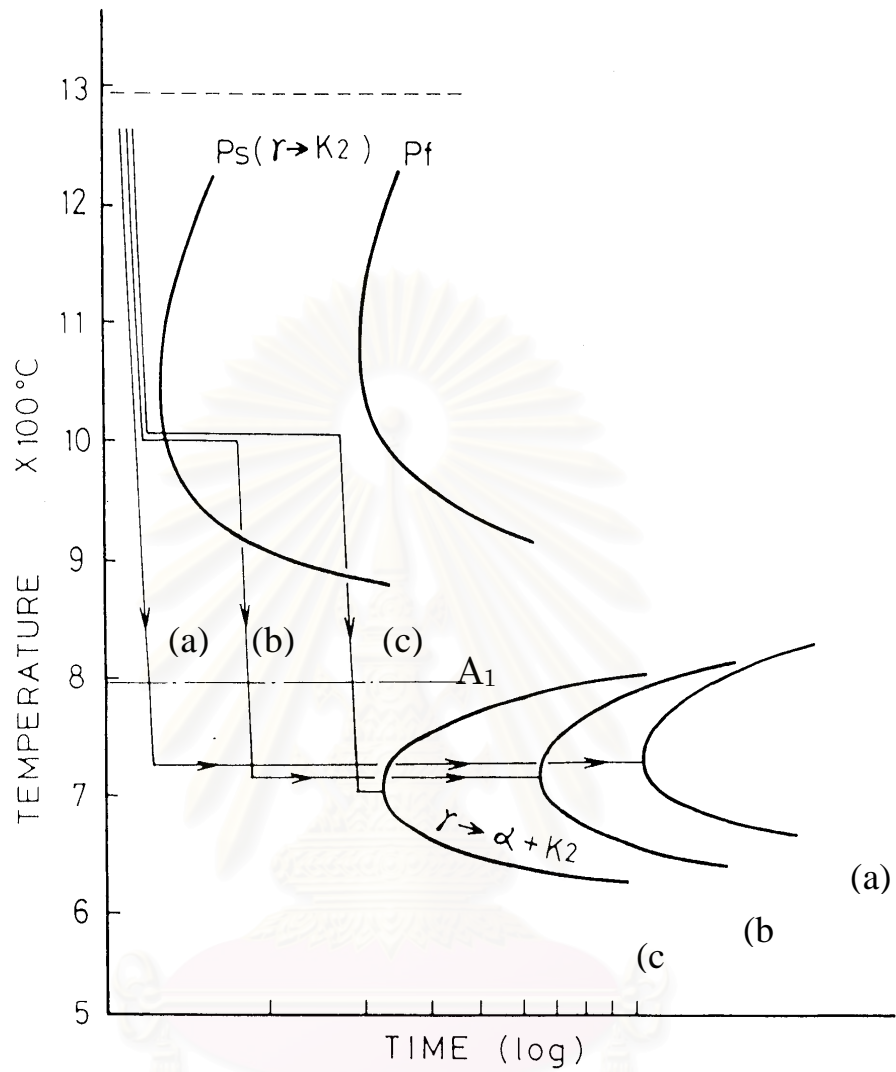
Fig. 2.5 Schematic explanation of destabilization heat treatment on IT diagram of high chromium white cast iron. [22]

time has to be taken for destabilization.

The typical IT diagram of 20% Cr - 1% Mo cast iron is shown in Fig. 2.6 (a) for the cast iron in as-cast condition while Fig. 2.6 (b) for the cast iron after destabilizing at 1000 ^{o}C.[45] The secondary precipitation curve displays a "C" curve and the nose of curve is around 1000 ^{o}C. At the higher temperatures, 920 to 1060 ^{o}C, the austenite is destabilized and the reaction can be described as;

$$\gamma \rightarrow \gamma^* + \text{secondary carbides (M}_7\text{C}_3 \text{ or M}_{23}\text{C}_6)$$

where the γ^* is austenite with a lower alloy content than the original austenite. This reaction depletes C and Cr in austenite. At the lower tempering temperature in Fig. 2.6 (b), if enough time is given, the austenite is full destabilized and transform into pearlite. It is found from Fig. 2.6 (b) that the pearlite transformation is shifted to the long time side. Due to the precipitation of carbides during destabilization, the alloy concentration in austenite reduces and therefore Ms temperature goes up over room temperature, in other word, martensite transformation appears. Hence, during cooling to the room temperature, the retained austenite transforms to martensite. This is one of reasons why retained austenite in as-hardened state contributes to increase the tempered hardness.

The types of secondary carbides which precipitate in austenite are M_3C, M_7C_3 and/or $M_{23}C_6$ depending on chemical composition and condition of heat treatment. [46] In 25% to 30% Cr cast irons, the $M_{23}C_6$ carbides are formed, and M_7C_3 and $M_{23}C_6$ types of carbide are found in 15% to 20% Cr cast irons. [47] The M_3C carbides can also form in low Cr cast iron. [1,46-49] Powell [1,27,28] reported that the precipitation of secondary carbide produces in two stages. The $M_{23}C_6$ carbide precipitates first and then transform to M_7C_3 when it is held for a long time. Powell and Laird [28,46] predicted the types of secondary carbides precipitated by using the isothermal section at 1000 ^{o}C and 870 ^{o}C of C-Cr-Fe ternary shown in Fig. 2.7 (a) and (b). [41] And they reported that after
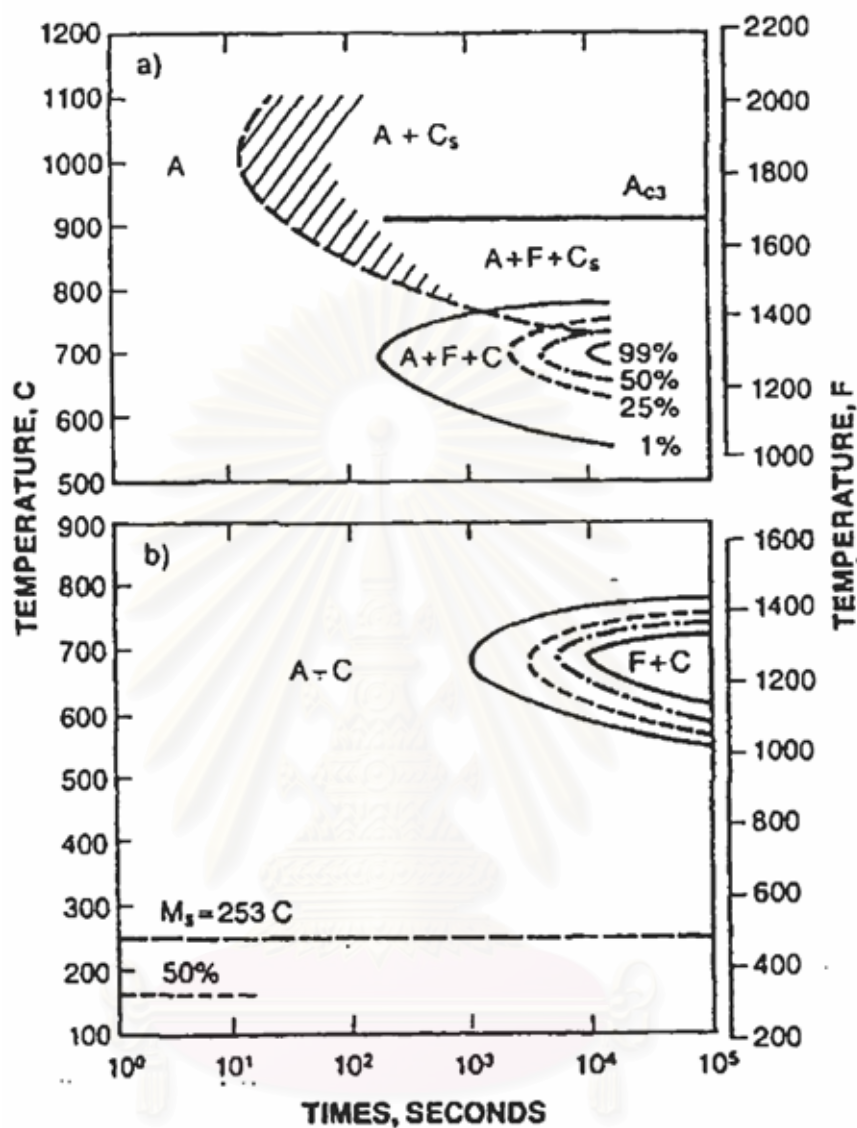
Fig. 2.6 Isothermal transformation diagrams of high-Cr white iron containing 2.5%C-20%Cr-1%Mo; a) before and b) after destabilizing austenite: A= austenite; C= pearlite; F= ferrite; Ms= martensite start; Cs= secondary carbide. [45]
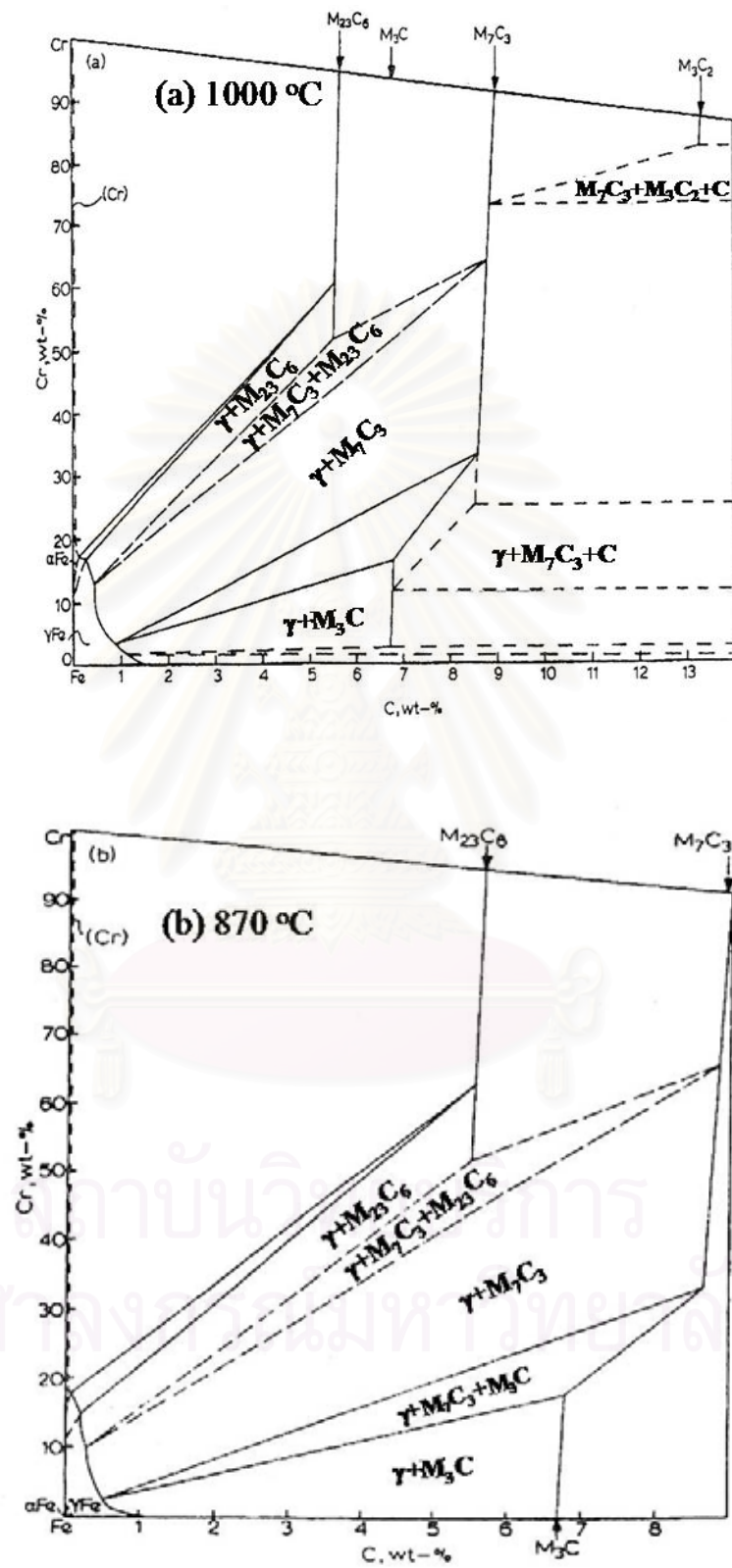
Fig. 2.7 Solid-state isotherms of C-C-Fe system at (a) 1000 °C and (b) 870 °C. [41]

destabilization of three cast irons with 10% Cr, 18% Cr and 30% Cr at 870 ^{o}C and 1000 ^{o}C, the main types of secondary carbides precipitated are M_3C in 10% Cr, M_7C_3 in 18% Cr and $M_{23}C_6$ in 30% Cr cast irons, respectively. [28]

The destabilization temperature has a major effect on the transformation of austenite into martensite and controls the final hardness. Maratray and Poulalion [18] suggested that the important factors controlling the amount of retained austenite are chemical composition, destabilization temperature and cooling rate. It is reported that the maximum hardness is obtained at the austenitizing temperature between 930 to 1030 ^{o}C.[18] With an increase in the austenitizing temperature, the solubility of C in austenite increases and resultantly, hard martensite is obtained on subsequent cooling. However, the higher C content in the matrix lowers the Ms temperature, producing more retained austenite which cause a decrease in the hardness.

As for high chromium cast iron, it can be said that an important goal of heat treatment is to increase the hardness for the wear resistance. Maratray [18] reported that the highest hardness is obtained when the matrix contains 20% retained austenite in as-hardened state. Cr content has a significant influence on the optimum austenitizing temperature and the relationship between austenitizing temperature and hardness is shown in Fig. 2.8. [14] According to Fig. 2.7, it is found that as Cr content increases, the C content in austenite decreases. Therefore, the higher austenitizing temperature is required in order to get the same C content in austenite. For this reason, as Cr content increases, the optimum destabilizing temperature increases. It is clear Fig. 2.8 that the higher level of chromium content needs the higher austenitizing temperature to obtain the highest as-hardened hardness, around 930 ^{o}C in 15% Cr cast iron and 1030 ^{o}C in 28% Cr cast iron.

The volume fraction of carbide increases as the C content rises. Resultantly chromium concentration in matrix is decreased if carbon content is the same. Therefore, a parameter of Cr/C value has been

introduced to understand the effect of both the C and Cr content in the cast iron. The alloying elements such as Mo, Ni, Cu and Mn are usually added to high chromium cast iron in order to improve the hardenability. They delay the transformation of austenite into pearlite. Most of the alloying element decreases the Ms temperature, in other words, it stabilizes austenite. Maratray also reported that austenite stability is reduced with decreasing the cooling rate. [14]
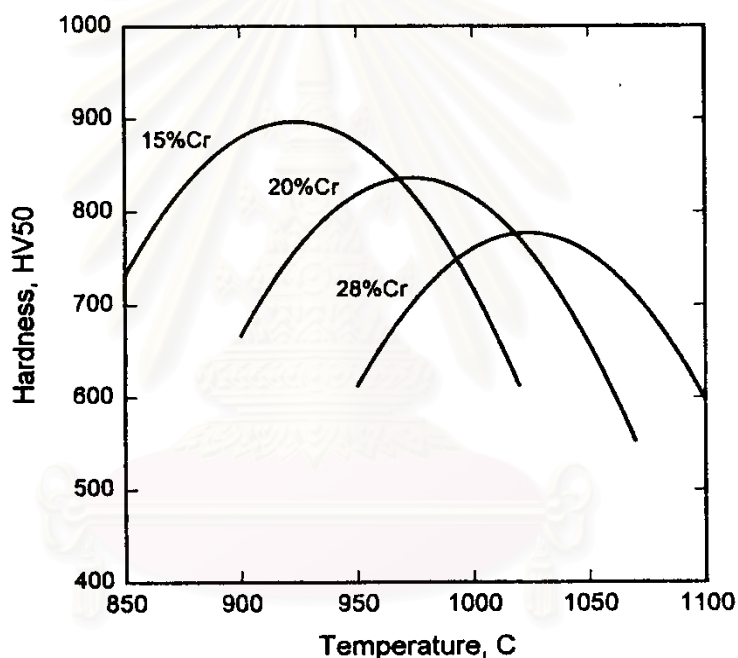
Fig. 2.8 Influence of Cr contention on optimum hardening
temperature in high chromium cast irons. [14]

2.2.2 Tempering or subcritical heat treatment

Tempering or subcritical heat treatment is always conducted after hardening in order to transform retained austenite into martensite and allows the precipitation of secondary carbide.

As described previously, martensite formation in high chromium cast iron usually occurs at low temperature and then the high quantity of austenite retained in the matrix in as-hardened state. In this case, the subzero treatment must be given to obtain more or full martensitic matrix structure. According to the effect of alloying elements on the Ms temperature of steel, carbon has a greatest effect followed by the other elements of Mn, Ni, Cr and Mo. A following equation has been proposed experimentally [36],

$$Ms \ (^{o}C) = 550 - 350 \ x \ \%C - 35 \ x \ \%V - 20 \ x \ \%Cr - 17 \ x \ \%Ni$$
$$-10 \ x \ \%Cu - 10 \ x \ \%Mo \qquad (2.4)$$

While cooling from austenitizing temperature to A_1 temperature, precipitation of carbides occurs along with A_{cm} line due to a decrease of solubility of carbon in the matrix and the ratio of precipitation is varied by the cooling rate, the higher the cooling rate, the less the precipitation. Some papers said that the spalling resistance decreased as the retained austenite increases. [4,10,45] This should be due to too much retained austenite in the matrix. To overcome this weakness, the tempering or subcritical heat treatment is taken.

The tempering temperature and holding time must be carefully chosen so that the martensite can not be over-tempered, in other words, so that the tempered martensite can be left greatly in the matrix. Over-tempering leads to a decrease in hardness and strength of the matrix. In subcritical heat treatment, the chromium carbides of $M_{23}C_6$ are precipitated from retained austenite at high temperature over 450 ^{o}C and this precipitation results in the destabilization of austenite and transformation into martensite during cooling to room temperature. [21] Low tempering temperature between 200 to 250 ^{o}C is too low to transform the retained austenite and therefore, higher temperature in the range of 450 to 600 ^{o}C are normally used. [45] Maratray [18] reported that in the range of tempering temperature from 480 to 650 ^{o}C, $M_{23}C_6$

carbide is more stable than M_7C_3 carbide. Biss [20] showed that the tempering at 650 ^{o}C produced $M_{23}C_6$ carbide and he also found that some martensite still exists in the matrix. Sare et al. [21] reported that in an alloyed white cast iron, the hardness does not change until the tempering temperature was risen to 450 ^{o}C but over 500 ^{o}C, it gradually decreases as the tempering temperature increases. Pearce[50] has been studied on the effect of tempering temperature on the hardness of 20% Cr-1.7% Mo cast iron. It is reported that at 450 ^{o}C to 500 ^{o}C tempering, the secondary carbides precipitated and reduced the retained austenite resulting in the secondary hardening. When the tempering temperature over 600 ^{o}C, the hardness decreases as the secondary carbides coarsen, or austenite decomposed to be pearlite.

It is preferable, if the cast iron could self hardened as it cooled within the mold. Bureau and CSIRO [28] reported using addition of Si to 3%C - 17% Cr - 2% Mo - 1% Cu-or Ni that Si lowers the solubility of C in austenite and promotes the carbide formation. As C content in austenite is lowered, the Ms temperature increases and allows the transformation of austenite into martensite.

2.3 Wear Resistance

2.3.1 Concept of abrasion wear

In the fields of mining, iron and steel, electric power plant and cement industries, various kinds of machines are used for digging, crushing, milling or pulverizing and rolling. Abrasive wear usually occurs in the parts that are used in the machines. Abrasive wear can be classified into three types,

(1) Gouging abrasion which arises when surface of the part is scooped out by the large mass of abrasives such as ores or stones with heavy impact load.

(2) Grinding or high-stress abrasion which takes place when mineral or cement clinker is pulverized between two moving

metals, say, roller and table.

(3) Scratching abrasion or low-stress abrasion which occurs when small abrasives are touching on the surface of working part and when low stress is sufficient to crush or grind the abrasives.

Generally, the combination wear of two or three types occurs on the surface of part during service. As we know, wear resistance of high chromium cast iron is closely related to the microstructure consisting of the morphology and amount of carbide and the matrix structure, which are factors to determine the macro-hardness of cast iron. These factors may also determine the mechanical properties, mainly toughness and strength. All these factors influence finally on the abrasion wear resistance. As the eutectic carbide changes little in both of the quantity and morphology after solidification, the matrix structure becomes a very important factor to improve the wear property.

2.3.2 Relationship between wear resistance and retained austenite

The parameters to determine the wear performance are both eutectic carbide and matrix structure. Many literatures reported [4,12,21] that too much amount of retained austenite in the matrix deteriorates only spalling resistance in applications under impact loading. The wear resistance of high chromium cast iron in as-cast state is studied by Dogan [10]. The results showed that pearlitic matrix has extremely poor wear resistance compared with the matrix structure mixed with austenite and martensite. Many researches [3-5] reported that a large volume fraction of retained austenite was preferable to the abrasive wear resistance against the heavy abrasive load or high stress abrasion, whereas, in light abrasive condition, martensitic matrix is preferable. Even for a general cast iron to be used under an abrasive load, a certain amount of retained austenite is considered to be effective. It is well known that the retained austenite may often lead to a generation crack during serving, because of a great deal of expansion by a stress-induced martensite transformation. This

phenomenon is solved by using heat treatment which decomposes the retained austenite to be at a low level. I.R. Sare [4,21] reported that the lowest wear loss is achieved at the intermediate level of retained austenite like 30-40%, as shown in Fig. 2.9. It is also reported that the abrasive wear resistance of heat-treated cast iron with martensitic matrix is higher than that in as-cast cast iron with austenitic matrix. Laird II and et al. [15] studied on pin-on-disk wear test of 28% Cr cast iron and showed that the highest wear resistance is obtained in as-hardened state that contained some retained austenite. S.K. Yu et al. [3] investigated the effect of volume fraction of retained austenite (Vγ) on the rate of wear (Rw) in hypoeutectic high chromium white cast iron. As shown in Fig. 2.10, the Rw decreases with an increase in the Vγ. It is because the retained austenite transforms more and more into martensite by stresses.
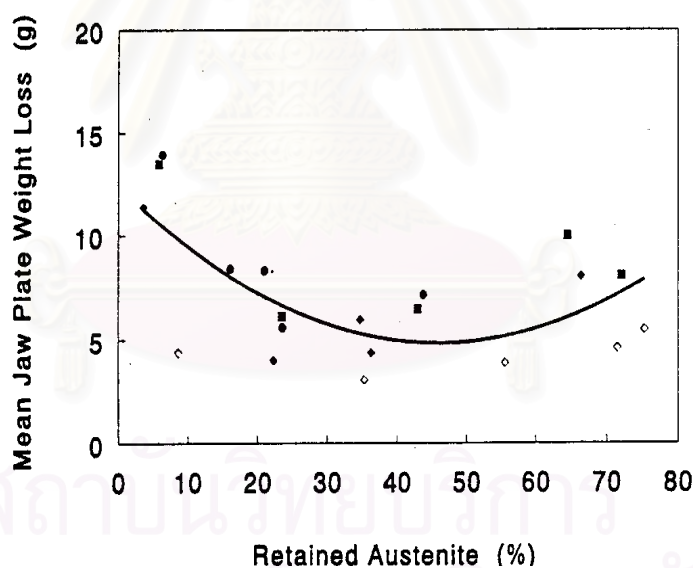
Fig. 2.9 Relationship between mean weight loss(g) and volume fraction
of retained austenite by jaw plate test. [4]
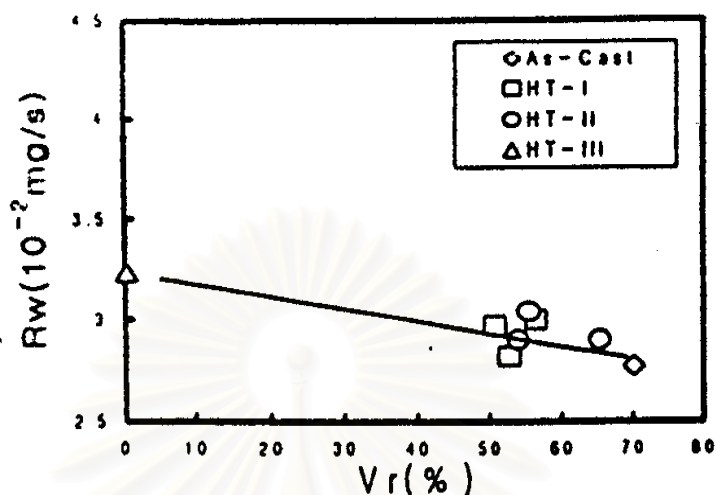
Fig. 2.10 The relationship between wear rate and volume fraction of
retained austenite (Vγ). [3]

2.3.3 Relationship among wear resistance, volume fraction of carbide and hardness

Abrasion wear resistance can be also related to the volume fraction of carbide (Vc). O.N. Dogan [10] used 15% and 26% Cr cast irons in as-cast state to investigate the wear resistance and connected the wear rate to the Vc value that was calculated by the equation (2.5) proposed by Maratray [14]. The relationship between Vc and wear rate is shown in Fig. 2.11. The wear rate decreases as the Vc value increases and the decreasing rate is greater in 15% Cr cast iron, but the quantity of wear at the same Vc value is three times as higher as in 15% Cr cast iron than in 26% Cr cast iron. As shown in Fig. 2.12, the wear rate decreases roughly in proportion to the hardness. From the above reviews, it can be concluded that the abrasive wear resistance of 26%Cr cast iron, which has more austenite in matrix and high volume fraction of carbide, is greater than that of 15% Cr cast iron with bainitic and pearlitic matrix and lower volume fraction of carbide.
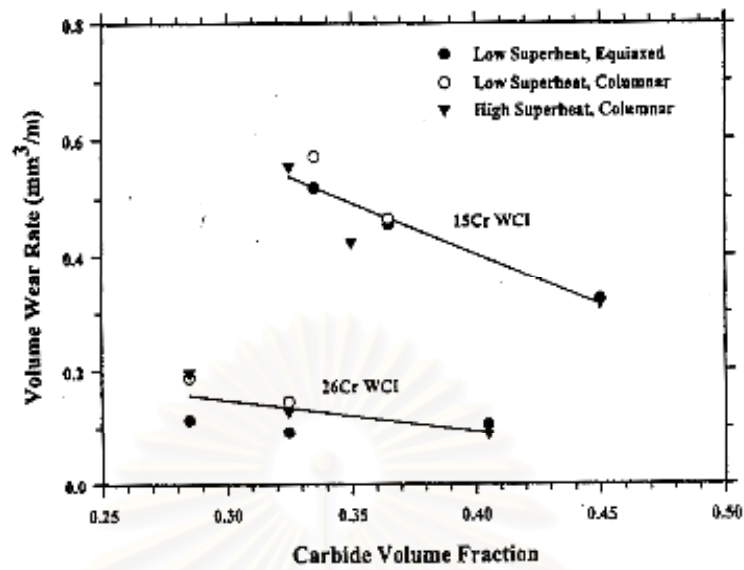
Fig. 2.11 Effect of volume fraction of carbide on wear rate of high chromium cast irons. [10]
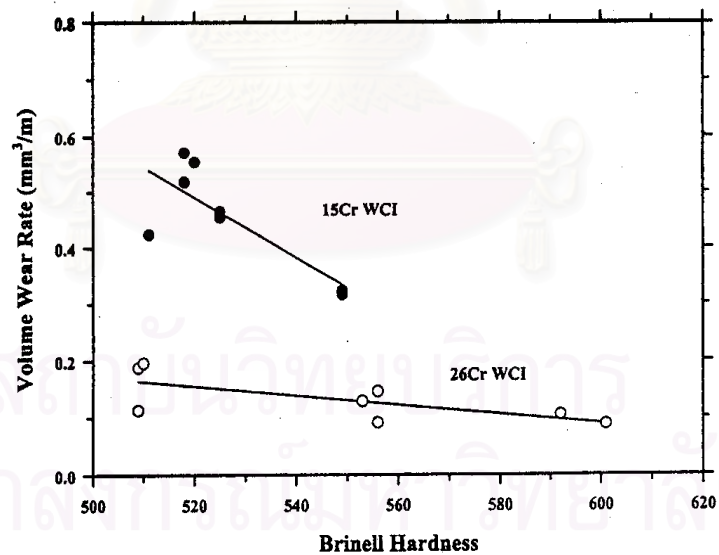
Fig. 2.12 Relationship between wear resistance and hardness of the 15 %Cr and 26 % Cr cast irons. [10]

The effect of heat treatment on the gouging abrasion resistance or the high stress abrasion resistance of alloyed white cast iron was investigated by I.R. Sare and B.K. Arnold [4,21] using a jaw crusher. As shown in Fig. 2.13, though the data are scattered, it is presumed that the weight loss decreases roughly in proportion to the hardness. In high-stress abrasive condition, the effects of austenitizing temperature on the wear losses in as-cast and as-hardened states are shown in Fig. 2.14. The abrasion resistance of double heat treatment, that is, tempered state is low, and the highest wear resistance is obtained in as-hardened state from about 1373 K austenitization. In tempered state, as shown in Fig. 2.15, the wear loss decreases gradually as the tempering temperature rises to 723 K (500 ^{o}C) and then increases as the tempering temperature rises. This can be explained by the fact that over the 798 K (525°C), the secondary carbides formed by tempering starts to aggregate to be coarser. Results of pin-on-disk wear test are shown in Fig. 2.16. It is clear that the wear resistance in tempered state is in good accordance with the macro-hardness and it decreases as the hardness increases. To obtain high hardness, the tempering temperature must be chosen by considering the amount of retained austenite in the matrix. Wanaporn et al. [23] has clarified the same relation in multi-component white cast irons and suggested that the higher tempering temperature should be adopted as volume fraction of retained austenite increases.
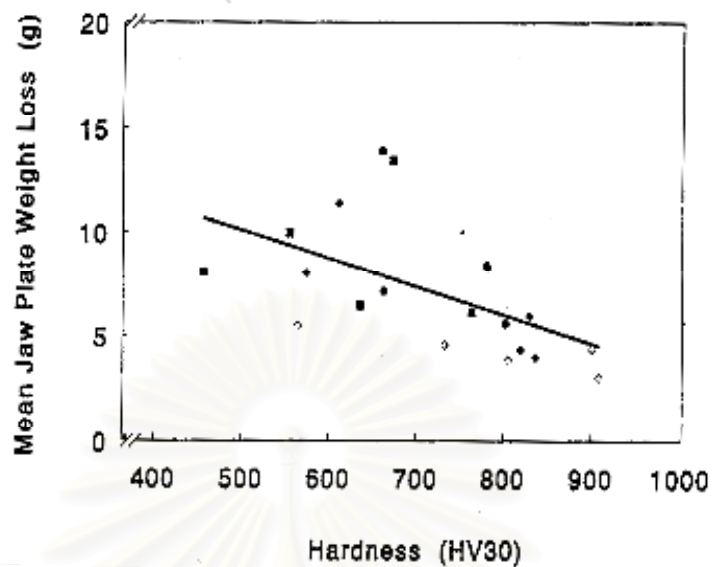
Fig. 2.13   Relationship between weight loss and hardness by Jaw-plate
test. [21]
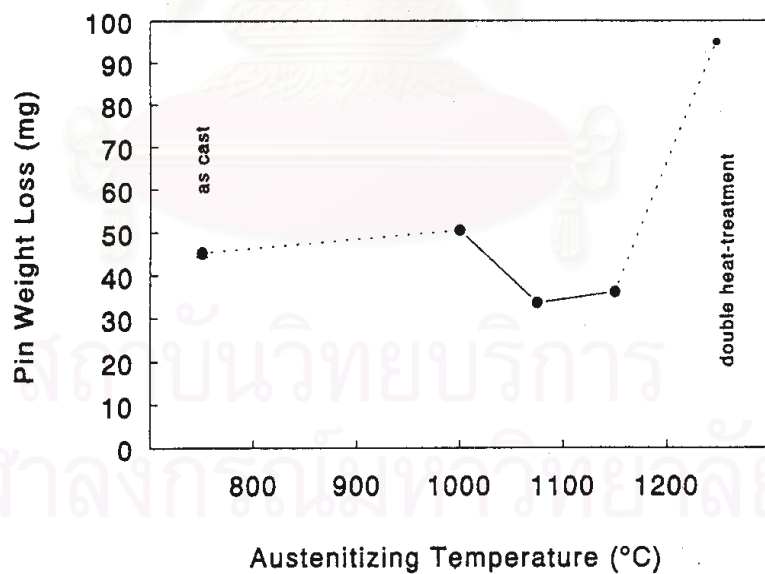
Fig. 2.14   Relationship between pin weight loss (mg) and austenitizing
temperature(^{o}C) of 27% Cr cast iron. Data are also shown in
the as-cast and as-hardened condition. [21]
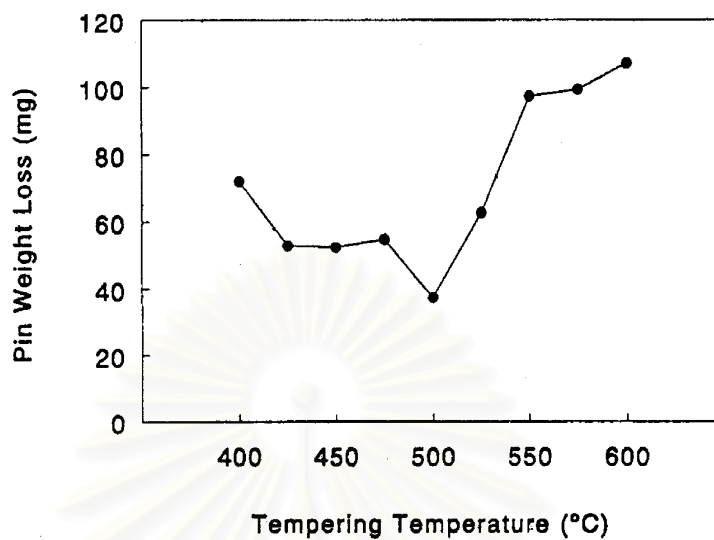
Fig. 2.15 Relationship between pin weight loss(mg) and tempering temperature(^{o}C) of 27% Cr cast iron. [21]
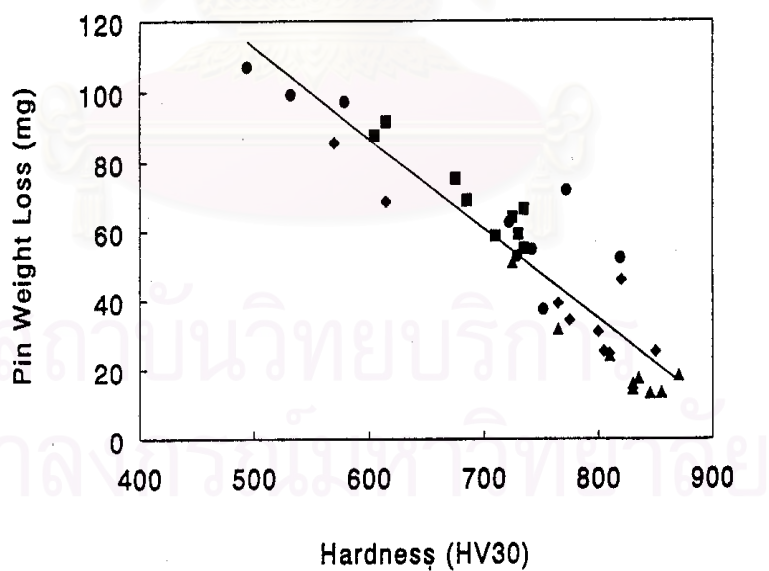
Fig. 2.16 Relationship between weight loss and hardness in tempered state by Pin-on-Disk wear test. [21]

CHAPTER III

EXPERIMENTAL PROCEDURES

3.1 Preparation of Specimens

3.1.1 Mold design and test piece

The shape and dimension of the CO_2 mold is shown in Fig. 3.1.The wood pattern or cavity consists of a portion (25 mm x 65 mm) for test piece and the riser on it. The cast specimen was sliced by a wire-cut EDM (Electric Discharge Machine) to obtain the disk-shaped test piece with 7 mm in thickness.
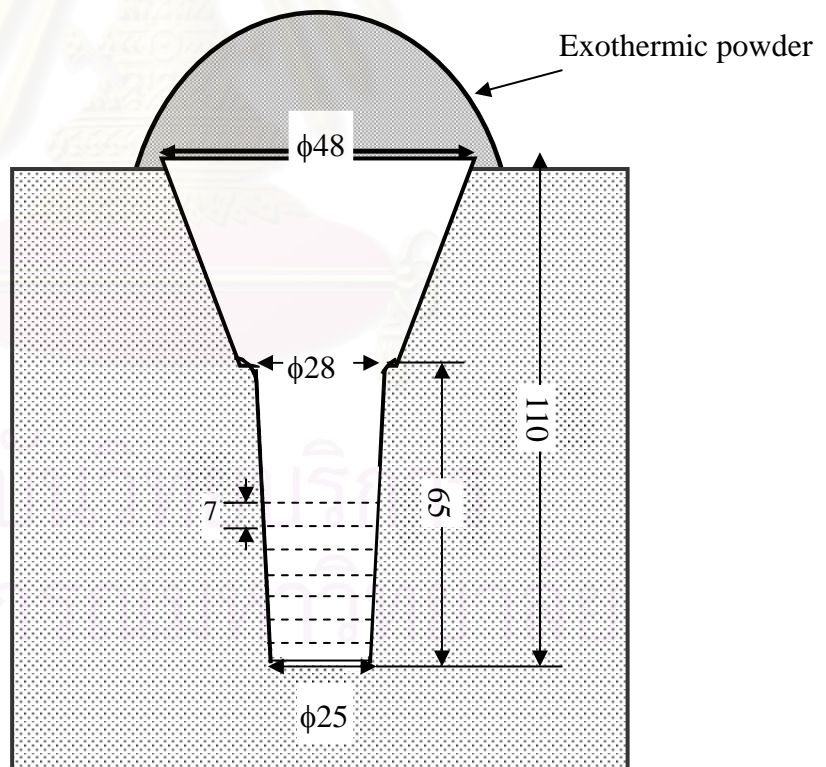
Fig. 3.1 Schematic drawings of CO_2 mold. Unit: mm

3.1.2 Production of specimens

The charge calculations were carried out for the target chemical compositions of eutectic and hypo-eutectic cast irons. As raw materials, mild steel scrap, pig iron, ferroalloys and pure metals were used. The chemical compositions of raw materials are shown in Table 3.1. The total weight of 30 kg was melted down in 30 kg-capacity high frequency induction furnace with alumina (Al_2O_3) lining and superheated at 1853 K (1580 °C). After holding the melt, it was cast from the pouring temperature of 1773-1793 K (1500-1520 °C) into the preheated CO_2 mold shown in Fig. 3.1. The melt was immediately covered with dry exothermic powder to hold the temperature of riser high. The aim chemical compositions of plain high chromium cast iron, eutectic and hypo-euetctic cast irons with alloying elements are respectively summarized in Table 3.2 to Table 3.4. Four series of plain high chromium cast irons with 10% Cr, 16% Cr, 20% Cr and 26% Cr were prepared. In each chromium series, the carbon content was varied so that the eutectic ratio could range widely from 100%. At the same time, the 16 %Cr and 26 %Cr eutectic and hypoeutectic cast irons without alloying element and with a single addition of Ni, Cu up to 2% and Mo, V up to 3% were produced.

3.2 Heat Treatment Procedure

For the investigation of heat treatment characteristics, the conditions of heat treatment listed in Table 3.5 were introduced. Each heat treatment cycle are illustrated in Fig. 3.2.

Table 3.1 Chemical composition of raw materials.

Materials	Element (mass%)										
	C	Cr	Ni	Cu	Mo	V	Si	Mn	P	S	Fe
Mild steel scrap	0.05	-	-	-	-	-	0.02	0.28	0.011	0.011	bal
Pig iron	4.44	-	-	-	-	-	1.14	0.19	0.08	0.019	bal
Fe-Cr (HC)	8.42	62.02	-	-	-	-	1.02	-	0.025	0.036	bal
Fe-Cr (LC)	0.02	69.24	-	-	-	-	0.25	-	0.030	0.005	bal
Fe-Mn(L)	0.96	-	-	-	-	-	0.24	75.3	0.144	0.012	bal
Fe-Si	0.047	-	-	-	-	-	75.00	-	0.016	-	bal
Fe-V	0.1	-	-	Al = 1.7	-	79.4	0.7	-	0.030	0.01	bal
Fe-Mo	0.05	-	-	0.38	62.7	-	0.7	-	0.04	0.09	bal
Pure Cu	-	-	-	100	-	-	-	-	-	-	-
Pure Ni	-	-	100	-	-	-	-	-	-	-	-

Table 3.2 Chemical composition and Cr/C value of plain high chromium cast irons.

Specimen	Element (mass%)				Cr/C
	C	Cr	Si	Mn	
No.1	3.68	10	0.5	0.5	2.64
No.2	3.12	10	0.5	0.5	3.17
No.3	2.94	10	0.5	0.5	3.54
No.4	3.45	16	0.5	0.5	4.64
No.5	3.01	16	0.5	0.5	5.48
No.6	2.62	16	0.5	0.5	6.08
No.7	3.28	20	0.5	0.5	6.06
No.8	2.90	20	0.5	0.5	6.94
No.9	2.57	20	0.5	0.5	7.91
No.10	3.00	26	0.5	0.5	8.96
No.11	2.65	26	0.5	0.5	9.65
No.12	2.32	26	0.5	0.5	11.00

* Cr, Si and Mn contents are aim composition.

Table 3.3 Aim chemical composition of eutectic cast irons with
alloying elements.

Number	Element(mass%)							
	C	Cr	Si	Mn	Ni	Cu	Mo	V
No.1	3.45	16	0.5	0.5	-	-	-	-
No.2	3.45	16	0.5	0.5	1.0	-	-	-
No.3	3.45	16	0.5	0.5	2.0	-	-	-
No.4	3.45	16	0.5	0.5	-	1.0	-	-
No.5	3.45	16	0.5	0.5	-	2.0	-	-
No.6	3.45	16	0.5	0.5	-	-	1.0	-
No.7	3.45	16	0.5	0.5	-	-	2.0	-
No.8	3.45	16	0.5	0.5	-	-	3.0	-
No.9	3.45	16	0.5	0.5	-	-	-	1.0
No.10	3.45	16	0.5	0.5	-	-	-	2.0
No.11	3.45	16	0.5	0.5	-	-	-	3.0
No.12	3.0	26	0.5	0.5	-	-	-	-
No.13	3.0	26	0.5	0.5	1.0	-	-	-
No.14	3.0	26	0.5	0.5	2.0	-	-	-
No.15	3.0	26	0.5	0.5	-	1.0	-	-
No.16	3.0	26	0.5	0.5	-	2.0	-	-
No.17	3.0	26	0.5	0.5	-	-	1.0	-
No.18	3.0	26	0.5	0.5	-	-	2.0	-
No.19	3.0	26	0.5	0.5	-	-	3.0	-
No.20	3.0	26	0.5	0.5	-	-	-	1.0
No.21	3.0	26	0.5	0.5	-	-	-	2.0
No.22	3.0	26	0.5	0.5	-	-	-	3.0

Table 3.4 Aim chemical composition of hypo-eutectic cast irons with alloying elements.

Number	Element (mass%)							
	C	Cr	Si	Mn	Ni	Cu	Mo	V
No.1	3.0	16	0.5	0.5	-	-	-	
No.2	3.0	16	0.5	0.5	1.0	-	-	-
No.3	3.0	16	0.5	0.5	2.0	-	-	-
No.4	3.0	16	0.5	0.5	-	1.0	-	-
No.5	3.0	16	0.5	0.5	-	2.0	-	-
No.6	3.0	16	0.5	0.5	-	-	1.0	-
No.7	3.0	16	0.5	0.5	-	-	2.0	-
No.8	3.0	16	0.5	0.5	-	-	3.0	-
No.9	3.0	16	0.5	0.5	-	-	-	1.0
No.10	3.0	16	0.5	0.5	-	-	-	2.0
No.11	3.0	16	0.5	0.5	-	-	-	3.0
No.12	2.65	26	0.5	0.5	-	-	-	-
No.13	2.65	26	0.5	0.5	1.0	-	-	-
No.14	2.65	26	0.5	0.5	2.0	-	-	-
No.15	2.65	26	0.5	0.5	-	1.0	-	-
No.16	2.65	26	0.5	0.5	-	2.0	-	-
No.17	2.65	26	0.5	0.5	-	-	1.0	-
No.18	2.65	26	0.5	0.5	-	-	2.0	-
No.19	2.65	26	0.5	0.5	-	-	3.0	-
No.20	2.65	26	0.5	0.5	-	-	-	1.0
No.21	2.65	26	0.5	0.5	-	-	-	2.0
No.22	2.65	26	0.5	0.5	-	-	-	3.0

3.2.1 Annealing

In order to remove the micro-segregation produced during solidification, the specimen was coated with an anti-oxidation liniment to prevent the decarburization. Specimens were cold-charged in an electric furnace and heated up by a heating rate of 0.1 K/s. At 1173 K (900 ˚C), the specimens were held for 10.8 ks (3 hours) and cooled in the furnace (FC) down to the room temperature.

3.2.2 Hardening

Two austenitizing temperatures were adopted for hardening. Specimens homogenized by annealing were heated up at 1273 K (1000 ˚C) and 1323 K (1050 ˚C) for austenitization. After holding for 5.4 ks (1.5 hours) at the austenitizing temperatures, the specimens were hardened by force air cooling (FAC).

3.2.3 Tempering

The hardened specimens were arranged on the alumina boat and held in the electric furnace at several temperatures from 573 K to 873 K for 7.2 ks (2 hours). The tempering temperatures were changed at an interval of 50 K. After the tempering finished, they were cooled to the room temperature in the still air (AC).

3.3 Observation of Microstructure

3.3.1 Optical microscopy

To observe the microstructure of specimen by means of an optical microscope (OM), test piece was polished using emery papers in the order of #180, 320, 400 and 600 and finished by a buff cloth with extremely fine alumina powder of 0.3 μm in diameter. The microstructure was revealed using the etchants shown in Table 3.6.

Table 3.5   Heat treatment conditions

Heat Treatment Process	Annealing	Hardening	Tempering
Temperature (K)	1173	1273 1323	573 623 673 723 773 823 873
Holding Time (ks)	10.8	5.4	7.2
Cooling Conditon	FC	FAC	AC
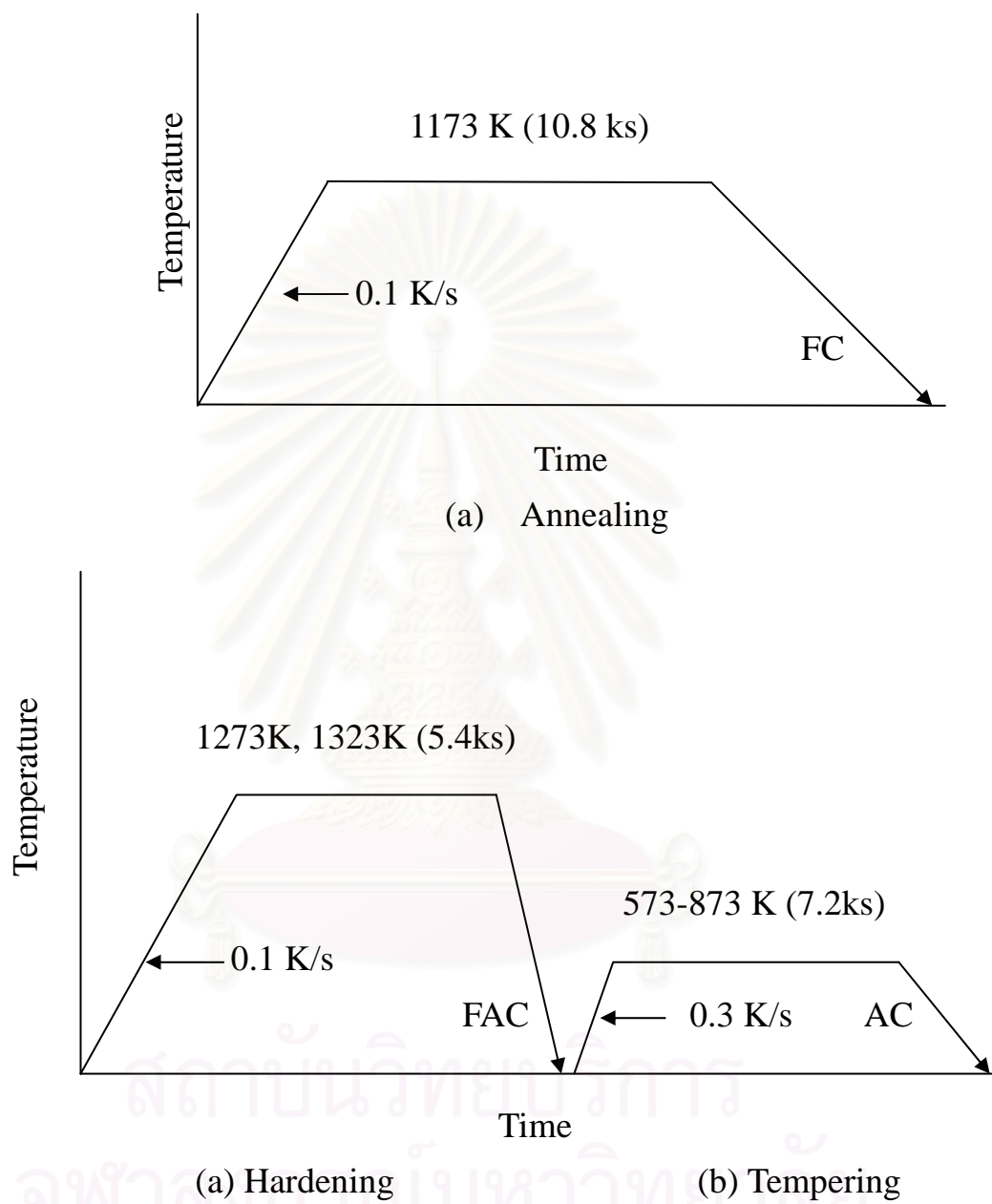
Fig. 3.2   Heat treatment cycles for annealing, hardening and tempering.

Table 3.6 List of etchants.

Type	Etchant	Etching method	Attack
A	Picric acid 1 g HCl 5 cc Ethanol 100 cc	Immersion at room temperature	Carbide and matrix
B	Nital reagent HNO_3 5 cc Ethanol 95 cc	Immersion at room temperature	Matrix

3.3.2 Scanning electron microscopy

For more discussions, the microstructure involving secondarily precipitated carbides was observed in detail using a Scanning Electron Microscope (SEM) of Hitachi Model S2380 N. A polished specimen was lighly etched using the B etchant to reveal the microstructure. The microphotographs mainly focusing on carbide morphology in matrix were taken by high magnifications.

3.4 Hardness Measurement

Macro-hardness of specimen was measured by means of Vickers hardness tester (Akashi Model AVK) applying the load of 297 N (30 kgf). Five indentations were taken at random and the average value was adopted. On the other hand, micro-hardness of matrix was also measured five times by Micro-Vickers hardness tester (Akashi Model MVK-G1) applying the load of 1 N (100 gf) and the measured values were averaged.

3.5 Measurement of Volume Fraction of Austenite

3.5.1 Theory for measurement of austenite by X-ray diffraction method

Quantitative measurment of austenite in matrix is not so easy because the bulk test specimen with strong orientation of dendrite must be used. In the methods to measure the volume fraction of austenite, X-ray diffraction method is convenient when the texture is cancelled as if the powder sample is used.

The basic equation of diffraction intensity of a phase is expressed as

$$I_{hkl} = K(FF^*)(LPF)me^{-2M}A(\theta)V_i/v_i^2 \qquad (3.1)$$

where,

K = proportional constant

FF^* = structure factor of the unit cell of the interest phase, equal to $4f^2$ and $16f^2$ for diffraction lines of α(martensite/ferrite) and γ (austenite), respectively, where f is the atomic scattering factor obtained from atoms which make up the unit cell : f relates to $(\sin \theta)/\lambda$

LPF = Lorenz Polarization Factor, $(1+\cos^2 2\theta)/\sin^2\theta\cos\theta$

m = multiplicity factor, the number of {hkl} planes in a unit cell

e^{-2M} = Debye –Waller temperature factor where

M = $(B\sin^2\theta) / \lambda^2$: B is a material constant

$A(\theta)$ = absorption factor, independent of θ if sample is flat

V_i = volume fraction of the phase

and

v_i = volume of unit cell

Let,

$$K´ = K \times A(\theta) \qquad (3.2)$$

and

$$R_{hkl} = [FF^*(LPF)me^{-2M}]/v_i^2 \qquad (3.3)$$

Here, Debye-Waller temperature factor is negligible. By substitutes K´

and R_{hkl} for the equation (3.1), the equation (3.4) is obtained.

$$I_{hkl} = K'R_{hkl}V_i \tag{3.4}$$

When several peaks in the diffraction pattern participate in the calculation, the above equation is expressed by the next equation (3.5),

$$\Sigma I_{hkl} = K'(\Sigma R_{hkl})(V_i) \tag{3.5}$$

Therefore, total intensity of ferrite and/or martensite (α) peaks and that of austenite (γ) peaks are respectively shown as follows,

$$\Sigma I_{\alpha} = K'(\Sigma R_{\alpha})(V_{\alpha}) \tag{3.6}$$

$$\Sigma I_{\gamma} = K'(\Sigma R_{\gamma})(V_{\gamma}) \tag{3.7}$$

Besides,

$$V_{\alpha} + V_{\gamma} + V_c = 1 \tag{3.8}$$

Where, V_c is the volume fraction of other phase.

Assuming that only α and γ phases exist in the specimen, the equation (3.8) is,

$$V_{\alpha} + V_{\gamma} = 1 \tag{3.9}$$

The relationship between V_{α} and V_{γ} from the equation (3.6) and (3.7) can be obtained by as the next equation (3.10).

$$V_{\alpha} = [\Sigma I_{\alpha} \cdot \Sigma R_{\gamma} / \Sigma I_{\gamma} \cdot \Sigma R_{\alpha}] \times V_{\gamma} \tag{3.10}$$

Solving the equation (3.9) and the equation (3.10) to obtain the volume fraction of austenite which relates to the diffraction peak intensity and R values, the following equation is finally given,

$$V_{\gamma} = 1 / [1 + (\alpha \Sigma I_{\alpha} \cdot \Sigma R_{\gamma} / \Sigma I_{\gamma} \cdot \Sigma R_{\alpha})] \tag{3.11}$$

For the determination of the amount of austenite, R values must be obtained by equation (3.3), and I_{α} and I_{γ} values by measuring the areas under the diffraction peaks of α and γ. Resultantly, the volume fraction of austenite ($V\gamma$) is attained numerically.

3.5.2 Equipment and measuring condition

The measurement of Vγ is carried out using X-ray diffraction method which was developed for steel by R.L. Miller and then for high chromium white iron by C. Kim. [24] The measuring condition is demonstrated in Table 3.7. In this experiment, the simultaneously rotating and swinging sample stage was employed to cancel the influence of preferred orientation or textural configulation of austenite in the cast iron. The sample stage is shown in Fig. 3.3. Fig. 3.4 shows the results of preliminary tests using this experimental specimen to prove the advantage for the use of this sample stage. It is edivident that the peaks of γ200 and γ311 are stronger in the case of rotating and swinging (a) than those in the both cases of only rotaing (b) and of without rotating and swinging (c). On the other hand, the peaks of α200 and α220 are weaker in the case of stage with rotaing and swinging. However, volume fraction of retained austenite calculated from the diffraction pattern measured using the rotating and swinging sample stage is much higher than the other cases. It is clear that the rotaing and swinging could cancle the preferred orientation or texture of austenite. This sample stage has been used in this research.

The test piece for X-ray diffraction was prepared by grinding the surface and followed by polishing it in the same way as the specimen for microphotography was prepared. Mo-Kα characteristic line with a wavelength of 0.007 nm (0.711 A°) filtered by Zr was used as a source of X-ray beam.
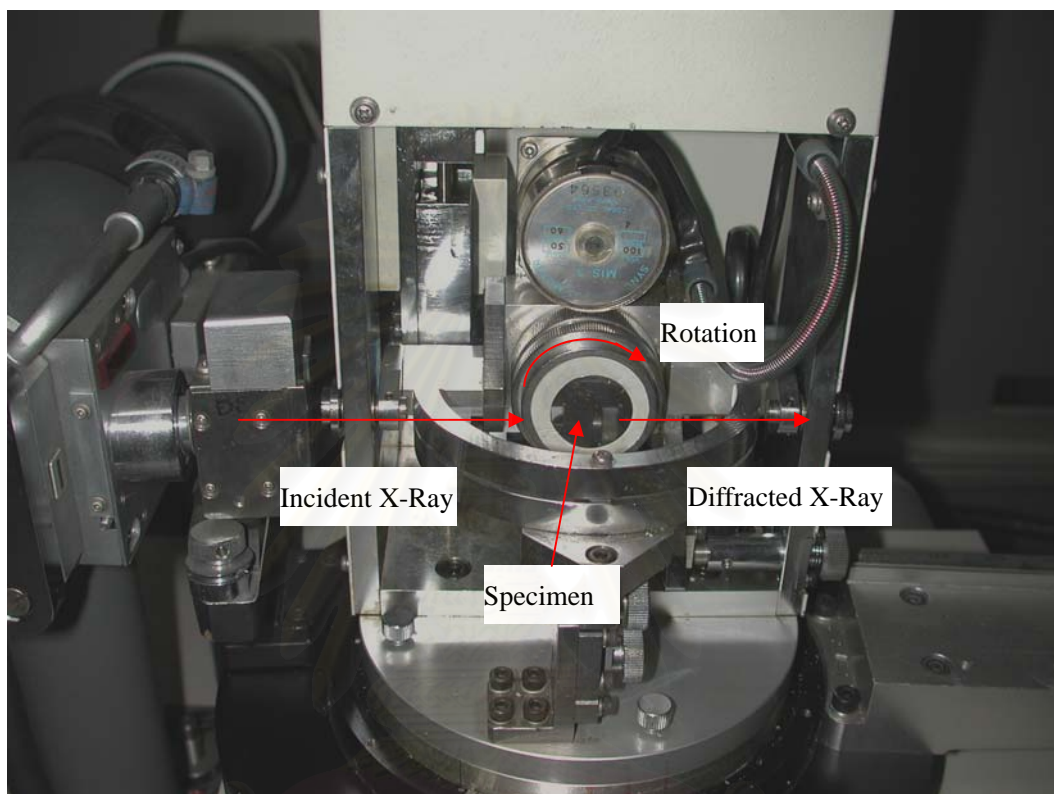
Fig. 3.3   Photograph of special sample stage for retained austenite
            measurement by X-ray diffraction.
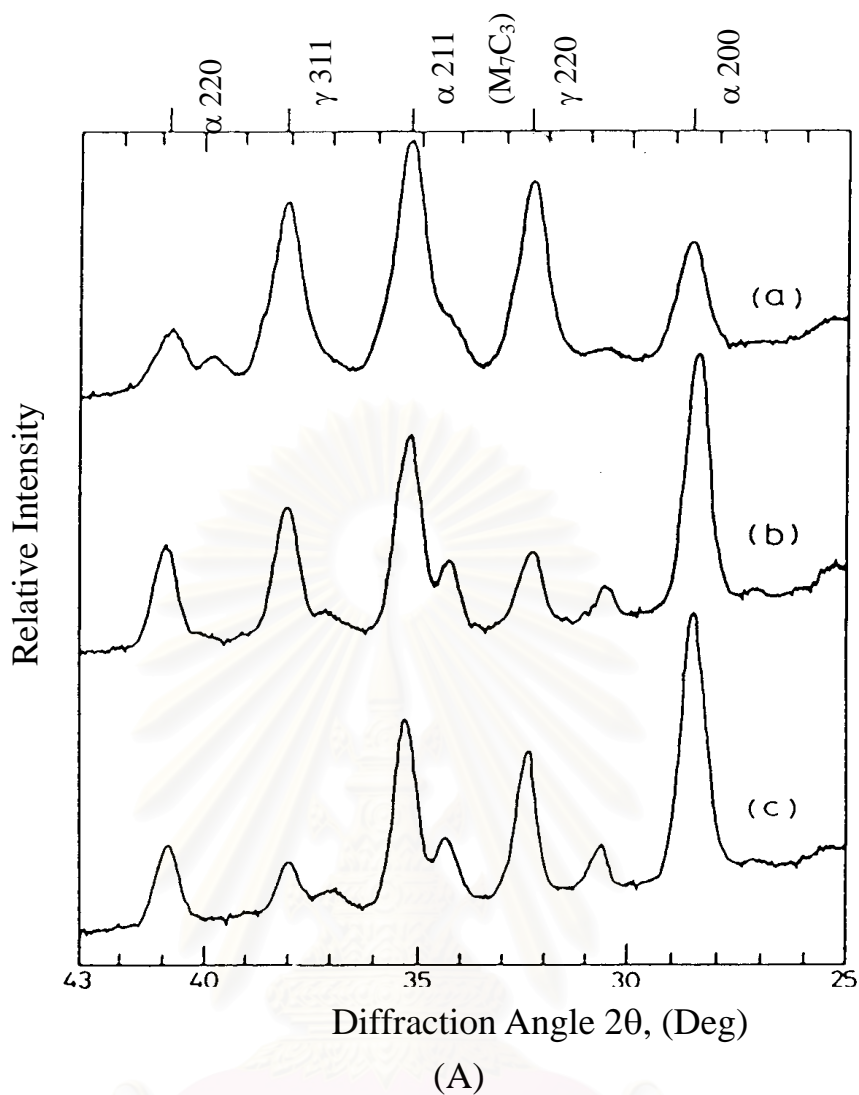
Fig.3.4   Effect of sample stage condition on diffraction pattern(A),
and volume fraction of retained austenite(Vγ) (B) calculated
from the profiles in (A).

Table 3.7 Condition of X-ray diffraction to measurethe volume fraction of retained austenite.

Target metal	Mo
Tube Voltage · Current	50 kV · 30mA
Slits	Divergence Slit: 1˚ Receiving Slit: 1.5 mm Scattering Slit: 1˚
Filter	Zr
Scanning Range	24-44 deg
Scanning Speed	0.5 deg/min
Step/Sampling	0.01 deg

3.5.3 Calculation of volume fraction of austenite

In this investigation, the diffraction peaks from crystal planes availed for the calculation are (200), (220) of ferrite or/and martensite and (220), (331) of austenite because these four peaks are independent or not interfering from peaks of other phases like carbides. The diffraction patterns of three specimens with different $V\gamma$ are shown for comparison in Fig. 3.5. The reason why the α_{211} peak in these patterns is not taken into account is that this peak is overlapped with a strong peak of chromium carbide (M_7C_3). The integrated areas of these peaks were obtained using an image analyzer (Nireco Model Luzex IIIU). The calculation of $V\gamma$ was done by a computer for three combination of peaks, $\alpha_{200} - \gamma_{311}$, $\alpha_{200} - \Sigma\gamma(220,311)$ and $\Sigma\alpha(200,220) - \gamma_{311}$. The averages of values calculated from three combinations were used for plotting.

3.6 Abrasion Wear Test

A schematic drawing of an abrasion wear tester is illustrated in Fig. 3.6. Under the load of 10N(1kgf), the abrading wheel (44 mm in

diameter and 12 mm in thickness) on which 180 mesh SiC abrasive paper was stuck on the circumference was revolved intermittently while moving back and forth by 35 mm traveling stoke on the same area of the test piece in dry condition. The revolving speed of the abrading wheel was 0.345 mm/s and the worn area was 420 (12x35) mm^2. The abrasion wear loss of the test piece was measured using an electronic balance after one cycle test which takes 400 s, and the test was repeated up to eight times for one test piece.
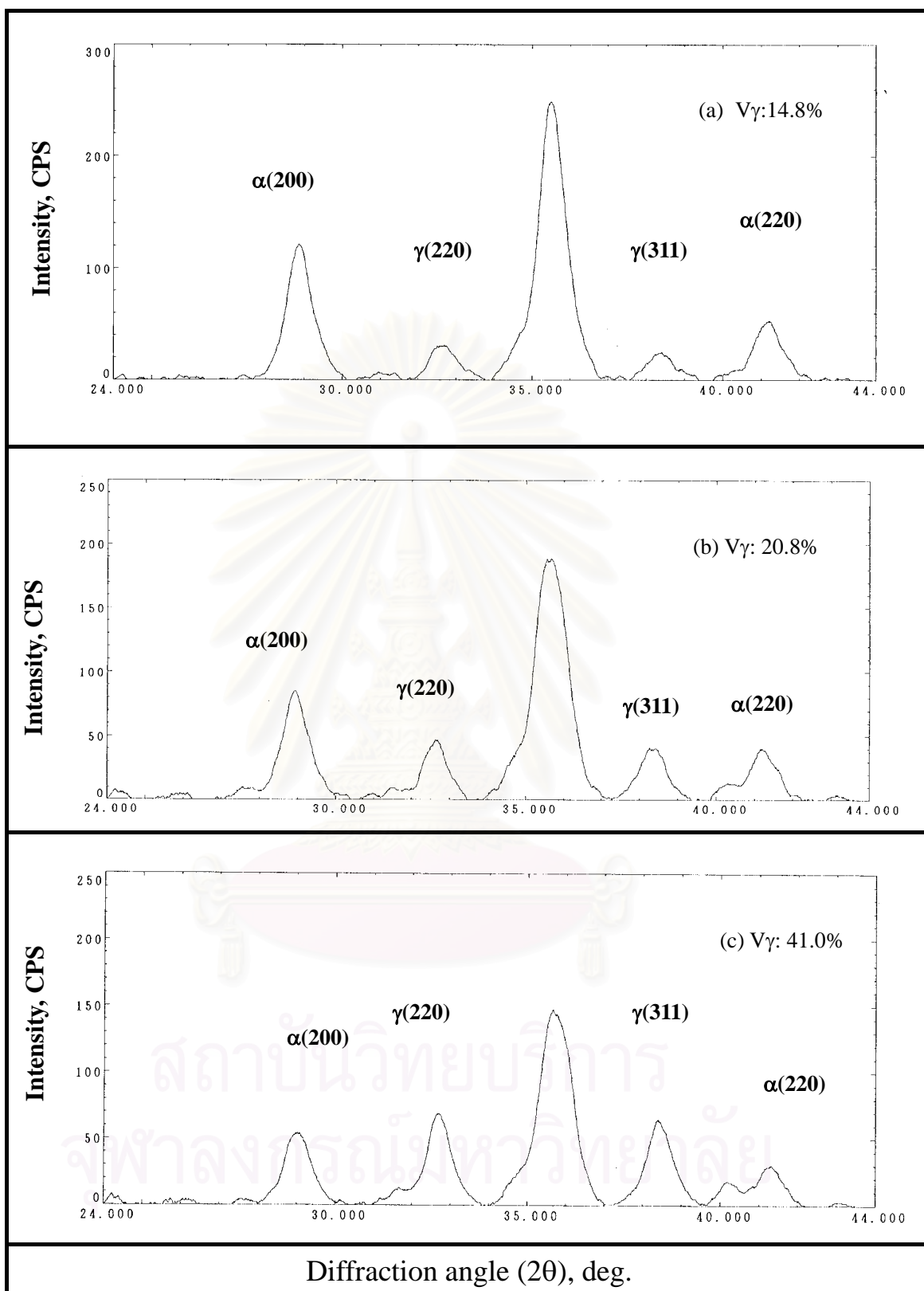
Fig 3.5 X-ray diffraction patterns of specimens with different volume fraction of retained austenite (Vγ): (a) 14.8%, (b) 20.8%, (c) 41.0%.
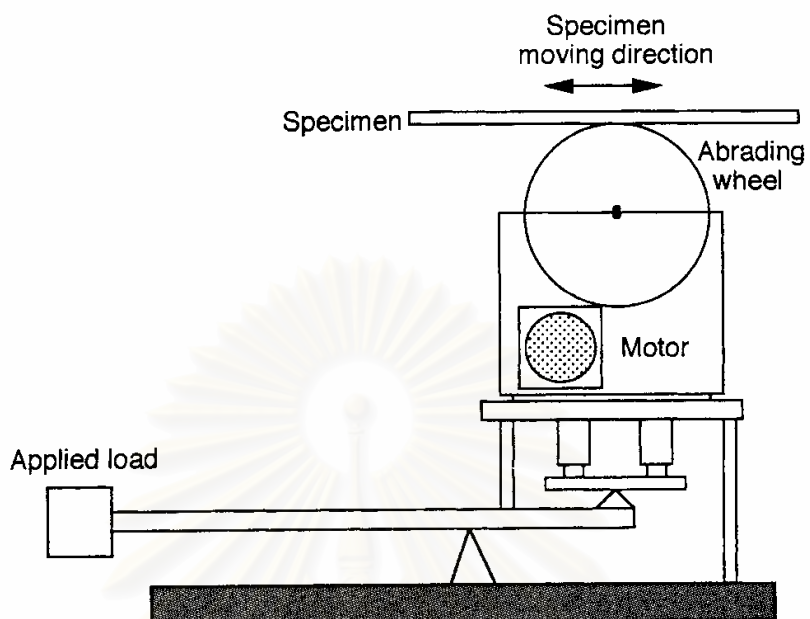
Fig. 3.6 Schematic drawing of abrasion wear testing machine.

CHAPTER IV

EXPERIMENTAL RESULTS

4.1 Heat Treatment Behavior of Plain High Chromium Cast Iron

4.1.1 Introduction

The eutectic and hypoeutectic cast irons with chromium content varied from 10% to 26% are prepared, and general heat treatments of hardening after annealing and tempering were given to them. Particularly, the investigations are focused on the variation of hardness and the volume fraction of retained austenite ($V\gamma$) connected to the heat treatment conditions. Then, the relationship between heat treatment behavior and carbon and chromium contents are obtained in details.

4.1.2 Test specimens in as-cast state

Chemical compositions of the test specimens are shown in Table 4.1. In each chromium content, one eutectic and two hypoeutectic cast irons with different carbon level are produced, and their positions are displayed on R.S. Jackson's Fe-Cr-C liquidus surface diagram as shown in Fig. 4.1. The specimens with eutectic composition, No. 1, No.4, No.7 and No.10, are located very close to the ($\gamma+M_7C_3$) eutectic line. The other hypoeutectic specimens are away from the eutectic line.

As-cast microstructures of the test specimens are shown in Fig. 4.2 for 10% Cr and 16% Cr cast irons and Fig. 4.3 for 20% Cr and 26% Cr cast irons, respectively. The microstructures of specimen No. 1, No.4, No.7 and No.10 show mostly eutectic structure consisting of matrix and eutectic carbides, and those of hypoeutectic specimens consist of primary dendrite and ($\gamma+M_7C_3$) eutectic. The morphologies of eutectic structure in eutectic and hypoeutectic specimens are similar. At the same chromium level, it is found that the amount of eutectic carbide decreases with a

Table 4.1 Chemical compositions and Cr/C values of test specimens.

Specimen	Element (mass%)				Cr/C
	C	Cr	Si	Mn	
No.1 (Eut)	3.68	9.70	0.56	0.60	2.64
No.2 (Hypo)	3.12	9.90	0.53	0.58	3.17
No.3 (Hypo)	2.94	10.42	0.54	0.62	3.54
No.4 (Eut)	3.45	16.01	0.39	0.67	4.64
No.5 (Hypo)	3.01	16.48	0.62	0.78	5.48
No.6 (Hypo)	2.62	15.93	0.41	0.69	6.08
No.7 (Eut)	3.28	19.88	0.56	0.56	6.06
No.8 (Hypo)	2.90	20.12	0.60	0.53	6.94
No.9 (Hypo)	2.57	20.34	0.48	0.50	7.91
No.10 (Eut)	2.99	26.78	0.51	0.54	8.96
No.11(Hypo)	2.65	25.56	0.37	0.51	9.65
No.12(Hypo)	2.32	25.53	0.37	0.54	11.00

*S and P are less than 0.06 mass%
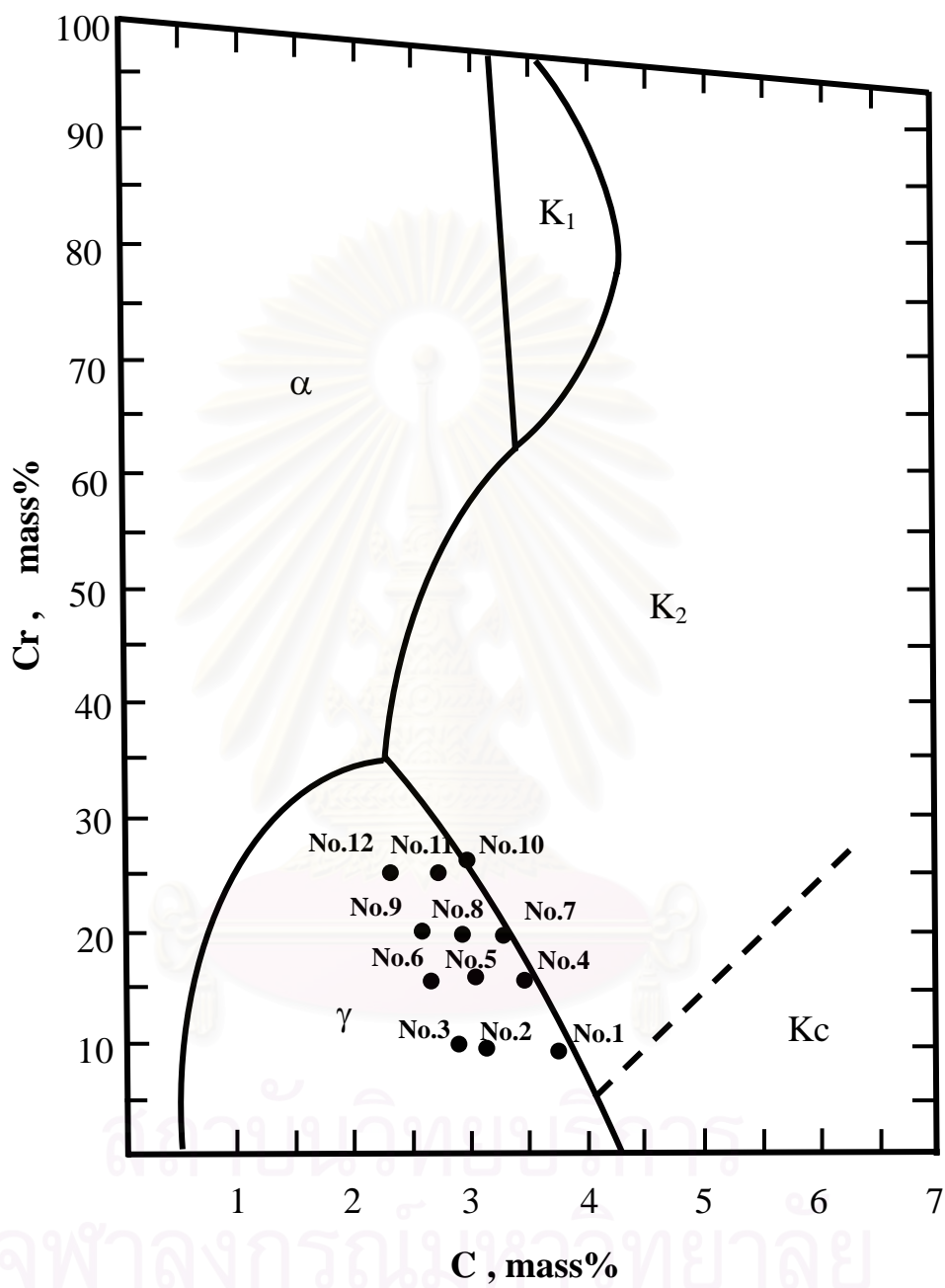
Fig. 4.1 The liquidus surface diagram of Fe-Cr-C system[34]. (Kc = M_3C, $K_2 = M_7C_3$, $K_1 = M_{23}C_6$)

10% Cr	16% Cr
No. 1 : 3.68 %C	No. 4 : 3.45 %C
No. 2 : 3.12 %C	No. 5 : 3.01 %C
No. 3 : 2.94 %C	No. 6 : 2.62 %C
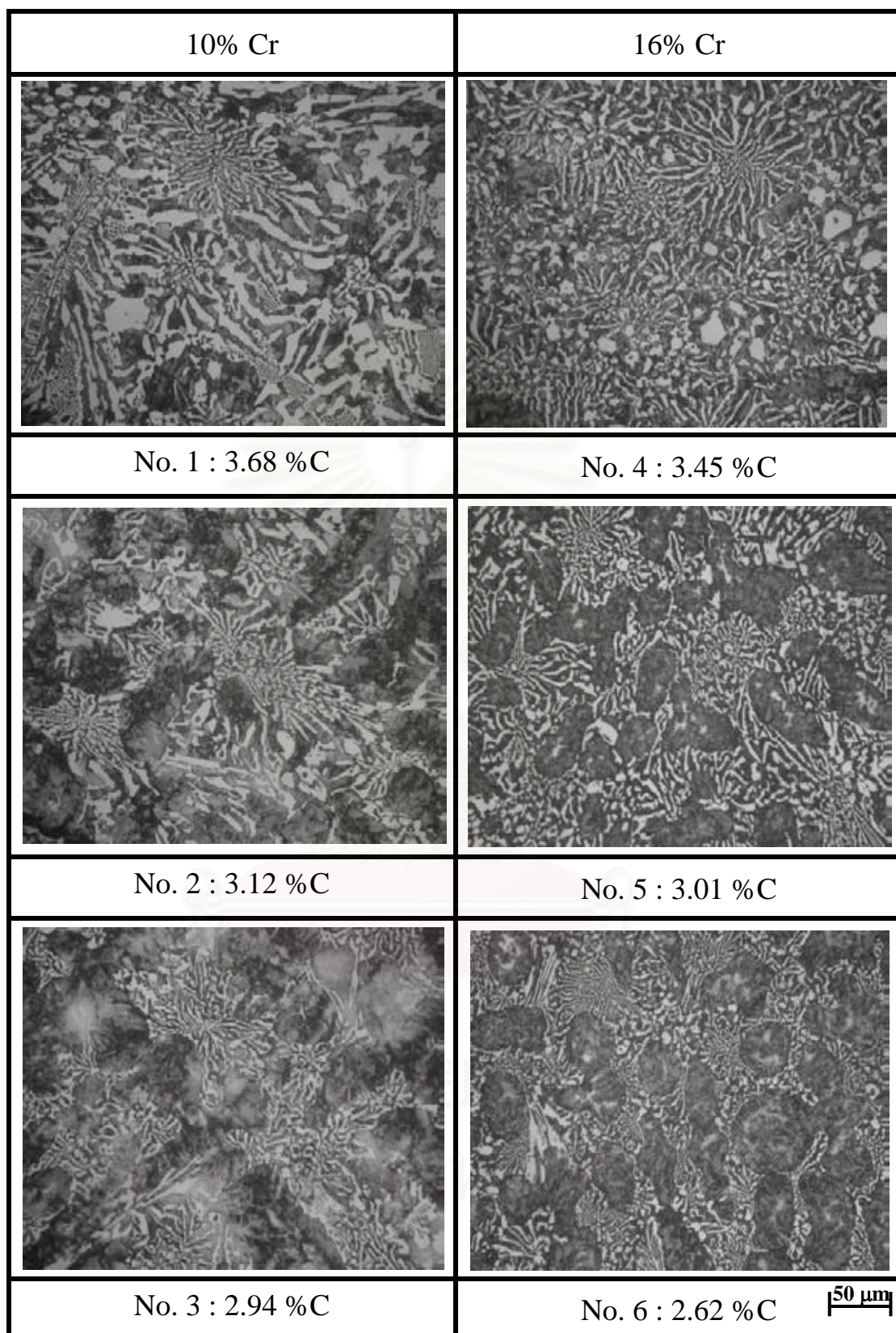
Fig. 4.2 As-cast microstructures of 10% Cr and 16%Cr cast irons. Microstructure consists of (γ+M_7C_3) eutectic and pearlitic matrix. M_3C carbides appear in ledeburite morphology in 10% Cr cast irons.

20% Cr	26% Cr
No. 7 : 3.28 %C	No. 10 : 2.99 %C
No. 8 : 2.90 %C	No. 11 : 2.65 %C
No. 9: 2.57 %C	No. 12: 2.32 %C
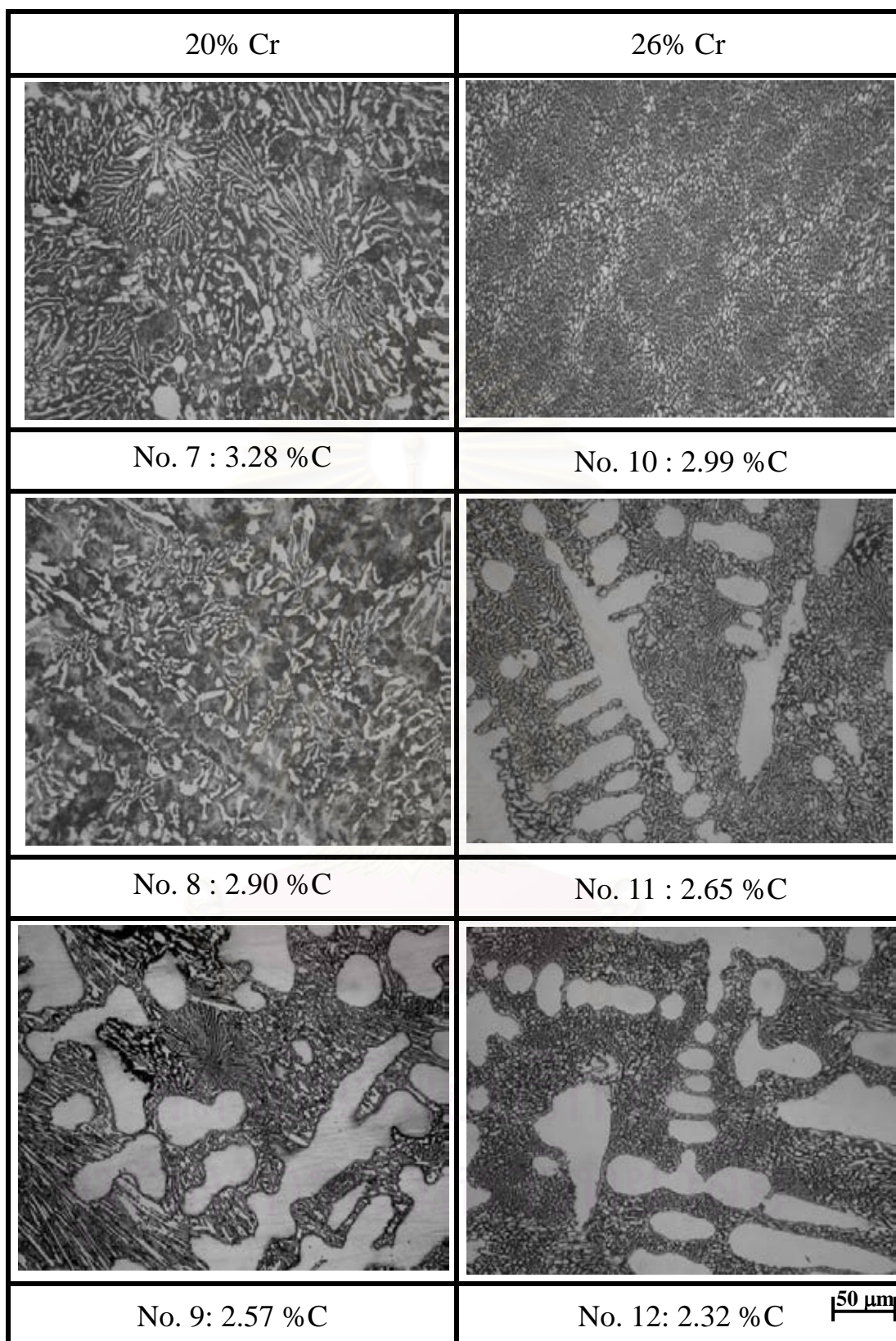
Fig. 4.3 As-cast microstructures of 20% Cr and 26% Cr cast irons. The (γ+M$_7$C$_3$) eutectic structures coexist with pearlitic matrix in 20% Cr with high C content and with austenitic matrix in 20% Cr cast iron with low C content and in all of 26% Cr cast irons.

decrease in carbon content. In the microstructures of 10% Cr specimen, most of M_7C_3 carbides are coexisting with some M_3C carbides in ledeburitic morphology. The M_7C_3 carbides are solely seen in the specimens with chromium content more than 16%. The eutectic structure of 26% Cr specimen is very fine. According to a paper by Matsubara et al.[2], the eutectic carbides are mostly M_7C_3 type and $M_{23}C_6$ carbides do not precipitate in the cast irons with chromium content between 15% and 30%. As for the morphology of eutectic structure, it shows a colony shape because ($\gamma+M_7C_3$) eutectic grows with a cellular interface having fine rod-like M_7C_3 carbides in the central region and coarse string-like M_7C_3 carbides growing to the colony boundary.[7] The colony size is affected by chromium content in the cast iron. It can be said that the size of colony is largest in 10% Cr cast iron and becomes small with an increase in chromium content. It is well known that the eutectic carbides are three-dimensionally interconnected.[12] With respect to the size of chromium carbides themselves, the carbide particles are especially very fine in the 26% Cr cast iron. The 20% Cr specimens show the intermediate microstructures between 16% Cr and 26% Cr cast irons.

When the cooling rate is similar, matrix structure is determined by the kind and amount of elements dissolved in austenite during solidification. The matrices of 10%, 16% and 20% Cr specimens are mostly pearlitic except for 20% Cr specimen with 2.57% C (No. 9) in which austenitic primary phase and eutectic matrix transformed into pearlite coexist. From the microstructures of 20% Cr specimen in Fig. 4.3, it is said that the transformation of matrix into pearlite is carried out by decreasing carbon content. In 26% Cr specimen, the matrix structures consist of austenite and possibly some martensite. However, the difference in the matrix structure due to the difference in carbon content can not be distinguished from the microphotographs.

In order to confirm the results mentioned above, macro-hardness and volume fraction of retained austenite ($V\gamma$) in as-cast state are measured and digital data are listed in Table 4.2. It is found that the

macro-hardness does not vary by Cr content. At the same chromium level, the hardness seems to decrease as the C content decreases and it ranges from 520 – 580 HV30. This is due to a decrease in the amount of eutectic carbide when the matrix structure is similar. The Vγ values of 10% Cr, 16% Cr and 20% Cr specimens are zero except for 20% Cr specimen with 2.57% C (No.9) which is 63% Vγ. It means that most of austenite in the specimens transformed to pearlite during cooling in the sand mold. In the case of 26% Cr specimens, the Vγ is clearly related to the carbon content of the cast iron. The Vγ increases abruptly from 34% to 71% as the C content decreases from 2.99% to 2.32%. These results agree with the microphotographs in Fig. 4.2 and Fig. 4.3. However, the large different in Vγ of 26% Cr specimen can not be judged from their microphotographs.

Anyway, the various matrix structures in as-cast state are changed by the following heat treatments for the improvement of wear resistance and mechanical properties.

4.1.3 Variation of macro-hardness and volume fraction of retained austenite (Vγ) during heat treatment

- As-hardened state

The macro-hardness in as-hardened state is determined depending on type and quantity of eutectic carbide and matrix structure. In particular, the matrix hardness is greatly influenced by the Vγ, the more the Vγ, the lower the macro-hardness. After annealing, the specimens were austenitized at 1273 K and 1323 K for 5.4 Ks and then cooled rapidly to the room temperature by fan air cooling. The macro-hardness and Vγ are shown in Table 4.3. The effect of carbon and chromium on the macro-hardness and Vγ are shown in Fig. 4.4 for 10% Cr, Fig. 4.5 for 16% Cr, Fig. 4.6 for 20% Cr and Fig. 4.7 for 26% Cr specimens, respectively. In all specimens, the hardness changes within 50 HV30 according to carbon content. At the same carbon content, the hardness seems to be a little higher in the case of higher austenitization.

Table 4.2 Hardness and volume fraction of retained austenite (Vγ) in as-cast specimens.

Specimen	%C	%Cr	Hardness (HV30)	Vγ (%)	Cr/C
No.1 (Eut)	3.68	9.70	580	0	2.64
No.2 (Hypo)	3.12	9.90	549	0	3.17
No.3 (Hypo)	2.94	10.42	542	0	3.54
No.4 (Eut)	3.45	16.01	578	0	4.64
No.5 (Hypo)	3.01	16.48	572	0	5.48
No.6 (Hypo)	2.62	15.93	554	0	6.08
No.7 (Eut)	3.28	19.88	568	0	6.06
No.8 (Hypo)	2.90	20.12	569	0	6.94
No.9 (Hypo)	2.57	20.34	546	63.2	7.91
No.10 (Eut)	2.99	26.78	584	33.7	8.96
No.11 (Hypo)	2.65	25.56	561	67.8	9.65
No.12 (Hypo)	2.32	25.53	520	71.3	11.00

Table 4.3 Macro-hardness and volume fraction of retained austenite
(Vγ) of as-hardened specimens.

Specimen			Austenitizing temperature			
			1273 K		1323 K	
No.	%C	%Cr	Hardness (HV30)	Vγ (%)	Hardness (HV30)	Vγ (%)
No.1 (Eut)	3.68	9.70	773	4.2	798	26.4
No.2 (Hypo)	3.12	9.90	746	20.8	757	24.4
No.3 (Hypo)	2.94	10.42	740	26.0	751	42.0
No.4 (Eut)	3.45	16.01	763	28.8	740	41.0
No.5 (Hypo)	3.01	16.48	775	18.1	730	31.8
No.6 (Hypo)	2.62	15.93	780	18.8	775	27.5
No.7 (Eut)	3.28	19.88	798	14.2	792	33.5
No.8 (Hypo)	2.90	20.12	792	8.4	792	21.7
No.9 (Hypo)	2.57	20.34	769	7.3	792	19.2
No.10 (Eut)	2.99	26.78	740	3.8	780	12.1
No.11 (Hypo)	2.65	25.56	743	4.1	757	11.8
No.12 (Hypo)	2.32	25.53	749	3.2	760	11.2

The hardness of 10% Cr specimen increases ranging from 740 HV30 to 725 HV30 in 1273 K and 750 HV30 to 790 HV30 in 1323 K austenitization as the carbon content increases. However, the hardness is not influenced so much by the austenitizing temperature. In the case of 16% Cr specimen, the hardness decreases gradually with increasing carbon content and it ranges from 780 HV30 to 765 HV30 in 1273 K austenitization. In the case of 1323 K austenitization, the hardness decreases first and then increases a little with an increase in C content, resulting within 775 HV30 to 730 HV30. An increase in austenitizing temperature lowers the hardness. In 20% Cr specimen, the hardness increases from 769 HV30 to 798 HV30 in 1273 K austenitization and it is almost the same value of around 790 HV30 in 1323 K austneitization even though the C content is changed. In the 26% Cr specimen, the hardness in high austenitization is overall a little higher and it increases from 760 HV30 to 780 HV30, but the hardness in 1273 K austenitization decreases slightly from 750 HV30 to 740 HV30 in 1323 K austenitization.

With respect to the effect of Cr content on the hardness illustrated in Fig. 4.8 (a), the clear relationship between the hardness and Cr content can not be seen but the hardness of 20% Cr specimens are found to show the highest value in both austenitizing temperatures.

As for the Vγ, it varies depending on C content and austenitizing temperatures. In 1273 K austenitization, the Vγ of 10% Cr specimen decreases gradually with increasing C content, ranging from 26% to 4%. In 1323 K austenitization, the Vγ decreases abruptly from 42% to 24% and after that it changes a little as carbon content rises. The Vγ values in 16% Cr and 20% Cr specimens increase with increasing C content. It ranges from 19% to 29% in 16% Cr specimens and 7% to 14% in 20% Cr specimens in 1273 K austenitization and 28% to 41% in 16% Cr, 19% to 34% in 20% Cr specimens in 1323 K austenitization, respectively. The Vγ of 26% Cr specimens does not change by C content, around 4% in 1273 K and 12% in 1323 K austenitization.

The effect of Cr content on the Vγ is displayed in Fig. 4.8 (b). It is found that the Vγ is overall more in the specimen hardened from high austenitizing temperature of 1323 K. In eutectic specimen, the Vγ increases up to 16% Cr and then decreases gradually as the Cr content increases, and the highest Vγ values obtained in 16% Cr specimen are 28% in 1273 K and 41% in 1323 K austenitization. On the other hand, the Vγ decreases uniformly in the hypoeutectic specimens, from 28.8% to 3.8% in 1273 K and 41% to 12.1% in 1323 K austenitization, as the Cr content rises.

Comparing the hardness and Vγ by the austenitizing temperature, the hardness do not show affixed temperature dependence when the austenitizing temperature is increased. However, the Vγ is overall much higher in the case of 1323 K austenitization. This is because more carbon and chromium dissolve in austenite at higher austenitizing temperature and they stabilize the austenite more.

When these results are compared with those of as-cast specimens, remarkable difference is observed in the behavior of Vγ. The Vγ values are almost zero in as-cast 10%, 16% and 20% Cr specimens, whereas those in as-hardened specimens are high. This reason is due to a great difference in the cooling rate between as-cast and hardening conditions. In 26% Cr irons, on the other hand, the Vγ values in as-hardened specimens are very low in comparison with those in as-cast specimens. The reason could be that the carbon and chromium supersaturated in as-cast austenite form chromium carbides during austenitization and resultantly the C and Cr contents in austenite are reduced and hence Ms temperature rises over the room temperature. The decrease of Vγ due to the reasons mentioned above can be also explained from the fact that some martensite are observed in the matrix.

In order to comprehend the transformed matrix structure in detail, SEM microphotographs were taken at 2500 magnification focusing on matrix. Typical SEM photographs of each specimen hardened from 1323 K are shown in Fig 4.9 for 10% and 16% Cr specimens and in Fig. 4.10

for 20% and 26% Cr specimens. In 10 % Cr specimen, small amount of coarse carbides precipitate in the matrix in which some pearlite and a small amount of martensite could be existed, but they are not clear in this microphotograph. This may be because 10% Cr cast iron has poor hardenability in the velocity of forced air cooling and therefore, the $V\gamma$ is less. In the case of specimens containing 16% Cr, 20% Cr and 26% Cr, the matrix structure consists of comparably large amount of fine precipitated carbides, martensite and large amount of retained austenite. Large particles of carbides could already exist in the annealed state and grow up during austenitizing. G. Laird II [15] reported in his work that the secondary carbides precipitated in as-hardened state of high chromium cast iron are mostly M_7C_3 and $M_{23}C_6$ types.

In each chromium group specimens, the degree of carbide precipitation is more in the hypoeutectic specimens than in the eutectic specimens. The microphotographs in Fig. 4.9 show that austenite and/or pearlite existed in as-cast state is greatly reduced, and instead, more carbides are precipitated. This proves that the austenite were decomposed during austenitization. These secondary carbides seem to be more in the central region of primary austenite and less near the eutectic carbides. It may be explained by that the C and Cr content are low around eutectic carbides or that precipitated carbides diffuses to the massive eutectic carbides.
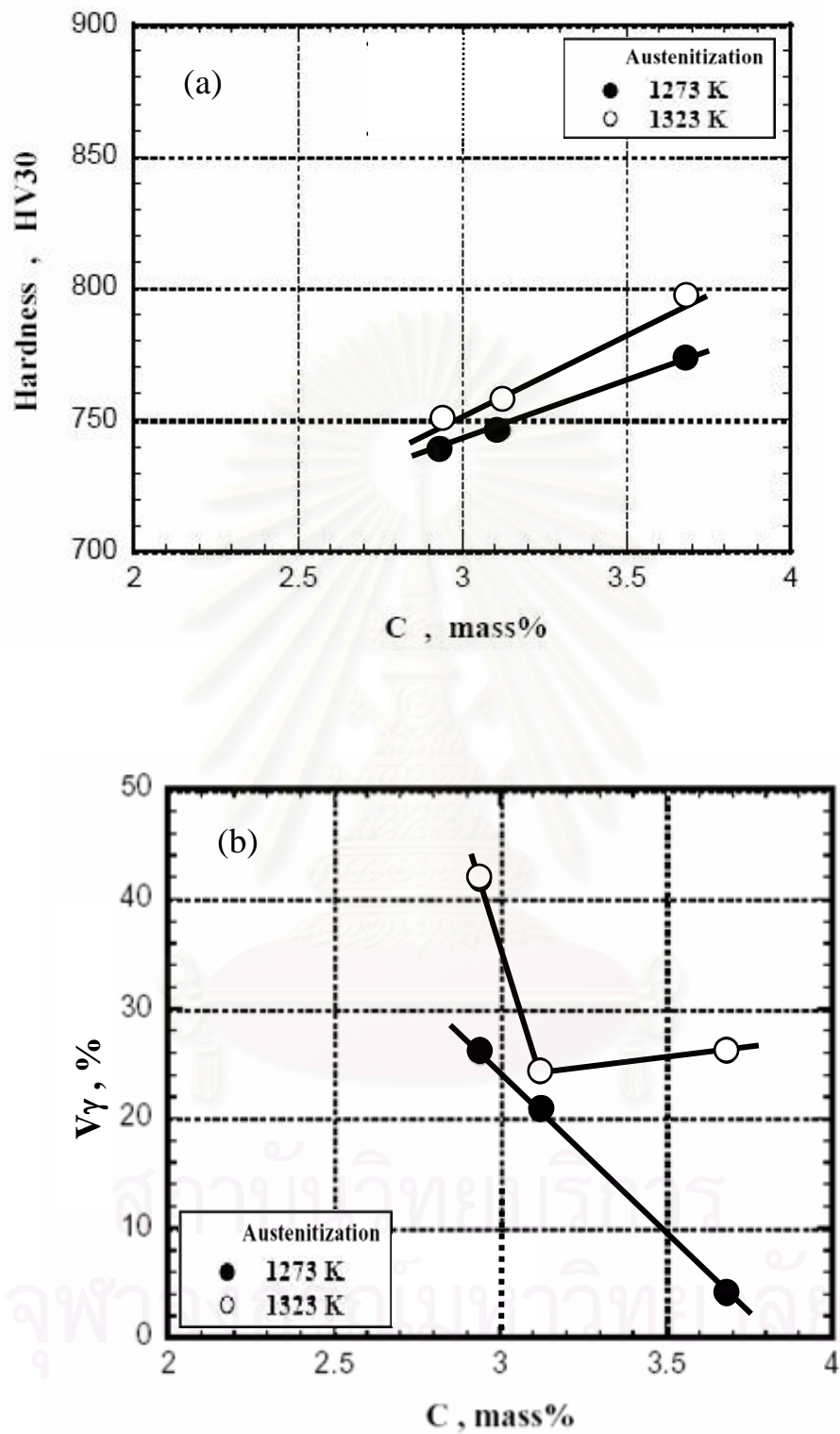
Fig. 4.4 Effect of C content on macro-hardness (a) and Vγ (b) of 10% Cr
specimens.
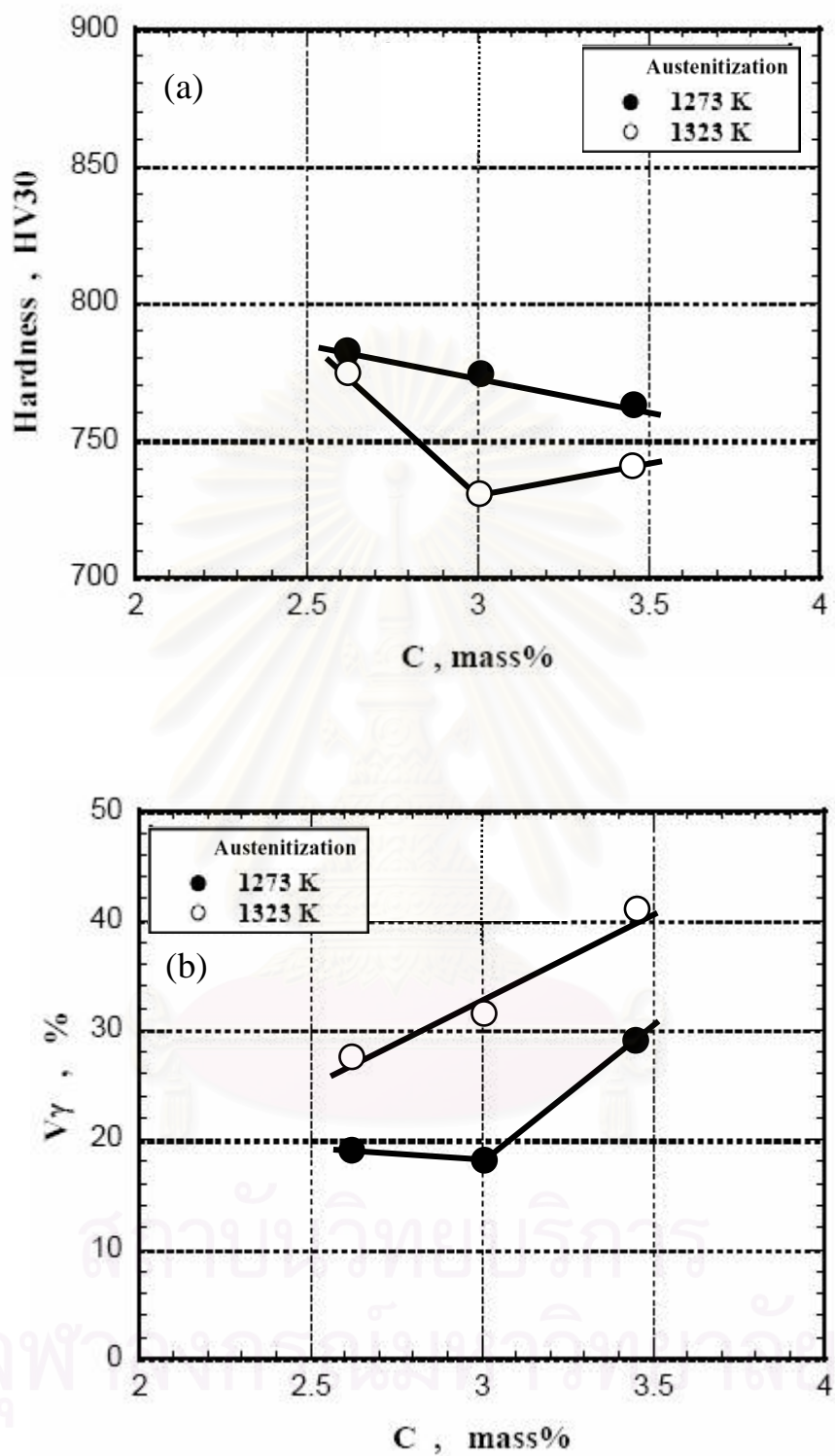
Fig.4.5 Effect of C content on macro-hardness (a) and Vγ (b) of 16% Cr specimens.
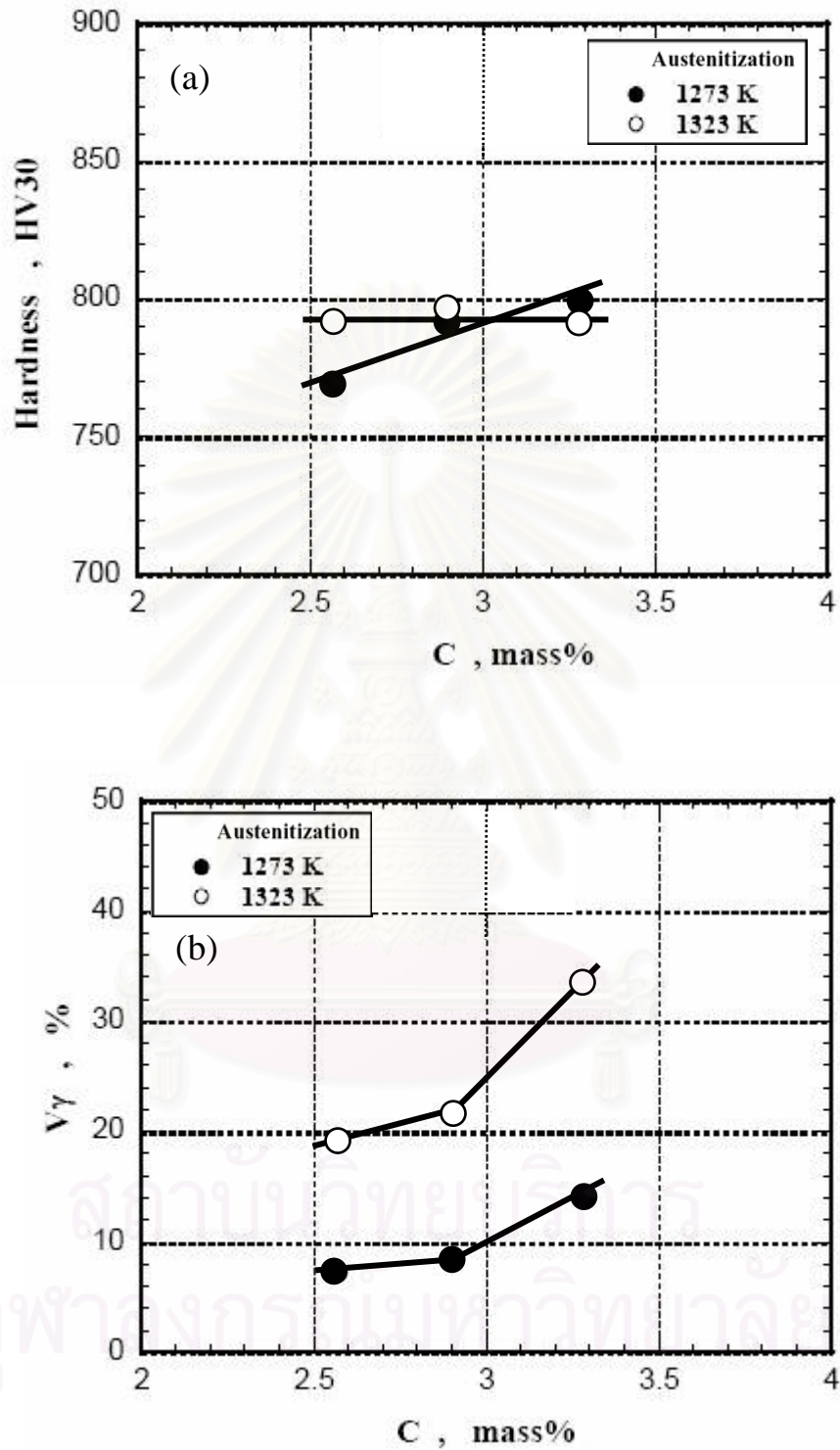
Fig. 4.6 Effect of C content on macro-hardness (a) and Vγ (b) of 20% Cr
specimens.
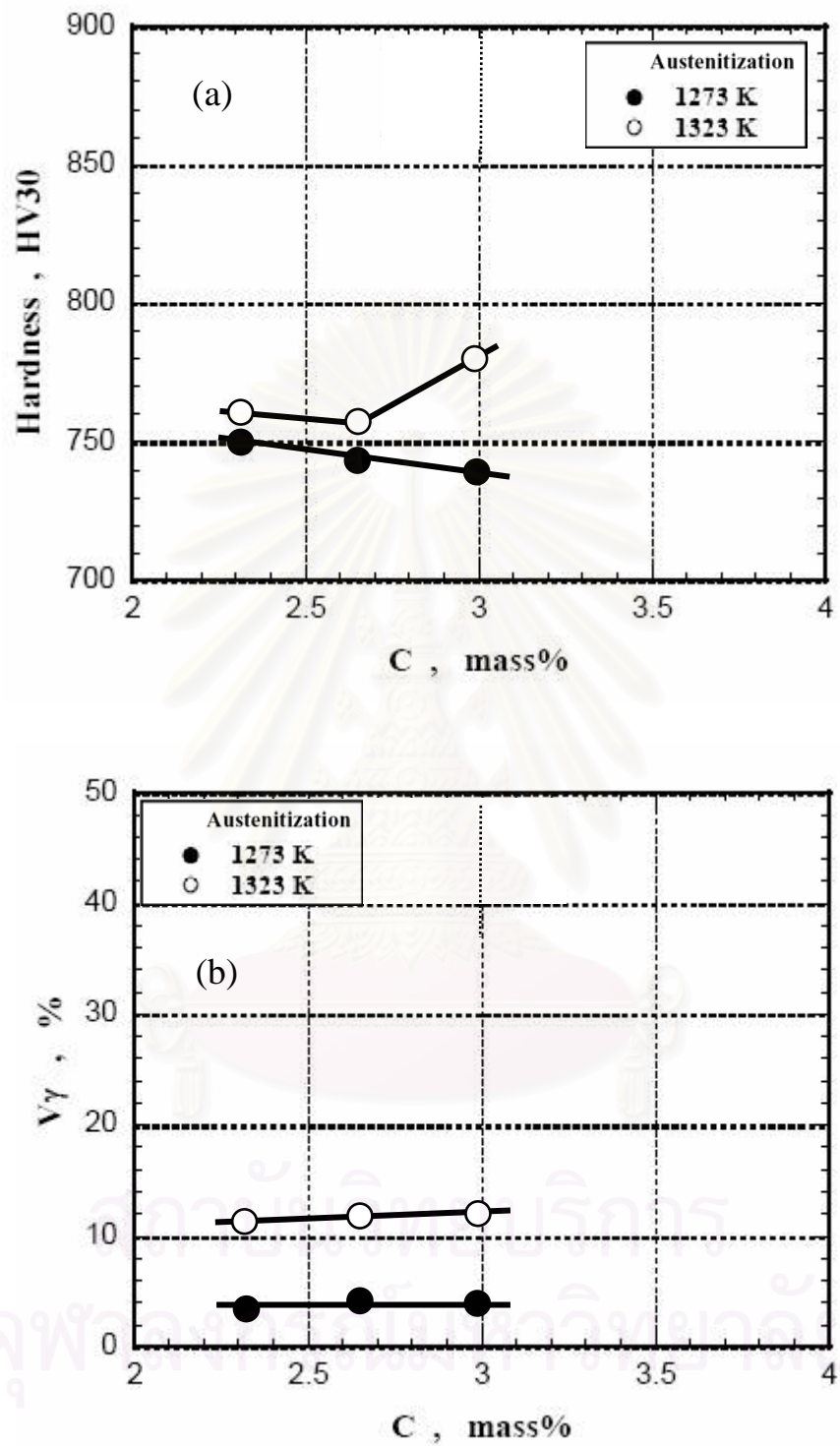
Fig.4.7 Effect of C content on macro-hardness (a) and Vγ (b) of 26% Cr
specimens.
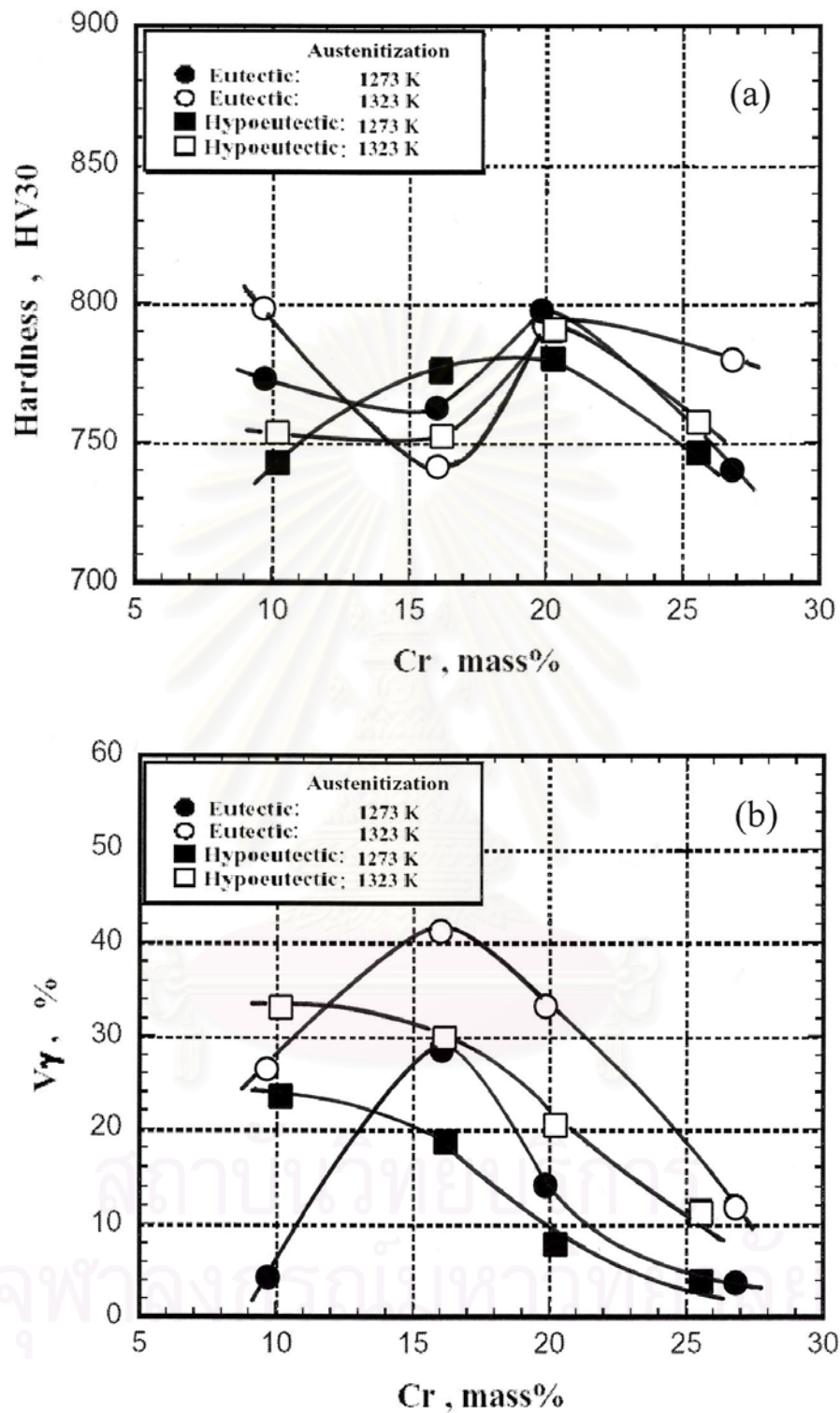
Fig.4.8 Effect of Cr content on macro-hardness (a) and Vγ (b) the test
specimens.

10% Cr	16% Cr
No. 1 : 3.68%C	No. 4 : 3.45%C
No. 2: 3.12%C	No. 5 : 3.01%C
No. 3: 2.94%C	No. 6 : 2.62%C

Fig. 4.9 SEM microphotographs of as-hardened 10% Cr and 16% Cr cast irons austenitized at 1323 K. Fine secondary carbides precipitate in matrices of martensite and retained austenite.

20% Cr	26% Cr
No. 7 : 3.28%C	No. 10 : 2.99%C
No. 8 : 2.90%C	No. 11 : 2.65%C
No. 9: 2.57%C	No. 12: 2.32%C
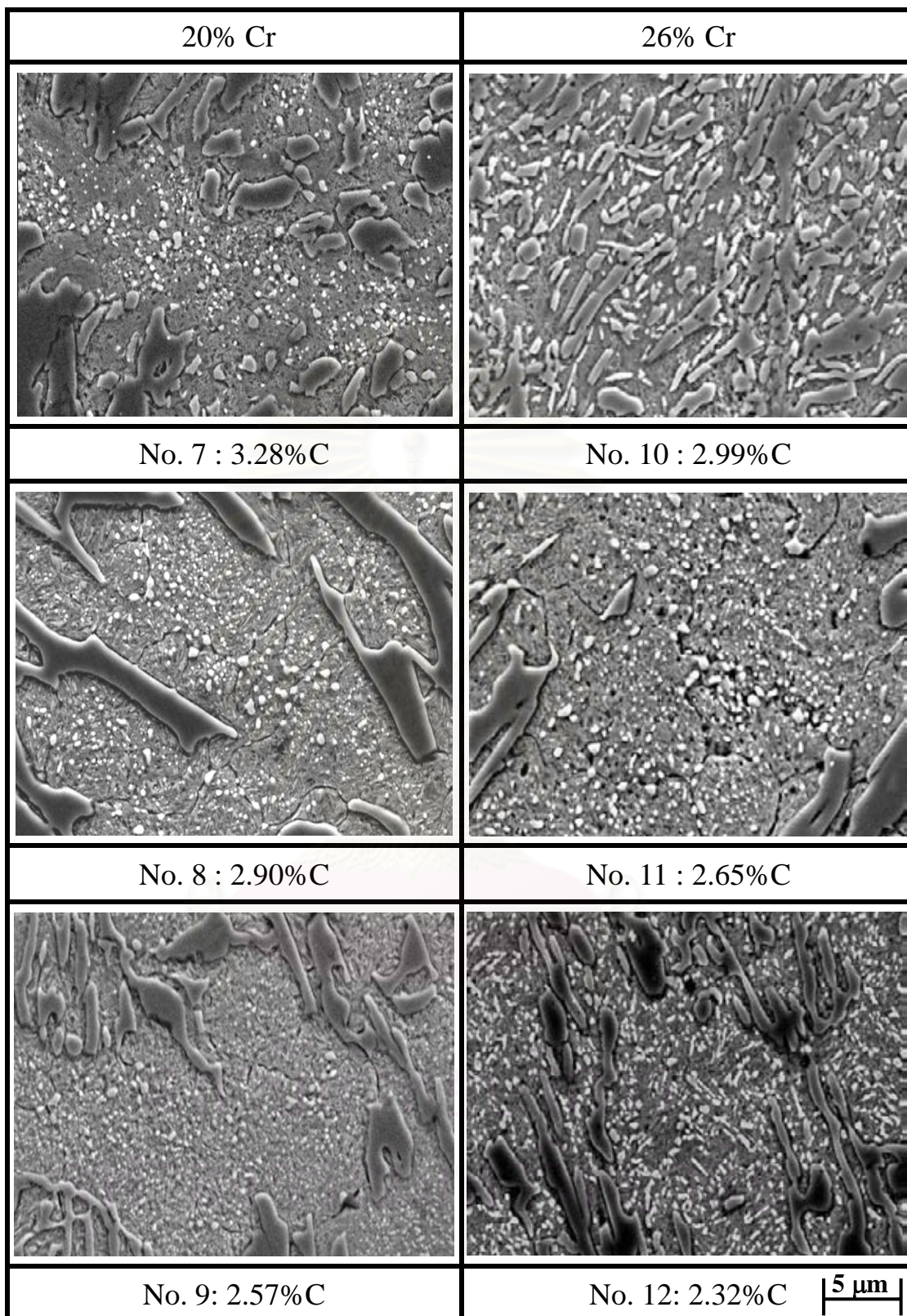
Fig. 4.10 SEM microphotographs of as-hardened 20% Cr and 26% Cr cast irons austenitized at 1323 K. Fine secondary carbides precipitate matrices of martensite and retained austenite more than those in 10% Cr and 26% Cr cast irons.

- Tempered state

Hardness and Vγ also change depending on the tempering condition. To clarify the relationship between the hardness, Vγ and tempering condition, the tempered hardness curve is usually made. The hardness in tempered state could be lower than that in as-hardened state because martensite is tempered and transformed to be carbide and ferrite. On the other hand, Vγ is reduced by its decomposition during tempering, and martensite transformation takes place in the rest of destabilized austenite during the cooling down after tempering. This behavior makes the hardness increase. Therefore, the macro-hardness measured is a sum of both the decrease in hardness of martensite and the increase in hardness due to the transformation of martensite from austenite remained in destabilized condition.

After the specimens were air-hardened from two levels of austenitizing temperatures, 1273 K and 1323 K, they were tempered at several temperatures between 573 K and 873 K. Relationships between macro-hardness, Vγ and tempering temperature are shown in Fig.4.11 to Fig.4.13 for 10 % Cr, Fig. 4.14 to Fig. 4.16 for 16% Cr, Fig. 4.17 to Fig. 4.19 for 20% Cr and Fig. 4.20 to Fig. 4.22 for 26% Cr specimens, respectively. In each diagram, as-hardened hardness are plotted. In each specimen, the tempered hardness curve increases first to the maximum point and then decreases with an increase in tempering temperature. The tempered hardness shows more or less a secondary hardening due to the precipitation of secondary carbides and martensite transformed from destabilized austenite. The degree of secondary hardening, which is defined as the difference in hardness between the maximum tempered hardne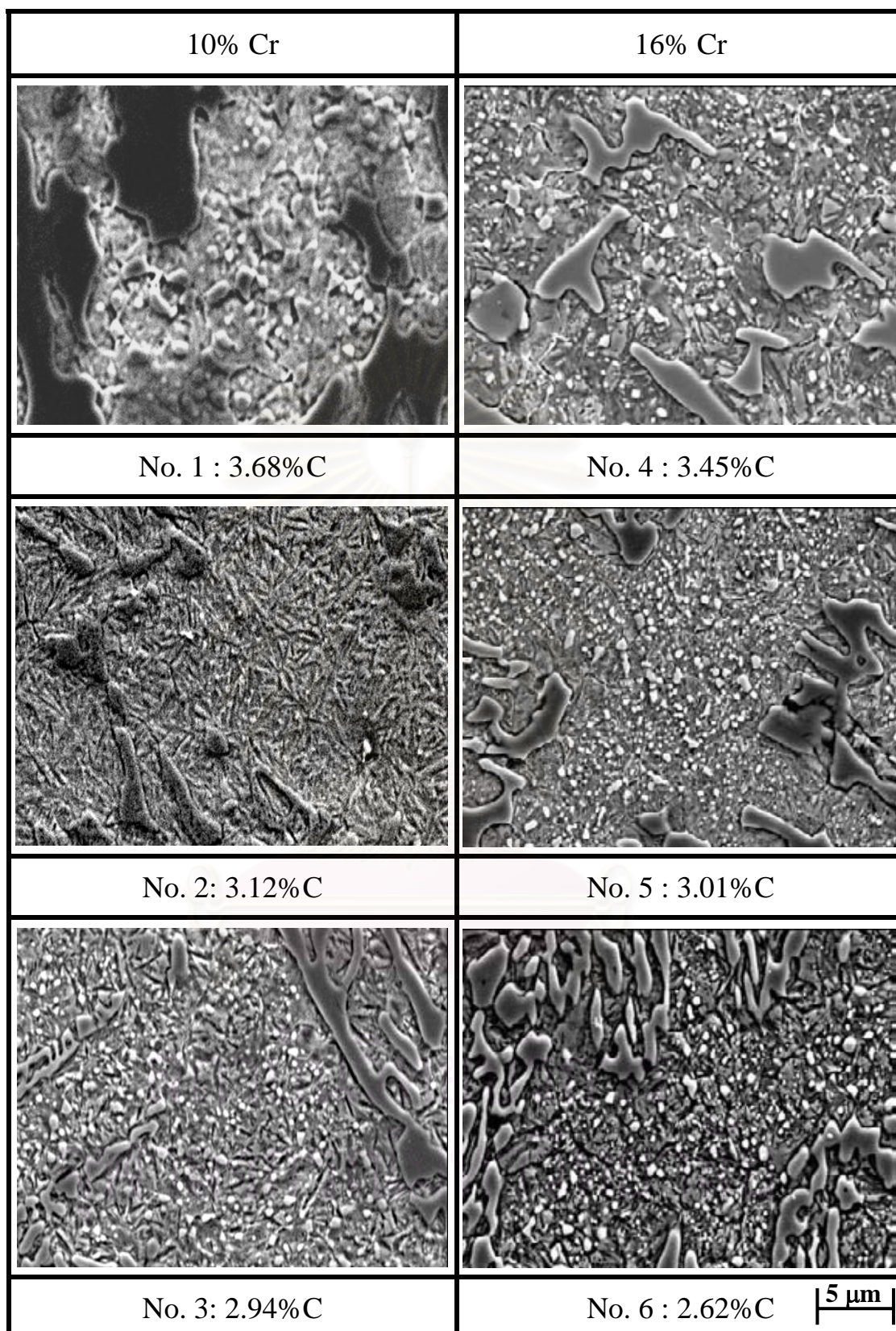ss (H_{Tmax}) and the hardness at which the secondary hardening begins, are respectively shown in Table 4.4. However, the degree of the hardening in high chromium cast iron is less than those of alloyed tool steel and the multi-component white cast iron [25]. The Vγ decreases gradually as the tempering temperature rises.

Table 4.4 Degree of the secondary hardening of test specimens.

Specimen	%C	%Cr	Degree of secondary hardening (HV30)		Cr/C
			1273 K austenitization	1323 K austenitization	
No.1	3.68	9.70	34	47	2.64
No.2	3.12	9.90	39	30	3.17
No.3	2.94	10.42	37	70	3.54
No.4	3.45	16.01	45	85	4.64
No.5	3.01	16.48	33	83	5.48
No.6	2.62	15.93	35	77	6.08
No.7	3.28	19.88	15	65	6.06
No.8	2.90	20.12	15	51	6.94
No.9	2.57	20.34	20	48	7.91
No.10	2.99	26.78	18	44	8.96
No.11	2.65	25.56	20	34	9.65
No.12	2.32	25.53	15	34	11.00

(i) 10% Cr cast iron

Fig. 4.11 shows the relationship between tempered hardness, $V\gamma$ and tempering temperature of the specimen No.1 with almost eutectic composition (3.68% C, 9.70% Cr). The hardness lowers once due to the tempering effect, and increases as the tempering temperature rises. The hardness of the specimens hardened from high austenitizatizing temperature of 1323 K are overall higher when compared with those in the case of low austenitizing temperature of 1273 K. The degree of the secondary hardening is greater in the case of higher austenitization, that is, 34 HV30 in 1273 K and 47 HV30 in 1323 K austenitization. The H_{Tmax} are 775 HV30 at 673 K tempering in the case of 1273 K austenitization, and 798 HV30 at 743 K tempering in 1323 K austenitization, respectively. It can be said that the higher H_{Tmax} is obtained by higher austenitizing temperature. The hardness decreases gradually after reaching the H_{Tmax} as the tempering temperature increases.

Around 4.2% $V\gamma$ existed in the as-hardened specimen hardened from 1273 K austenitization. It disappears at the tempering temperature of 723 K. When the austenitizing temperature rises up to 1323 K, 26.4% $V\gamma$ existed in as-hardened state decreases gradually as the tempering temperature rises and then it becomes 0% at 773 K. The $V\gamma$ values at the H_{Tmax} are 2% at 673 K in 1273 K austenitization and 7% at 723 K in 1323 K austenitization.

In the case of specimen No. 2 with hypoeutectic composition (3.12% C, 9.90% Cr) shown in Fig. 4.12, the tempered hardness curves show similar behavior to those in eutectic specimen (No. 1), that is, the tempered hardness of the specimen hardened from 1273 K austenitization are overall lower than that in the case of hardening from 1323 K austenitization and they also show the secondary hardening. The degrees of the secondary hardening are 39 HV30 in 1273 K and 30 HV30 in 1323 K austenitization. At the same Cr level, however the degree of the
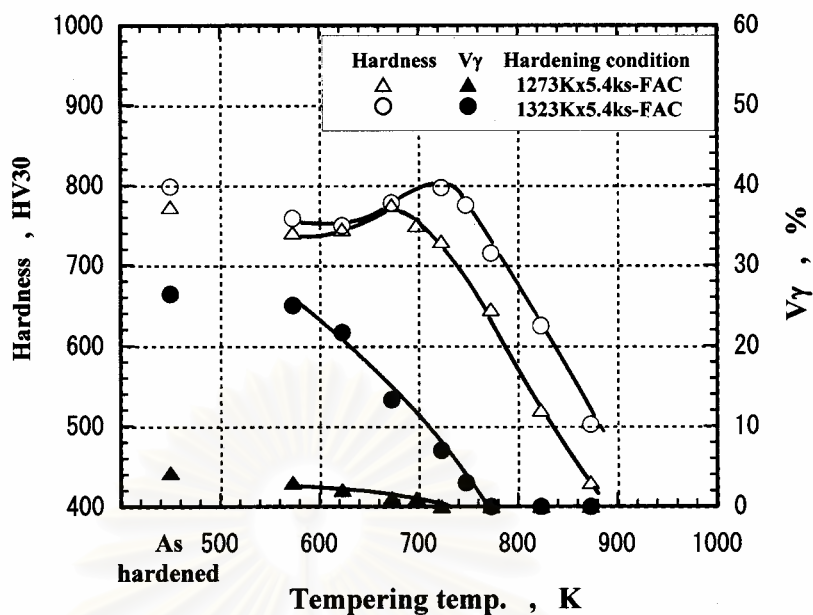
Fig. 4.11 Relationship between macro-hardness, volume fraction of retained austenite (Vγ) and tempering temperature. (Specimen No.1)
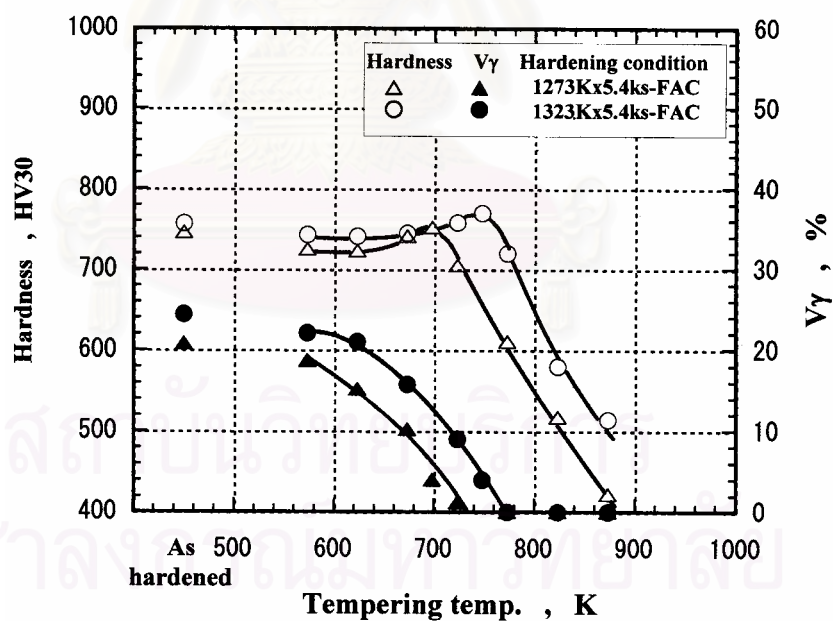
Fig. 4.12 Relationship between macro-hardness, volume fraction of retained austenite (Vγ) and tempering temperature. (Specimen No.2)
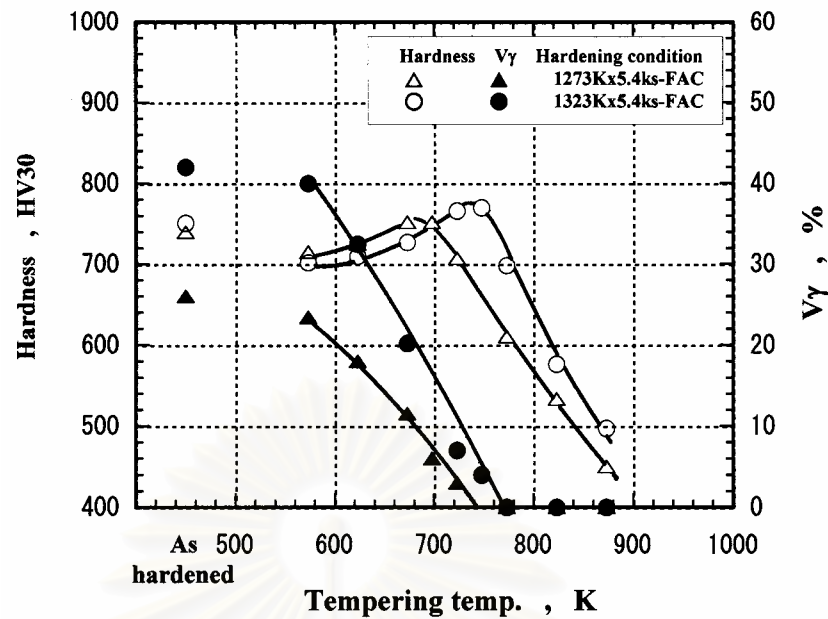
Fig. 4.13 Relationship between macro-hardness, volume fraction of retained austenite (Vγ) and tempering temperature. (Specimen No.3)

secondary hardening in hypoeutectic specimen is greater in 1273 K. The H_{Tmax} of 752 HV30 was obtained in the specimen hardened from 1273 K and tempered at 698 K, and 770 HV30 in 1323 K austenitization and 748 K tempering.

The Vγ values in as-hardened state are 20.8% in 1273 K and 24.4% in 1323 K austenitization, and they are more than those of the specimen No. 2. Both of the Vγ gradually reduces with an increase in the tempering temperature. Finally, the Vγ is fully decomposed at 723 K in the case of hardening from 1273 K and at 748 K 1323 K austenitization. The Vγ values at the H_{Tmax} are 4% and 9% at 698 K and 748 K tempering in 1273 K and 1323 K austenitization, respectively.

The tempered hardness curves of specimen No. 3 with more hypoeutectic composition (2.94% C, 10.42 % Cr) are shown in Fig. 4.13. The tempered hardness curves show different tendency from those of specimen No.1 and No.2. In the temperature ranges up to 698 K, however, the tempered hardness of specimens hardened from 1323 K is lower than those of specimens hardened from 1273 K, and it is reversed over the

tempering temperature of 698 K. The degrees of the secondary hardening are 37 HV30 in 1273 K and 70 HV30 in 1323 K austenitization and they are greater than eutectic specimen. In 10% Cr specimens, the degree of secondary hardening is broadly larger in the case of high austenitizing temperature. The H_{Tmax} in the specimen hardened from 1273 K is 752 HV30 but that in the case of 1323 K austenitization is 770 HV30.

In the specimens hardened from 1273 K and 1323 K, the $V\gamma$ values are 26% and 42%, they decrease abruptly as the tempering temperature increases and the tempering temperature at 0% $V\gamma$ are 740 K in the case of 1273 K and 773 K in 1323 K austenitization. It is clear that the tempering temperature at which the retained austenite disappears is high when austenitizing temperature is high under the same holding time. This behavior corresponds well with the variation of H_{Tmax}. The $V\gamma$ values at the H_{Tmax} are 6 % at 673 K and 4% at 748 K tempering in 1273 K and 1323 K austenitization, respectively.

(ii) 16% Cr cast iron

Fig.4.14 shows the tempered hardness curves and variation of $V\gamma$ of eutectic specimen No. 4 (3.45% C, 16.01% Cr). The hardness curves show different behavior from those of the specimens No. 1 and No. 2 but similar behavior to specimen No. 3 in the case of 10% Cr cast iron. At the tempering temperature is 698 K or less, the hardness of specimens hardened from 1323 K are lower than those hardened from 1273 K. This is because the more retained austenite left in the tempered state. At the temperature range over 698 K, the hardness changes off. Irrespective of the austenitizing temperatures, the tempered hardness increases from 623 K as the tempering temperature rises and gets to the H_{Tmax}. After the H_{Tmax}, the hardness decreases because of coarsening of precipitated carbides.

The degree of the secondary hardening is greater in 16% Cr specimens than in 10% Cr specimens, which are 45 HV30 in 1273 K and

85 HV30 in 1323 K austenitization. The H_{Tmax} values are 790 HV30 at 698 K tempering in 1273 K austenitization and 798 HV30 at 748 K tempering in 1323 K austenitization. From these results, it is found that the H_{Tmax} does not make much difference by austenitizing temperature even if the degree of the secondary hardening is greater in the case of 1323 K austenitization. The tempering temperature to obtain the H_{Tmax} is shifted to the high temperature side by increasing the austenitizing temperature.

The $V\gamma$ begins to reduce abruptly over the tempering temperature of 623 K and the tempering temperatures at which $V\gamma$ gets 0% are 723 K and 773 K in 1273 K and 1323 K austenitization, respectively. The $V\gamma$ values when the H_{Tmax} are obtained are almost 5% regardless of austenitizing temperature. It is clear that the more the $V\gamma$ value, the higher tempering temperature is necessary to eliminate the retained austenite.

In the case of hypoeutectic specimens No.5 (3.01% C, 16.48% Cr) as shown in Fig.4.15, the tempered hardness curves and the show similar behavior to those of eutectic specimen No.4 (Fig. 4.14). The degrees of the secondary hardening are 33 HV30 in 1273 K and 83 HV30 in 1323 K austenitization. When compared with eutectic specimen (No. 4), in each specimen, the degree of the secondary hardening is higher in high austenitization but lower in hypoeutectic specimen. The H_{Tmax} of 798 HV30 is obtained in the specimen hardened from 1323 K and tempered at 700 K, and it is a little larger than that of 783 HV30 tempered at 698 K in hardening from 1273 K. The tempering temperature at which the H_{Tmax} is obtained is about 50 K higher in the specimens hardened from 1323 K than those hardened from 1273 K. Both of the tempered hardness decrease gradually as the tempering temperature increases over the H_{Tmax}. The relation of $V\gamma$ vs tempering temperature shows good correspondence to that of the hardness vs tempering temperature. The tempering temperature, at which is 623 K and then the $V\gamma$ value begins to drop greatly.

The $V\gamma$ of 18.1% and 31.8 % in as-hardened state begin to drop at

Fig.4.14 Relationship between macro-hardness, volume fraction of retained austenite (Vγ) and tempering temperature . (Specimen No.4)

Fig. 4.15 Relationship between macro-hardness, volume fraction of retained austenite(Vγ) and tempering temperature. (Specimen No.5)

Fig. 4.16 Relationship between macro-hardness, volume fraction of retained austenite (Vγ) and tempering temperature. (Specimen No.6)

tempering temperature of 623 K where the secondary precipitation hardening starts. Over 673 K, they reduce greatly with an increase in the tempering temperature, and they disappears when the specimens are tempered at 730 K in 1273 K and 773 K in 1323 K austenitization. The Vγ values at the H_{Tmax} are 7% and 5% at 698 K and 748 K tempering in 1273 K and 1323 K austenitization, respectively.

The correlation between hardness, Vγ and tempering temperature of specimen No. 6 with more hypoeutectic composition (2.62% C, 15.93% Cr) is shown in Fig.4.16. The tempered hardness curves show the similar tendency in a family of 16% Cr specimens, that is, at the tempering temperatures is 698 K or less, the hardness of specimens hardened from 1323 K are lower than those hardened from 1273 K and it is reversed in when the tempering temperature rises over 698 K. However, the degree of the secondary hardening is much larger in the case of high austenitization, i.e., 35 HV30 in 1273 K and 77 HV30 in 1323 K austenitization, respectively. The degree is smallest when compared with other 16% Cr specimens. The H_{Tmax} values are 770 HV30 in the case of

1273 K and 782 HV30 in 1323 K austenitization. The Vγ values at the H$_{Tmax}$ are 4% and 8% in the specimen austenitized at 1273 K and 1323 K, respectively.

The 18.8% and 27.5% Vγ existed in the as-hardened state gradually reduce over 623 K and they reach 0% at 723 K in 1273 K and 773 K in 1323 K austenitization. This suggests that the use of high austenitizing temperature requires high tempering temperature in order to decompose a large volume fraction of retained austenite fully under the same holding time.

(iii) 20% Cr cast iron

Fig. 4.17 shows the results of the specimen No. 7 with eutectic composition (3.28% C, 19.88% Cr). The tempered hardness curves show the same behavior as those in 16% Cr specimens. In the temperature range up to 698 K, the hardness in the case of low austenitization is high in comparison with that in high austenitization of 1323 K. The hardness gradually increases until the maximum hardness and then decreases as the tempering temperature rises. The degree of the secondary hardening is smaller compared with 16% Cr specimens. It is clear that the degree of secondary hardening is larger in the case of high austenitization, i.e. 15 HV30 in 1273 K and 75 HV30 in 1323 K austenitization. However, the H$_{Tmax}$ does not make much difference, 798 HV30 in 1273 K and 810 HV30 in 1323 K austenitization, respectively.

The Vγ values of 14.2% in 1273 K and 33.5% in 1323 K austenitization in as-hardened state start to decrease gradually over 623 K and get to 0% at 740 K and 773 K tempering, respectively. Here, it is found that the high temperature is needed to decompose all the retained austenite in the specimen with higher Vγ. The Vγ values at the H$_{Tmax}$ are 9% at 698 K and 2% at 748 K tempering in 1273 K and 1323 K, respectively.
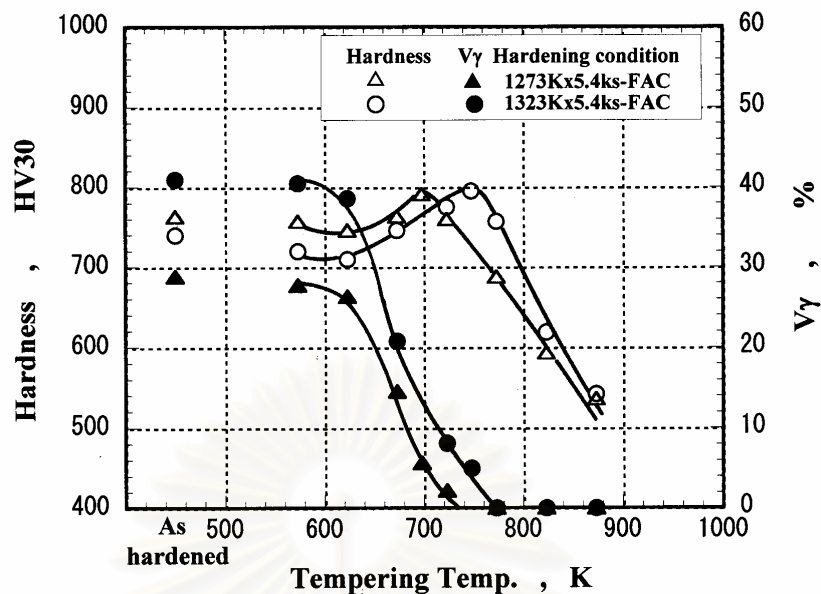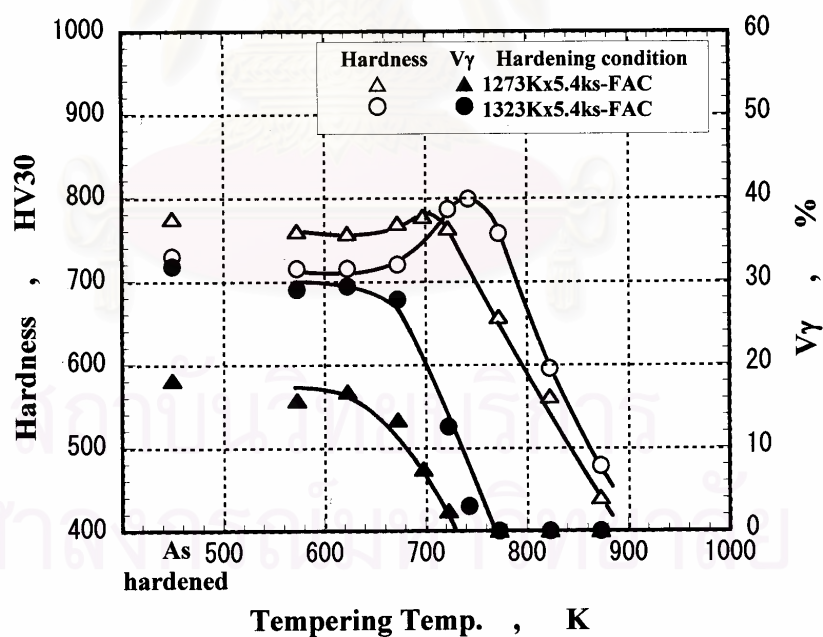
Fig. 4.17 Relationship between macro-hardness, volume fraction of retained austenite (Vγ) and tempering temperature. (Specimen No.7)

Fig. 4.18 Relationship between macro-hardness, volume fraction of retained austenite (Vγ) and tempering temperature. (Specimen No.8)
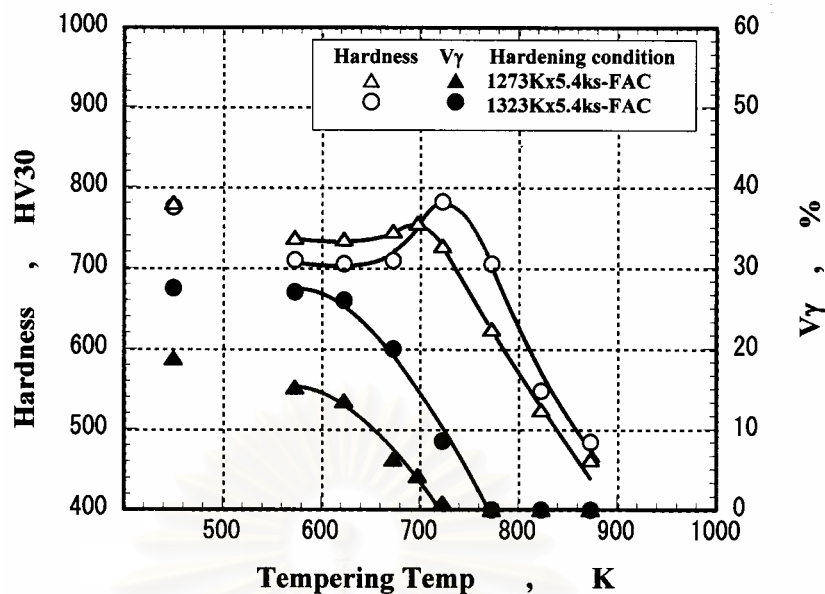
Fig. 4.19 Relationship between macro-hardness, volume fraction of retained austenite (Vγ) and tempering temperature. (Specimen No.9)

The results of the specimen No. 8 with hypoeutectic composition (2.90% C, 20.12% Cr) is shown in Fig. 4.18. The shapes of tempered hardness curves are similar to the eutectic specimen (No. 7). The degree of the secondary hardening is 15 HV30 and 51 HV30 in 1273 K and 1323 K austenitization, respectively, and they are almost same value as in eutectic specimen. The H_{Tmax} of 792 HV30 in 1323 K austenitization is a little higher than that of 775 HV30 in 1273 K austenitization.

The Vγ values in as-hardened state are 8.4% and 21.7% in 1273 K and 1323 K austenitization. Both the Vγ values do not change until 623 K tempering and then gradually decrease with an increase in the tempering temperature. The tempering temperatures at which the retained austenite disappears are 740 K and 760 K in 1273 and 1323 K austenitization. The Vγ values at the H_{Tmax} are 5% at 698 K and 2% at 748 K tempering in the 1273 K and 1323 K austenitization.

Fig. 4.19 shows the results of the specimen No. 9 with hypoeutectic composition (2.57% C, 20.34% Cr). Both tempered hardness curves show the secondary hardening and the degree is high in the case of higher austenitization, 20 HV30 in 1273 K and 48 HV30 in

1323 K austenitization. It is almost same as the eutectic specimen in 1273 K austenitization but smaller in 1323 K austenitization. The H_{Tmax} are 756 HV30 and 784 HV30 in 1273 K and 1323 K austenitization.

The $V\gamma$ in the specimen hardened from 1273 K is 7.3% and that in the specimen hardened from 1323 K is 19.2%. The former does not change until 673 K and begins to decrease gradually from 723 K. The latter starts to reduce from 623 K. The $V\gamma$ values at the H_{Tmax} are 4% and 2% in the specimens austenitized at 1273 K and 1323 K, respectively.

(iv) 26% Cr cast iron

The results of the specimen No.10 with eutectic composition (2.99% C, 26.78% Cr) are shown in Fig. 4.20. It is clear that the behavior of tempered hardness curves shows different tendency from those of 16% Cr and 20% Cr cast irons, that is, the hardness obtained from 1323 K austenitization are overall high compared with those obtained from low austenitization. It is similar that the degree of secondary precipitation is more in the case of high austenitization, 18 HV30 in 1273 K and 44 HV30 in 1323 K austenitization. However, the degree is small compared with 16% and 20% Cr specimens. The tempering temperature at the H_{Tmax} is located in high temperature side when the austenitizing temperature is high. The H_{Tmax} values are 770 HV30 in 1273 K and 780 HV30 in 1323 K austenitization.

The $V\gamma$ values are 3.8% and 12.1% in the specimens hardening from 1273 K and 1323 K, respectively. In 1273 K austenitization, the $V\gamma$ does not change until 723 K and gets to 0% at 773 K. In 1323 K austenitization, on the other side, the $V\gamma$ begins to decrease gradually over 573 K to 773 K. In both cases, the $V\gamma$ becomes 0% at 773 K. The $V\gamma$ values at H_{Tmax} are 3% at 698 K in 1273 K and 5% at 723 K tempering in 1323 K austenitization, respectively.

Fig. 4.21 shows the results of specimen No. 11 with hypoeutectic composition (2.65% C, 25.56% Cr). The tempered hardness curves show
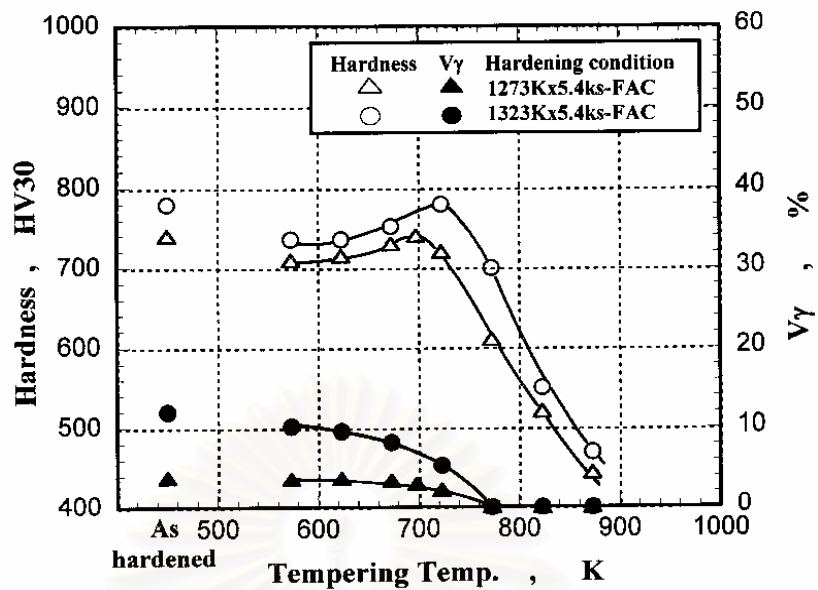
Fig. 4.20 Relationship between macro-hardness, volume fraction of retained austenite ($V\gamma$) and tempering temperature. (Specimen No.10)
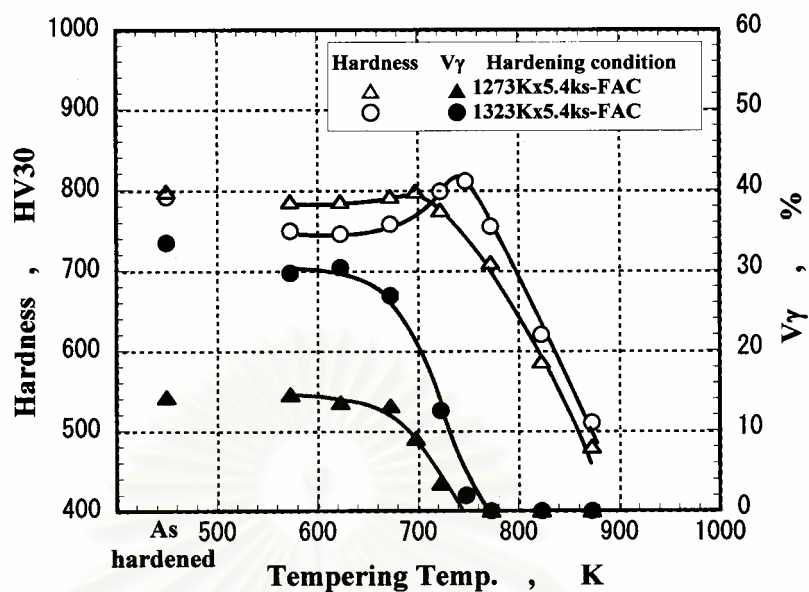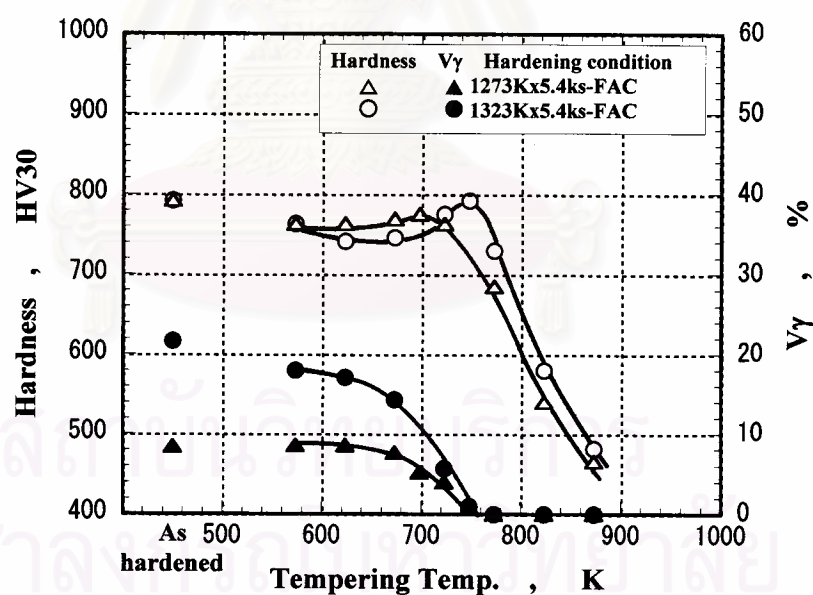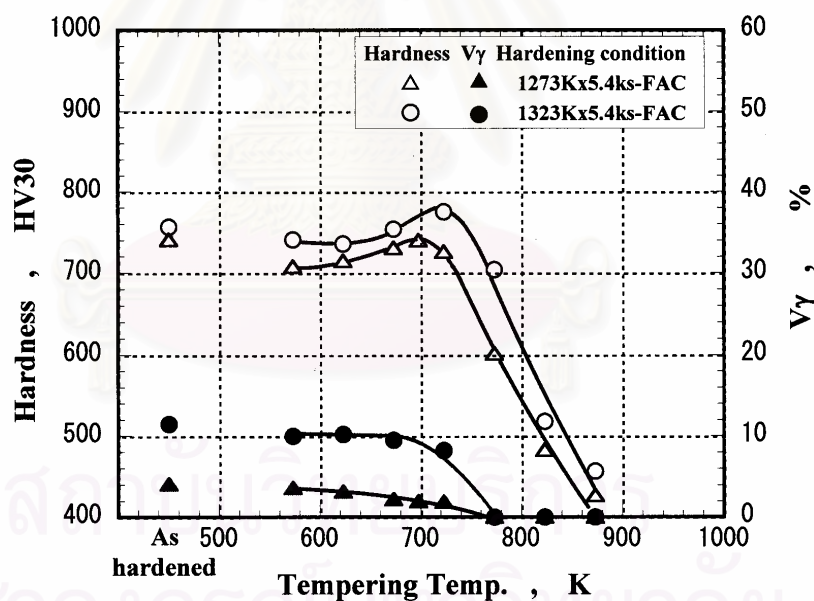

Fig. 4.21 Relationship between macro-hardness, volume fraction of retained austenite ($V\gamma$) and tempering temperature. (Specimen No.11)
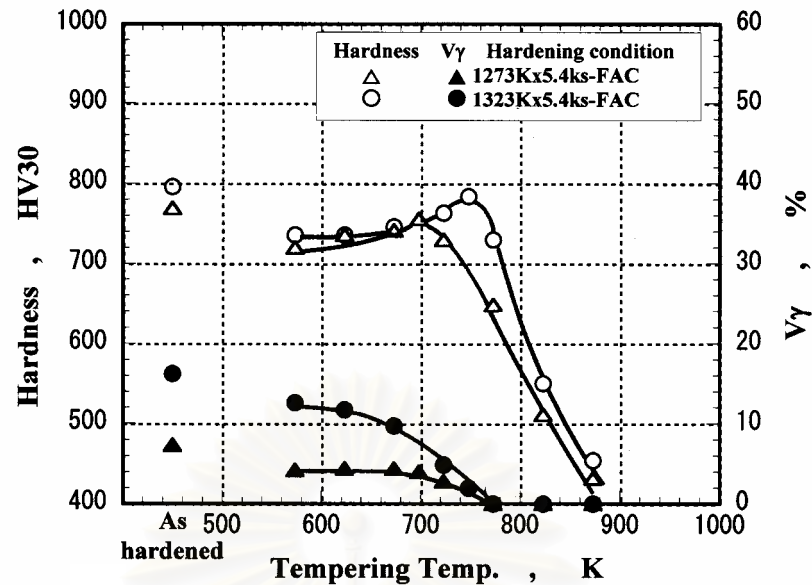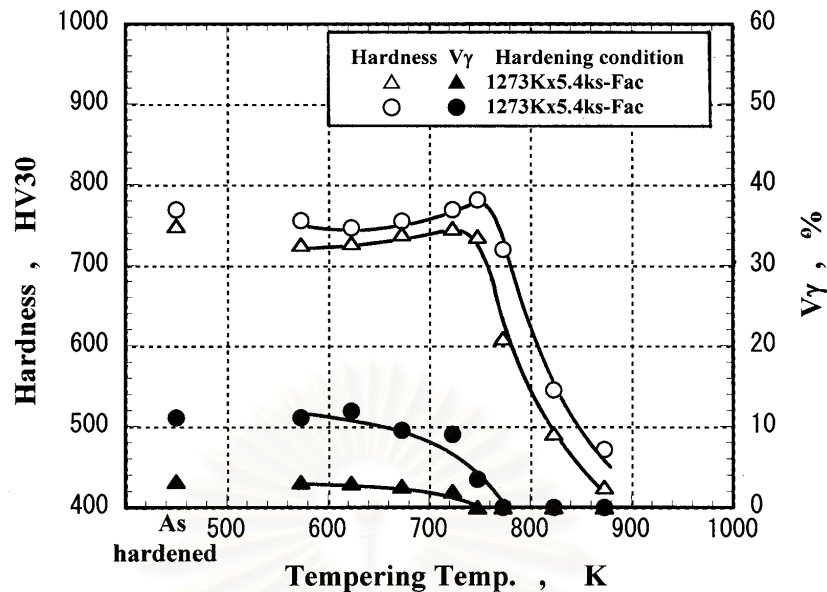
Fig. 4.22 Relationship between macro-hardness, volume fraction of retained austenite (Vγ) and tempering temperature. (Specimen No.12)

the similar behavior as those in the eutectic specimen (No. 10). The high tempered hardness is obtained in the specimens hardened from 1323 K. The secondary precipitation hardening appears in both of the specimens and the degrees are 20 HV30 in 1273 K and 34 HV30 in 1323 K austenitization. The H_{Tmax} is 740 HV30 at 690 K in 1273 K and 775 HV30 at 723 K tempering in 1323 K austenitization, respectively.

The Vγ values in as-hardened state are 4.1 % in 1273 K and 11.8% in 1323 K austenitization. In the specimen with 4% Vγ, the reduction of Vγ is very less in spite of increasing the tempering temperature. In the specimen with 12% Vγ, the reduction of Vγ is little until 723 K and then it decreases gradually. Both reach 0% at the same temperature of 773 K. The Vγ values at H_{Tmax} are 2% in 1273 K and 8% in 1323 K austenitization.

Fig. 4.22 shows the results of specimen No.12 with hypoeutectic composition (2.32% C, 25.53% Cr). The behavior of the tempered hardness and the Vγ value are quite similar to those of specimen No. 11. The degrees of the secondary hardening are 15 HV30 in 1273 K and 34 HV30 in 1323 K austenitization and they are smallest in the group of

26% Cr specimens. The H_{Tmax} values are 740 HV30 and 780 HV30 in 1273 K and 1323 K austenitization, respectively.

The Vγ values in as-hardened state are 3.2% in 1273 K and 11.2% in 1323 K austenitization and they decrease little until 723 K. Over 723 K, they reduce abruptly to 0% at 750 K in 1273 K and 773 K in 1323 K austenitization. The Vγ values at H_{Tmax} are 2% at 723 K in 1273 K austenitization and 3% at 748 K tempering in 1323 K austenitization.

Here, it should be described that in 26% Cr cast iron, the tempered hardness of specimens hardened from high austenitizatizing temperature of 1323 K is always high.

4.1.4 Relationship between micro-hardness of matrix and tempering temperature

The strength of matrix can be widely varied by heat treatment and it influences the mechanical properties including wear resistance. Though it is impossible to measure the strength of matrix itself in cast iron, it is possible to estimate the strength qualitatively from the matrix hardness. Therefore, it is worthy to measure the micro-hardness of matrix relating to the condition of heat treatment. The employed specimens are hypoeutectic cast irons that were tempered.

The measurement results of micro-hardness in the matrices are shown in Fig.4.23 and Fig. 4.24 for 10% Cr, Fig. 4.25 and Fig. 4.26 for 16% Cr, Fig. 4.27 and Fig. 4.28 for 20% Cr and Fig. 4.29 and Fig. 4.30 for 26% Cr specimens, respectively. In each diagram macro-hardness curves shown in section 4.1.3 are displayed for comparison. As an increase in the tempering temperature, the micro-hardness increases to the maximum point and after that, it decreases abruptly. In every specimen, the micro-hardness curve shows similar behavior to the macro-hardness curve and it lies at lower position than the macro-hardness. This suggests that the macro-hardness shows total hardness of both the eutectic carbide and the matrix. In the micro-hardness curve, the secondary precipitation hardening appears in the same manner as in the macro-hardness curve.

The degrees of the secondary hardening of micro-hardness are listed in Table 4.5. The degrees of secondary hardening in the case of 1273 K austenitization are 24 - 25 HV0.1 in 10% Cr, 25-34 HV0.1 in 16% Cr, 13 - 35 HV0.1 in 20% Cr and 22-38 HV0.1 in 26% Cr specimens, and those in 1323 K austenitization are 31-54 HV0.1 in 10% Cr, 50-55 HV0.1 in 16% Cr, 47- 50 HV0.1 in 20% Cr and 52 - 55 HV0.1 in 26% Cr specimens, respectively. It is clear that the degree of the secondary hardening is larger in the specimen hardened from higher austenitizing temperature of 1323 K.

The maximum or peak micro-hardness are shown in Table 4.6. In the same group of Cr content, there are not so large differences in the hardness between the specimens with different C content. However, they are certainly higher in the case of higher austenitization. The maximum micro-hardness of the specimens hardening from 1273 K vary from 612 HV0.1 to 624 HV0.1 in 10% Cr, 697 HV0.1 to 695 HV0.1 in 16% Cr, 695 HV0.1 to 675 HV0.1 in 20% Cr and 683 HV0.1 to 661 HV0.1 in 26% Cr and those hardened from 1323 K are 642 HV0.1 to 639 HV0.1 in 10% Cr, 706 HV0.1 to 703 HV0.1 in 16% Cr, 710 HV0.1 to 695 HV0.1 in 20% Cr and 703 HV0.1 to 698 HV0.1 in 26% Cr, respectively. The tempering temperatures at which the peaks of micro-hardness are obtained agree exactly with those of macro-hardness. The difference between macro-hardness and micro-hardness results in due to the existence of eutectic carbides that are usually much harder than the matrix. The differences at the H_{Tmax} are 140 HV0.1 in 10 % Cr, 90 HV0.1 in 16% Cr, 80-90 HV0.1 in 20% Cr and 90 HV30 in 26% Cr specimens, respectively.

From above results, it is clear that the variation of macro-hardness follows that of the matrix micro-hardness, and therefore, it might as well discuss the heat treatment behavior of matrix by adopting macro-hardness in stead of the micro-hardness.

Table 4.5 Degree of secondary hardening of micro-hardness.

Specimen	%C	%Cr	Degree of secondary hardening (HV30)		Cr/C
			1273 K austenitization	1323 K austenitization	
No.2	3.12	9.90	26	31	3.17
No.3	2.94	10.42	24	54	3.54
No.5	3.01	16.48	25	55	5.48
No.6	2.62	15.93	34	50	6.08
No.8	2.90	20.12	13	50	6.94
No.9	2.57	20.34	35	47	7.91
No.11	2.65	25.56	22	52	9.65
No.12	2.32	25.53	38	55	11.00

Table 4.6 Maximum micro-hardness of matrix.

Specimen	%C	%Cr	Maximum micro-hardness (HV0.1)		Cr/C
			1273 K austenitization	1323 K austenitization	
No.2	3.12	9.90	612	642	3.17
No.3	2.94	10.42	624	639	3.54
No.5	3.01	16.48	697	706	5.48
No.6	2.62	15.93	695	703	6.08
No.8	2.90	20.12	695	710	6.94
No.9	2.57	20.34	675	695	7.91
No.11	2.65	25.56	683	703	9.65
No.12	2.32	25.53	661	698	11.00

Fig. 4.23 Relationship between micro-hardness of matrix and tempering temperature of 10% Cr cast iron. (Specimen No. 2)

Fig. 4.24 Relationship between micro-hardness of matrix and tempering temperature of 10% Cr cast iron. (Specimen No. 3)

Fig. 4.25 Relationship between micro-hardness of matrix and tempering temperature of 16% Cr cast iron. (Specimen No. 5)
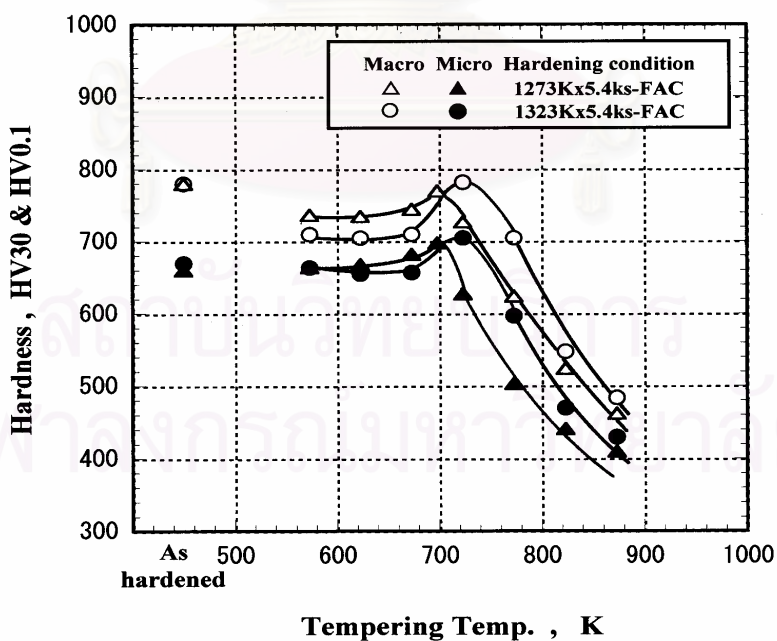
Fig. 4.26 Relationship between micro-hardness of matrix and tempering temperature of 16% Cr cast iron. (Specimen No. 6)
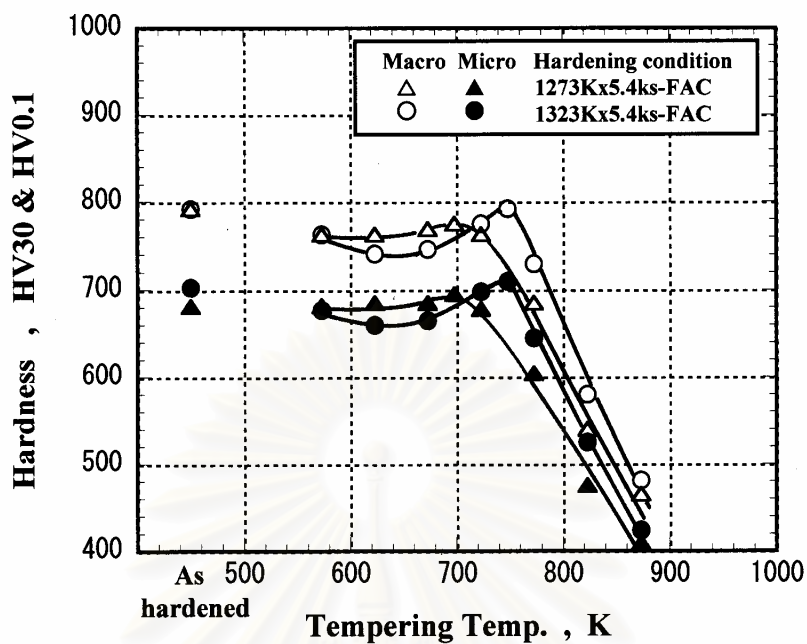
Fig. 4.27 Relationship between micro-hardness of matrix and tempering temperature of 20% Cr cast iron. (Specimen No. 8)
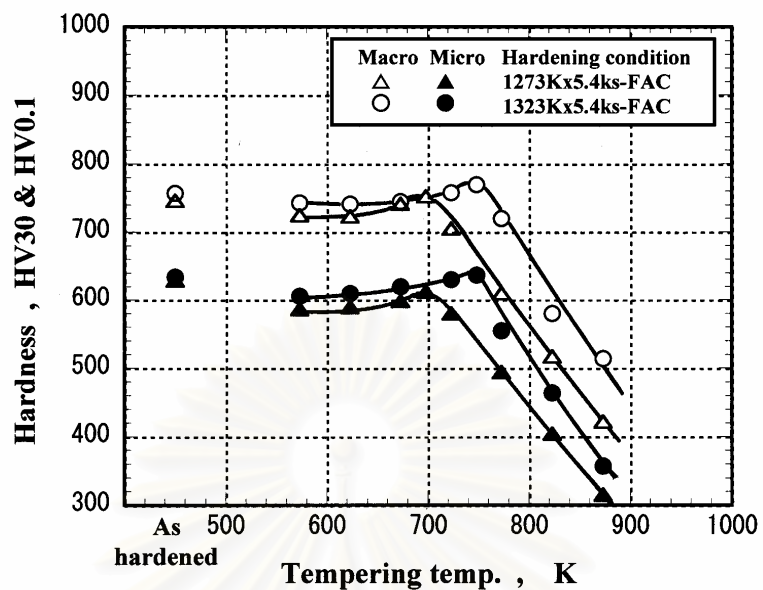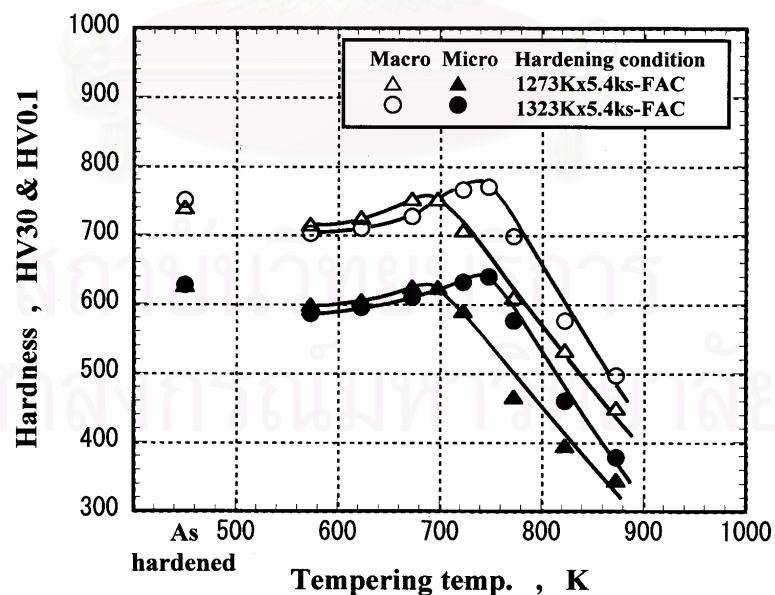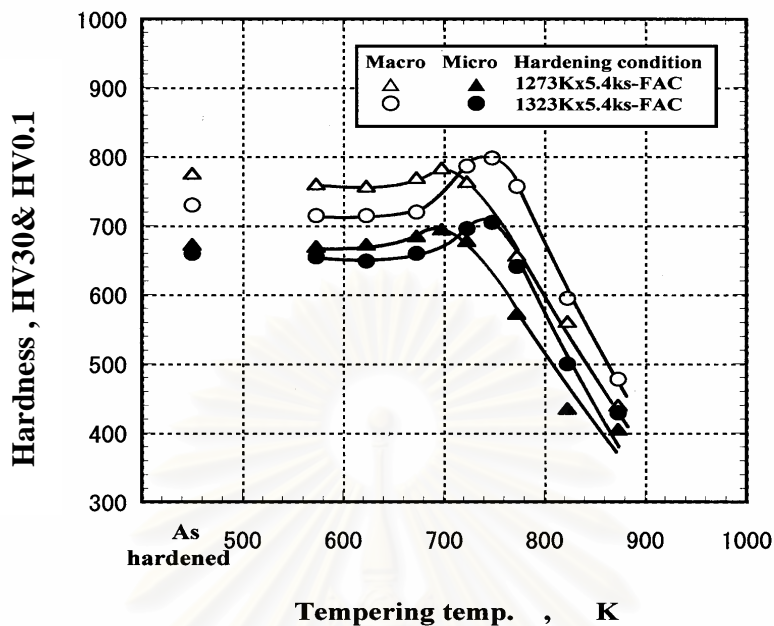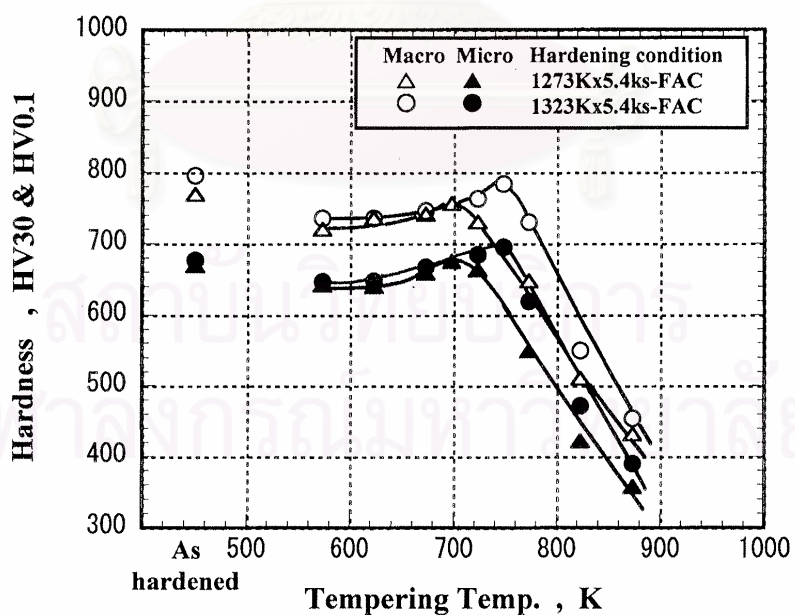

Fig. 4.28 Relationship between micro-hardness of matrix and tempering temperature of 20% Cr cast iron. (Specimen No. 9)
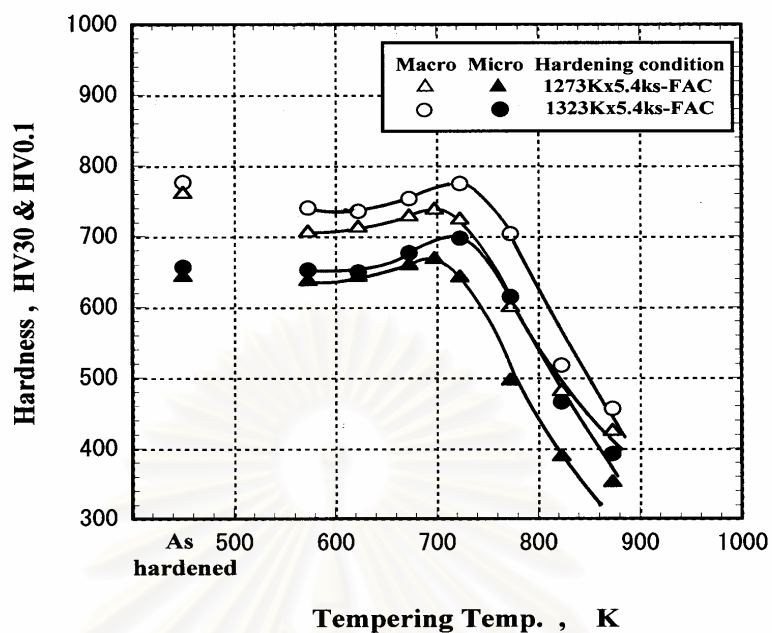
Fig. 4.29 Relationship between micro-hardness of matrix and tempering temperature of 26% Cr cast iron. (Specimen No. 11)
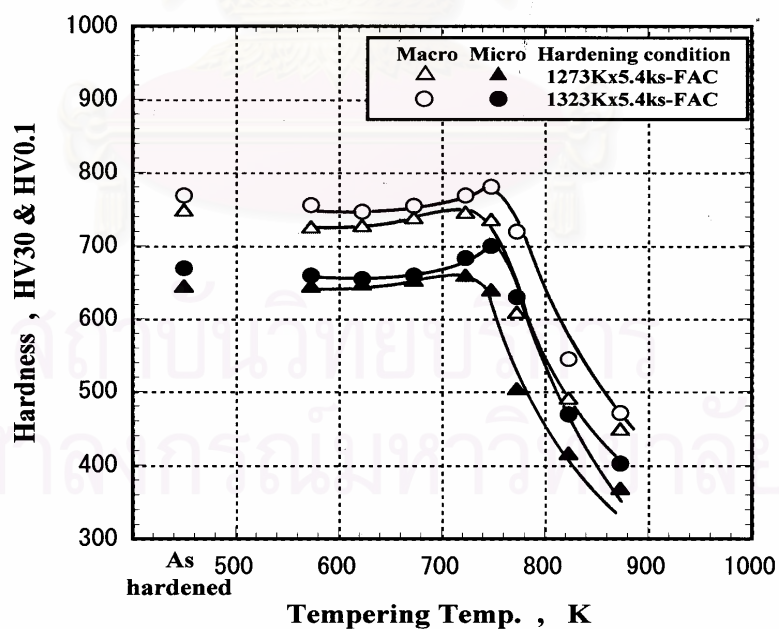
Fig. 4.30 Relationship between micro-hardness of matrix and tempering temperature of 26% Cr cast iron. (Specimen No. 12)

4.2 Effects of Alloying Elements on Heat Treatment Behavior of High Chromium Cast irons Containing 16% Cr and 26% Cr

4.2.1 Introduction

It is well known that the 15% to 16% Cr cast irons have been preferably used for rolling mill rolls in steel industry, and 25% to 28% Cr cast irons for rollers, tables of pulverizing mills in mining and cement industries. Such materials require more hardness and wider range of mechanical properties. For such purposes, 16% and 26% Cr cast irons with eutectic and hypoeutectic composition were selected as the base materials to investigate the effect of alloying elements on the heat treatment behavior. As the additional alloying elements, nickel and copper were employed to improve the hardenability and Mo and V to promote the formation of secondary special carbides with higher hardness than chromium carbides.

In this section, correlation among condition of heat treatment, hardness and volume fraction of retained austenite ($V\gamma$) and effect of alloying elements on the correlation are described in detail.

4.2.2 Eutectic high chromium cast irons

4.2.2.1 Effect of nickel (Ni)
(a) Test specimen in as-cast state

The chemical compositions of the test specimens are listed up in Table. 4.7. The specimens were separated into two groups of 16% Cr and 26% Cr, and Ni was added up to 2% in the both groups. As-cast microstructures of specimens without alloying element and with Ni addition are shown in Fig. 4.31. The microstructures consist of matrix and eutectic M_7C_3 carbides. The microstructures of the 16% Cr specimens are mostly eutectic and those of 26% Cr specimens are perfectly eutectic. The ($\gamma+M_7C_3$) eutectic structure shows a colony morphology, and the sizes of

Table 4.7 Chemical compositions of test specimens.

Specimen	Element (mass%)							
	C	Cr	Si	Mn	Ni	Cu	Mo	V
No.1	3.45	16.01	0.39	0.67	-	-	-	-
No.2	3.40	16.16	0.56	0.69	1.10	-	-	-
No.3	3.29	15.65	0.63	0.63	2.16	-	-	-
No.4	2.99	25.78	0.51	0.54	-	-	-	-
No.5	3.01	25.94	0.68	0.58	0.99	-	-	-
No.6	3.00	26.00	0.64	0.54	2.03	-	-	-

*S and P are less than 0.06 mass%

eutectic colony and eutectic carbides in 26% Cr specimens are much smaller than those in 16%Cr specimens. The carbide morphology does not change by Ni content compared with alloy-free specimen.

In 16% Cr specimens, the matrix of alloy-free and 1% Ni specimen is mostly pearlitic but that in 2% Ni specimen is austenitic mixed with pearlite and small amount of martensite. In 26%Cr specimens, the matrices of all specimens consist of austenite and possibly some martensite, and the difference in microstructure due to the amount of Ni can not be distinguished from the microphotographs.

The results of macro-hardness and Vγ are shown in Table 4.8. The hardness ranges from 565 HV30 to 658 HV30 in 16% Cr and 581 HV30 to 664 HV30 in 26% Cr specimens. In 16% Cr specimen, the hardness is high in 1%Ni specimen and low in 2% Ni specimen when compared with alloy-free specimen. In 26% Cr specimens, the hardness decreases gradually with an increase in Ni content.

The Vγ of alloy-free specimen with 16% Cr is zero percent and it increases abruptly from 7% to 77% as Ni content increases from 1% to 2%. In 26% Cr specimens, the Vγ increases with increasing Ni content, ranging from 34% in 0% Ni to 59% in 2% Ni specimens. This is because the addition of Ni delays the pearlite transformation and stabilizes

Alloy	16% Cr	26 %Cr
Alloy-free		
1% Ni		
2% Ni		

50 μm
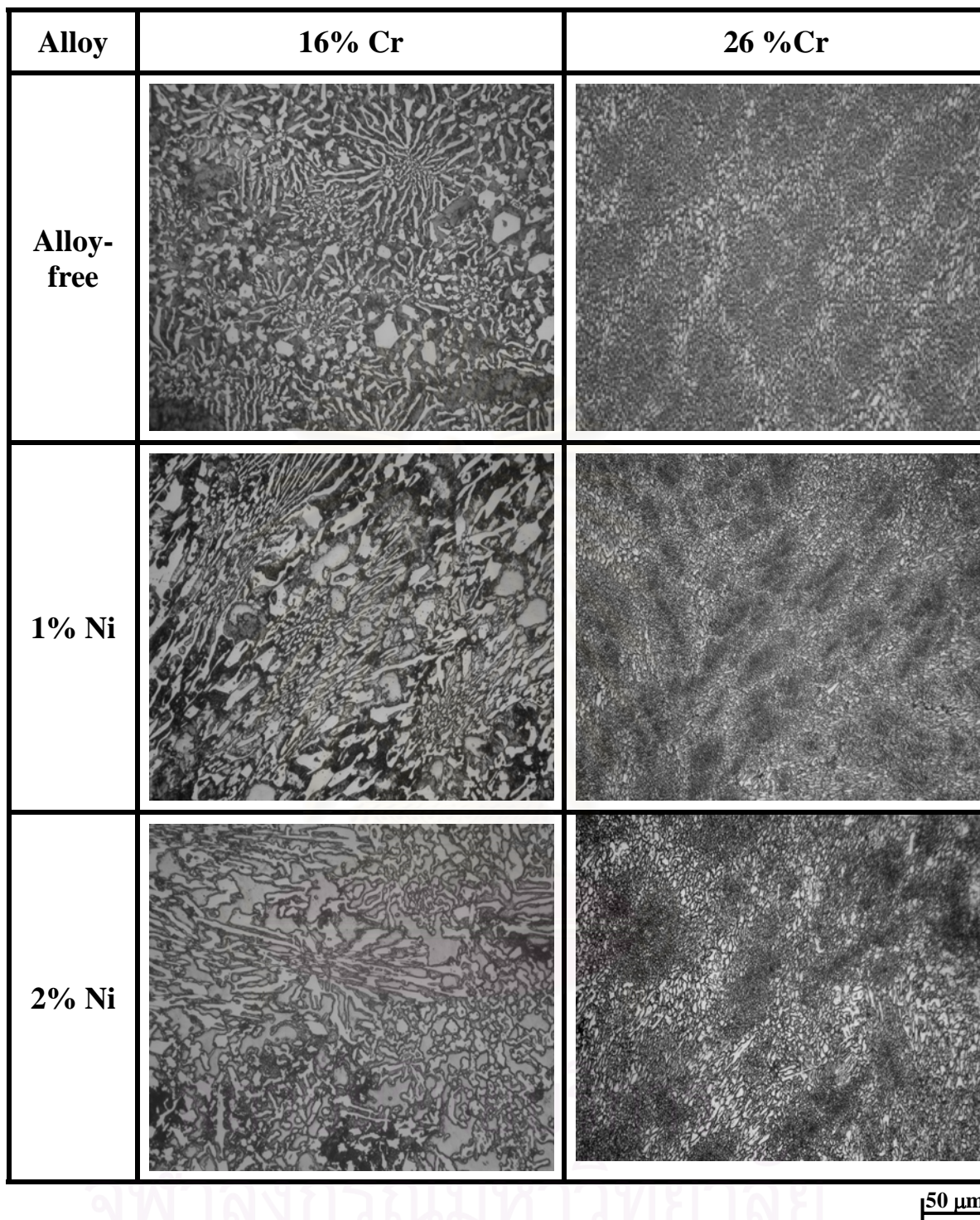
Fig. 4.31 As-cast microstructures of 16% Cr and 26% Cr eutectic cast irons with and without Ni. Matrices of 16% Cr cast irons change from pearlitic to austenitic with an increase in Ni content but those in 26% Cr cat irons are austenitic regardless of Ni content.

Table 4.8 Macro-hardness and volume fraction of retained austenite (Vγ)
of as-cast specimens.

Specimen	Element (mass%)		HV30	Vγ, %
	Cr	Ni		
No. 1		-	578	0
No. 2	16	1	658	7.1
No. 3		2	565	77.3
No. 4		-	664	33.7
No. 5	26	1	652	53.3
No. 6		2	581	59.4

austenite. This large amount of retained austenite in the matrix decreases
the macro-hardness in 2% Ni specimens.

(b) Effects of Ni content on variation of macro-hardness and volume fraction of retained austenite (Vγ) during heat treatment

-As-hardened state

The macro-hardness and Vγ of as-hardened specimens are listed up
in Table 4.9. In the both series of the test specimens, the hardness and the
Vγ vary greatly depending on Ni content and austenitizing temperature.
The effect of Ni content on the hardness and Vγ is shown in Fig. 4.32 (a)
and (b), respectively. In 16% Cr specimens, as shown in (a), the hardness
changes a little in the specimens hardened from 1273 K, ranging from
763 HV30 to 798 HV30 but it reduces greatly from 740 HV30 to 619
HV30 in the specimens hardened from 1323 K when Ni content
increases. In the 26% Cr specimens, the hardness reduces remarkably
with an increase in Ni content and it ranges from 770 HV30 to 685 HV30
in 1273 K and 780 HV30 to 709 HV30 in 1323 K austenitization,
respectively.

Table 4.9 Macro-hardness and volume fraction of retained austenite (Vγ)
of as-hardened specimens.

Specimen	Element (mass %)		Austenitizing Temperature (K)			
	Cr	Ni	1273		1323	
			HV30	Vγ, %	HV30	Vγ, %
No. 1	16	-	763	28.8	740	41.0
No. 2		1	798	36.0	700	62.4
No. 3		2	787	48.3	619	75.2
No. 4	26	-	770	3.8	780	12.1
No. 5		1	725	5.8	741	24.0
No. 6		2	685	11.5	709	33.6

As shown in Fig. 4.32 (b), the Vγ varies depending on Ni content and austenitizing temperature. Regardless of austenitizing temperature, the Vγ values increase with an increase in Ni content. In the case of 1273 K austenitization, the Vγ ranges from 29% to 48% in 16% Cr and from 4% to 12% in 26%Cr specimens. In 1323 K austenitization, the Vγ is increased remarkably by increasing Ni content, from 41% to 75% in 16% Cr specimens and from 12% to 34% in 26% Cr specimens, respectively. At the same Ni content, the Vγ is overall more in 16% Cr specimen compared with 26% Cr specimen. By comparing the hardness and Vγ with austenitizing temperature, it is found that the hardness is substantially low in 16%Cr specimens but high in 26%Cr specimens when the specimens are hardened from higher austenitizing temperature of 1323 K. On the other side, the high Vγ is obtained when the austenitizing temperature is high. This is because an increase in austenitizing temperature makes mainly C and Cr dissolve more into austenite and stabilizes it.

The as-hardened microstructures of the specimen hardened from 1323 K are shown as examples in Fig.4.33. In 16%Cr specimens, the matrix structure consists of comparably large amount of fine carbides, martensite and some retained austenite. Pearlite and austenite which existed much more in the as-cast state is greatly reduced, and instead,
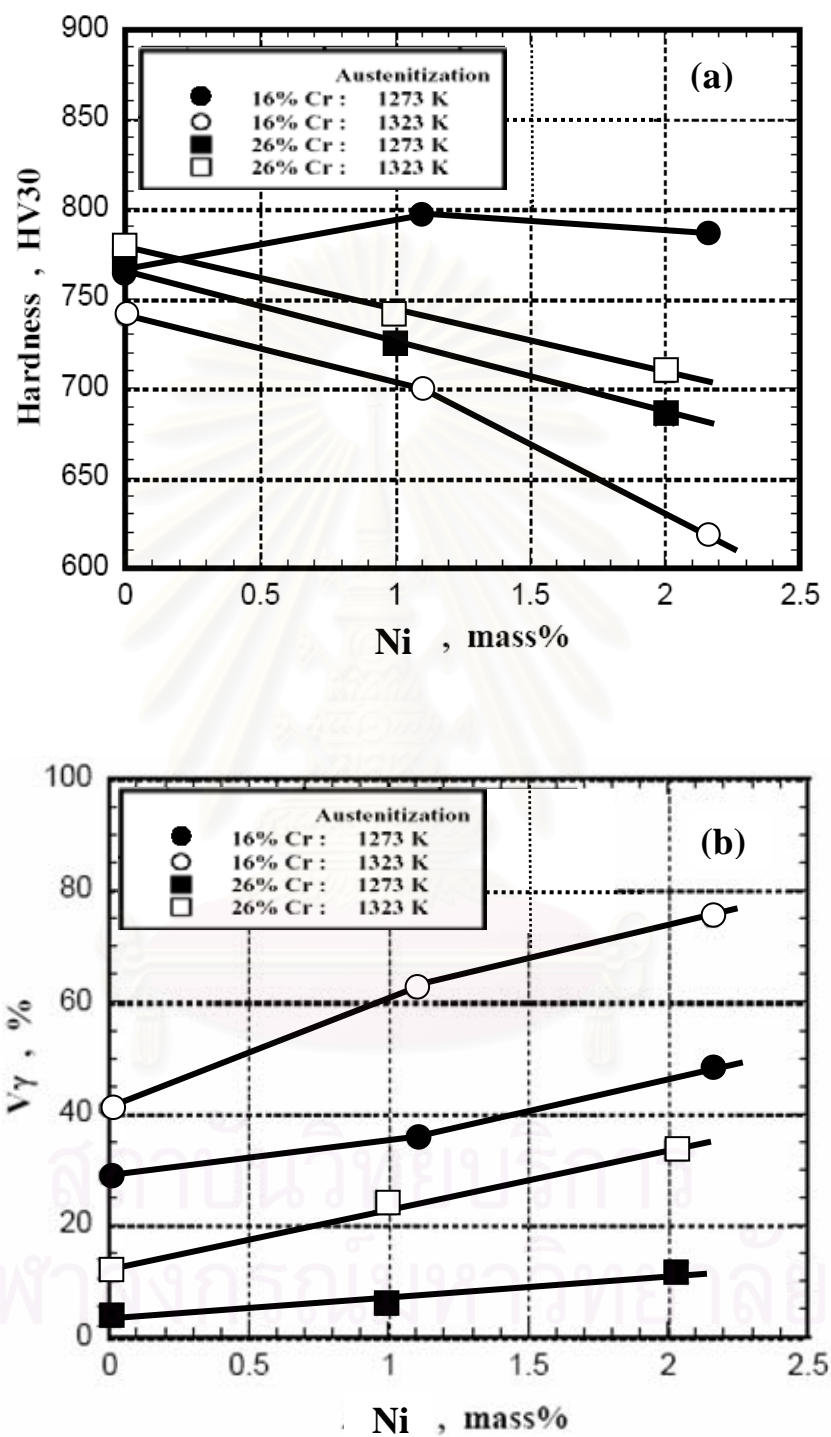
Fig. 4.32 Effect of Ni content on hardness (a) and Vγ (b) in as-hardened
state.

Alloy	16% Cr	26 %Cr
Alloy - free		
1%Ni		
2%Ni		

5 µm
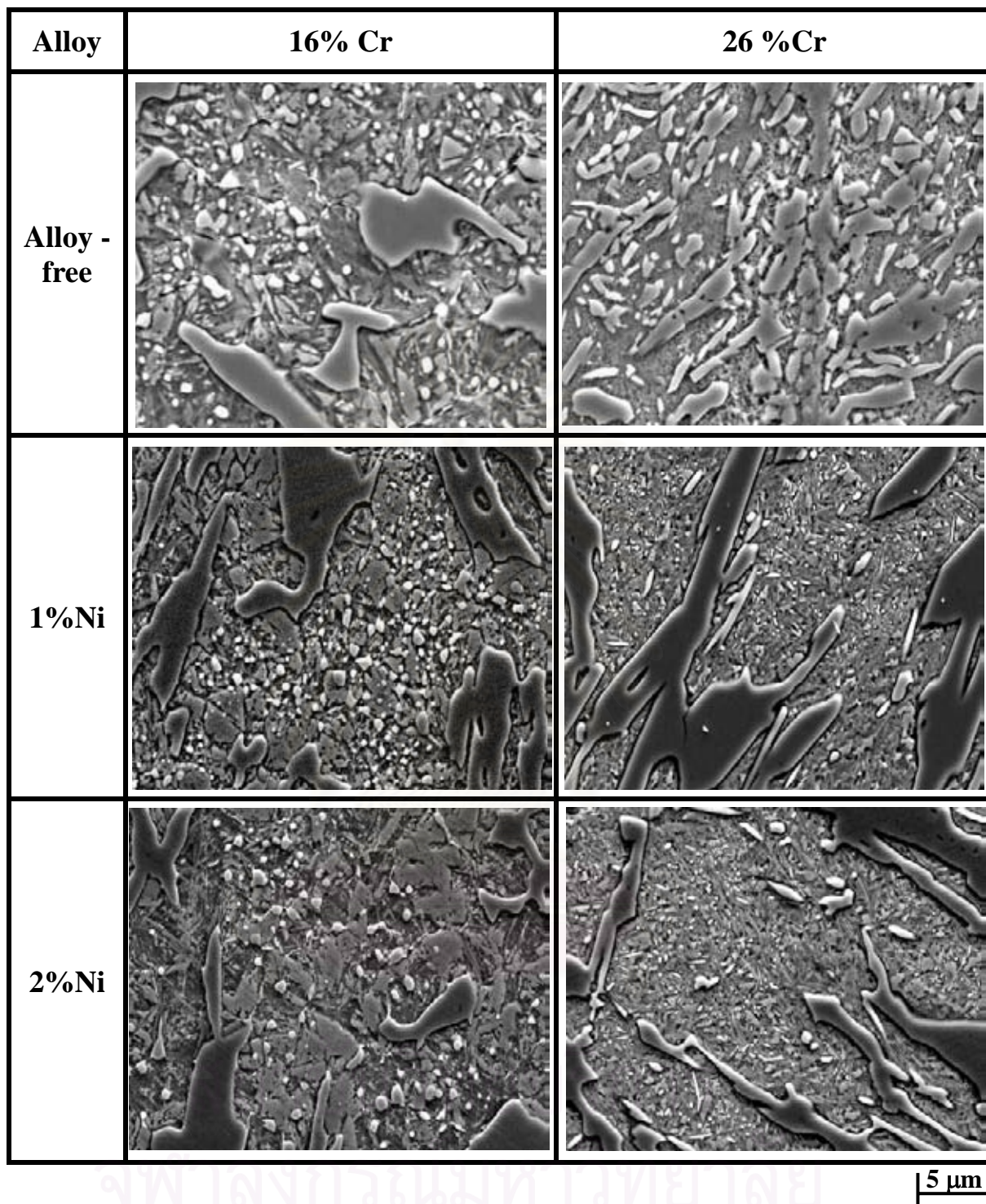
Fig. 4.33 SEM microphotographs in as-hardened state of 16% Cr and 26% Cr eutectic cast irons with and without Ni. Matrices consist of fine secondary carbides, martensite and retained austenite. Number of secondary carbides is much more in 16% Cr cast irons.

more carbide can be precipitated. In the case of 26%Cr specimens, the matrix is also dominated by secondary carbides, martensite and some austenite. However, the secondary carbides are less and the sizes of them seem to be a little larger.

- Tempered state

After the specimens were air hardened from two levels of austenitizing temperatures, 1273 K and 1323 K, they were tempered at several temperatures from 573 K to 873 K. Relationship between macro-hardness and $V\gamma$ and tempering temperature are respectively shown in Fig. 4.34 to Fig 4.36 for 16% Cr specimens and 4.37 to Fig. 4.39 for 26% Cr specimens. In each diagrams, hardness and $V\gamma$ of as-hardened specimens are plotted for comparison. The tempering curves show the secondary hardening and the degree of secondary hardening are summarized in Table 4.10.

(i) 16%Cr cast iron

The relationship between hardness, $V\gamma$ and tempering temperature of the specimen without alloying element (No.1) and with almost eutectic composition is shown in Fig. 4.34. In the range of lower tempering temperatures less than 723 K, however, the hardness of specimens hardened from 1323 K are lower than those hardened from 1273 K. When the specimens are tempered at the temperature range over 723 K, the hardness are conversely higher. Regardless of the austenitizing temperatures, the tempered hardness decreases abruptly as the tempering temperature rises after the tempered hardness curve shows H_{Tmax}. It is due to the over tempering. The degree of the secondary hardening is 45 HV30 and 85 HV 30 in 1273 K and 1323 K austenitization, respectively. The H_{Tmax} of 790 HV30 is obtained from the specimen hardened by 1273 K

Table 4.10 Degree of secondary hardening of test specimens.

Specimen	Element (mass %)		Degree of secondary hardening (HV30)	
	Cr	Ni	1273 K austenitization	1323 K austenitization
No. 1	16	-	45	85
No. 2		1	50	193
No. 3		2	83	224
No. 4	26	-	18	44
No. 5		1	73	92
No. 6		2	101	133

austenitization and tempered at 698 K and 798 HV30 is obtained from the specimen hardened by 1323 K austenitization and tempered at 748 K. The $V\gamma$ value of 28% in as-hardened state obtained by 1273 K austenitization and that of 41% by 1323 K austenitization begin to reduce gradually when the tempering temperature rises to 623 K and then they decreases abruptly over it. The tempering temperatures at which $V\gamma$ gets to 0% are 723 K and 773 K in 1273 K and 1323 K austenitization, respectively. The $V\gamma$ values at the H_{Tmax} are approximately 5% regardless of austenitizing temperature.

The results of 1% Ni specimen (No. 2) are shown in Fig. 4.35. The shape of tempered hardness curves is similar to alloy-free specimen of No.1. Up to 723 K tempering, the hardness of specimen hardened from low austenitizing temperature of 1273 K is higher than that in the case of high austenitizing temperature of 1323 K and over 730 K, it is reversed. As the tempering temperature rises, the hardness decreases from 573 K tempering and then it increases. Both of the tempered hardness curves show the secondary hardening and the degree is greater in the specimen hardened from higher austenitization. The degrees are 50 HV30 in 1273 K and 193 HV30 in 1323 K austenitization and they are much greater compared with alloy-free specimen. Both hardness curves decreases remarkably after the H_{Tmax}. The H_{Tmax} values of 800 HV30 and 823 HV30

are obtained at 723 K and 748 K tempering in 1273 K and 1323 K austenitization, respectively.

The Vγ of 29% in the specimen hardened from 1273 K and 41% in the hardening from 1323 K decrease gradually up to 673 K with an increase in tempering temperature and they decrease rapidly over 673 K. The Vγ values disappear all at 760 K and 773 K in 1273 K and 1323 K austenitization, respectively, and those at the H$_{Tmax}$ are 15% in the case of 1273 K and 16% in 1323 K austenitization.

The results of 2% Ni specimen (No. 3) are shown by Fig. 4.36. The curves of tempered hardness are similar to the specimens No.1 and No.2. When the tempering temperature rises over 623 K, the hardness gradually increases to the H$_{Tmax}$ and reduces remarkably after arriving there regardless of austenitizing temperature. Both of the hardness curves show the greatest secondary hardening in the group of 16% Cr specimens and the degree is much greater in the case of higher austenitizing temperature of 1323 K. The degrees of the secondary hardening are 83 HV30 in the case of 1273 K and 224 HV30 in 1323 K austenitization. The H$_{Tmax}$ of 805 HV30 is obtained by tempering at 735 K in 1273 K austenitization and 808 HV30 at 773 K in 1323 K austenitization, respectively.

The Vγ values in as-hardened state are 48% in 1273 K and 75% in 1323 K austenitization. Both the Vγ decrease fast when the specimens are tempered over 623 K, and they become 0% at 770 K and 780 K tempering in 1273 K and 1323 K austenitization, respectively. When the hardness is corresponded to the Vγ, it is understood that the H$_{Tmax}$ can be obtained near the tempering temperature at which the retained austenite is reduced less than 5%. From the view point of Vγ, it can be said that the more the Vγ in as-hardened state, the more the degree of secondary hardening. However, it is interesting that the H$_{Tmax}$ value does not vary even if there is a large difference in the degree of secondary hardening. From the experimental results of 16% Cr specimens, it is clear that the tempering temperature to obtain the H$_{Tmax}$ is shifted to the high

Fig. 4.34 Relationship between macro-hardness, volume fraction of retained austenite (Vγ) and tempering temperature of 16% Cr cast iron without alloying element. (Specimen No. 1)

Fig. 4.35 Relationship between macro-hardness, volume fraction of retained austenite (Vγ) and tempering temperature of 16%Cr cast iron with 1% Ni. (Specimen No. 2)

Fig. 4.36 Relationship between macro-hardness, volume fraction of retained austenite (Vγ) and tempering temperature of 16%Cr cast iron with 2% Ni. (Specimen No. 3)

temperature side by increasing the austenitizing temperature.

(ii) 26%Cr cast iron

The results of alloy-free specimen (No. 4) are shown in Fig. 4.37. The hardness of 26% Cr specimens shows the different behavior from 16%Cr specimens, that is, the hardness of specimens hardened from high austenitizing temperature of 1323 K are overall more than that hardened from low temperature of 1273 K. It is similar that the tempered hardness curves show the secondary hardening and the degree is more in the case of high austenitizing temperature of 1323 K, that is, 18 HV30 in 1273 K and 44 HV30 in 1323 K austenitization. The hardness gradually increases from 623 K to the highest point (H_{Tmax}) and then decreases with increasing the tempering temperature. The tempering temperature at H_{Tmax} is shifted to the higher temperature side. The H_{Tmax} values are 770 HV30 in 1273 K and 780 HV30 in 1323 K austenitization.

The $V\gamma$ values of specimens hardened from 1273 K and 1323 K are 4% and 12%, respectively. In 1273 K austenitization, the $V\gamma$ decreases gradually from 723 K and gets to 0% at 773 K. In the case of 1323 K austenitization, the $V\gamma$ settles at the same value until 673 K and after that, it begins to reduce remarkably as the tempering temperature increases and gets to 0% at 773 K. The $V\gamma$ values at the H_{Tmax} are 3% at 698 K in 1273 K and 8% at 723 K tempering in 1323 K austenitization, respectively.

The results of 1% Ni specimen (No. 5) are shown in Fig. 4.38. The tempered hardness curves show the different tendency from alloy-free specimen (No. 4). The hardness of specimens hardened from 1273 K are lower than those hardened from 1323 K except for tempering temperature between 673 K and 710 K, and the hardness do not make much difference by the difference in austenitizing temperature. However, when the tempering temperature rises over 673 K, both the tempered hardness curves show the remarkable secondary hardening compared with alloy-free specimen and much greater secondary hardening is obtained in the specimen hardened from 1323 K. The degrees are 73 HV30 in 1273 K and 92 HV30 in 1323 K austenitization. The H_{Tmax} are 780 HV30 in 1273 K and 804 HV30 in 1323 K austenitization, respectively.

In as-hardened state, the 6% and 24% $V\gamma$ exist in the specimens hardened from 1273 K and 1323 K austenitization, respectively. The $V\gamma$ decreases gradually in the former case and reduces remarkably in the latter case, and they become 0% at 773 K regardless of austenitizing temperature. The $V\gamma$ values at H_{Tmax} are 4 % at 698 K in 1273 K and 9% at 748 K tempering in 1323 K austenitization.

As shown in Fig. 4.39 for the results of 2% Ni specimen (No. 6), the tempered hardness curves show the different tendency from alloy-free and 1% Ni specimens under the same tempering condition but it is similar to that of 16% Cr specimens. In the range of tempering temperature lower than 720 K, the hardness of specimens hardened from 1323 K are lower than those hardened from 1273 K, and they are reversed over 720 K. Both hardness curves increase gradually from 573 K to the highest point
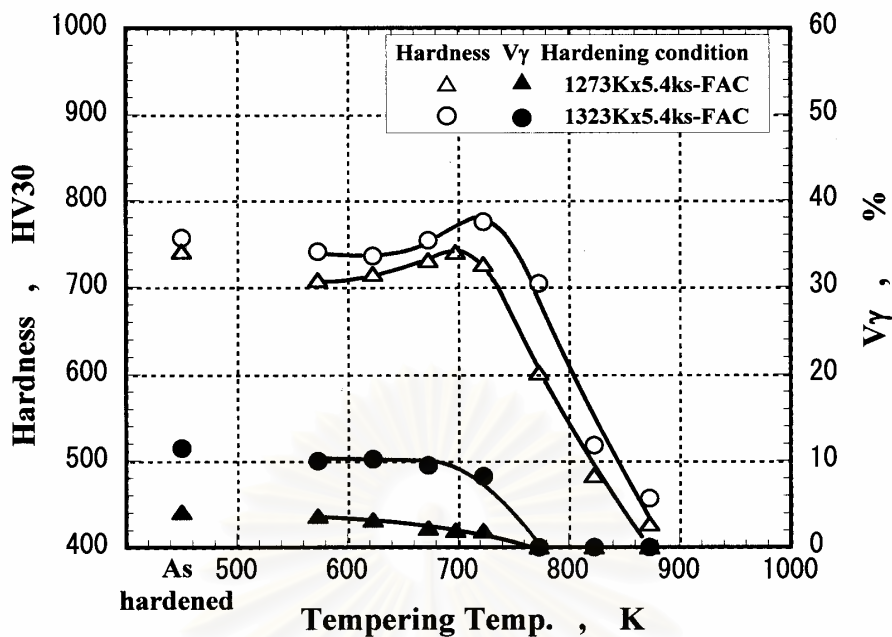
Fig. 4.37 Relationship between macro-hardness, volume fraction of retained austenite (Vγ) and tempering temperature of 26% Cr cast iron without alloying element. (Specimen No. 4)
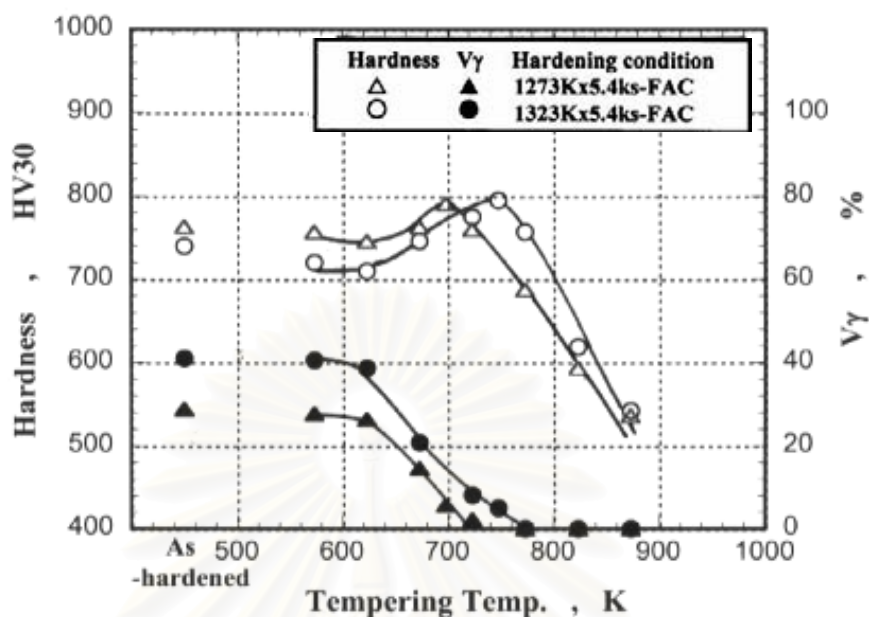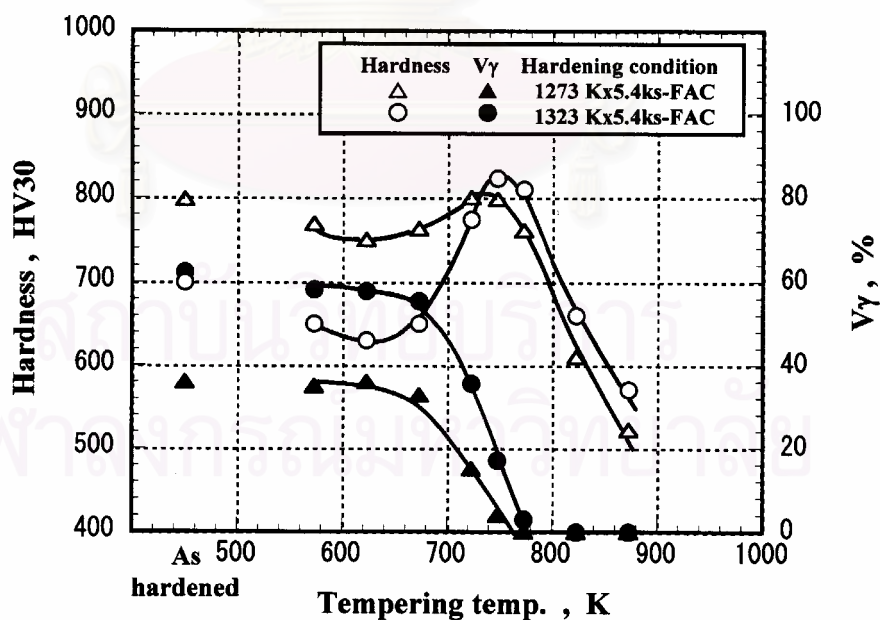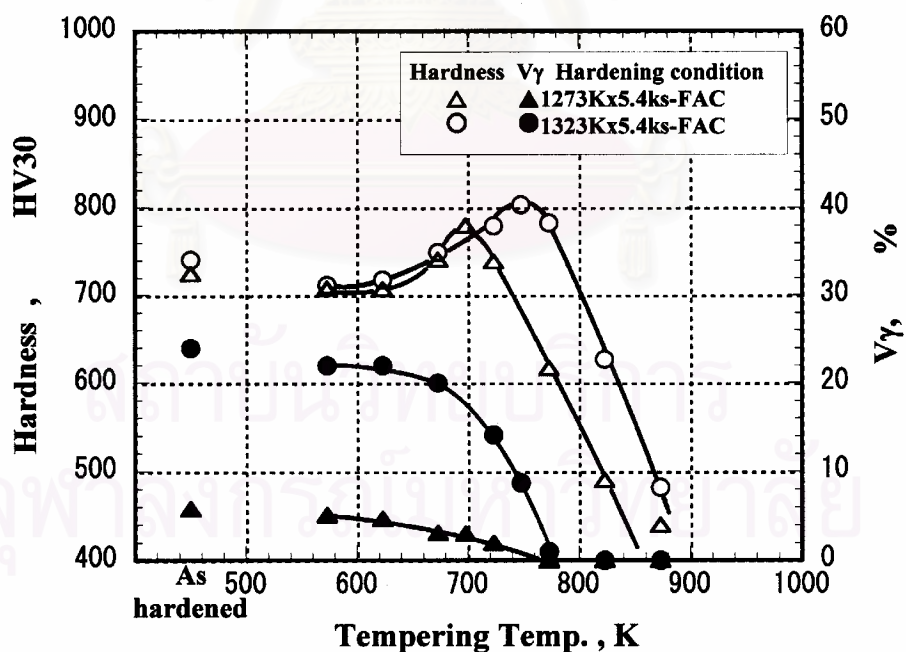

Fig. 4.38 Relationship between macro-hardness, volume fraction of retained austenite (Vγ) and tempering temperature of 26% Cr cast iron with 1% Ni. (Specimen No. 5)

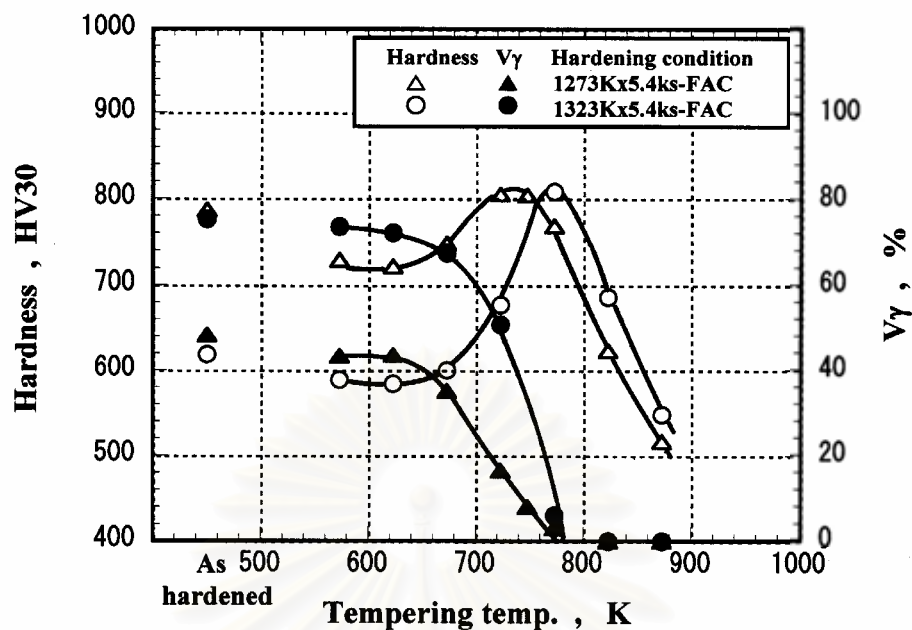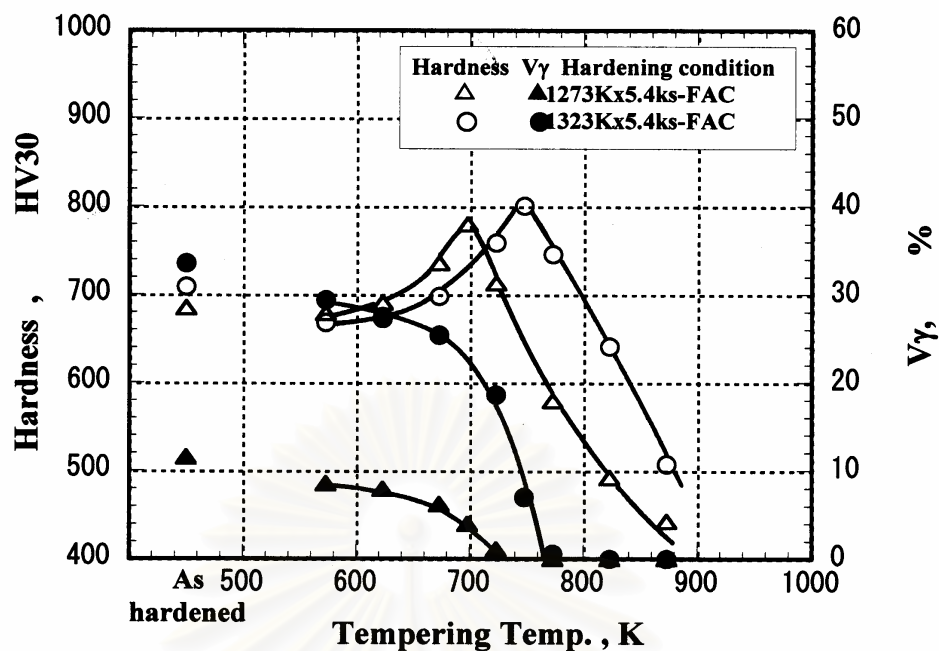Fig. 4.39 Relationship between macro-hardness, volume fraction of
retained austenite (Vγ) and tempering temperature of 26% Cr cast
iron with 2% Ni. (Specimen No. 6)

(H$_{Tmax}$) and after that, they decreases remarkably due to the
agglomeration of secondary carbides as the tempering temperature
increases. The degrees of secondary hardening during tempering are 101
HV30 and 133 HV30 in 1273 K and 1323 K austenitization, respectively.
The H$_{Tmax}$ value in 1273 K austenitization is 780 HV30 and that in 1323
K austenitization is 801 HV30. From these results, it can be said that the
degree of secondary hardening obtained from the specimen hardened
from 1323 K is largest in the group of 26% Cr specimens.

As-hardened Vγ values of 12% in 1273 K and 34% in 1323 K
austenitization decrease gradually as the tempering temperature
increases. The tempering temperature at which the Vγ becomes 0% is
730 K in 1273 K and 773 K in 1323 K austenitization. The Vγ values at
the H$_{Tmax}$ are 4% at 698 K in 1273 K and 7% at 748 K tempering in 1323
K austenitization.

4.2.2.2 Effect of copper (Cu)

(a) Test specimen in as-cast state

   Chemical compositions of the test specimens are respectively shown in Table 4.11. Cu was added up to 2% into both the 16% Cr and 26% Cr specimens. The as-cast microstructures are respectively shown in Fig. 4.40. The microstructures of 16% Cr specimens are nearly eutectic and those in 26% Cr specimens are perfectly eutectic. The morphology and the size of eutectic carbide are similar to the alloy-free specimens in both 16% Cr and 26% Cr specimen. The eutectic colony size and the size of eutectic carbide are much larger in 16% Cr specimens than those in 26% Cr specimens.

   The matrix structure of all 16% Cr specimens is pearlitic but in 26% Cr specimen is austenitic possibly mixing with martensite. This means that the as-cast austenite fully transformed to pearlite during cooling even if the addition of Cu rises up to 2% in 16% Cr specimens. In 26% Cr specimens, the change of the matrix due to the addition of Cu can not distingue by these microphotographs. However, it can be said that an increase in Cr content to 26% caused to stabilize the austenite.

   Here, macro-hardness and volume fraction of retained austenite ($V\gamma$) of as-cast specimens are quantitatively measured and the results are shown in Table 4.12. The hardness gradually increases in 16%Cr specimen but it decreases in 26%Cr specimen with an increase in Cu content.

   The $V\gamma$ of 16%Cr specimens are zero regardless of Cu content. This result supports the microphotographs in Fig. 4.40. In the case of 26% Cr specimens, the $V\gamma$ is greatly related to Cu content, that is, it increases remarkably from 34% to 57% with increasing Cu content from 1% to 2%.

Table 4.11 Chemical composition of test specimens.

Specimen	Element(mass%)							
	C	Cr	Si	Mn	Ni	Cu	Mo	V
No.1	3.45	16.01	0.39	0.67	-	-	-	-
No.4	3.38	15.67	0.56	0.56	-	1.00	-	-
No.5	3.45	15.59	0.55	0.46	-	2.03	-	-
No.12	2.99	25.78	0.51	0.54	-	-	-	-
No.15	3.00	25.96	0.65	0.54	-	1.05	-	-
No.16	3.01	25.78	0.41	0.55	-	1.94	-	-

* S and P are less than 0.06 mass%

Table 4.12 Macro-hardness and volume fraction of retained austenite

(Vγ) of as-cast specimens.

Specimen	Element (mass%)		HV30	Vγ, %
	Cr	Cu		
No. 1		-	578	0
No. 2	16	1	617	0
No. 3		2	628	0
No. 4		-	664	33.7
No. 5	26	1	654	45.7
No. 6		2	626	55.6

Table 4.13 Macro-hardness and volume fraction of retained austenite

(Vγ) of as-hardened specimens.

Specimen	Element (mass%)		Austenitizing Temperature (K)			
	Cr	Cu	1273		1323	
			HV30	Vγ, %	HV30	Vγ, %
No. 1		-	763	28.8	740	41.0
No. 2	16	1	800	33.8	716	49.8
No. 3		2	780	38.0	675	59.3
No. 4		-	770	3.8	780	12.1
No. 5	26	1	759	3.5	778	13.2
No. 6		2	740	4.1	780	14.1

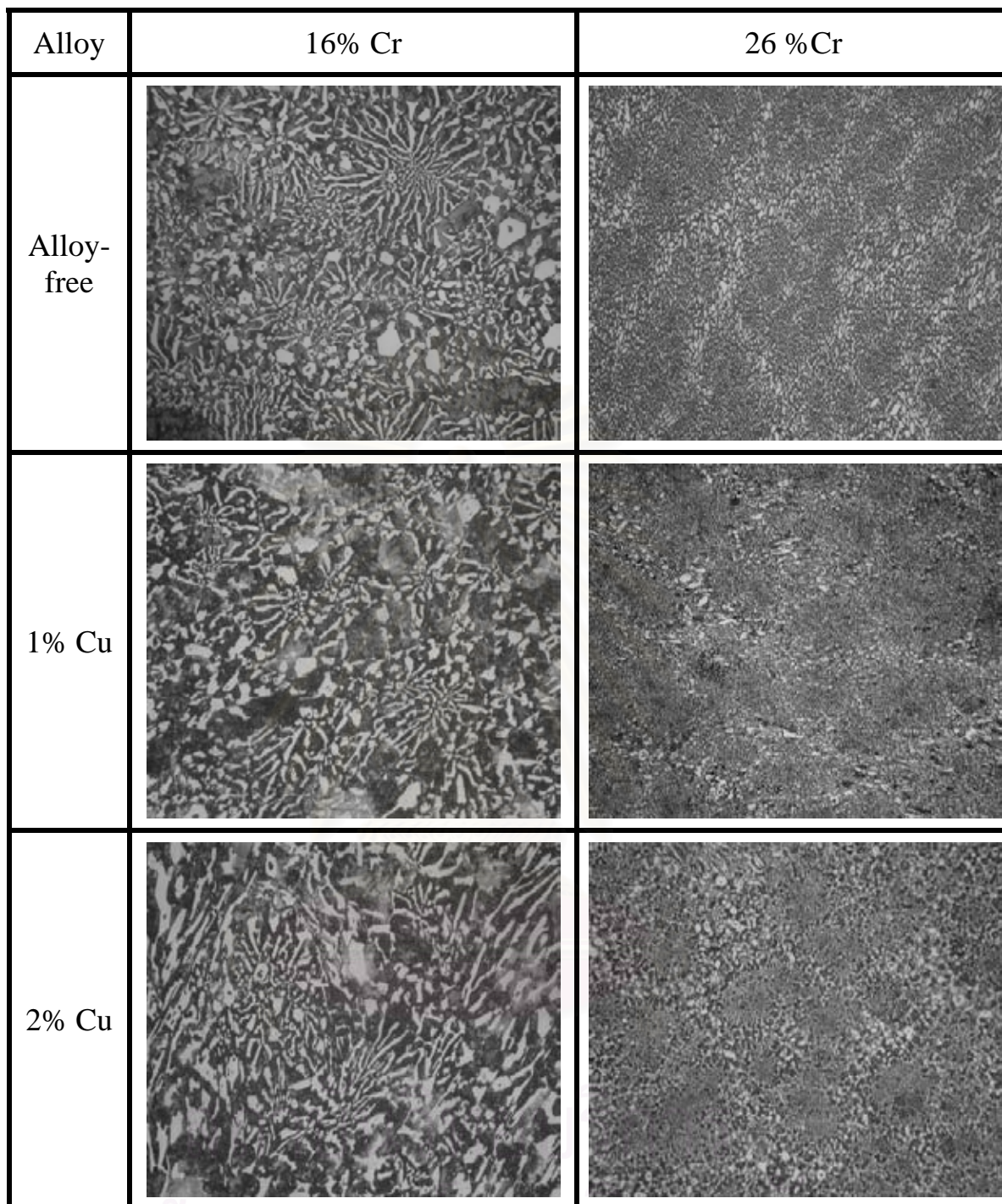| Alloy	16% Cr	26 %Cr
Alloy-free		
1% Cu		
2% Cu		

50 μm

Fig. 4.40 As-cast microstructures of 16% Cr and 26% Cr eutectic cast irons with and without Cu. Matrices of 16% Cr cast irons are all prarlitic regardless of Cu content. Those in 26% Cr cast irons are all austenitic possibly with martensite but it can not distinguish from this microphotographs.

(b) Effect of Cu content on variation of macro-hardness and volume fraction of retained austenite (Vγ) during heat treatment

-As-hardened state

Macro-hardness and Vγ of as-hardened specimens are shown in Table 4.13. The hardness is closely related to the chemical composition and condition of heat treatment. Effect of Cu content on the macro-hardness and Vγ is shown in Fig. 4.41 (a) and (b). In the case of 1273 K austenitization, the hardness of 16% Cr specimen increases a little while that of alloy-free specimens decreases greatly as Cu content increases, ranging from 763 HV30 to 800 HV30. On the other hand, the hardness of 26% Cr specimens gradually decreases from 770 HV30 to 740 HV30 as Cu content increases. In the case of 1323 K austenitization, the hardness of 16% Cr specimens decreases from 740 HV30 to 675 HV30, but that of 26%Cr specimens does not change at about 780 HV30 with an increase in Cu content. At the same Cu content, an increase in the austenitizing temperature results in low hardness in 16%Cr specimens and high hardness in 26%Cr specimens. According to an increase in Cu content, the Vγ of 16%Cr specimens increases from 28.8% to 38% in 1273 K and 41% to 59.3% in 1323 K austenitization and that of 26% Cr specimens from 3.8% to 4.1% in 1273 K and 12.1% to 14.1% in 1323 K austenitization. It is found that the Vγ changes little in both chromium specimens even if the austenitizing temperature is varied.

The microstructures of as-hardened 16% Cr and 26% Cr specimens are shown in Fig. 4.42. The matrix structures of all specimens consist of small particle of carbide, austenite and martensite. In 16%Cr specimens, most of pearlite which existed in as-cast state is greatly reduced, and instead, secondary carbides, austenite and martensite are appeared. In 26% Cr specimens, austenite in as-cast state is destabilized and replaced by martensite and secondary carbides. It is found that the amount of secondary carbides seems to be more in 16%Cr specimens than that in
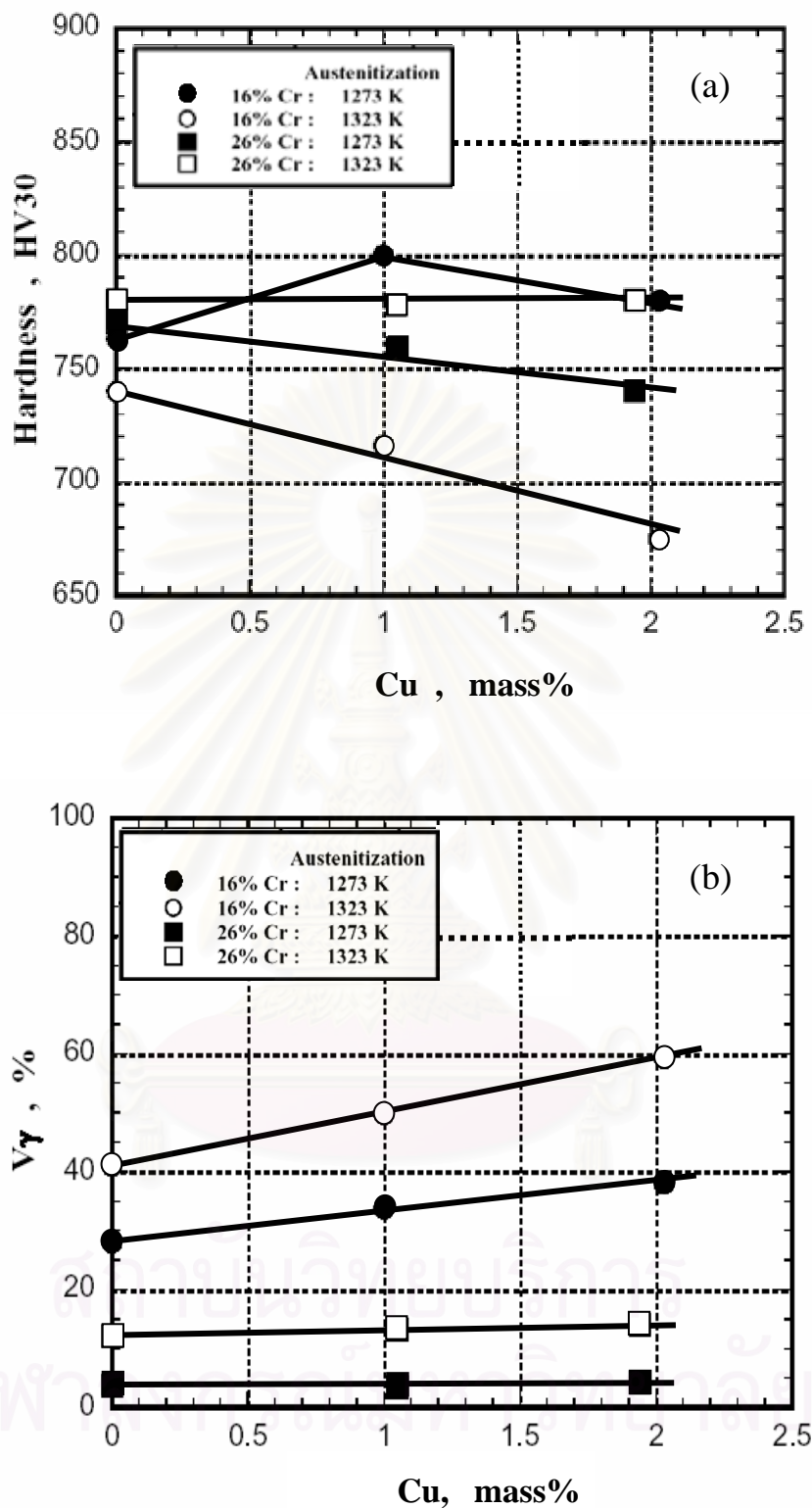
Fig. 4.41 Effect of Cu content on macro-hardness (a) and Vγ (b) of as-hardened specimens.

Alloy	16% Cr	26 %Cr
Alloy-free		
1% Cu		
2% Cu		

5 µm
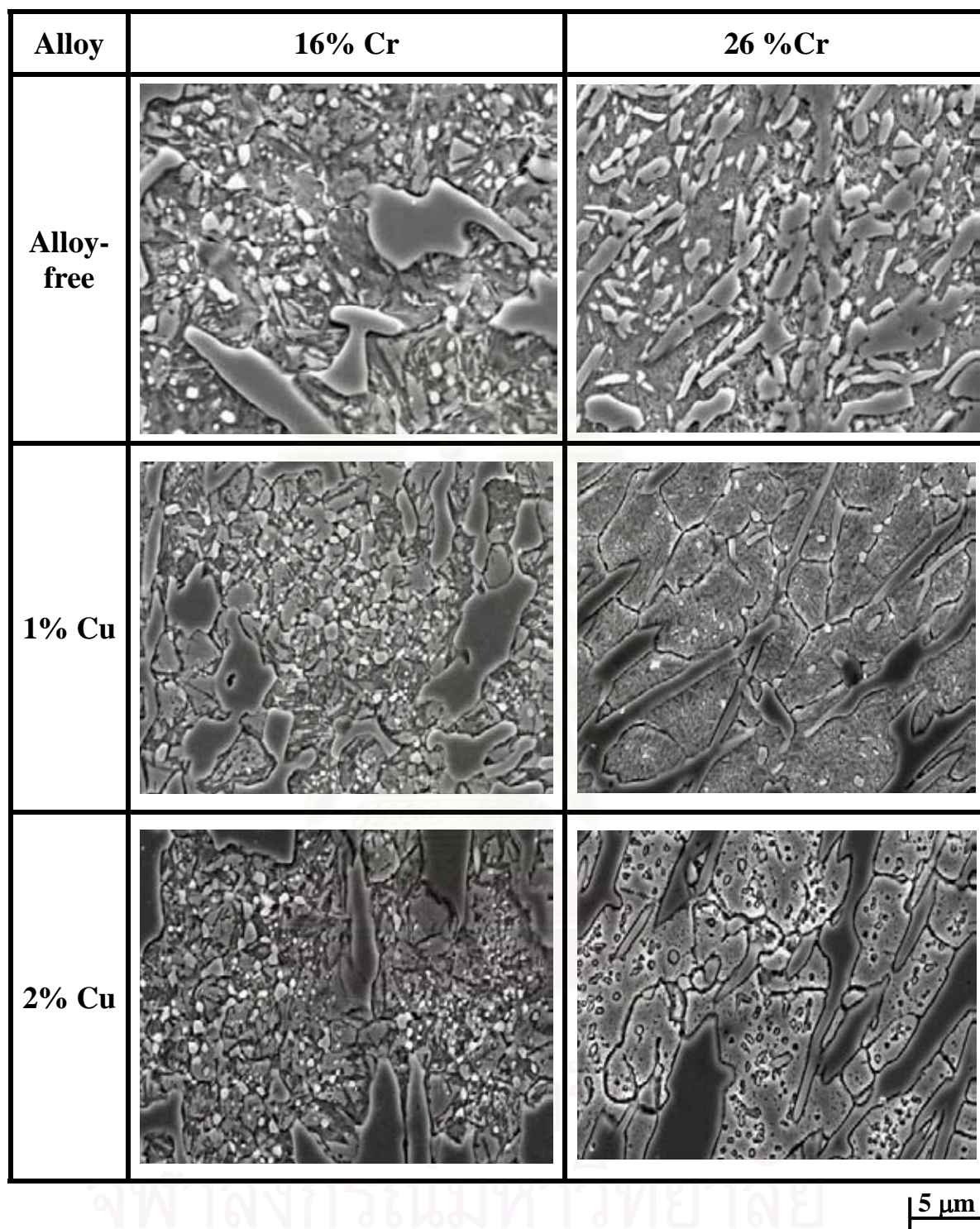
Fig. 4.42 As-hardened microstructures of 16% Cr and 26% Cr eutectic high chromium cast irons with and without Cu. Secondary carbides precipitate in the matrices of austenite and martensite but number of precipitated carbides is more in 16% Cr cast irons.

26% Cr specimens when compared with the same Cu level.

- Tempered state

In the same way, the specimens hardened from two levels of austenitization, 1273 K and 1323 K were tempered at several temperatures from 573 K to 873 K. The relationship between hardness, Vγ and tempering temperature of alloy-free specimen are already shown in the previous section, Fig. 4.34 for 16% Cr specimen (No.1) and Fig. 4.37 for 26% Cr specimen (No. 4) specimen, respectively. The results of tempering behaviors of alloyed cast irons with a third alloying element are shown in Fig. 4.43 and Fig. 4.44 for 16%Cr specimens and Fig. 4.45 and Fig. 4.46 for 26% Cr specimens. The degree of secondary hardening in each specimen is summarized in Table 4.14. It is noted that the degree becomes greater when Cu is added to the cast iron.

Table 4.14 Degree of secondary hardening of specimens.

Specimens	Element (mass %)		Degree of secondary hardening (HV30)	
	Cr	Cu	1273 K austenitization	1323 K austenitization
No. 1	16	-	45	85
No. 2		1	48	161
No. 3		2	91	226
No. 4	26	-	18	44
No. 5		1	64	87
No. 6		2	87	100

(i) 16%Cr cast iron

Fig. 4.43 shows the relationship between macro-hardness, $V\gamma$ and tempering temperature of specimen with 1% Cu (No.2). In the tempered hardness curves, the hardness of specimens hardened from 1323 K are lower than those hardened from 1273 K while the tempering temperature is less than 730 K. This reason is due to the fact that much more retained austenite exists in the matrix. When the specimens are tempered at over 730 K, the hardness are reversed. In the case of 1273 K austenitization, the hardness increases gradually when tempering temperature rises over 673 K. However, the hardness begins to increase from 623 K in the case of 1323 K austenitization. As shown in Table 4.14, the degrees of secondary hardening are 48 HV30 in 1273 K and 161 HV30 in 1323 K austenitization, respectively. The H_{Tmax} values of 823 HV30 and 849 HV30 are obtained in the specimens tempered at 760 K in 1273 K and 780 K in 1323 K austenitization, respectively. It is clear that the H_{Tmax} is high in the case of high austenitization and the tempering temperature to obtain the H_{Tmax} shifts to the high temperature side.

It is a same way that the $V\gamma$ decreases as the tempering temperature increases. The tempering temperatures at which the $V\gamma$ gets to 0% are 760 K in 1273 K and 780 K in 1323 K austenitization. The $V\gamma$ values at H_{Tmax} are about 10% in both the austenitizing temperatures.

The results of 2% Cu specimen (No. 3) are shown in Fig. 4.44. The tempering behaviors are similar to those of specimen No. 2. The degree of secondary hardening is much larger in the specimen hardened from the higher austenitizing temperature of 1323 K, 226 HV30, but it is remarkable even in the specimens hardened from 1273 K, 91 HV30. The H_{Tmax} values are 830 HV30 in 1273 K and 848 HV30 in 1323 K austenitization. The tempering temperature at the H_{Tmax} is higher of about 25 K in 1323 K austenitization than in 1273 K austenitization.

The tempering temperatures at which the retained austenite disappears all are 760 K in 1273 K and 780 K in 1323 K austenitization.

Fig. 4.43 Relationship between macro-hardness, volume fraction of retained austenite (Vγ) and tempering temperature of 16% Cr eutectic high chromium cast iron with 1% Cu. (Specimen No. 2)

Fig. 4.44 Relationship between macro-hardness, volume fraction of retained austenite (Vγ) and tempering temperature of 16% Cr eutectic high chromium cast iron with 2% Cu. (Specimen No. 3)

The $V\gamma$ values at the H_{Tmax} are 4% at 748 K in 1273 K and 10% at 748 K tempering in 1323 K austenitization, respectively.

(ii) 26%Cr cast iron

Fig. 4.45 shows the relationship between hardness, $V\gamma$ and tempering temperature of 1% Cu specimen (No.5). The behaviors of tempered hardness curves are a little different from those of 16%Cr specimens, that is, the hardness of specimen hardened from 1323 K are overall higher than those hardened from 1273 K. The degrees of secondary hardening are more compared with alloy-free specimen and they are 64 HV30 in 1273 K and 87 HV30 in 1323 K austenitization. The H_{Tmax} values are 769 HV30 at 723 K in 1273 K and 820 HV30 at 748 K tempering in 1323 K austenitization, respectively.

The $V\gamma$ values in as-hardened state of 4% in 1273 K and 13% in 1323 K austenitization decrease with an increase in the tempering temperature. In the case of 1273 K, the $V\gamma$ does not change until the tempering temperature of 623 K and then it decreases to 0% at 723 K. In the case of 1323 K austenitization, the $V\gamma$ decreases gradually to 773 K at which the $V\gamma$ is 0%. The $V\gamma$ values at H_{Tmax} are almost 0% in 1273 K and 4% in 1323 K austenitization.

Fig. 4.46 shows the results of 2% Cu specimen (No.6). The remarkable secondary hardening can be seen in both austenitizing temperatures. The degrees are greatest in Cu containing specimens, 87 HV30 in 1273 K and 100 HV30 in 1323 K austenitization. The H_{Tmax} values are 760 HV30 in 1273 K and 823 HV30 in 1323 K austenitization. The tempering temperatures at the H_{Tmax} are 723 K and 748 K in 1273 K and 1323 K austenitization, respectively.

By tempering, the $V\gamma$ in 1273 K austenitization slightly decreases to 0% at 723 K and that in 1323 K austenitization reduces greatly to 0% at 773 K. The $V\gamma$ values at the H_{Tmax} are 2% in 1273 K and 5% in 1323 K austenitization.

Fig. 4.45 Relationship between macro-hardness, volume fraction of retained austenite (Vγ) and tempering temperature of 26% Cr eutectic high chromium cast iron with 1% Cu. (Specimen No. 5)
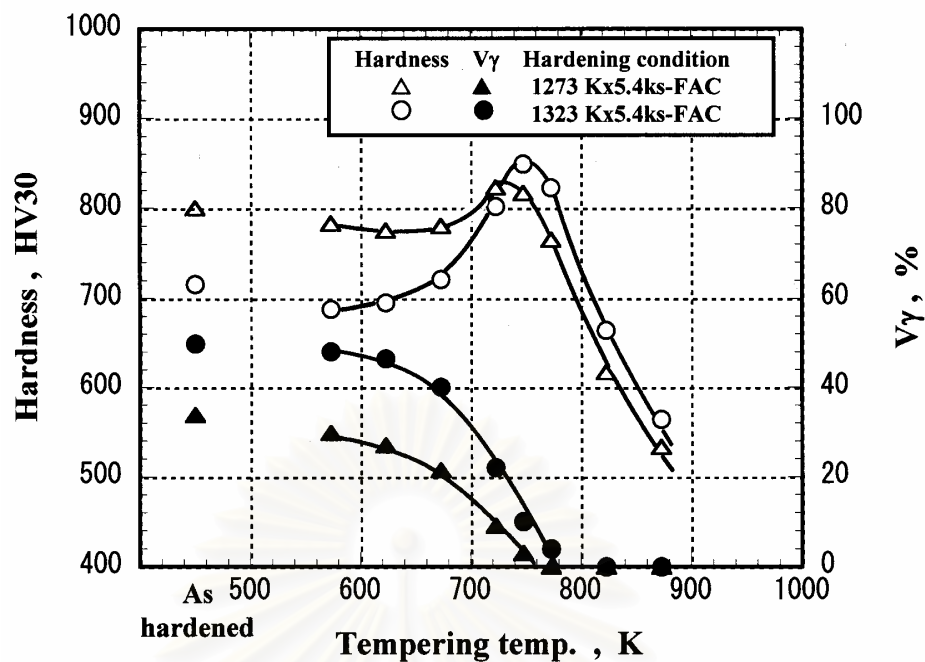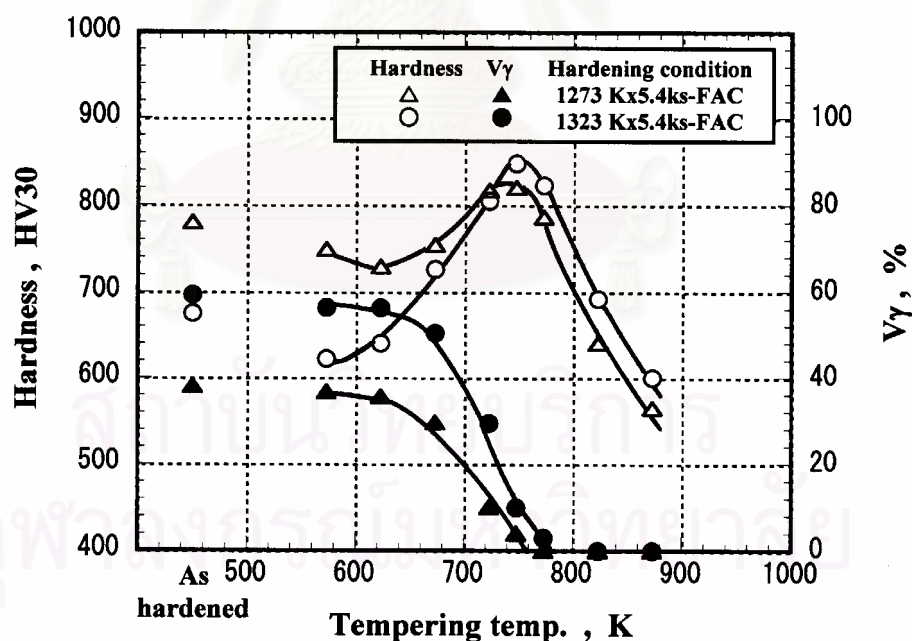

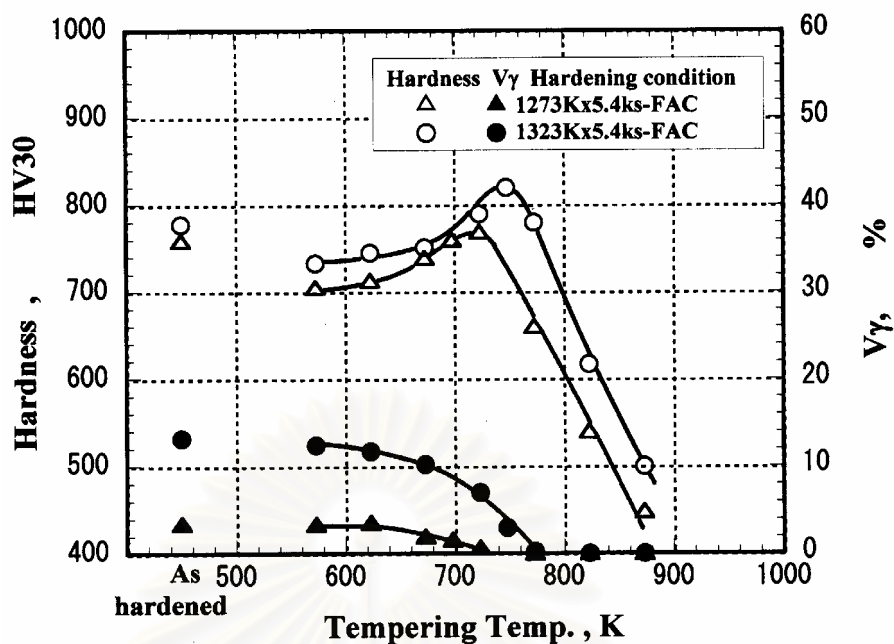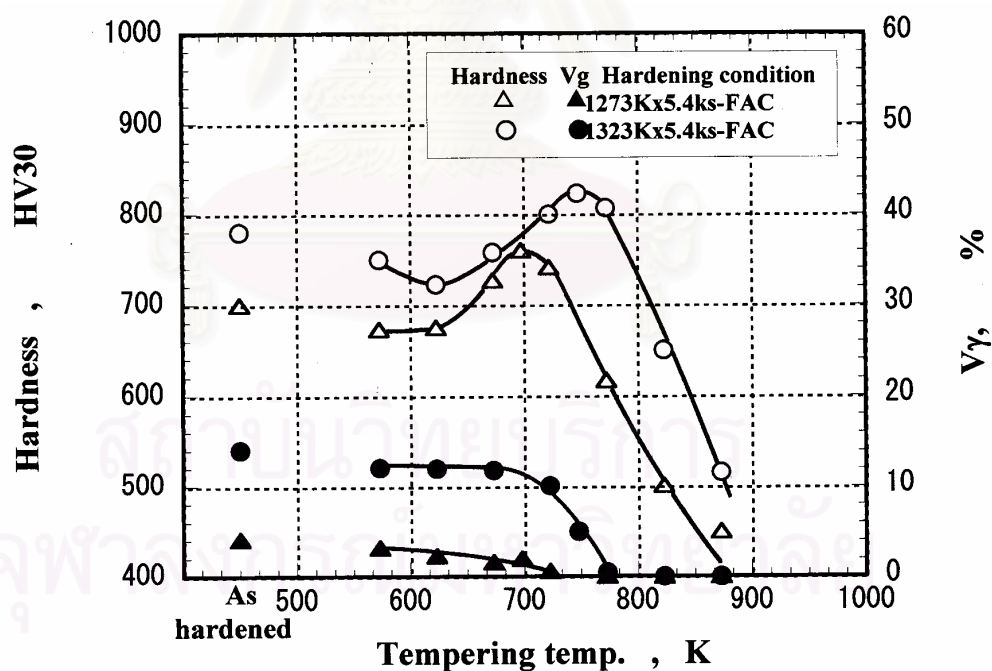Fig. 4.46 Relationship between macro-hardness, volume fraction of retained austenite (Vγ) and tempering temperature of 26% Cr eutectic high chromium cast iron with 2% Cu. (Specimen No. 6)

4.2.2.3 Effect of molybdenum (Mo)

(a) Test specimen in as-cast state

The chemical compositions of test specimens are shown in Table 4.15. Mo was added up to 3% in the both 16% Cr and 26% Cr cast irons. The as-cast microstructures of alloy-free and Mo specimens are shown in Fig. 4.47. The carbide structure seems to be coarser in Mo specimens compared with alloy-free specimen and it becomes larger with increasing Mo content. Particularly, the eutectic colony size enlarges by the addition of Mo. In 16% Cr specimens, the matrix structure of alloy-free specimen is pearlitic. The matrix in 1% Mo specimen is mostly pearlite with some retained austenite. The greater part of matrix in specimens with Mo content over 2% is mixture of austenite and small amount of martensite. In 26% Cr specimens, the matrices of the specimens with or without Mo consist of austenite and possibly some martensite but the difference in matrix structure according to the amount of Mo can not be distinguished from the microphotographs.

Macro-hardness and Vγ of the specimens without and with Mo in as-cast state are summarized in Table 4.16. Regardless of Cr content, the hardness of specimens with 1% Mo are higher than that in alloy-free specimens. However, an increase in Mo content makes the hardness low and those with 3% Mo are lower than those of alloy-free specimens. The hardness values range from 543 HV30 to 710 HV30 in 16% Cr specimens, 630 HV30 to 670 HV30 in 26% Cr specimens. The Vγ value varies remarkably depending on Mo content. The Vγ in alloy-free specimen with 16% Cr is zero and it increases by the addition of Mo, 8.7% at 1% Mo to 85.2% at 3% Mo. In 26% Cr specimens, the Vγ of alloy-free specimen is 33.7% and it increases from 56.8% at 1% Mo to 70.4% at 2% Mo. These variations of Vγ give good correspondence to those of the hardness.

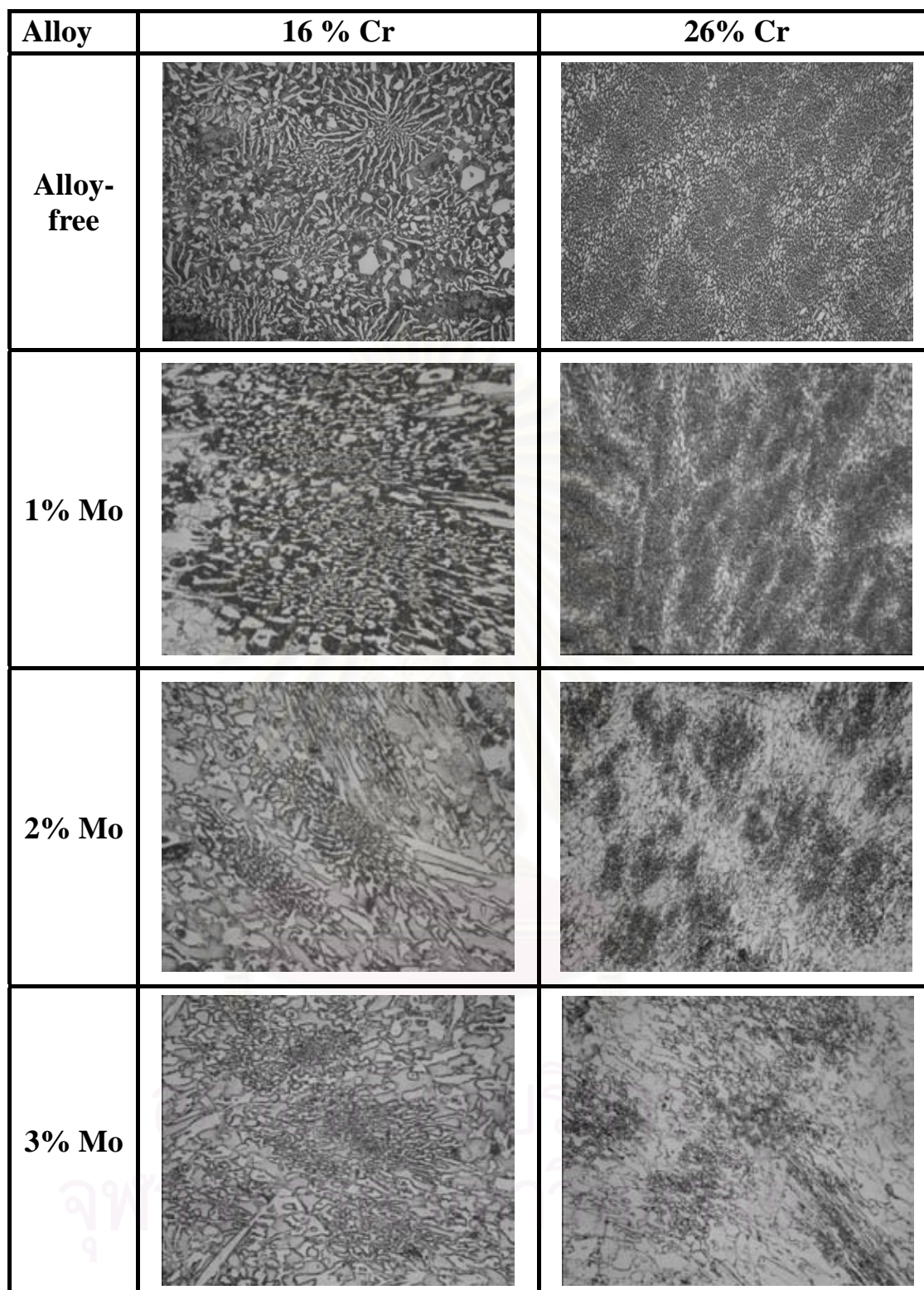| Alloy	16 % Cr	26% Cr
Alloy-free		
1% Mo		
2% Mo		
3% Mo		

50 µm

Fig. 4.47 As-cast microstructures of 16% Cr and 26% Cr eutectic cast irons with and without Mo. Austenitic increases with an increase in Mo content in 16% Cr cast irons but matrices are all austenitic in 26% Cr cast irons regardless of Mo content.

Table 4.15 Chemical compositions of test specimens.

Specimen	Element (mass%)							
	C	Cr	Si	Mn	Ni	Cu	Mo	V
No.1	3.45	16.01	0.39	0.67	-	-	-	-
No.2	3.56	15.74	0.57	0.45	-	-	0.92	-
No.3	3.64	15.52	0.51	0.49	-	-	2.02	-
No.4	3.70	15.93	0.53	0.49	-	-	2.96	-
No.5	2.99	25.78	0.51	0.54	-	-	-	-
No.6	3.00	25.55	0.68	0.54	-	-	1.05	-
No.7	2.98	25.59	0.66	0.53	-	-	2.00	-
No.8	2.90	25.88	0.57	0.63	-	-	2.85	-

* S and P are less than 0.06 mass%

Table 4.16 Macro-hardness and volume fraction of retained austenite ($V\gamma$) of as-cast specimens.

Specimen	Element (mass%)		HV30	$V\gamma$, %
	Cr	Mo		
No. 1		-	578	0.0
No. 2	16	1	710	8.7
No. 3		2	621	43.7
No. 4		3	543	85.2
No. 5		-	664	33.7
No. 6	26	1	670	56.8
No. 7		2	638	69.2
No. 8		3	630	70.4

(b) Effect of Mo content on variation of macro-hardness and volume fraction of retained austenite (Vγ) during heat treatment

-As-hardened state

The results of macro-hardness and Vγ of test specimens are shown in Table 4.17 and they are graphically shown in Fig. 4.48 (a) and (b). In both Cr specimens, the hardness are overall higher than those of alloy-free specimen and they increase roughly in proportion to Mo content. In 16%Cr specimens, it rises from 763 HV30 at 0% Mo to 936 HV30 at 3% Mo in 1273 K and 740 HV30 at 0% Mo to 793 HV30 at 3% Mo in 1323 K austenitization, respectively. The hardness of 26% Cr specimens increase from 770 HV30 to 850 HV30 in 1273 K and 780 HV30 to 910 HV30 in 1323 K austenitization, respectively, when Mo content rises from 0% to 3%.

The Vγ increases proportionally as Mo content increases except for 16% Cr specimen hardened from 1273 K of which hardness change little by Mo content. The Vγ of 16% Cr specimens hardened from 1323 K varies from 51% at 1% Mo to 61% at 3% Mo. In 26% Cr specimens, the Vγ values are lower than those of 16% Cr specimens and they increase from 3.8% at 0% Mo to 14% at 3% Mo in 1273 K and 12.1 % at 0% Mo to 23 % at 3% Mo in 1323 K austenitization, respectively. With respect to the effect of austenitizing temperature, the hardness is substantially lower and the Vγ is much higher in 16% Cr specimens when the austenitizing temperature is increased from 1273 K to 1323 K. This is because Mo as well as C and Cr dissolves more in austenite at higher austenitizing temperaturea and makes austenite stable.

As-hardened microstructures are shown in Fig. 4.49. The matrix structures of all specimens consist of secondary carbides, austenite and martensite. The secondary carbides were densely precipitated in the central region of austenite and less near eutectic carbides. It is found that the pearlitic and austenitic matrices in as-cast state are replaced by those

Table 4.17 Macro-hardness and volume fraction of retained austenite (Vγ) of as-hardened specimens.

Specimen	Element (mass%)		Austenitizing Temperature (K)			
	Cr	Mo	1273		1323	
			HV30	Vγ, %	HV30	Vγ, %
No. 1	16	-	763	28.8	740	41.0
No. 2		1	854	28.0	756	51.0
No. 3		2	890	29.7	780	56.5
No. 4		3	936	30.3	793	61.1
No. 5	26	-	770	3.8	780	12.1
No. 6		1	787	6.5	836	12.5
No. 7		2	812	10.4	876	17.6
No. 8		3	850	14.0	910	23.0

of fine secondary carbides, austenite and martensite. In the specimens with the same Mo content, the secondary carbide particles are smaller in 26% Cr specimen than those in 16% Cr specimen.

-Tempered state

The relationships between macro-hardness, Vγ and tempering temperature are shown in Fig. 4.50 to Fig. 4.52 for 16% Cr specimens and Fig. 4.53 to Fig. 4.55 for 26%Cr specimens, respectively. In each diagram, the hardness and Vγ in as-hardened state are plotted for comparison. In this group of specimens, the secondary hardening occurs and then the digital data are listed in Table 4.18.

(i) 16%Cr cast iron

Fig. 4.50 shows the relationship between the macro-hardness, Vγ and tempering temperature of 1% Mo specimen (No. 2). When compared with alloy-free specimen in Fig. 4.34, the tempered hardness curves show similar behavior. In the range of tempering temperature less than 773 K,
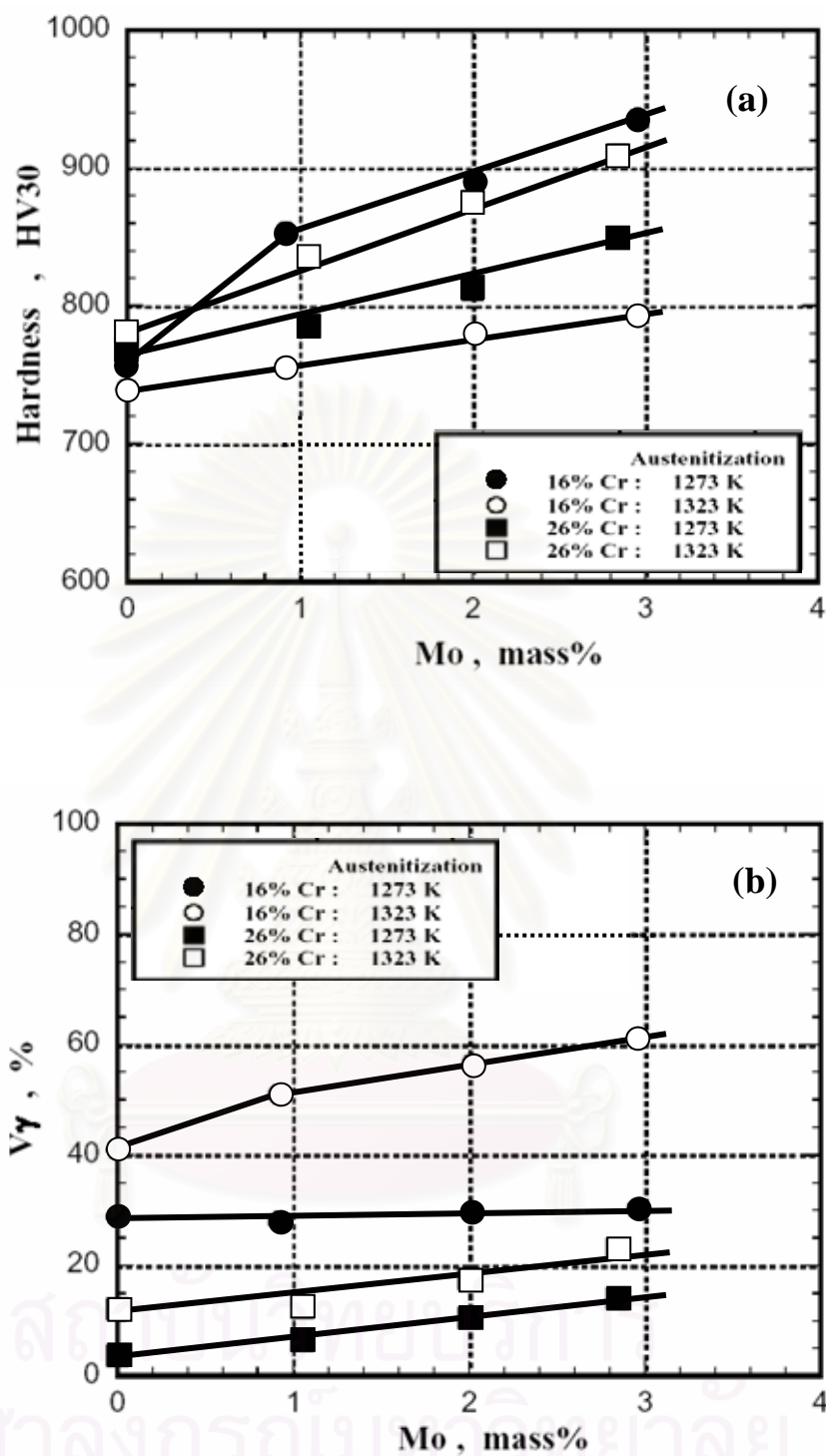
Fig. 4.48 Effect of Mo content on macro-hardness (a) and Vγ (b) in as-hardened state.

Alloy	16 % Cr	26% Cr
Alloy-free		
1% Mo		
2% Mo		
3% Mo		

Fig.4.49 SEM microphotographs in as-hardened state of 16% Cr $\vdash$5 μm$\dashv$ and 26% Cr eutectic cast irons with and without Mo. Matrix consist of secondary carbides, martensite and retained austenite in all cast irons. However, numbers of secondary carbides in 16% Cr and 26% Cr cast irons are less than in cast irons with alloying elements of Ni and Cu.

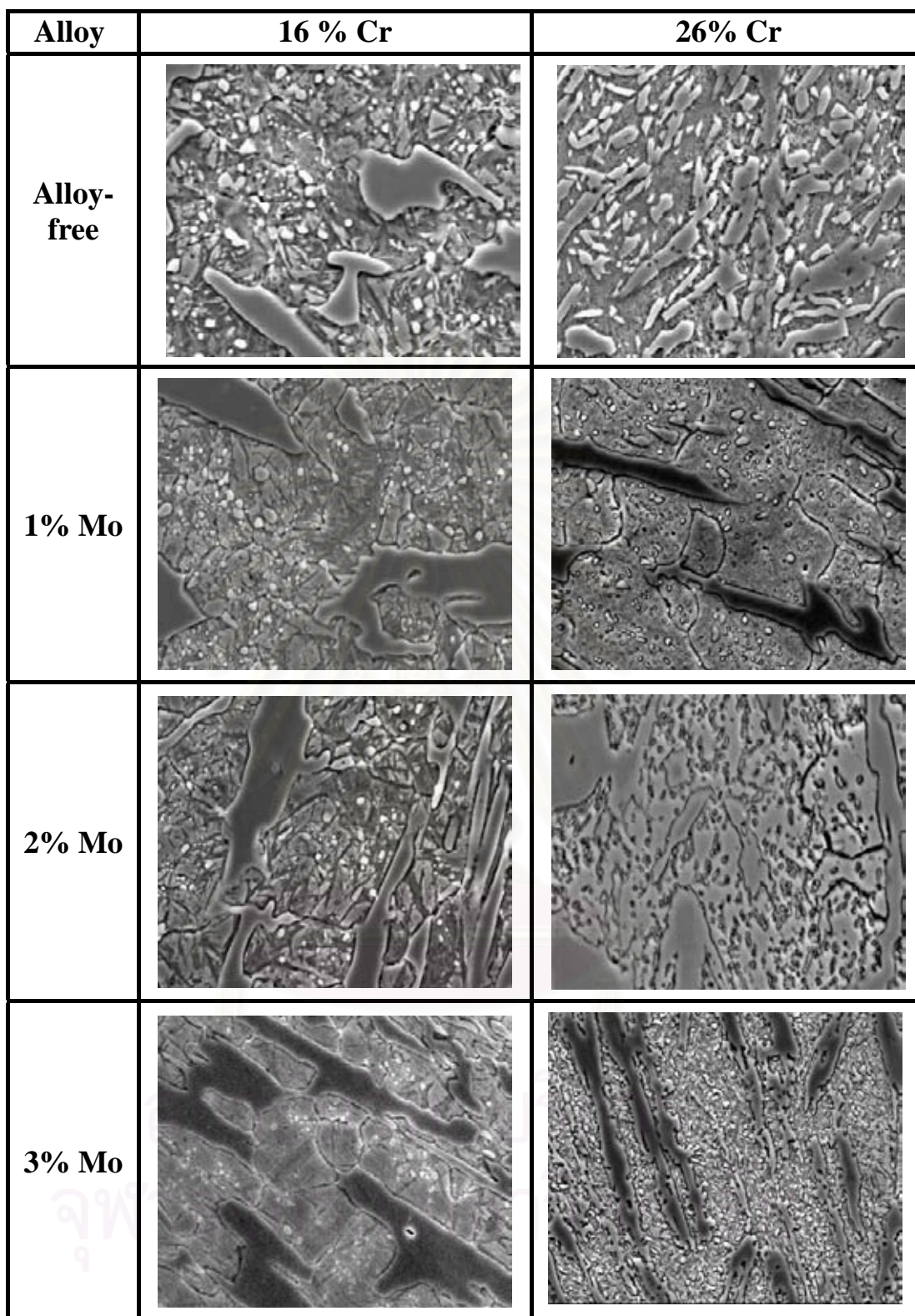Table 4.18 Degree of the secondary hardening of test specimens.

Specimen	Element (mass%)		Degree of the secondary hardening (HV30)	
	Cr	Mo	1273 K austenitization	1323 K austenitization
No. 1	16	-	45	85
No. 2		1	74	129
No. 3		2	50	168
No. 4		3	78	196
No. 5	26	-	18	44
No. 6		1	55	50
No. 7		2	78	81
No. 8		3	55	93

the hardness of specimens hardened from 1323 K are lower than those in 1273 K. Over 773 K, the hardness is conversed. The degree of the secondary hardening is much larger when compared with alloy-free specimen and also it is much greater in the specimens hardened from 1323 K, 74 HV30 in 1273 K and 129 HV30 in 1323 K austenitization. The H_{Tmax} obtained in the specimen hardened from 1273 K is 847 HV30 at 748 K and that in the specimen hardened from 1323 K is 856 HV30 at 798 K.

The $V\gamma$ values of 28% and 51% in as-hardened state begin to reduce remarkably as the tempering temperature rises over 673 K regardless of austenitizing temperature and gets to 0% at 773 K in 1273 K and 810 K in 1323 K austenitization. The $V\gamma$ value at the H_{Tmax} value is 4% in both austenitizing temperatures. It is clear from these results that the H_{Tmax} is high in the specimens obtained from high austenitization. The tempering temperature at the H_{Tmax} shifts to the high temperature side under the same holding time.

The results of 2% Mo specimen (No. 3) are shown in Fig. 4.51, the curves of tempered hardness behave the same tendency as those of alloy-free and 1% Mo specimens. In the range of low tempering temperature,

Fig. 4.50 Relationship between macro-hardness, volume fraction of retained austenite (Vγ) and tempering temperature of 16%Cr cast iron with 1% Mo. (Specimen No. 2)

Fig. 4.51 Relationship between macro-hardness, volume fraction of retained austenite (Vγ) and tempering temperature of 16%Cr cast iron with 2% Mo. (Specimen No. 3)
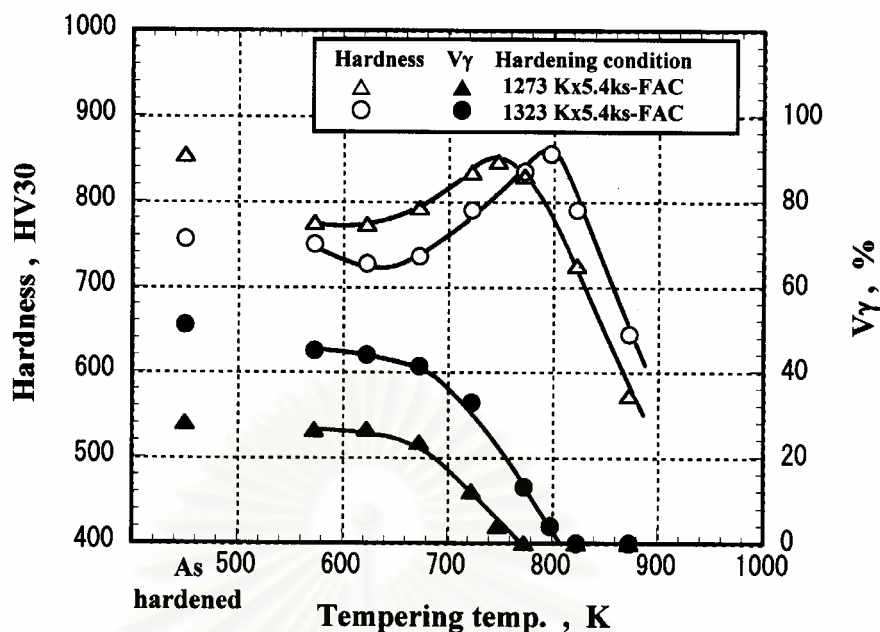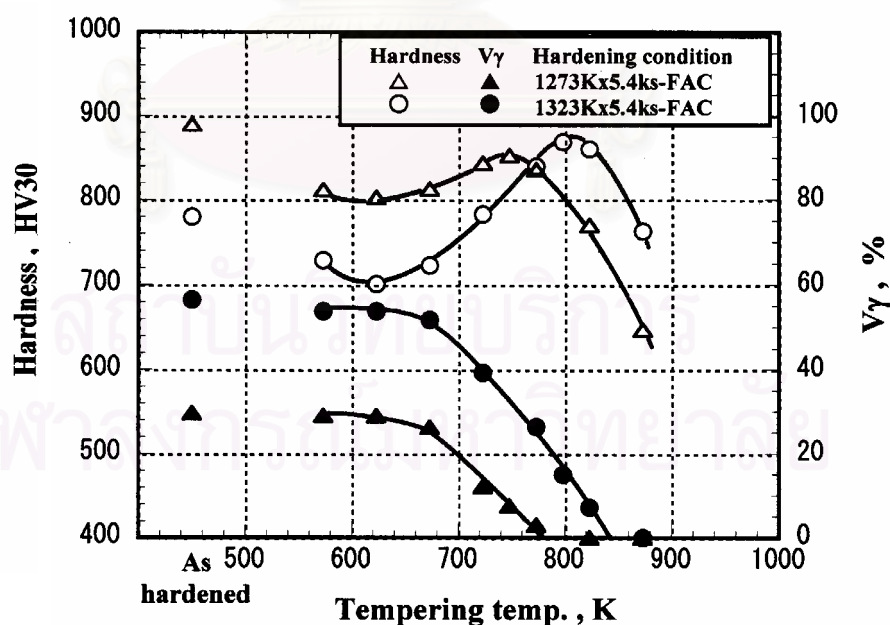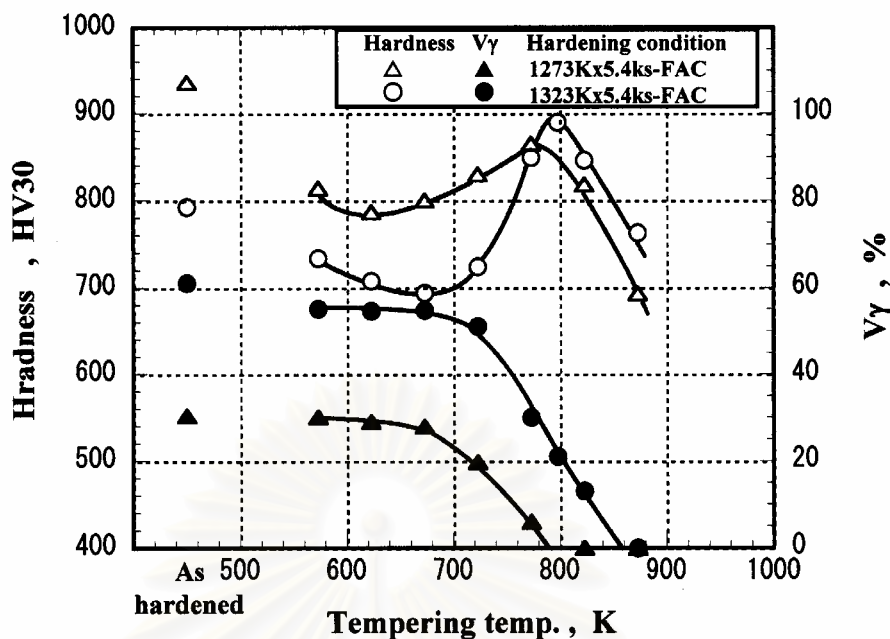
Fig. 4.52 Relationship between macro-hardness, volume fraction of retained austenite (Vγ) and tempering temperature of 16%Cr cast iron with 3%Mo. (Specimen No. 4)

the hardness of specimen hardened from 1273 K is high at lower temperature range than 773 K and it is conversed at the temperature over 773 K. The clear secondary hardening is obtained in each curve and it is greater when compared with alloy-free and 1% Mo specimens. An increase in the austenitizing temperature results in more degree of the secondary hardening, 50 HV30 in 1273 K and 168 HV30 in 1323 K austenitization. The H_{Tmax} is 870 HV30 at 773 K in the specimen hardened from 1323 K and 853 HV30 at 798 K in the specimen hardened from 1273 K, respectively.

The Vγ values begin to reduce gradually when the tempering temperature is raised over 673 K. The Vγ gets to 0% at 780 K in 1323 K and 840 K in 1323 K austenitization. The Vγ values at H_{Tmax} are 10% and 15% in 1273 K and 1323 K austenitization, respectively.

The results of the specimen No.4 with 3% Mo are shown in Fig. 4.52. The tempered hardness curves show similar behavior to those in other 16% Cr specimens. The degree of secondary hardening is greatest

in the same group of 16% Cr specimens. They are 78 HV30 in 1273 K and 196 HV30 in 1323 K austenitization. The H_{Tmax} values of 865 HV30 at 773 K in 1273 K and 890 HV30 at 798 K in 1323 K austenitization, respectively.

The $V\gamma$ values in as-hardened state of 30% in 1273 K and 61% in 1323 K austenitization start to decrease after 673 K. The tempering temperatures at which the $V\gamma$ becomes to 0% are 790 K and 860 K in the specimens hardened from 1273 K and 1323 K, respectively. It is evident that an increase in austenitizing temperature needs higher tempering temperature to decompose all the retained austenite existed much more in as-hardened state. The $V\gamma$ values at the H_{Tmax} are 5% in 1273 K and 21% in 1323 K austenitization, respectively.

(ii) 26%Cr cast iron

Fig. 4.53 shows the relationship between hardness, $V\gamma$ and tempering temperature of specimen No. 6 with 1% Mo. There is not interchange obtained by two different austenitizing temperatures. The hardness of specimen hardened from 1323 K are overall higher than those hardened from 1273 K. The degree of secondary hardening is more when compared with alloy-free specimen and it is not affected by the austenitizing temperature, 55 HV30 in 1273 K and 50 HV30 in 1323 K austenitization. The H_{Tmax} values are 820 HV30 and 836 HV30 in 1273 K and 1323 K austenitization, respectively. In the case of high austenitizing temperature, the H_{Tmax} value is obtained at higher tempering temperature side, 698 K in 1273 K and 748 K in 1323 K austenitization.

In the case of 1273 K austenitization, the $V\gamma$ does not change until 698 K and over the 698 K, it decreases to 0% at 773 K. In the case of 1323 K, the $V\gamma$ decreases gradually to 0% at 773 K as the tempering temperature increases. The $V\gamma$ values at the H_{Tmax} are about 4% in the both austenitization.

The results of 2% Mo specimen (No. 7) are shown in Fig. 4.54. Here appear twice interchange in tempered hardness curves. It is higher in the specimens hardened from 1273 K in the range of tempering temperatures between 673 and 730 K. It is found that the greater degree of precipitation hardening is obtained in this 2% Mo specimen when compared with alloy-free and 1% Mo specimen. The degrees are similar in both austenitization, 78 HV30 in 1273 K and 81 HV30 in 1323 K. The H_{Tmax} values are 884 HV30 at 723 K tempering in 1273 K austenitization and 905 HV30 at 748 K in 1323 K.

The Vγ values in as-hardened state are 10% in 1273 K and 18 % in 1323 K austenitization, respectively. With an increase in the tempering temperature, both of them gradually decrease to 0% at 800 K in 1273 K and 823 K in 1323 K austenitization. The Vγ values at the H_{Tmax} are 4% in 1273 K and 7% in 1323 K austenitization.

The results of specimen No. 8 with 3% Mo is shown in Fig. 4.55. One interchange occurs in the tempered hardness curves at 723 K. This tendency is different from other specimens in the 26% Cr cast irons and it resemble to the tendency of 16% Cr specimens. In the rang of low tempering temperature less than 723 K, the hardness of the specimens hardened from 1273 K are more than those hardened from 1323 K, and over 723 K, the hardness curves are interchanged. The high degree of the secondary hardening in the specimen hardened from 1323 K is very high and the values are 55 HV30 in 1273 K and 93 HV30 in 1323 K austenitization. The H_{Tmax} values of 895 HV30 in 1273 K and 920 HV30 in 1323 K austenitization are obtained in the specimen tempered at 698 K and 748 K, respectively.

The Vγ values of 14% in 1273 K and 23% in 1323 K austenitization lower gradually with an increase in tempering temperature and they get to 0% at 820 K in 1273 K and 870 K in 1323 K austenitization. The Vγ values at the H_{Tmax} are 6% in 1273 K and 15% in 1323 K austenitization.

Fig. 4.53 Relationship between macro-hardness, volume fraction of retained austenite (Vγ) and tempering temperature of 26%Cr cast iron with 1%Mo. (Specimen No. 6)

Fig. 4.54 Relationship between macro-hardness, volume fraction of retained austenite (Vγ) and tempering temperature of 26% Cr cast iron with 2%Mo. (Specimen No. 7)
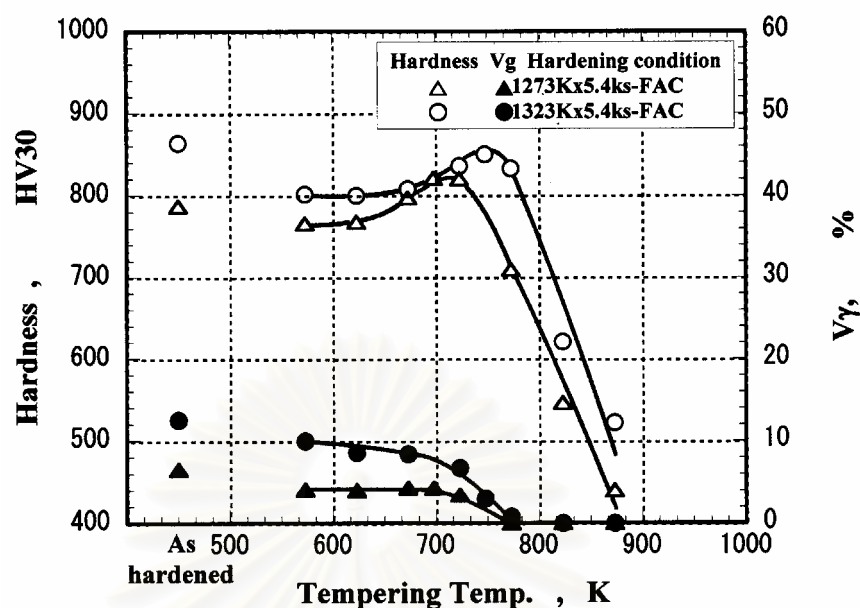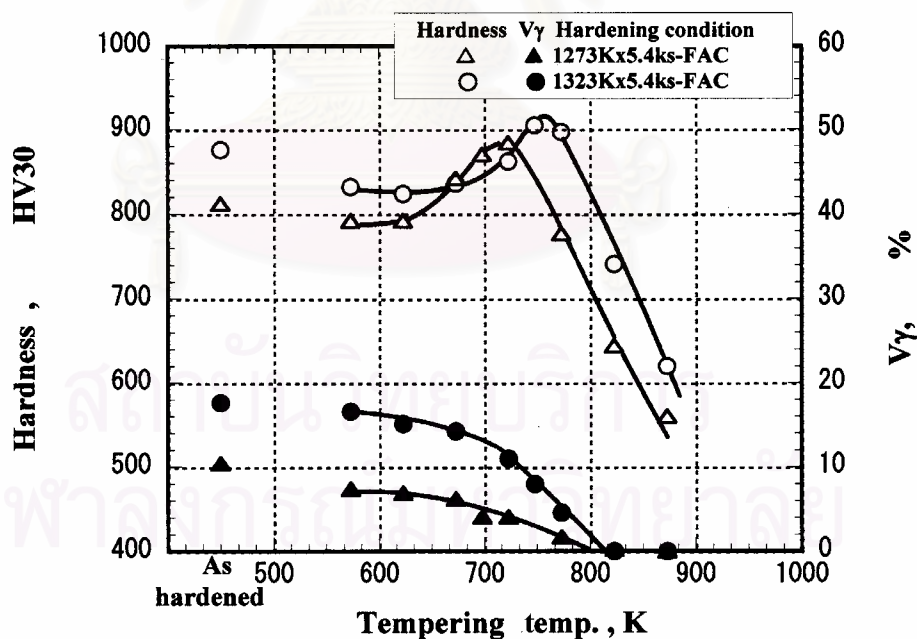
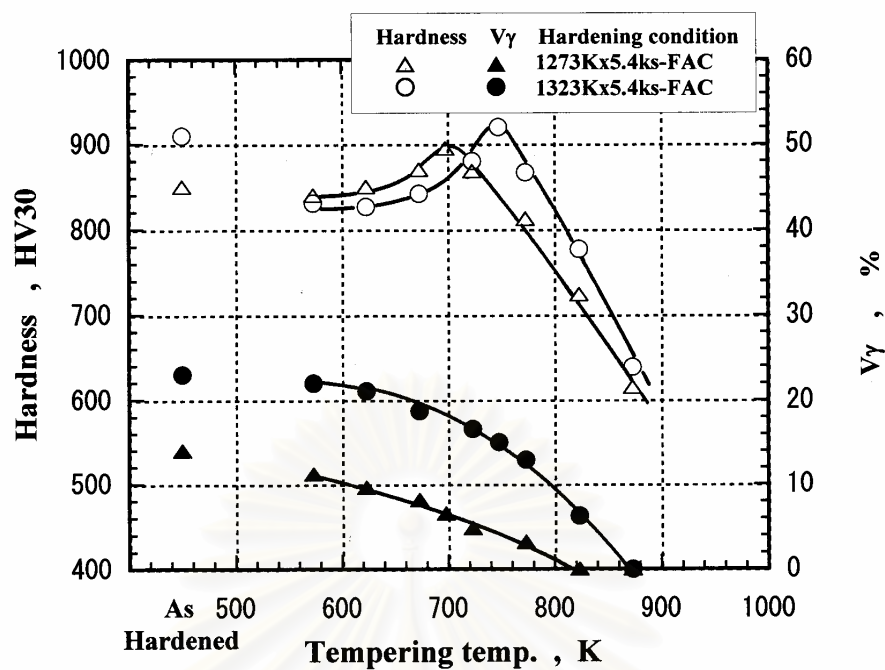Fig. 4.55 Relationship between macro-hardness, volume fraction of retained austenite (Vγ) and tempering temperature of 26% Cr cast iron with 3%Mo. (Specimen No. 8)

4.2.2.4 Effect of vanadium (V)

(a) Test specimen in as-cast state

The chemical compositions of test specimens are shown in Table 4.19. V was added up to 3% in both the 16% Cr and 26% Cr cast irons. As-cast microstructures of the test specimens are shown in Fig. 4.56. The 16% Cr specimens are mostly eutectic and 26% Cr specimens are perfectly eutectic. The microstructures consist of matrix and eutectic carbides which show the colony morphology. In the both groups of specimens, the sizes of eutectic carbides and $(\gamma+M_7C_3)$ eutectic colony seem to become small with an increase in V content. This is because V reduces the eutectic freezing range [51] and then fine eutectic structure is produced. The sizes of carbides and eutectic colony in 16% Cr specimens are much larger than those in 26% Cr specimens. The matrix structures of 16% Cr specimens are mostly pearitic but those in 26% Cr specimens are austenitic possibly with some martensite.

Macro-hardness and $V\gamma$ in as-cast specimens are shown in Table 4.20. The hardness does not change much even the V content increases and it seems to be a little high in 26% Cr specimens. They range from 564 HV30 to 586 HV30 in 16% Cr specimens and 664 HV30 to 695 HV30 in 26% Cr specimens. The $V\gamma$ values of 16% Cr specimens are all zero. This means that austenite fully transforms into pearlite as shown by the microphotographs in Fig. 4.52. In the case of 26%Cr specimens, on the other hand, the high $V\gamma$ values are measured and it decreases with an increase in V content, from 33.7% in 0% V to 10.1% in 3% V specimens. This suggests that V promote the transformation of austenite into pearlite.

Table 4.19 Chemical compositions of test specimens.

Specimen	Element(mass%)							
	C	Cr	Si	Mn	Ni	Cu	Mo	V
No.1	3.45	16.01	0.39	0.67	-	-	-	-
No.9	3.61	15.92	0.50	0.47	-	-	-	0.89
No.10	3.41	15.67	0.53	0.47	-	-	-	1.67
No.11	3.60	16.11	0.52	0.51	-	-	-	2.89
No.12	2.99	25.78	0.51	0.54	-	-	-	-
No.20	2.90	25.94	0.58	0.67	-	-	-	0.91
No.21	2.86	25.93	0.57	0.48	-	-	-	1.92
No.22	2.89	25.83	0.56	0.55	-	-	-	3.09

*S and P are less than 0.06 mass%

Table 4.20 Macro-hardness and volume fraction of retained austenite (Vγ) of as-cast specimens.

Specimen	Element (mass%)		HV30	Vγ, %
	Cr	V		
No.1	16	-	578	0
No.2		1	586	0
N0.3		2	585	0
No.4		3	564	0
No.5	26	-	664	33.7
No.6		1	695	34.4
No.7		2	680	22.1
No.8		3	668	10.1

Alloy	16%Cr	26% Cr
Alloy-free		
1%V		
2%V		
3%V		
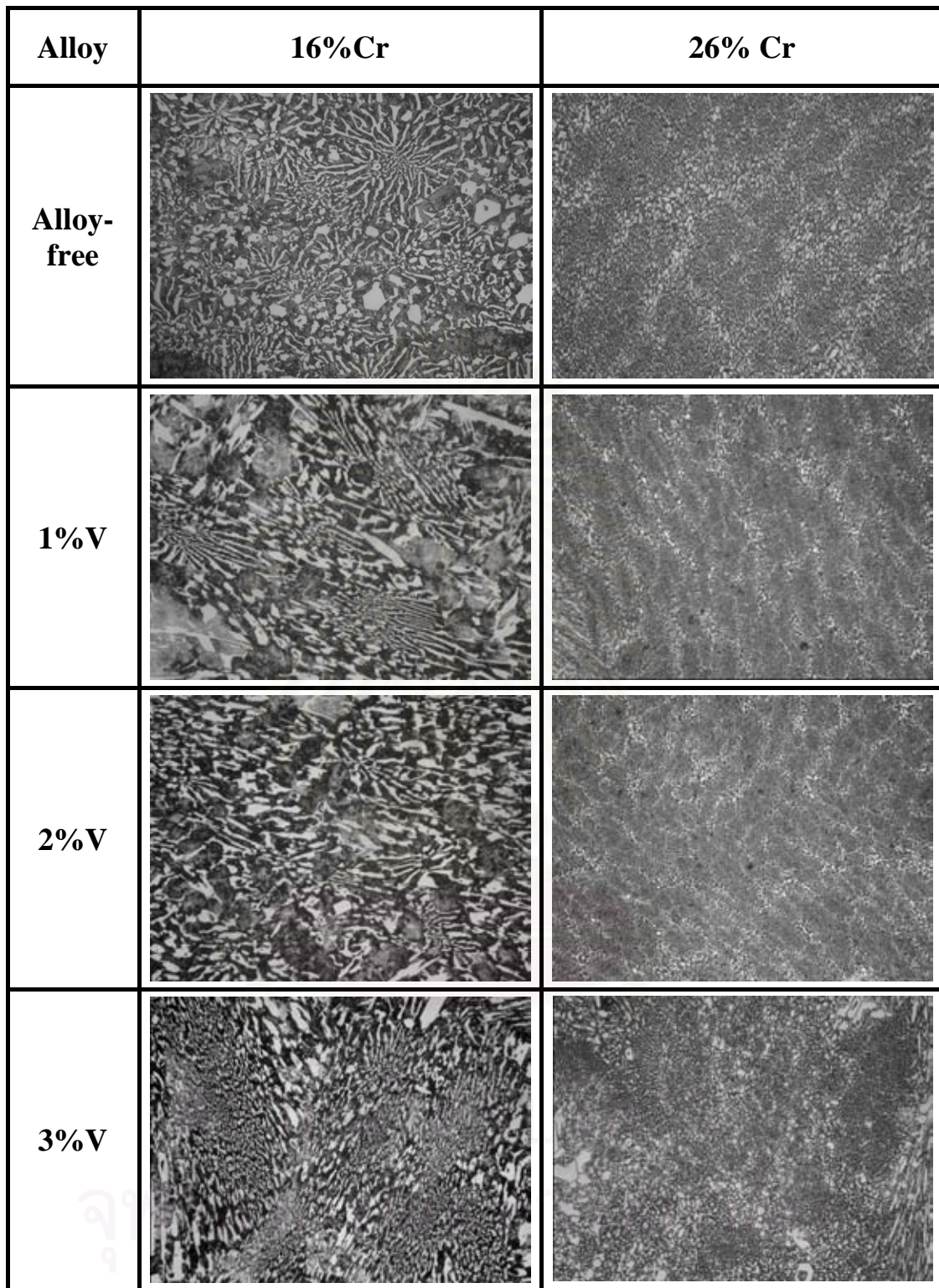
50 μm

Fig.4.56 As-cast microstructures of 16% Cr and 26% Cr eutectic cast irons with and without V. Matrices of 16% Cr cast irons are mostly pearlite but those in 26% Cr cast irons are austenitic and martensitic. Finer eutectic colony is obtained by V addition.

(b) Effect of V content on variation of macro-hardness and volume fraction of retained austenite (Vγ) during heat treatment

- As-hardened state

The hardness and Vγ of as-hardened specimens are shown in Table 4.21. The effects of V content are shown in Fig. 4.57 (a) and (b). As V content increases in 16% Cr specimens, the hardness increases remarkably from 763 HV30 in alloy-free specimen to 947 HV30 in 3% V specimen under 1273 K austenitization and 740 HV30 to 947 HV30 under 1323 K austenitization. In 26%Cr specimens, on the other hand, the hardness decreases with an increase in V content from 770 HV30 to 708 HV30 in 1273 K and 780 HV30 to 750 HV30 in 1323 K austenitization. At the same V content, the hardness of 16% Cr specimens is higher than that in 26% Cr specimen. Comparing the hardness by the austenitizing condition, the hardness is low in 16% Cr specimens but high in 26%Cr specimens at high austenitizing temperature of 1323 K.

As shown in Fig. 4.57 (b), the Vγ decreases with increasing V content in the both of 16% Cr and 26% Cr specimens. In 16% Cr specimens, the Vγ lowers in proportion to V content, from 28.8 % to 11.2% in 1273 K and 41% to 20.6% in 1323 K austenitization. In 26% Cr specimens, however, the reduction of Vγ is small and it ranges from 3% in alloy-free specimen to 0% at V% more than 1% in 1273 K and 12.1% to 2.5% in 1323 K austenitization. Even in the case of 1323 K austenitization, the reduction of Vγ is small in V containing specimens. The Vγ is overall more when the austenitizing temperature is high. From the above results, it is found that 26% Cr specimens have poor hardenability under the force air cooling, especially, in the specimens hardened from the low austenitizing temperature of 1273 K.

As-hardened SEM microphotographs of 16% Cr and 26% Cr eutectic specimens with V are shown in Fig. 4.58. The matrix structures in 16% Cr specimens consist of a larger number of secondary carbides, martensite and retained austenite. This suggests that the pearlite which exists much more in as-cast state dissolved back to the matrix by austenitization and resulted in high alloy concentration in austenite. In 26% Cr specimens, the

Table 4.21 Macro-hardness and volume fraction of retained austenite (Vγ)
of as-hardened specimens.

Specimen	Element (mass%)		Austenitizing Temperature (K)			
	Cr	V	1273		1323	
			HV30	Vγ, %	HV30	Vγ, %
No.1	16	-	763	28.8	740	41.0
No.2		1	840	20.6	800	36.6
No.3		2	913	16.0	850	29.0
No.4		3	947	11.2	947	20.6
No.5	26	-	770	3.8	780	12.1
No.6		1	750	0.0	780	5.0
No.7		2	738	0.0	745	4.0
No.8		3	708	0.0	750	2.5

microstructures resemble to those of 16%Cr specimens. In every matrix, the retained austenite in as-cast state is replaced by fine secondary carbides and martensite during austenitizing. From the digital data of hardness and Vγ, some pearlite may exist in the matrix of 26% Cr specimens with V content more than 2% but it can not be confirmed in the SEM microphotographs.

- Tempered state

The relationship between macro-hardness, Vγ and tempering temperature are shown in Fig. 4.59 to Fig. 4.61 for 16% Cr specimens and Fig 4.62 to Fig. 4.64 for 26% Cr specimens. In every diagram, the secondary hardening can be seen in the tempered hardness curves and the degrees are shown in Table 4.22. When they are compared with alloy-free specimens, they are roughly smaller in 16% Cr specimens and larger in 26% Cr specimens.

(i) 16%Cr cast iron
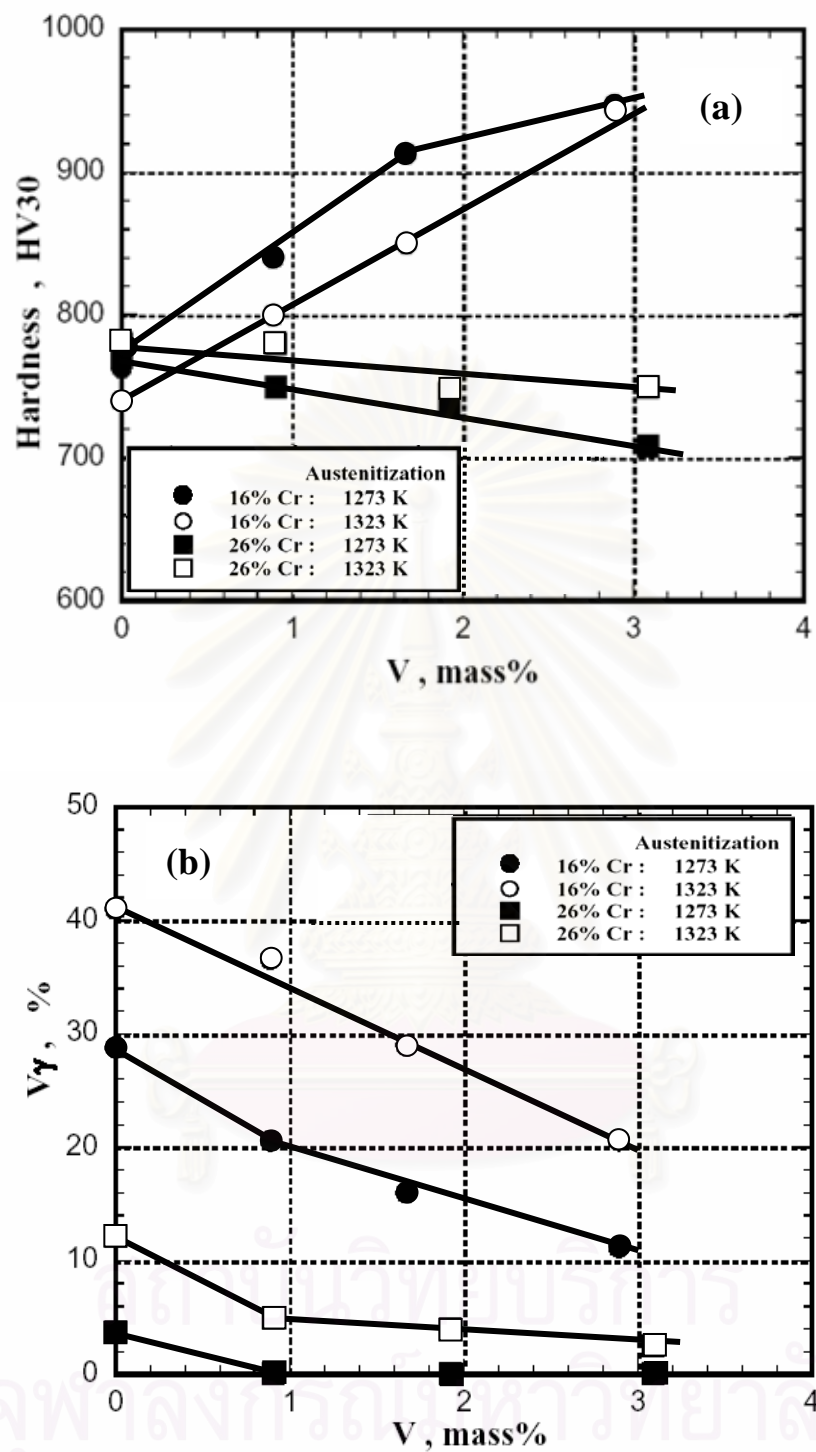
The relationship between macro-hardness, Vγ and tempering

Fig. 4.57 Effect of V content on macro-hardness (a) and Vγ (b) in as-hardened state.

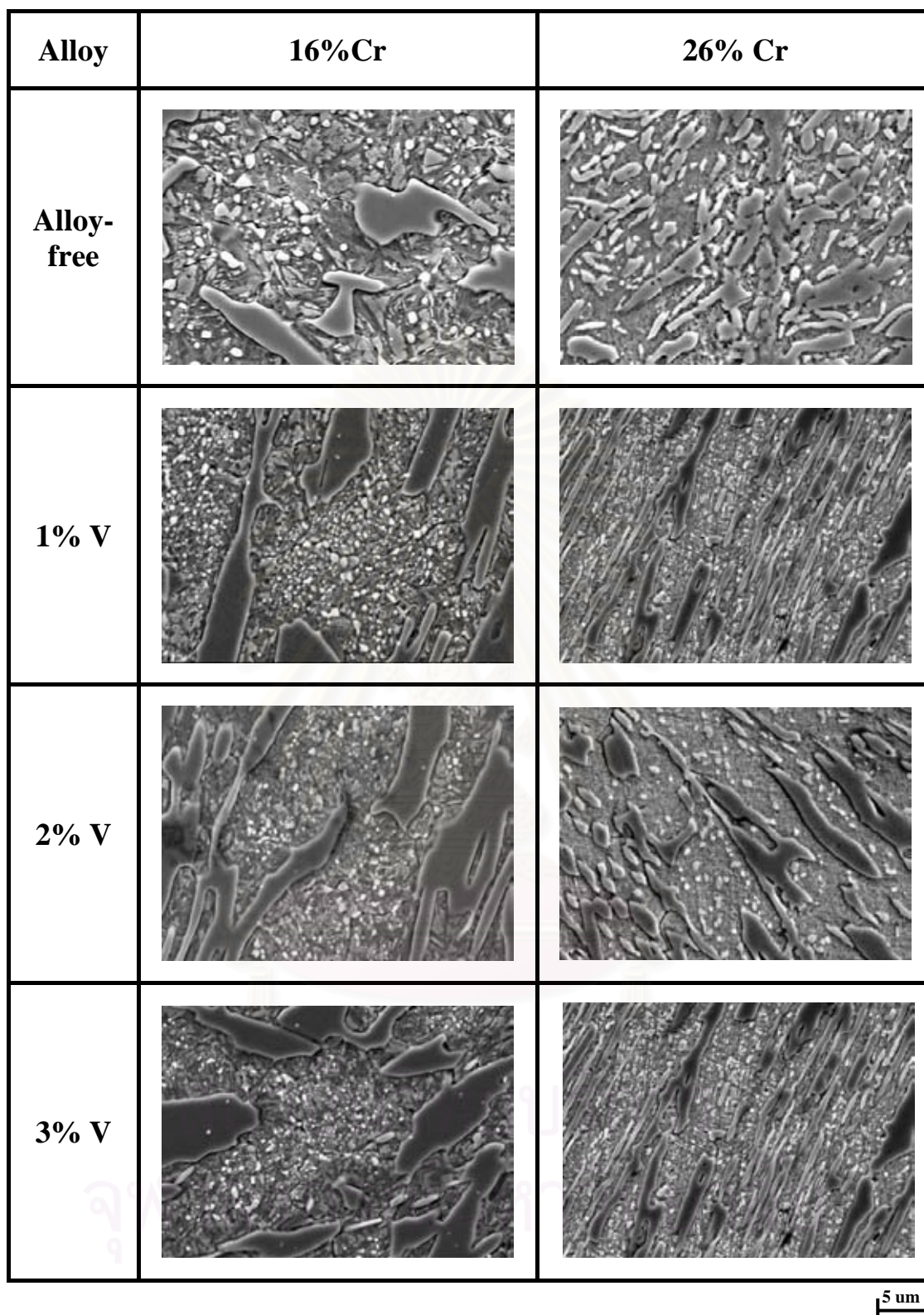| Alloy	16%Cr	26% Cr
Alloy-free		
1% V		
2% V		
3% V		

5 um

Fig. 4.58 SEM microphotographs in as-hardened state of 16% Cr and 26% Cr eutectic high chromium cast iron without and with V. Fine secondary carbide precipitate in matrix of martensite and retained austenite.

Table 4.22 Degree of the secondary hardening of test specimens.

Specimen	Element (mass%)		Degree of the secondary hardening (HV30)	
	Cr (mass%)	V (mass%)	1273 K austenitization	1323 K austenitization
No. 1	16	-	45	85
No. 2		1	37	118
No. 3		2	35	52
No. 4		3	33	43
No. 5	26	-	18	44
No. 6		1	39	71
No. 7		2	41	47
No. 8		3	65	45

temperature of 1% V specimens (No.2) is shown in Fig. 4.59. In the range of tempering temperature less than 720 K, the tempered hardness of the specimen hardened from 1323 K is lower than those hardened from 1273 K and it is reversed over 720 K. The secondary hardening occurs over 623 K. Their degrees are 37 HV30 in 1273 K and 118 HV30 in 1323 K austenitization. The H_{Tmax} in 1273 K austenitization is 823 HV30 and that in 1323 K austenitization is 850 HV30.

The 21% and 37% $V\gamma$ existed in as-hardened state decrease from 623 K and then the $V\gamma$ values get to 0% at 723 K in 1273 K and 760 K in 1323 K austenitization. The temperature at which the retained austenite disappears all is high in the case of high austenitizing temperature. This tendency corresponds well with the variation of H_{Tmax}. The tempering temperatures at the H_{Tmax} are 698 K in 1273 K and 748 K where the $V\gamma$ values are 6% and 4%, respectively.

As shown in Fig. 4.60, the hardness curves of 2% V specimen (No. 3) show similar tendency to alloy-free and 1% V specimens. However, the difference in hardness between two different austenitizations is very small in the temperature range lower than 710 K at which the hardness curves intersect. The degrees of the secondary hardening are 35 HV30 in 1273 K and 52 HV30 in 1323 K austenitization. The H_{Tmax} values are 836 HV30 in 1273 K and 842 in 1323 K austenitization.
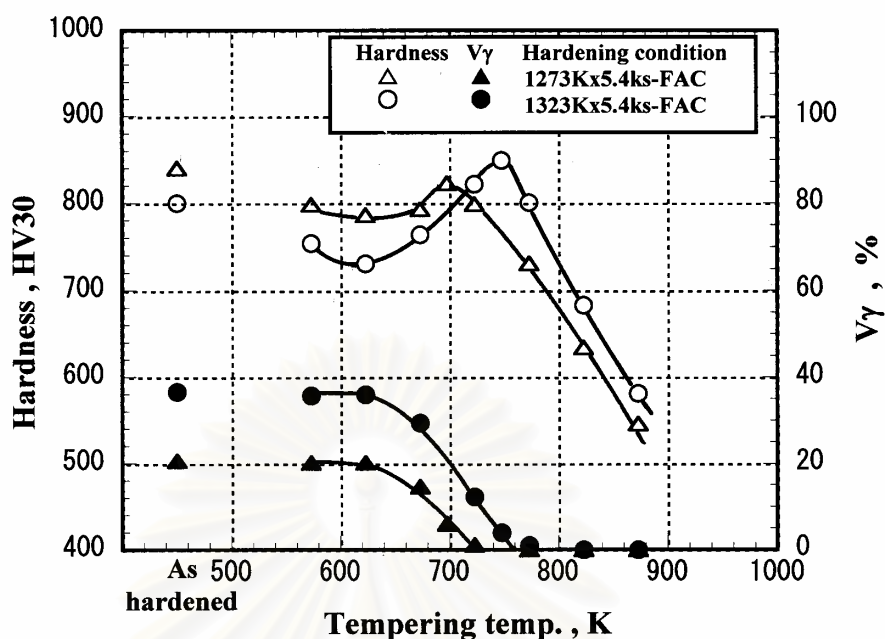
Fig. 4.59 Relationship between macro-hardness, volume fraction of retained austenite (Vγ) and tempering temperature of 16% Cr cast iron with 1% V. (Specimen No. 2)

Fig. 4.60 Relationship between macro-hardness, volume fraction of retained austenite (Vγ) and tempering temperature of 16%Cr cast iron with 2% V. (Specimen No. 3)
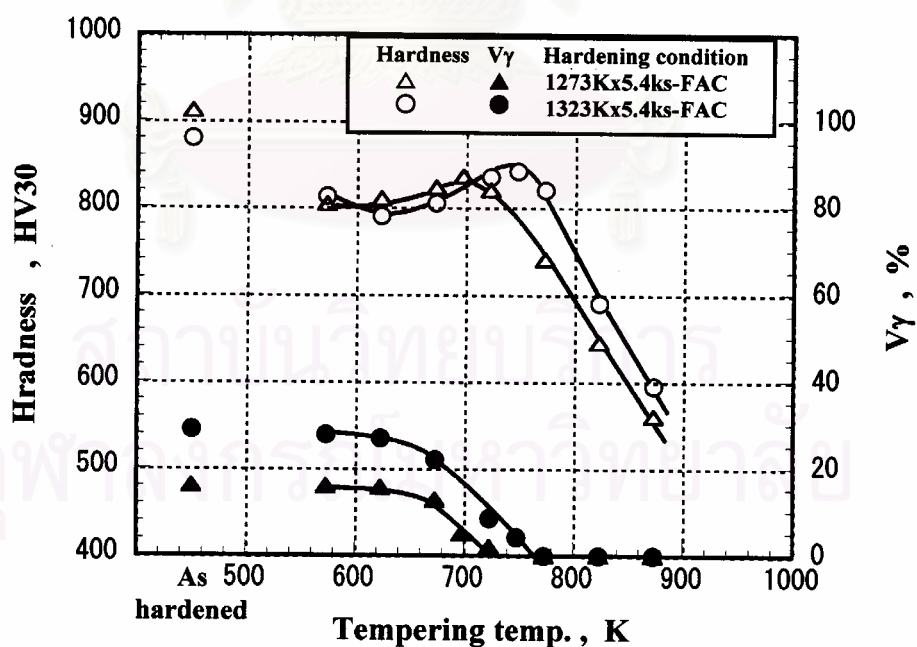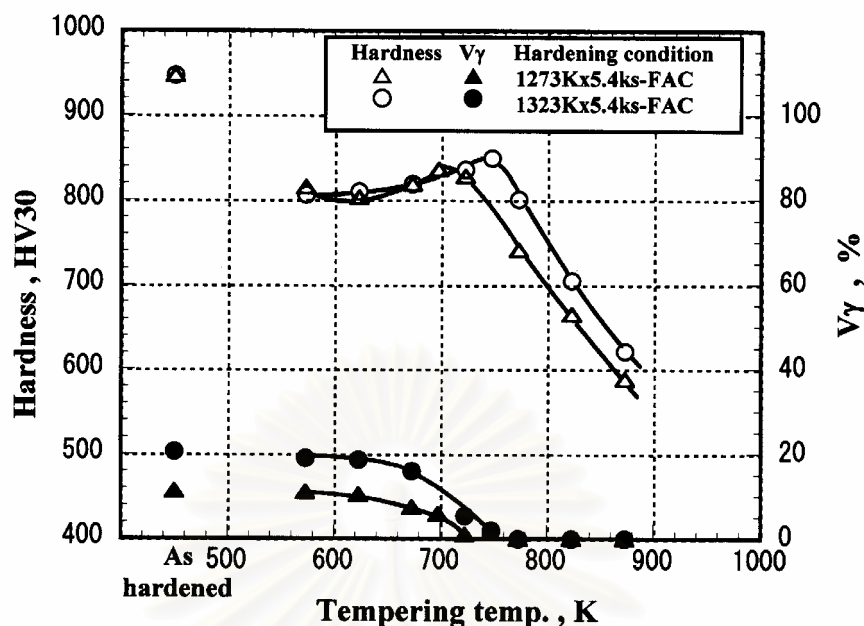
Fig. 4.61 Relationship between macro-hardness, volume fraction of retained austenite (Vγ) and tempering temperature of 16%Cr cast iron with 3% V. (Specimen No.4)

The Vγ values in as-hardened state are 16% in 1273 K and 29% in 1323 K austenitization. Both of the Vγ values decreases gradually over 623 K and finally they become 0% at 723 K in 1273 K and 760 K tempering in 1373 K austenitization. The Vγ values at the H_{Tmax} are 5% at 698 K in 1273 K and 4% at 748 K tempering in 1323 K austenitization, respectively.

Fig. 4.61 shows the results of 3% V specimen (No.4). The tempered hardness curves show a little different tendency from others specimens in the 16% Cr specimens. In the range of low tempering temperature lower than 723 K, the hardness are almost same value regardless of the austenitizing temperature. However, in the range over 723 K, the hardness in 1323 K austenitization are higher than those in 1273 K austenitization. The degrees of secondary hardening are smallest in the same group specimens, 33 HV30 in 1273 K and 43 HV30 in 1323 K austenitization. The H_{Tmax} of 836 HV30 and 849 HV30 are obtained at 698 K in 1273 K and 748 K tempering in 1323 K austenitization, respectively.

The Vγ in the specimen hardened from 1273 K is 11% and that hardened from 1323 K is 20%. Such Vγ values decrease to 0% at 723 K in 1273 K and 748 K in 1323 K austenitization. The Vγ values at the H_{Tmax} are obtained are 6% in 1273 K and 2% in 1323 K austenitization.

In the series of 16%Cr cast irons hardened from 1273 K, it is clarified that the more V content, the less Vγ, and resultantly the H_{Tmax} is low. At 1323 K austenitization, on the other hand, the H_{Tmax} does not change so much despite that the Vγ in as-hardened state decreases by increasing V content.

(ii) 26%Cr cast iron

Fig. 4.62 shows the results of specimen No. 6 with 1% V. The tempered hardness curve shows a similar behavior to alloy-free specimen shown in Fig. 4.34 but this is different from those of 16% Cr specimens. The tempered hardness in the case of 1323 K austenitization is higher than that in 1273 K austenitization. It is noted that this tendency appears in all the 26% Cr specimens with V. The hardness curves show the secondary hardening and the degree is larger in the case of high austenitization of 1323 K. The degrees are 39 HV30 in 1273 K and 71 HV30 in 1323 K austenitization which are higher compared with alloy-free specimen. The H_{Tmax} values of 759 HV30 in 1273 K and 798 HV30 in 1323 K austenitization are obtained at the tempering temperature of 723 K and 748 K, respectively.

The Vγ in as hardened state is 0% in 1273 K 5% in 1323 K austenitization. The Vγ of specimens hardened from 1323 K decreases to 0% at 773 K tempering, and the Vγ value at the H_{Tmax} is 2%.

In 2%V specimen (No.7) shown in Fig. 4.63, the tempered hardness curves show similar tendency to alloy-free and 1% V specimens. However, it is found that the difference in the hardness between the specimens hardened from 1273 K and 1323 K becomes larger in the low temperature range until the H_{Tmax}. The degrees of secondary hardening are 41 HV30 in 1273 K and 47 HV30 in 1323 K austneitization. The H_{Tmax} values are 730 HV30 at 723 K in 1273 K and 770 HV30 at 748 K tempering in 1323 K austenitization.

The Vγ values in as-hardened state are 0% in 1273 K and 4% in 1323 K austenitization. This is the reason why the less degree of secondary hardening was obtained. However, the secondary hardening appears in spite of 0% Vγ. This is because the special vanadium carbides are precipitated from martensite by the carbide reaction and result in an increase in the hardness. The decrease of Vγ in 1323 K austenitization is a very little. The Vγ is less than 2% or almost 0% at 748 K, and there the H_{Tmax} is obtained.

The results of 3% V specimen (No. 8) are shown in Fig. 4.64. The hardness curves show the secondary hardening in spite of very less Vγ in as-hardened state. The degrees are 65 HV30 in 1273 K and 45 HV30 in 1323 K austenitization. In spite of the high degree of secondary hardening, the H_{Tmax} value of specimen hardened from 1273 K (720 HV30) is lower than that that hardened from 1323 K (760 HV30). The tempering temperature of 698 K in 1273 K austenitization at H_{Tmax} is lower than those of other specimens with 26% Cr but 748 K in 1323 K austenitization is same.

The Vγ values in as-hardened state are less than 2% and they do not change even if the tempering temperature increases. This might be within a measuring error. The Vγ is less than 2% when H_{Tmax} is obtained. In spite the Vγ is very small in as-hardened state but the degree of secondary is much more. The reason is that the precipitation of vanadium carbides precipitated from martensite makes the hardness of the matrix increases.
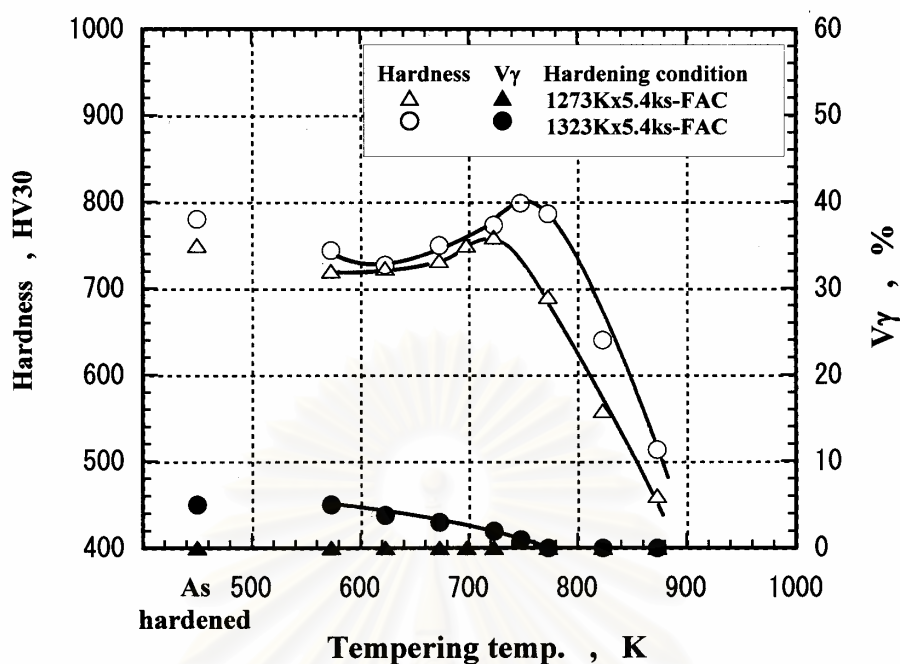
Fig. 4.62 Relationship between macro-hardness, volume fraction of retained
austenite (Vγ) and tempering temperature of 26%Cr cast iron with 1%
V. (Specimen No. 6)

Fig. 4.63 Relationship between macro-hardness, volume fraction of retained
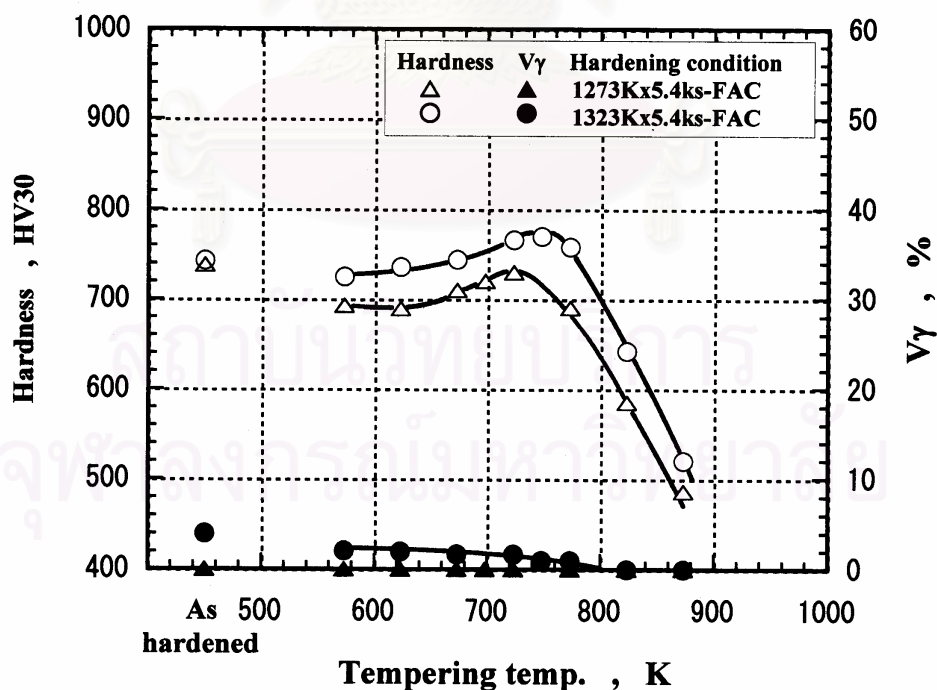austenite (Vγ) and tempering temperature of 26%Cr cast iron with 2%
V. (Specimen No.7)
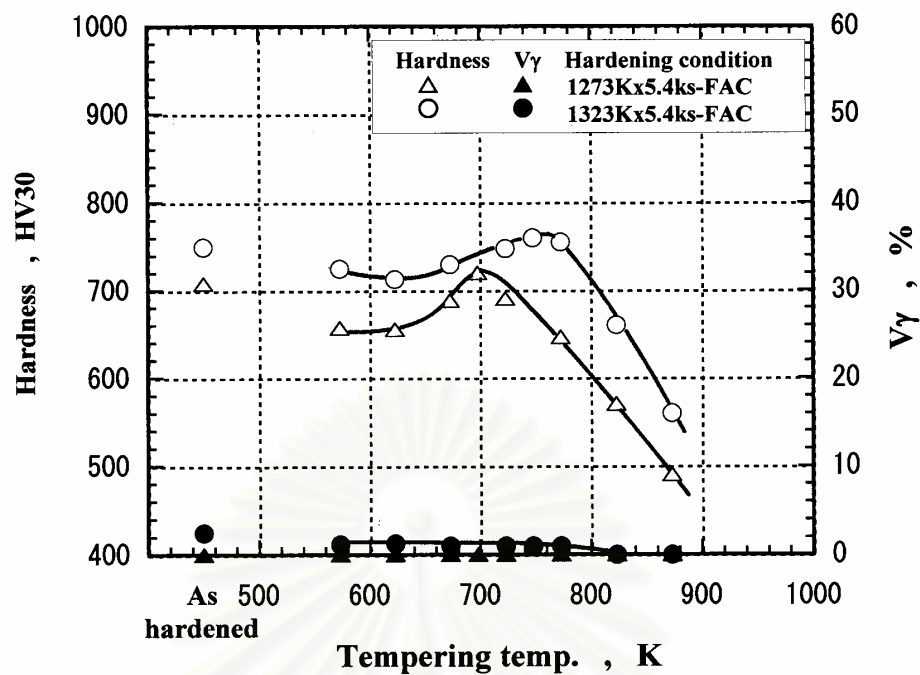
Fig. 4.64 Relationship between macro-hardness, volume fraction of retained austenite (Vγ) and tempering temperature of 26%Cr cast iron with 3% V. (Specimen No.8)

4.2.3 Hypoeutectic high chromium cast irons

4.2.3.1 Effect of nickel (Ni)

(a) Test specimen in as-cast state

Chemical compositions of specimens are listed up in Table 4.23. Ni is added up about 2% in the both 16% Cr and 26% Cr specimens. As-cast microstructures of alloy-free and Ni specimens are shown in Fig. 4.65. The microstructures consist of primary dendrites and $(\gamma+M_7C_3)$ eutectic in colony morphology and they are quite similar to those of plain high chromium cast iron. The matrices are mostly austenitic except for alloy-free 16% Cr specimen which is pearlitic. Even if Ni is added, the size of eutectic carbides is smaller in 26% Cr specimens than in 16% Cr specimens.

Macro-hardness and $V\gamma$ of as-cast specimens are shown in Table 4.24. Hardness decreases as Ni content increases in the both series of test specimens, from 572 HV30 to 530 HV30 in 16% Cr and 547 HV30 to 536 HV30 in 26% Cr specimens, respectively. On the other hand, the $V\gamma$ increases with an increase in Ni content, from 0% to 86.5 % in 16% Cr and 46.8% to 78.5% in 26% Cr specimens, respectively.

(b) Effect of Ni content on variation of macro-hardness and volume fraction of retained austenite ($V\gamma$) during heat treatment

-As-hardened state

Macro-hardness and $V\gamma$ in as-hardened state are shown in Table 4.25 and the effect of Ni on the macro-hardness and $V\gamma$ is shown in Fig. 4.66 (a) and (b), respectively. The hardness decreases as Ni content increases in all the specimens. The hardness of 16% Cr specimens gradually decreases from 775 HV30 to 730 HV30 in 1273 K and remarkably 730 HV30 to 650 HV30 in 1323 K austenitization,

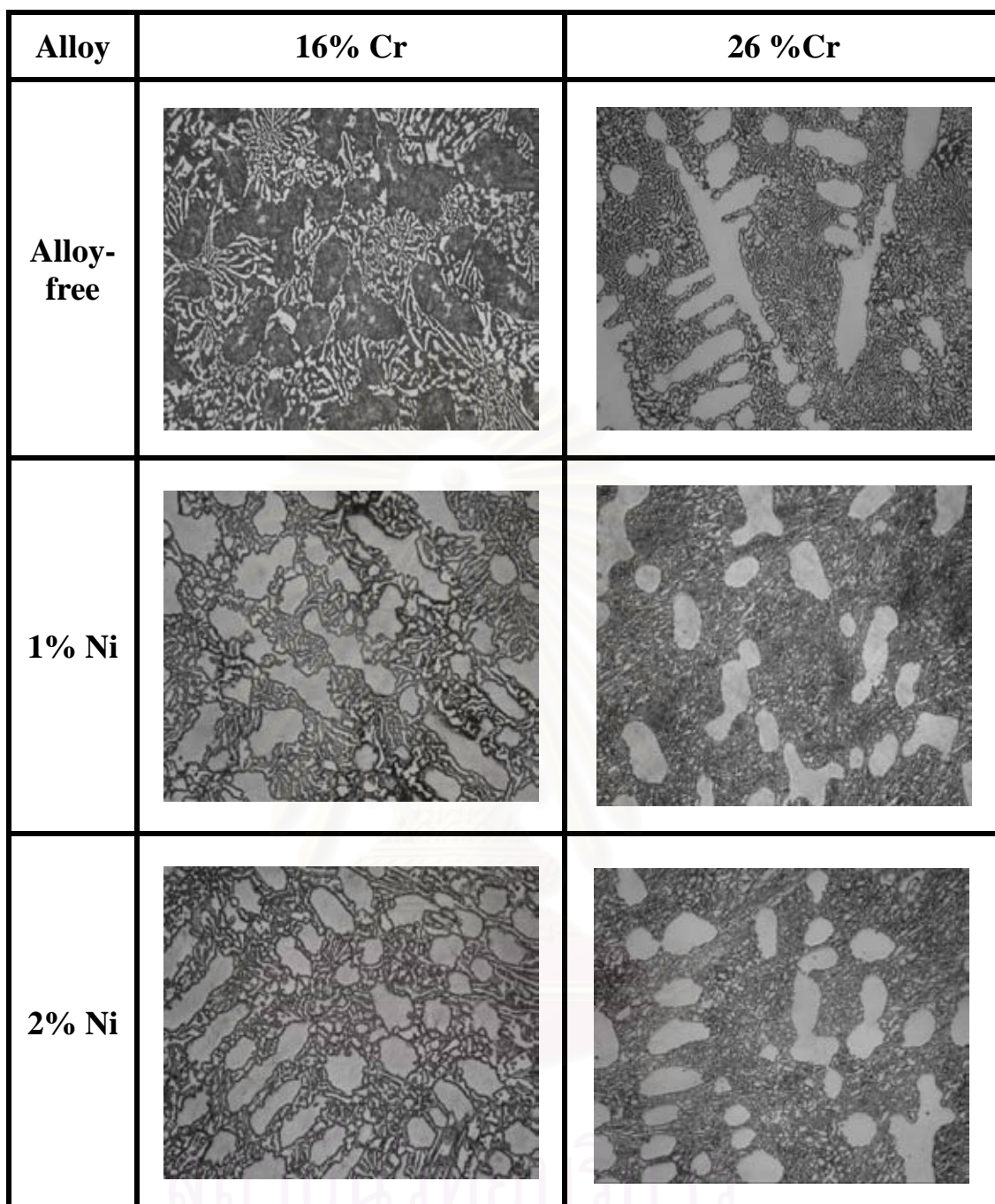Table 4.23 Chemical compositions of test specimens.

Specimen	Element (mass%)							
	C	Cr	Si	Mn	Ni	Cu	Mo	V
No.1	3.01	16.48	0.62	0.78	-	-	-	-
No.2	2.90	16.23	0.51	0.53	1.21	-	-	-
No.3	2.95	16.00	0.55	0.56	2.14	-	-	-
No.4	2.65	25.56	0.37	0.51	-	-	-	-
No.5	2.65	26.16	0.48	0.48	1.18	-	-	-
No.6	2.64	25.91	0.47	0.51	2.06	-	-	-

*S and P are less than 0.06 mass%

Table 4.24 Macro-hardness and volume fraction of retained austenite
(Vγ) of as-cast specimens.

Specimen	Element (mass%)		Hardness (HV30)	Vγ (%)
	Cr	Ni		
No. 1		-	572	0
No. 2	16	1	564	53.2
No. 3		2	530	86.5
No. 4		-	547	46.8
No. 5	26	1	541	67.8
No. 6		2	536	78.5

Alloy	16% Cr	26 %Cr
Alloy-free		
1% Ni		
2% Ni		

50 μm

Fig.4.65 As-cast microstructures of 16% Cr and 26% Cr hypoeutectic cast irons with and without Ni. Matrices of all cast irons with Ni and alloy-free 26% Cr cast iron are austenitic possibly with martensite.

Table 4.25 Macro-hardness and volume fraction of retained austenite

(Vγ) of as-hardened specimens.

Specimen	Element (mass%)		Austenitizing Temperature (K)			
			1273		1323	
	Cr	Ni	Hardness (HV30)	Vγ (%)	Hardness (HV30)	Vγ (%)
No. 1	16	-	775	18.1	730	31.8
No. 2		1	750	30	684	50.6
No. 3		2	730	34	650	57
No. 4	26	-	763	4.1	777	11.5
No. 5		1	731	4.2	758	14
No. 6		2	721	6.5	740	22

respectively. In 26%Cr specimens, the hardness lowers from 763 HV30 to 721 HV30 in 1273 K and 777 HV30 to 740 HV30 in 1323 K austenitization.

As for the Vγ in Fig. 4.63 (b), it is found that the effects of Ni content and austenitizing temperature appear clearly. In 16% Cr specimen, the Vγ increases from 18.1% at 0% Ni to 34% at 2% Ni in 1273 K and 31.8% at 0% Ni to 57% at 2% Ni in 1323 K austenitization. In 26% Cr specimen, the Vγ increases with an increase in Ni content, from 4.1% to 6.5% in 1273 K and 11.5% to 22% in 1323 K austenitization. It is clear that an increase in the austenitizing temperature makes the hardness low in 16%Cr specimens and high in 26%Cr specimens. From the variation of Vγ, a strong effect of Ni on stabilizing austenite is suggested.

In order to comprehend in detail the behavior of matrix structure in hardening process, the microstructure of as-hardened specimens were observed by SEM focusing on the matrix in which the secondary carbides are precipitated. The SEM microphotographs are representatively shown in Fig. 4.67. The matrices of all the specimens consist of large amount of fine carbides, certainly martensite and some retained austenite. When the size of precipitated carbides is compared, it is comparatively larger in the
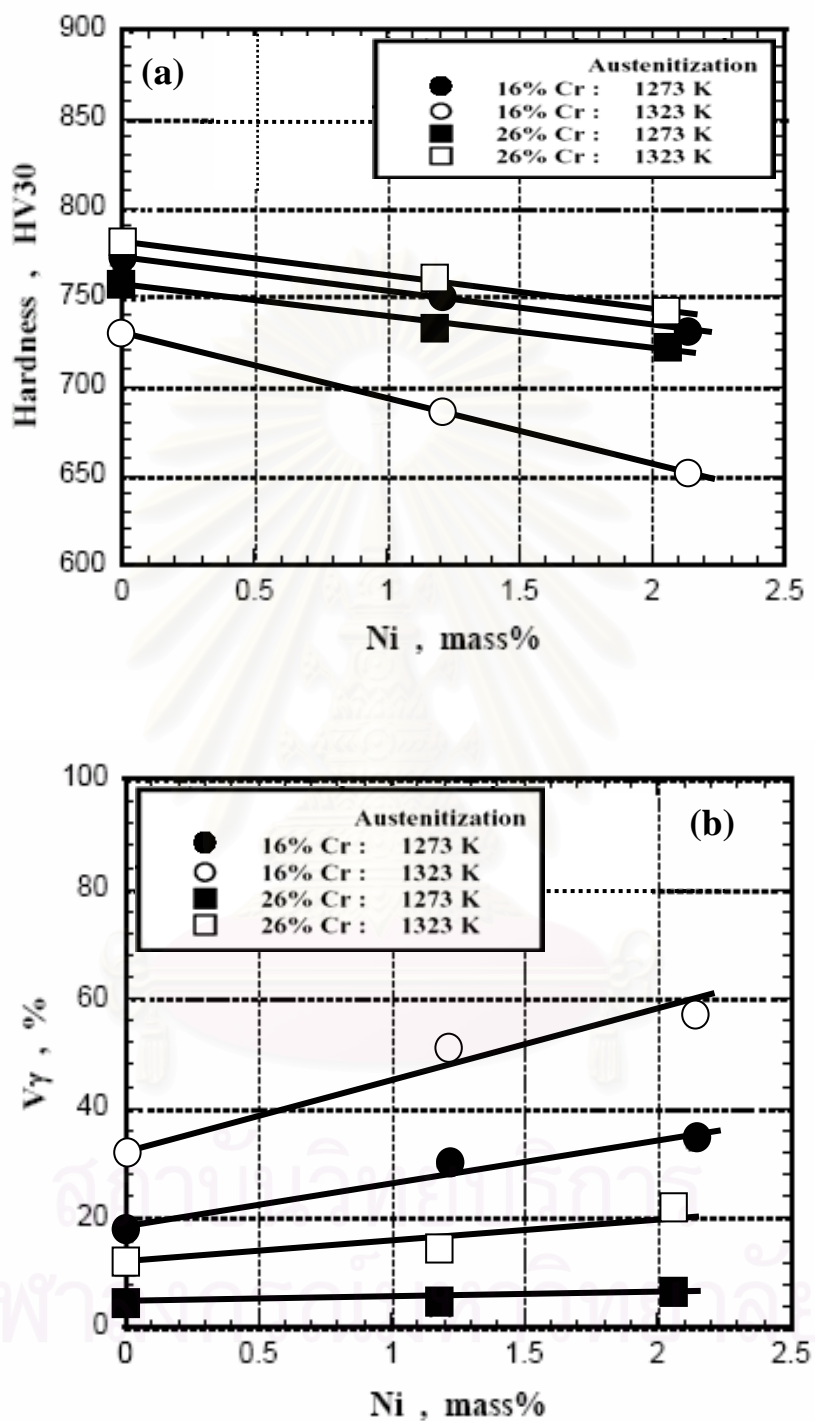
Fig. 4.66 Effect of Ni content on macro-hardness (a) and Vγ (b) in as-
hardened state.

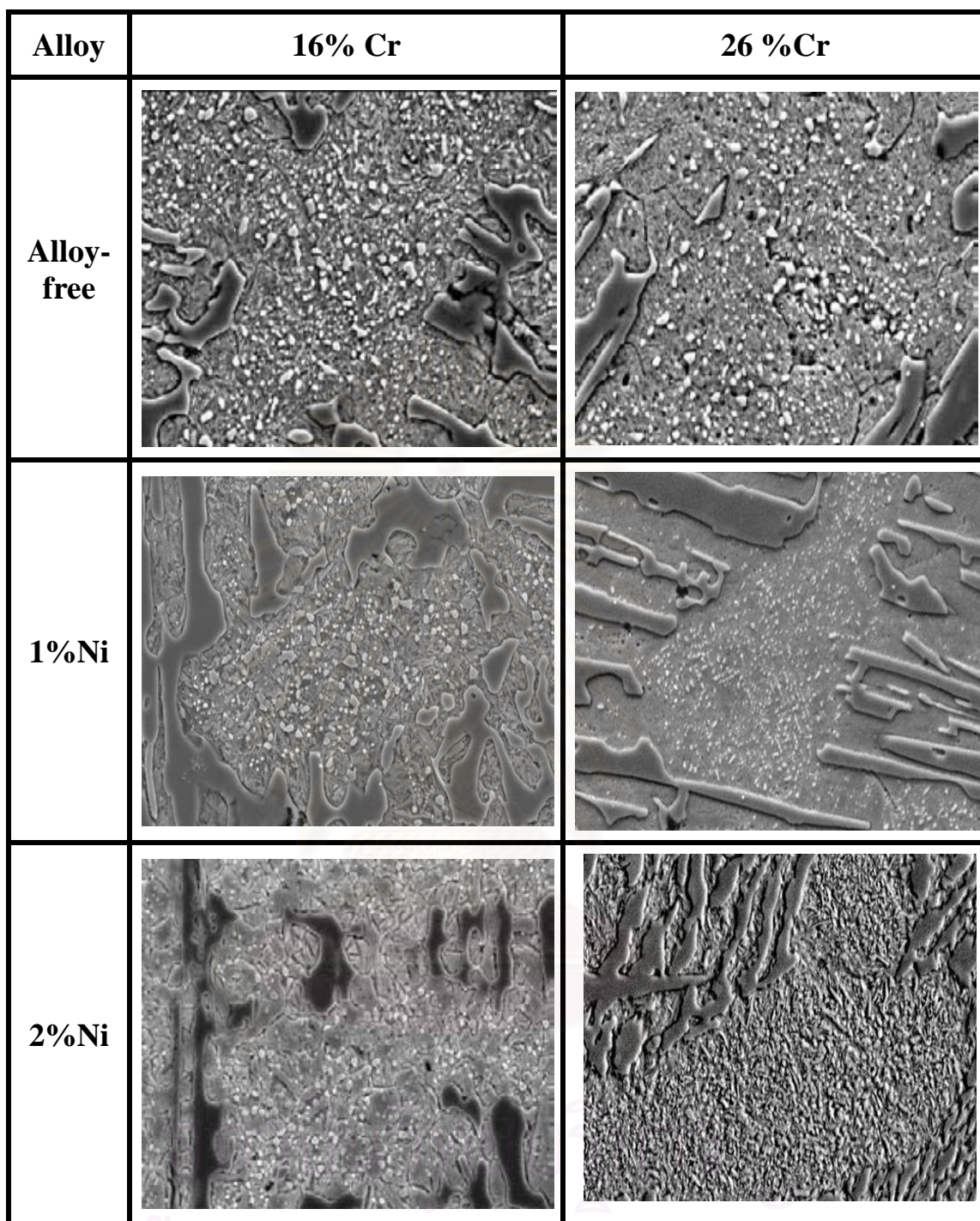| Alloy	16% Cr	26 %Cr
Alloy-free		
1%Ni		
2%Ni		

5 μm

Fig.4.67 SEM microphotographs in matrix of as-hardened 16% Cr and 26% Cr hypoeutectic cast irons with and without Ni. Fine secondary carbides precipitate in primary dendrite matrices of martensite and austenite. Numbers of precipitate carbides are much more than those of eutectic 16% CR and 26% Cr cast irons with Ni.

16% Cr specimens than that in 26%Cr specimens.

- **Tempered state**

Relationship between macro-hardness, Vγ and tempering temperature are shown in Fig. 4.68 to Fig 4.70 for 16% Cr specimens and Fig. 4.71 to Fig. 4.73 for 26% Cr specimens, respectively. In every diagram, the hardness and Vγ of as-hardened specimens are plotted for comparison. The tempered hardness curves show the remarkable secondary hardening. The degree of secondary hardening is greater in Ni specimen compared with alloy-free specimen and their degrees are listed in Table 4.26.

(i) 16%Cr cast iron

The relationship between hardness, Vγ and tempering temperature of alloy-free specimen (No.1) is shown in Fig. 4.68. In the temperature range up to 720 K, the tempered hardness of specimens hardened from 1323 K are lower than those hardened from 1273 K and over it, they are reversed. The degrees of secondary hardening are 33 HV30 and 83 HV30 in 1273 K and 1323 K austenitization, respectively. The H_{Tmax} obtained from specimen hardened from 1273 K is 780 HV30 at the tempering temperature of 698 K and that from 1323 K is 798 HV30 at 748 K. It is clear from these results that the higher the austenitizing temperature, the more both of the degree and the H_{Tmax}. The tempering temperature to obtain the H_{Tmax} is shifted to high temperature side by increasing the austenitizing temperature.

The Vγ values of 28.8% and 41% in as-hardened state begin to get down over 623 K in 1273 K and 673 K in 1323 K austenitization, and gets to 0% at 730 K in 1273 K and 773 K in 1323 K austenitization. The Vγ values at the H_{Tmax} are 7% in 1273 K and 2% in 1323 K austenitization. It is clear that the more the Vγ value, the higher

Table 4.26 Degree of the secondary hardening of test specimens.

Specimen	Element (mass %)		Degree of the secondary hardening (HV30)	
	Cr	Ni	1273 K austenitization	1323 K austenitization
No. 1	16	-	33	83
No. 2		1	56	134
No. 3		2	78	165
No. 4	26	-	20	34
No. 5		1	30	55
No. 6		2	52	72

tempering temperature is needed to eliminate the retained austenite.

The results of 1% Ni specimen (No. 2) are shown in Fig. 4.69, the shape of tempered hardness curves are similar to alloy-free specimen. In the tempering temperatures lower than 755 K, the hardness of specimens hardened from 1323 K is lower than those hardened from 1273 K and it is reversed when the tempering temperature gets over it. The tempered hardness curves show grater degree of secondary hardening compared with alloy-free specimen, 56 HV30 in 1273 K and 134 HV30 in 1323 K austenitization. The H_{Tmax} values of 763 HV30 in 1273 K and 778 HV30 in 1323 K austenitization are obtained at the tempering temperatures of 748 K and 773 K, respectively.

The 30% Vγ remained in the specimen hardened from 1273 K decreases from 623 K and disappears entirely at 748 K. In the case of 1323 K austenitization, about 50% Vγ existed in as-hardened state begins to decrease over 673 K and gets to 0% at 798 K tempering. The Vγ values at the H_{Tmax} are 3% at 748 K in 1273 K and 8.5 % at 775 K tempering in 1323 K austenitization, respectively.

The results of 2% Ni specimen (No. 3) are shown in Fig. 4.70. The shapes of tempered hardness curves are similar to those of alloy-free (No. 1) and 1% Ni (No. 2) specimens. Up to 760 K tempering, the hardness in 1273 K austenitization are overall more than those in the case of 1323 K austenitization and over 760 K it is reversed. The degree of the secondary
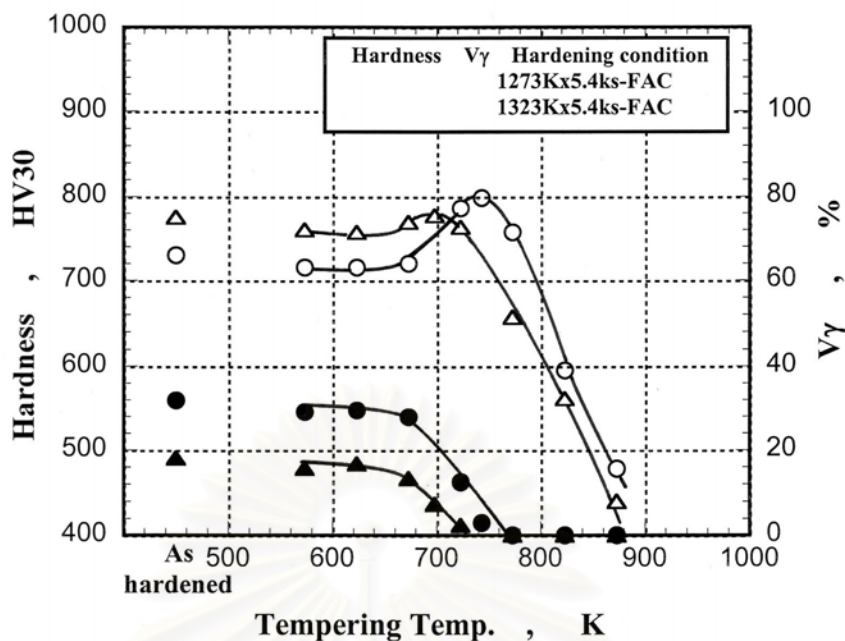
Fig. 4.68 Relationship between macro-hardness, volume fraction of retained austenite (Vγ) and tempering temperature of 16% Cr cast iron without alloying element. (Specimen No. 1)

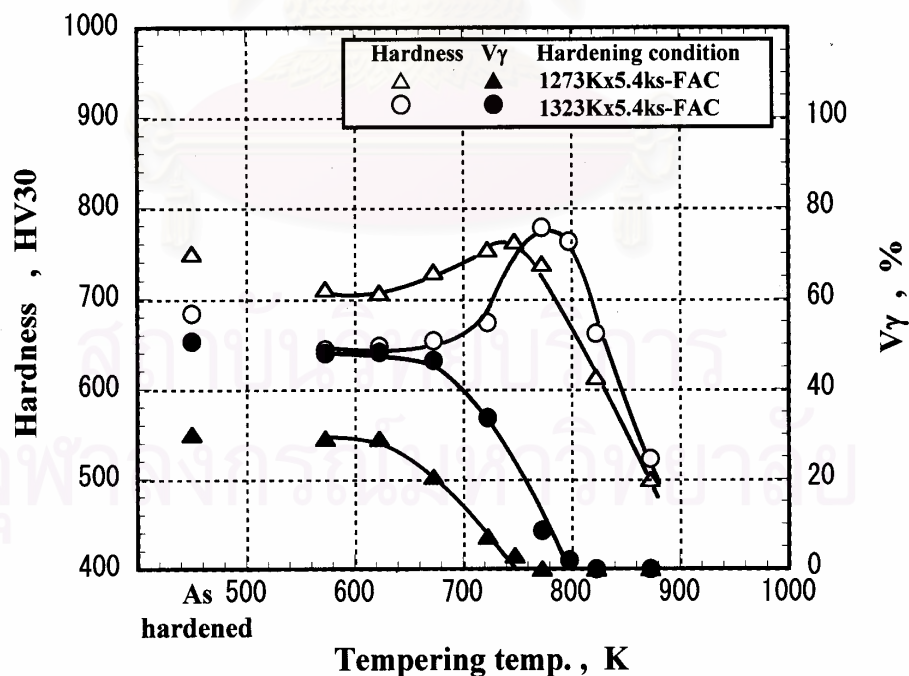Fig. 4.69 Relationship between macro-hardness, volume fraction of retained austenite (Vγ) and tempering temperature of 16% Cr cast iron with 1% Ni. (Specimen No. 2)
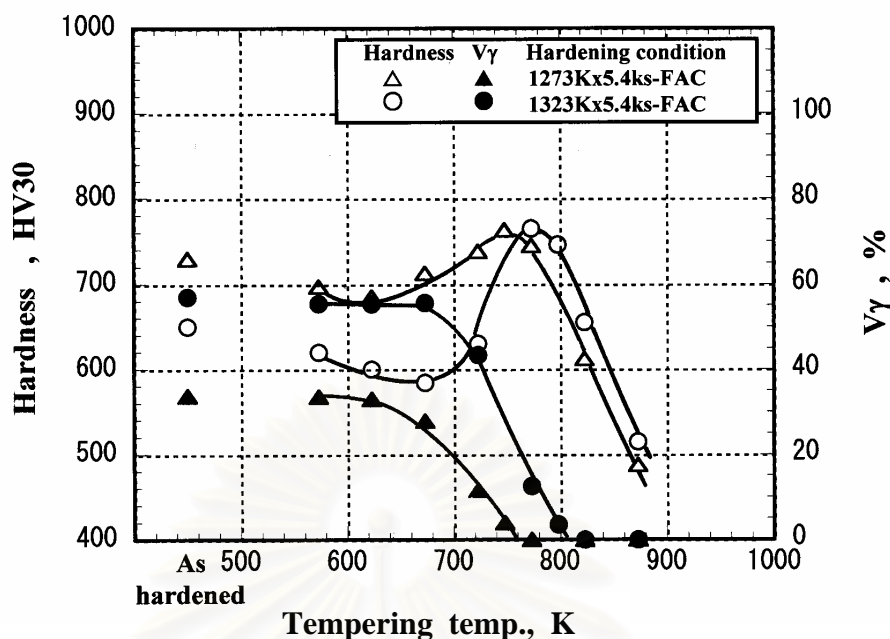
Fig. 4.70 Relationship between macro-hardness and volume fraction of
retained austenite (Vγ) and tempering temperature of 16% Cr cast
iron with 2% Ni. (Specimen No. 3)

hardening is largest in the 16% Cr specimens and they are 78 HV30 in
1273 K and 165 HV30 in 1323 K austenitization. It is clear that the
degree is much greater in the specimen with largest Vγ in as-hardened
state by hardening from higher austenitization. The H_{Tmax} values are 760
HV30 at 748 K in 1273 K and 765 HV30 at 773 K tempering in 1323 K
austenitization, and they are lowest in the 16% Cr specimens.

The 34% Vγ in as-hardened state in 1273 K decreases over 673 K
and gets to 0% at 760 K. The 57% Vγ in 1323 K austenitization starts to
lower over 623 K and gets to 0% at 805 K tempering. The Vγ values at
H_{Tmax} are 4% in 1273 K and 12.5% in 1323 K austenitization.

(ii) 26%Cr cast iron

The results of alloy-free specimen (No. 4) are shown in Fig. 4.71.
The behavior of tempered hardness curves shows different tendency from
that of 16% Cr specimens, that is, the hardness of the specimens hardened

from high austenitizing temperature of 1323 K are overall higher than those hardened from low temperature of 1273 K. In the case of high austenitization, however, it is similar that the degree of secondary hardening is more and that the H_{Tmax} is obtained at high temperature side. The degree of secondary hardening is smaller in comparison with 16% Cr specimens. The degrees are a little larger in the specimen hardened from 1323 K, 34 HV30 in 1323 K and 20 HV30 in 1273 K austenitization. The H_{Tmax} values are 770 HV30 at 698 K in 1273 K and 780 HV30 at 723 K tempering in 1323 K austenitization, respectively.

The 4% Vγ value in the specimen hardened from 1273 K decreases gradually by tempering to 0% at 773 K tempering, and 12% Vγ in 1323 K austenitization begins to lower from 723 K tempering and gets to 0% at 773 K. The Vγ values at the H_{Tmax} are 3% in 1273 K and 5% in 1323 K austenitization.

The results of 1% Ni specimen (No. 5) are shown in Fig. 4.72. The tempered hardness curves show same behavior as those in the alloy-free specimen. The degrees of secondary hardening are greater in 1% Ni specimen than the alloy-free specimen and also greater in 1323 K austenitization. They are 30 HV30 in 1273 K and 55 HV30 in 1323 K austenitization. The H_{Tmax} values are 720 HV30 at 698 K in 1273 K and 757 HV30 at 748 K tempering in 1323 K austenitization, respectively.

The 4% and 14% Vγ values existing in the as-hardened specimens hardened from 1273 K and 1323 K, respectively, begin to decrease gradually from 623 K tempering and both disappear at 780 K tempering. The Vγ values at the H_{Tmax} are 4% in 1273 K and 6% in 1323 K austenitization.

As shown in Fig. 4.73 for the results of 2% Ni specimen (No. 6), the tempered hardness curves show different tendency from alloy-free and 1% Ni specimens. In the range of tempering temperatures between 590 K and 723 K, the tempered hardness in 1323 K austenitization is lower in comparison with those in 1273 K austenitization, but it is reversed when the tempering temperature gets over 723 K. These results

are similar to the behavior of 16% Cr specimens. The secondary hardening is greatest in the 26% Cr specimens and the degree is greater in the case of high austenitization of 1323 K, 52 HV 30 in 1273 K and 72 HV30 in 1323 K austenitization. The H_{Tmax} values of 715 HV30 in 1273K and 731 HV30 in 1323 K austenitization are obtained when the specimen tempered at 698 K and 773 K, respectively.

The $V\gamma$ value in as-hardened state is 6.5% in 1273 K austenitization, and it begins to decrease from 623 K to 0% at 773 K tempering. The 22% $V\gamma$ in 1323 K austenitization gets down from 673 K to 0% at 773 K. The $V\gamma$ values at the H_{Tmax} are 4% and 2% in 1273 K and 1323 K austenitization, respectively.
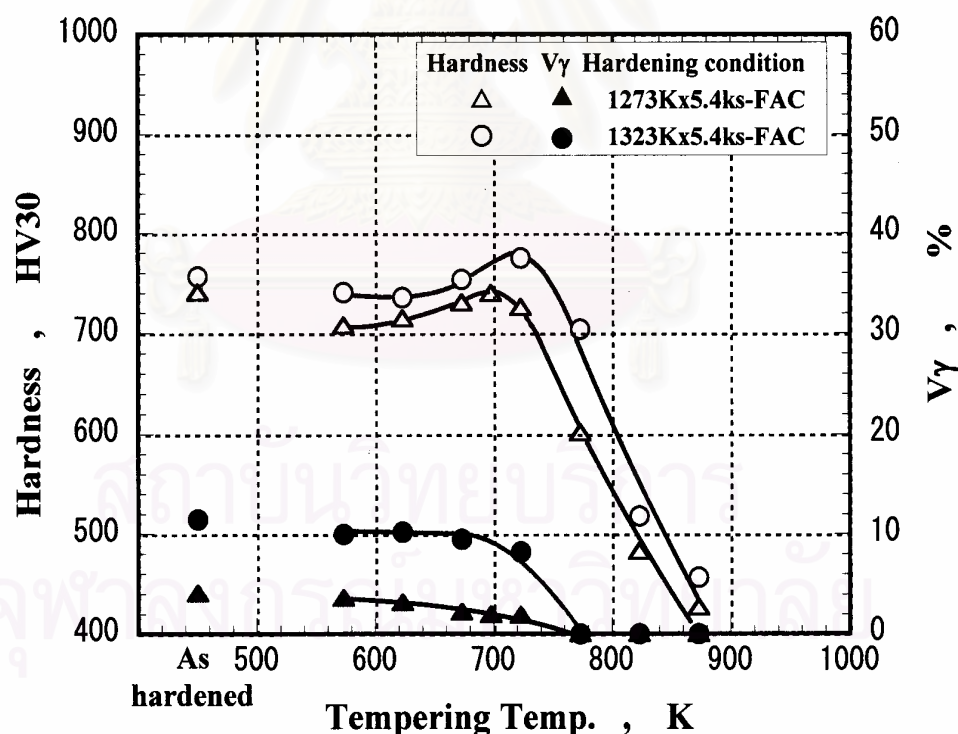

Fig. 4.71 Relationship between macro-hardness, volume fraction of retained austenite ($V\gamma$) and tempering temperature of 26% Cr cast iron without alloying element. (Specimen No. 4)
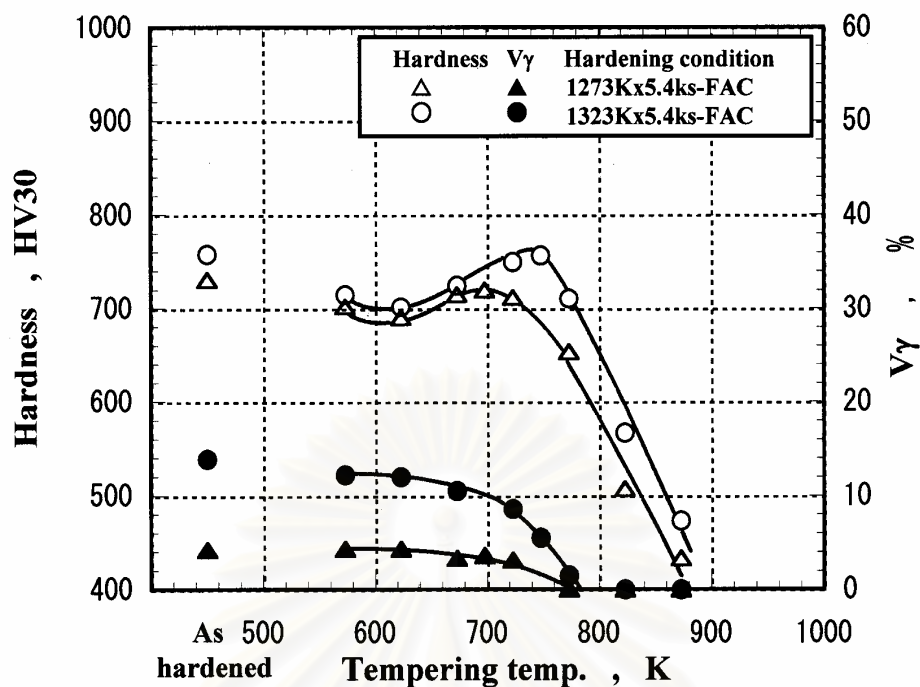
Fig. 4.72 Relationship between macro-hardness, volume fraction of retained austenite (Vγ) and tempering temperature of 26% Cr cast iron with 1% Ni. (Specimen No. 5)
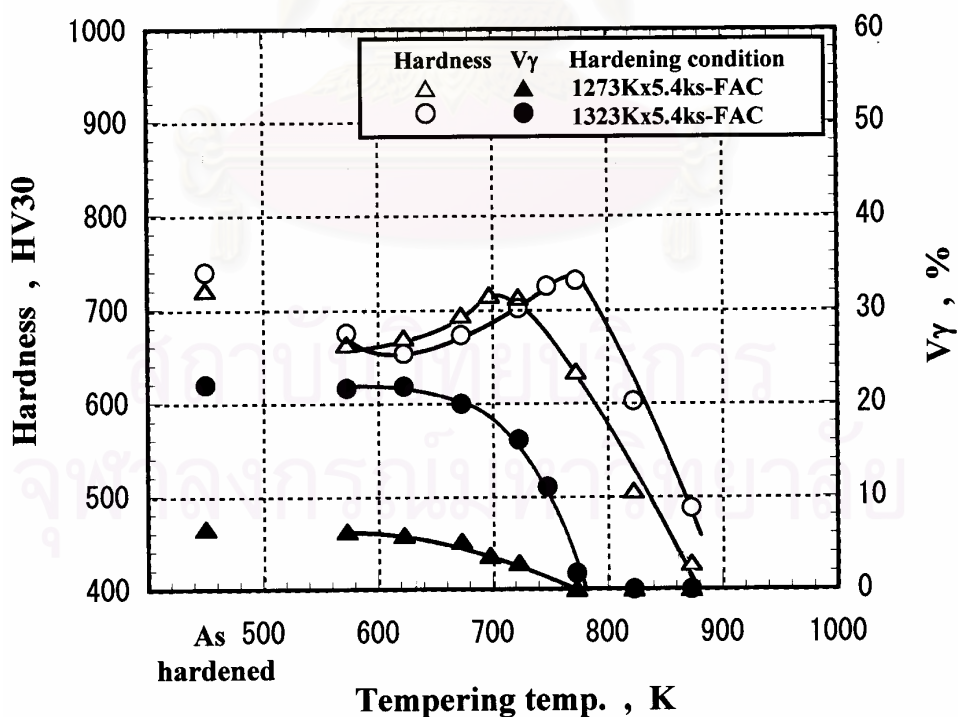

Fig. 4.73 Relationship between macro-hardness, volume fraction of retained austenite (Vγ) and tempering temperature of 26% Cr cast iron with 2% Ni. (Specimen No. 6)

(c) Relationship between micro-hardness of matrix and tempering temperature

In order to understand the transformation behavior of matrix, the matrix hardness was measured using micro-vicker hardness tester.

The relationships between micro-hardness of matrix in as-hardened and tempered states and tempering temperature are shown by solid symbols in Fig. 4.74 to Fig. 4.76 for 16% Cr and Fig. 4.77 to Fig. 4.79 for 26% Cr specimens, respectively. The macro-hardness curves are displayed in the same diagram for comparison. The micro-hardness increases with increasing tempering temperature and then decreases abruptly after reaching the maximum point of hardness. It is found that the profile of the micro-hardness curve is similar to that of macro-hardness curve and of course the micro-hardness is overall much lower than macro-hardness. The micro-hardness curve shows secondary hardening as the same manner as in macro-hardness curve.

The degrees of secondary hardening of micro-hardness are listed in Table 4.27. The degree in 16% Cr specimens changes from 25 HV0.1 at 0% Ni to 64 HV0.1 at 2% Ni in 1273 K and from 55 HV0.1 at 0% Ni to 134 HV0.1 at 2% Ni in 1323 K austenitization and those in 26% Cr specimens increase slightly from 22 HV0.1 at 0% Ni to 39 HV0.1 at 2% Ni in 1273 K and from 52 HV0.1 at 0% Ni to 60 HV0.1 at 2% Ni in 1323 K austenitization, respectively. From Table 4.27, it is clear that the degree is high in Ni specimens compared with alloy-free specimen and it increases remarkably with an increase in austenitizing temperature. At the same Ni content, the degree of secondary hardening in 16% Cr specimen is greater than that in 26% Cr specimen. The maximum micro-hardness are shown in Table 4.28. It decreases as Ni content increases. In 16% Cr specimen, the maximum micro-hardness lower from 697 HV0.1 at 0% Ni to 669 HV0.1 at 2% Ni in 1273 K and from 706 HV0.1 at 0% Ni to 669 HV0.1 at 2% Ni in 1323 K austenitization. The micro-hardness in 26% Cr specimens decrease from 683 HV0.1 to 530 HV0.1 in 1273 K and 703

HV0.1 to 555 HV0.1 in 1323 K austenitization, respectively. In 16% Cr specimens, the difference between macro-hardness and micro-hardness at H_{Tmax} are 80 HV0.1 to 95 HV in 1273 K and 90 HV0.1 to 100 HV0.1 in 1323 K austenitization, respectively. In the case of 26% Cr specimens, the differences between the maximum macro-hardness and the maximum micro-hardness are much higher compared with those 16% Cr specimens, and they are 90 HV to 180 HV in 1273 K and 90 HV to 190 HV in 1323 K austenitization.

Table 4.27 Degree of secondary hardening of micro-hardness.

Specimen	Cr (mass%)	Ni (mass%)	Degree of secondary hardening (HV0.1)	
			1273 K austenitization	1323 K austenitization
No.1	16	-	25	55
No.2		1	43	97
No.3		2	64	134
No.4	26	-	22	52
No.5		1	35	55
No.6		2	39	60

Table 4.28 Maximum micro-hardness of matrix.

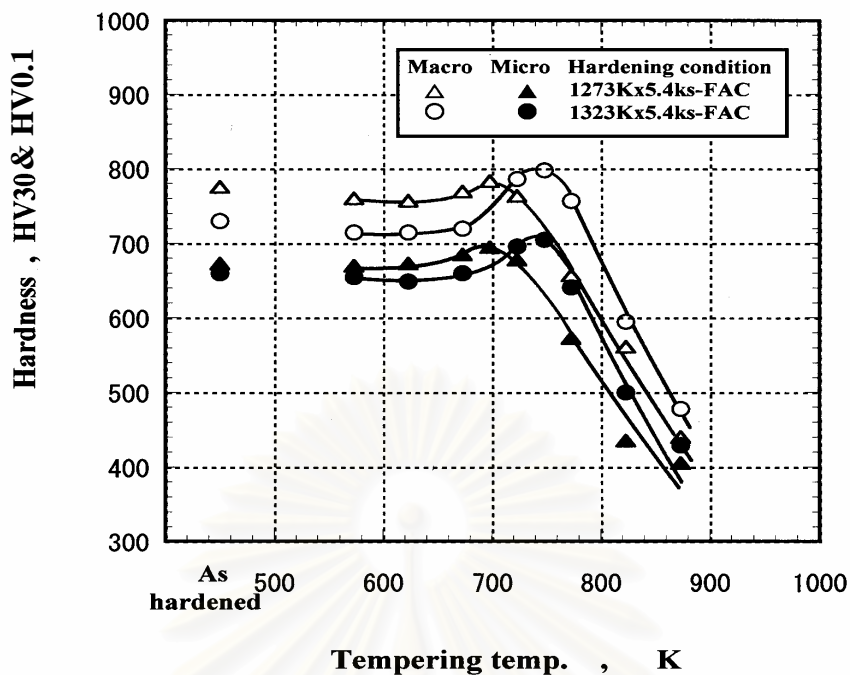| Specimen	Cr (mass%)	Ni (mass%)	Maximum micro-hardness (HV0.1)	
			1273 K austenitization	1323 K austenitization
No.1	16	-	697	706
No.2		1	678	677
No.3		2	669	669
No.4	26	-	683	703
No.5		1	550	572
No.6		2	530	555

Fig. 4.74 Relationship between micro-hardness of matrix and tempering
temperature of 16% Cr cast iron without alloying element.
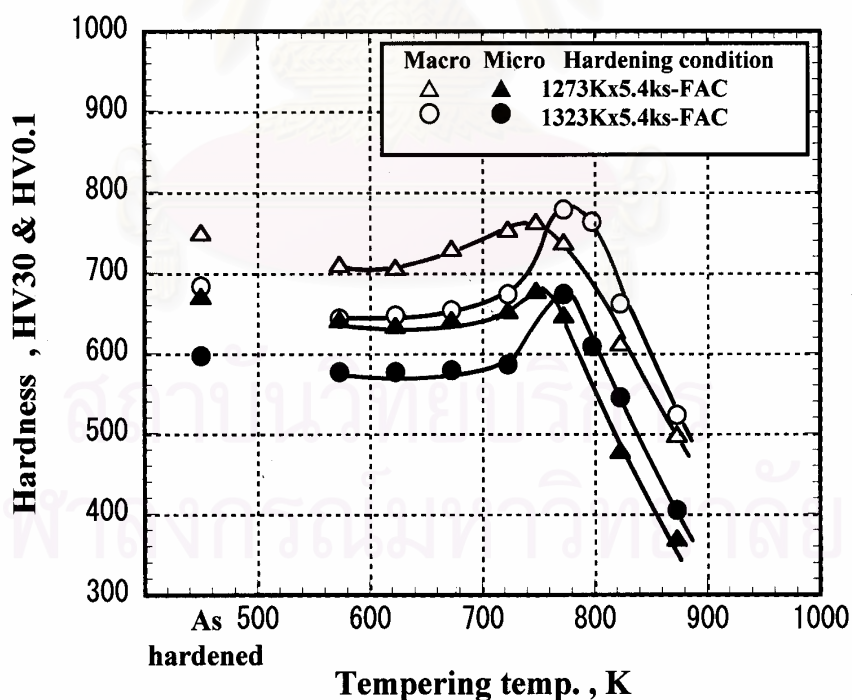(Specimen No. 1)

Fig. 4.75 Relationship between micro-hardness of matrix and tempering
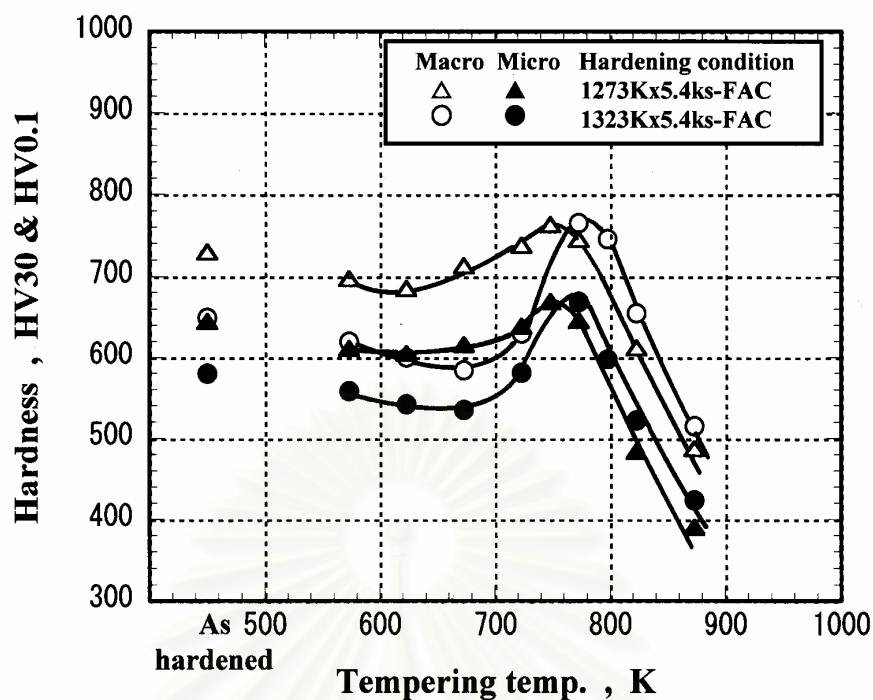temperature of 16% Cr cast iron with 1% Ni. (Specimen No. 2)

Fig. 4.76   Relationship between micro-hardness of matrix and tempering
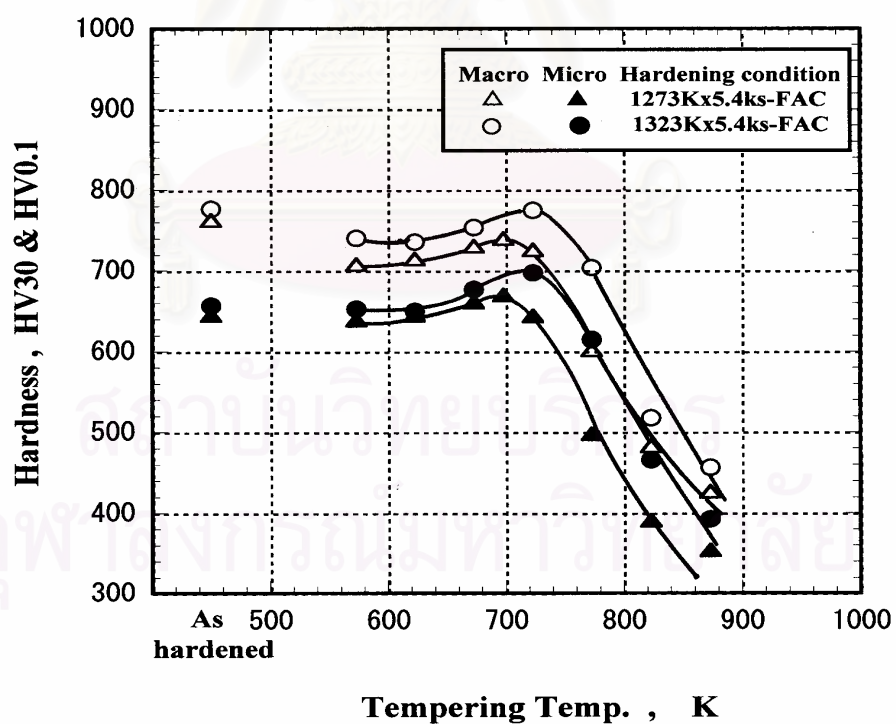temperature of 16% Cr cast iron with 2% Ni. (Specimen No. 3)

Fig.4.77   Relationship between micro-hardness of matrix and tempering
temperature of 26% Cr cast iron without alloying element.
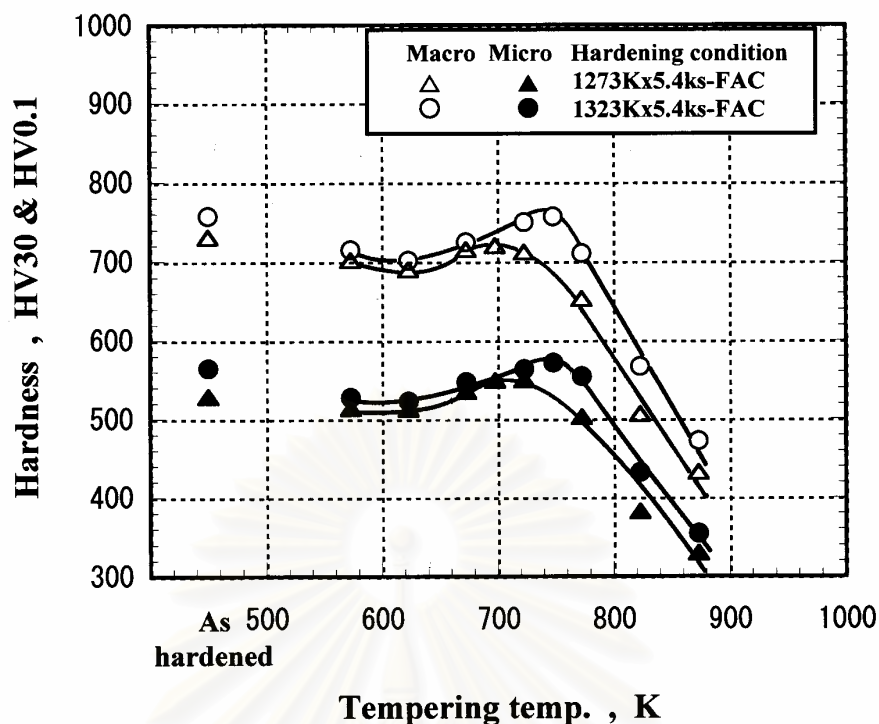(Specimen No. 4)

Fig. 4.78 Relationship between micro-hardness of matrix and tempering
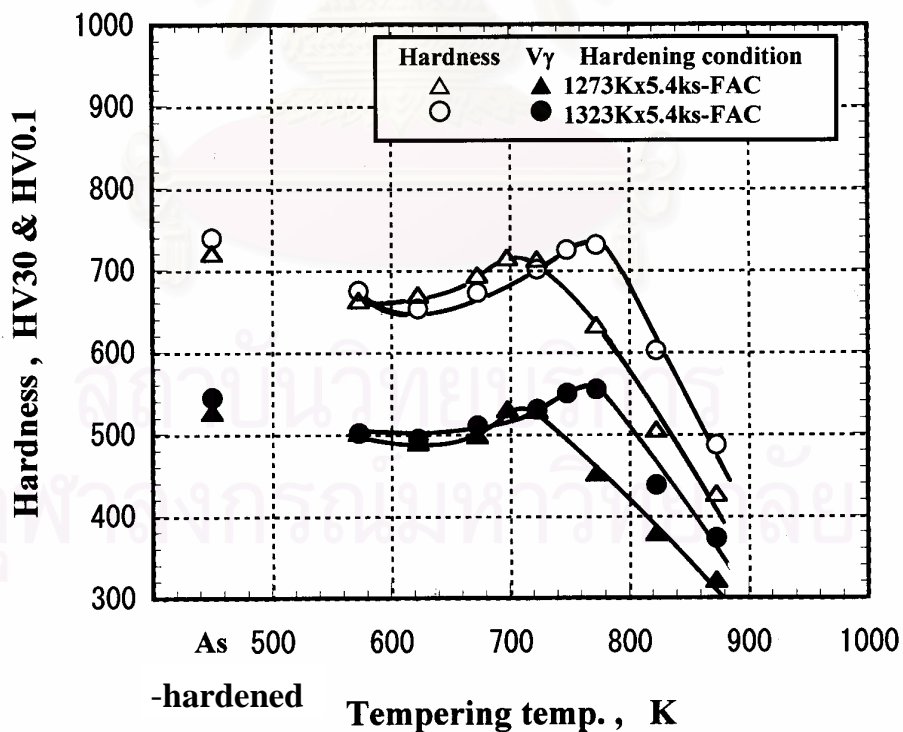temperature of 26% Cr cast iron with 1%Ni. (Specimen No. 5)

Fig. 4.79 Relationship between micro-hardness of matrix and tempering
temperature of 26% Cr cast iron with 2%Ni. (Specimen No. 6)

4.2.3.2 Effect of copper (Cu)

(a) Test specimen in as-cast state

Chemical compositions of the test specimens are shown in Table 4.29. Copper is added up to 2% to both of 16% Cr and 26% Cr specimens. The as-cast microstructures are shown in Fig. 4.80. Even when Cu content varies, the carbide morphology changes little compared with alloy-free specimen. However, the matrix changes remarkably depending on Cu content. As for the microstructures of 16% Cr specimens, most of matrix in alloy-free and 1% Cu specimens is pearlitic but that in 2 % Cu specimen is austenitic. In the case of 26 % Cr specimens, the matrices in all the specimens are austenitic, possibly containing some martensite. It is also same that sizes of eutectic colony and eutectic carbide particles of 26 % Cr specimens are much smaller than those of 16 %Cr specimens.

Macro-hardness and volume fraction of retained austenite (Vγ) in as-cast specimens are shown in Table 4.30. As Cu content increases, hardness rises from 572 HV30 to 607 HV30 in 16% Cr specimens but lowers slightly from 547 HV30 to 536 HV30 in 26% Cr specimens.

The Vγ values in 16% Cr specimens without and with 1% Cu are zero but that in 26% Cr specimen is 26%. This suggests that in 16% Cr hypoeutectic cast iron, 2% Cu is enough to delay the pearlite transformation in as-cast condition. In the case of 26% Cr specimens, the Vγ seems to be a little up from 46.7% to 50.6% by increasing Cu content.

Table 4.29 Chemical compositions of test specimens.

Specimen	Element (mass%)							
	C	Cr	Si	Mn	Ni	Cu	Mo	V
No.1	3.01	16.48	0.62	0.78	-	-	-	-
No.2	2.94	15.84	0.54	0.56	-	1.00	-	-
No.3	2.96	15.90	0.54	0.53	-	2.02	-	-
No.4	2.65	25.56	0.37	0.51	-	-	-	-
No.5	2.62	26.31	0.50	0.50	-	1.03	-	-
No.6	2.68	26.04	0.51	0.51	-	2.10	-	-

*S and P are less than 0.06 mass%

Table 4.30 Macro-hardness and volume fraction of retained austenite
(Vγ) of as-cast specimens.

Specimen	Element (mass%)		Hardness (HV30)	Vγ (%)
	Cr	Cu		
No. 1		-	572	0
No. 2	16	1	579	0
No. 3		2	607	26.1
No. 4		-	547	46.8
No. 5	26	1	544	48.4
No. 6		2	536	50.6

Table 4.31 Macro-hardness and volume fraction of retained austenite
(Vγ) of as-hardened specimens.

Specimen	Element (mass%)		Austenitizing Temperature (K)			
			1273		1323	
	Cr	Cu	Hardness (HV30)	Vγ (%)	Hardness (HV30)	Vγ (%)
No. 1		-	775	18.1	730	31.8
No. 2	16	1	780	29.0	710	40.8
No. 3		2	786	30.0	692	50.0
No. 4		-	763	4.1	777	11.5
No. 5	26	1	729	4.0	760	8.5
No. 6		2	696	4.5	730	9.3

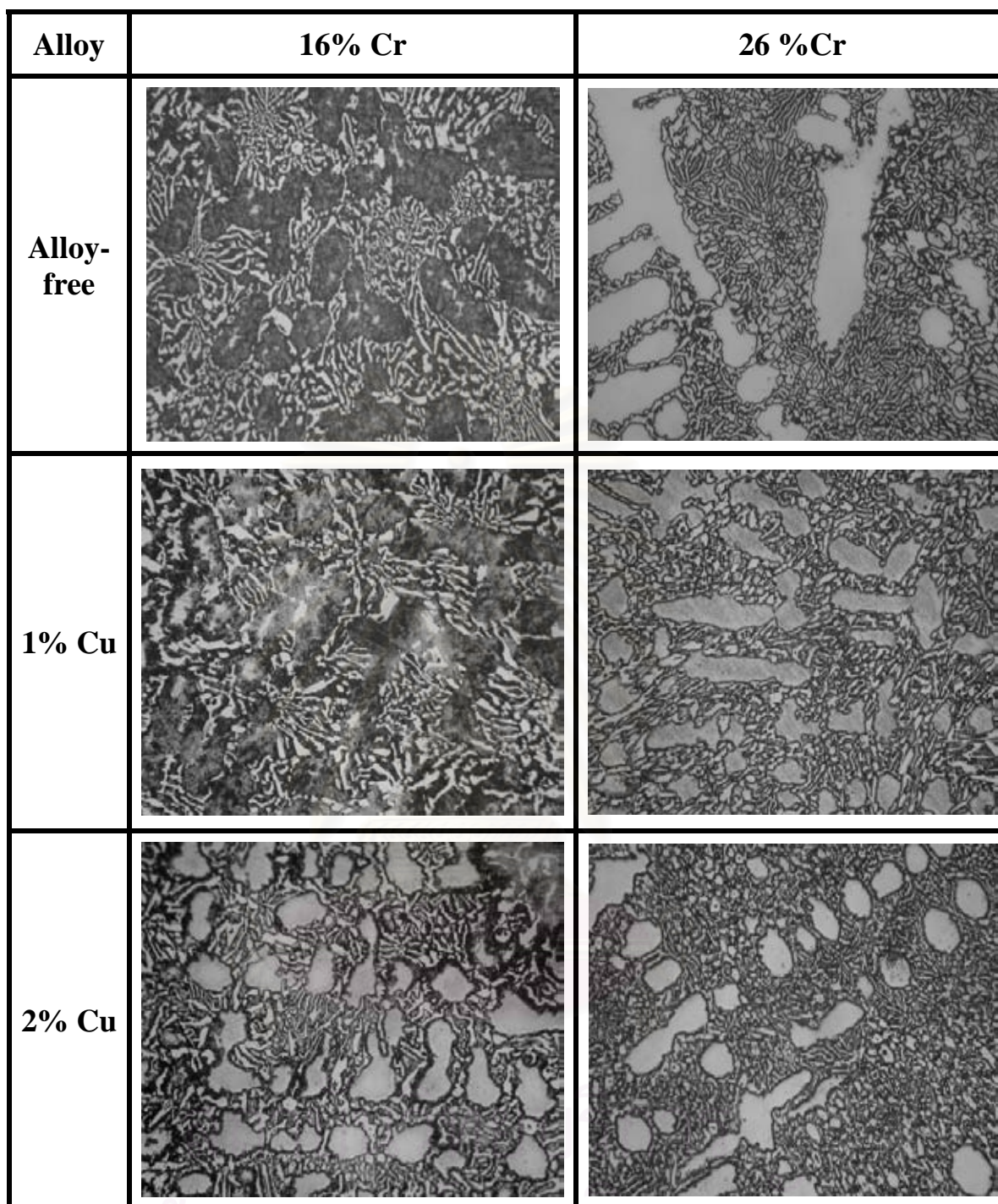| Alloy	16% Cr	26 %Cr
Alloy-free		
1% Cu		
2% Cu		

50 μm

Fig. 4.80 As-cast microstructures of 16% Cr and 26% Cr cast irons with and without Cu. Matrix of 16% Cr cast irons with Cu up to 1% Cu mostly pearlitic but that of 16% Cr cast iron with 2% Cu is austenitic. Matrices of alloy-free 26% Cr cast irons and those with Cu are austenitic possibly with some martensite.

(b) Effect of Cu content on variation of macro-hardness and volume fraction of retained austenite (Vγ) during heat treatment

-As-hardened state

Macro-hardness and Vγ of as-hardened specimens are shown in Table 4.31. As-hardened hardness is closely related to the chemical composition and austenitizing temperature that determine the transformation of matrix on the position of CCT curves. The effects of Cu content on macro-hardness and Vγ are shown in Fig. 4.81 (a) and (b), respectively. In 16% Cr specimens, the hardness in 1273 K austenitization increases a little from 775 HV30 at 0% Cu to 786 HV30 at 2% Cu as Cu content increase. In the case of 1323 K austenitization, on the other hand, it decreases from 730 HV30 to 692 HV30. In the case of 26% Cr specimens, the hardness reduces gradually regardless of austenitizing temperature from 763 HV30 at 0% Cu to 696 HV30 at 2% Cu in 1273 K and from 777 HV30 to 730 HV30 in 1323 K austenitization. It can be said that an increase in the austenitizing temperature makes the hardness low in 16% Cr specimen but high in 26% specimen.

As for the Vγ shown in Fig. 4.78 (b), it increases from 18.1% to 30% in 1273 K and from 31% to 50% in 1323 K austenitization in 16%Cr specimens, as Cu content increases to 2%. In 26% Cr specimens, however, the Vγ varies little at about 4% in 1273 K and at about 10% in 1323 K austenitization. In all the specimens, it is found that the Vγ is higher in the case of 1323 K austenitization.

The microstructures of as-hardened specimens of 16% and 26%Cr specimens are respectively shown in Fig. 4.82. A large amount of fine carbides, martensite and some retained austenite exists in the matrix. In each group of cast iron, austenite and/or pearlite existing in as-cast state is greatly reduced, and instead, a large amount of carbides can be seen. This is because the secondary carbides precipitated from austenite supersaturated with C and Cr during austenitization.
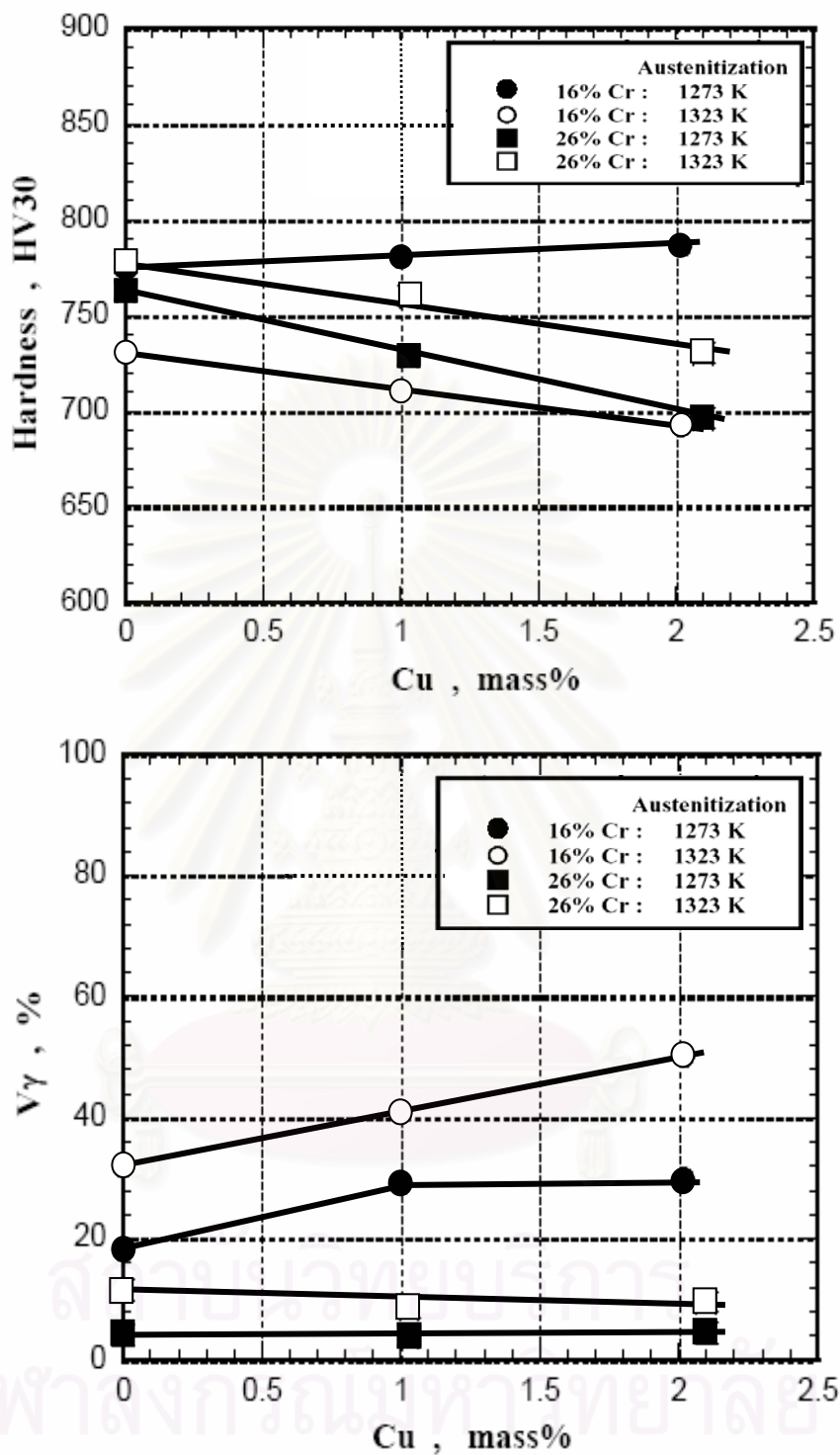
Fig. 4.81 Effects of Cu content on macro-hardness (a) and Vγ (b) in as-
hardened state.

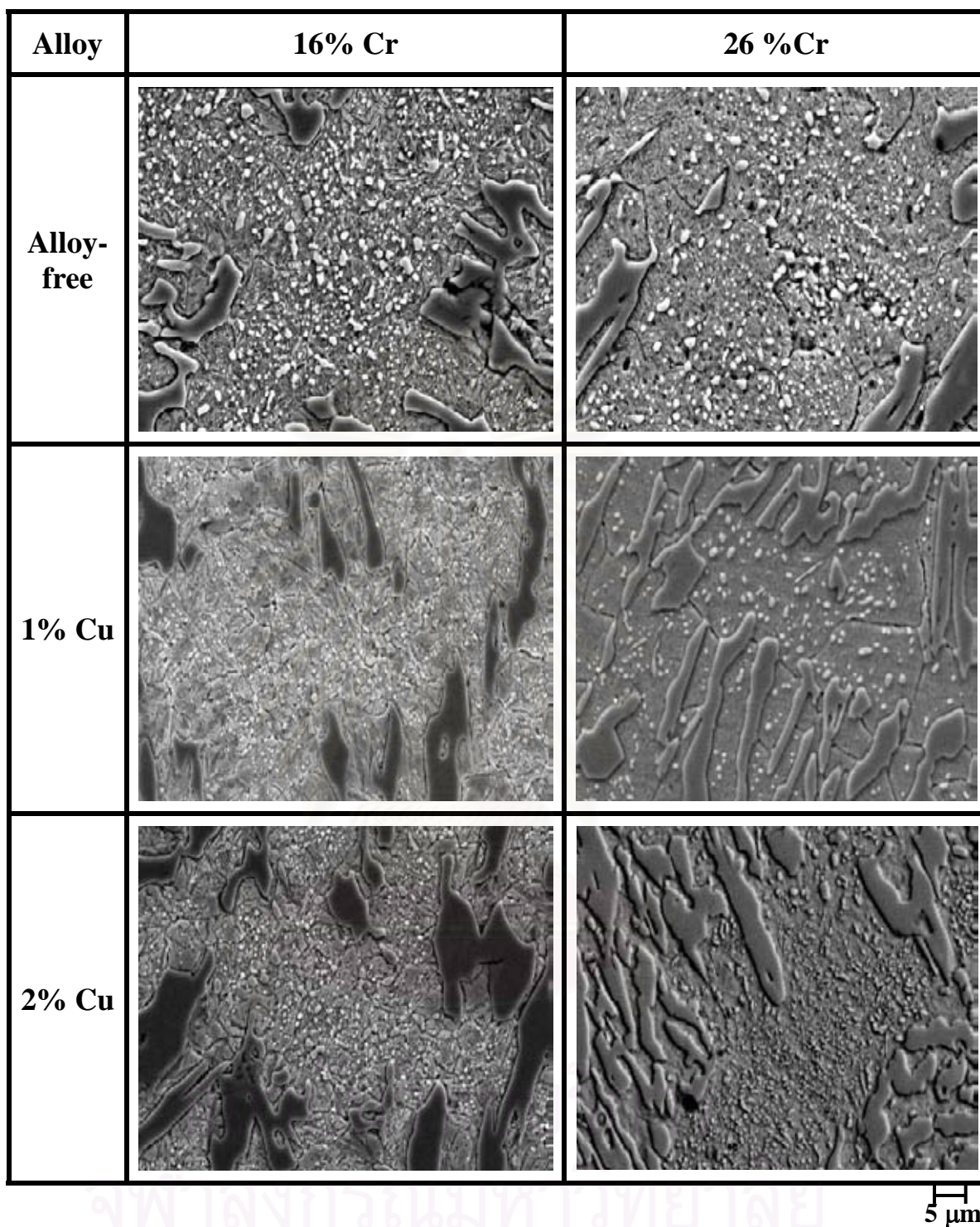| Alloy	16% Cr	26 %Cr
Alloy-free		
1% Cu		
2% Cu		

5 μm

Fig. 4.82 SEM microphotographs in as-hardened state of 16% Cr and 26% Cr hypoeutectic cast irons with and without Cu. Matrices of all cast irons consist of secondary carbides, martensite and retained austenite except for alloy-free 16% Cr cast iron.

- Tempered state

In order to clarify the effect of Cu content on the behavior of hardness and Vγ during tempering, the tempered hardness curves were constructed for each specimen. After hardening from two austenitizing temperatures, 1273 K and 1323 K, the specimens were tempered at several temperatures from 573 K to 873 K. The macro-hardness and Vγ were measured and the results are shown in Fig. 4.83 and Fig. 4.84 for 16% Cr specimens and Fig. 4.85 and Fig. 4.86 for 26% Cr specimens. The results of alloy-free specimens with 16% Cr and 26% Cr are already shown in the previous section, Fig. 4.68 for 16% Cr (No.1) and Fig. 4.71 for 26% Cr (No. 4) specimens, respectively. The degrees of secondary hardening are summarized in Table 4.32. It is found that the degree is increased by Cu addition.

(i) 16%Cr cast iron

The relationship between macro-hardness, Vγ and tempering temperature of 1% Cu specimen (No. 2) is shown in Fig. 4.83. The tempered hardness curves show the similar behavior to alloy-free specimen. In the range of tempering temperature lower than 748 K, the hardness of specimens hardened from 1323 K are lower than those hardened from 1273 K because more austenite was still left in the matrix after tempering. When the tempering temperature gets over 748 K, the hardness are reversed. The harness curves show remarkable secondary hardening and the degree is greater compared with alloy-free specimen. The degrees are 60 HV30 in 1273 K and 125 HV30 in 1323 K austenitization. The H_{Tmax} values are 775 HV30 at 723 K in 1273 K and 780 HV30 at 773 K tempering in 1323 K austenitization, respectively.

Irrespective of austenitizing temperature, the Vγ values in as-hardened state reduce from 623 K and get to 0% at 750 K in 1273 K and 780 K in 1323 K austenitization. The Vγ value at H_{Tmax} is 6% in 1273 K and 4% in 1323 K austenitization, respectively.

Table 4.32 Degree of the secondary hardening of test specimens.

Specimen	Element (mass %)		Degree of the secondary hardening (HV30)	
	Cr	Cu	1273 K austenitization	1323 K austenitization
No. 1		-	33	83
No. 2	16	1	60	125
No. 3		2	65	175
No. 4		-	20	34
No. 5	26	1	40	58
No. 6		2	85	95

In 2% Cu specimen (No. 3) as shown in Fig. 4.84, the tempered hardness curves show the similar tendency to the alloy-free and 1% Cu specimens. The degree of secondary hardening in the case of 1323 K austenitization is greatest in the 16% Cr specimens, and the pattern is quite similar to that of 2% Ni hypoeutectic specimen hardened from 1323 K. The degrees are 65 HV30 in 1273 K and 175 HV30 in 1323 K austenitization. The H_{Tmax} of about 780 HV30 is obtained in both austenitizing temperatures. The tempering temperature at H_{Tmax} is about 40 K higher in the specimen hardened from 1323 K than that hardened from 1273 K austenitization.

The Vγ also begins to reduce over 623 K in 1273 K and 673 K tempering in 1323 K austenitization, and they disappear at 760 K in 1273 K and 795 K in 1323 K austenitization. The Vγ values at H_{Tmax} are 6% at 735 K in 1273 K and 10% at 773 K in 1323 K austenitization.

(ii) 26%Cr cast iron

The results of 1% Cu specimen (No. 5) are shown in Fig. 4.85. The tempered hardness curves show the similar behavior to in alloy-free specimen, that is, the curve of specimen hardened from 1323 K lies overall at high hardness side compared with the specimen hardened from low temperature of 1273 K. This behavior is similar to 2% Cu specimen
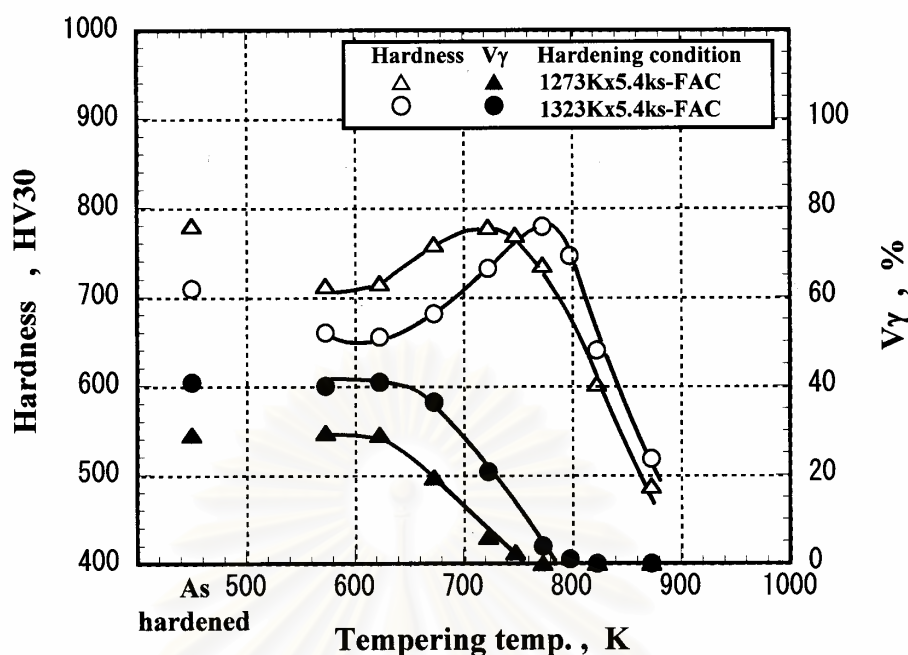
Fig. 4.83 Relationship between macro-hardness, volume fraction of retained austenite (Vγ) and tempering temperature of 16%Cr cast iron with 1% Cu. (Specimen No. 2)
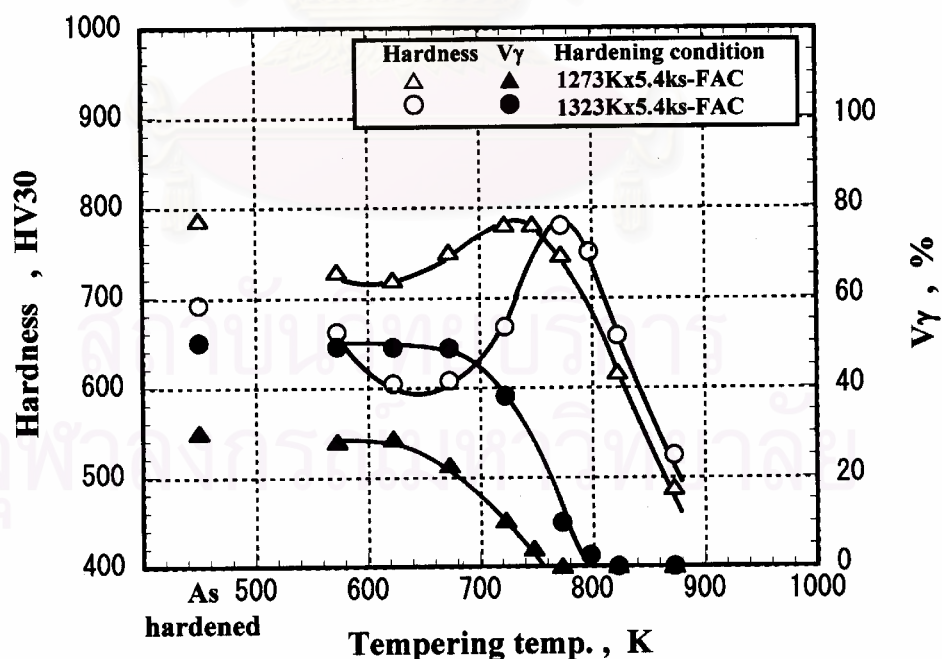

Fig. 4.84 Relationship between macro-hardness, volume fraction of retained austenite (Vγ) and tempering temperature of 16%Cr cast iron with 2% Cu. (Specimen No. 3)

but quite different from those of 16% Cr specimens with Cu. The degree of secondary hardening is a little greater in the case of high austenitization and the tempering temperature at H_{Tmax} is shifted to the higher temperature side. The degrees are 40 HV30 in 1273 K and 58 HV30 in 1323 K austenitization. The H_{Tmax} values of 730 HV30 in 1273 K and 763 HV30 in 1323 K austenitization are obtained at 698 K and 748 K tempering.

In the case of 1273 K and 1323 K austenitization, the $V\gamma$ decreases gradually with an increase in the tempering temperature and gets to 0% at 773 K and 800 K, respectively. The $V\gamma$ value at H_{Tmax} is about 3 % regardless of austenitizing temperature.

Fig. 4.86 shows the results of 2% Cu specimen (No. 6). The patterns of the tempered hardness curves are similar to alloy-free and 1% Cu specimens. The degree of secondary hardening is greatest in the 26% Cr specimens and they are smaller than that of 16% Cr specimens. The degrees are 85 HV30 in 1273 K and 95 HV30 in 1323 K austenitization. The H_{Tmax} values are 775 HV30 in 1273 K and 780 HV30 in 1323 K austenitization, respectively.

The $V\gamma$ decreases over 623 K in 1273 K and over 673 K in 1323 K austenitization, and reaches 0% at 773 K in 1273 K and 780 K in 1323 K austenitization. The $V\gamma$ values at H_{Tmax} are 2% in 1273 K and 5% in 1323 K austenitization.

(c) Relationship between micro-hardness of matrix and tempering temperature

Macro-hardness is changed in accordance with matrix structure because the hardness of eutectic carbide does not change at all. In order to make it sure, the matrix hardness of the tempered specimens were measured using Micro-Vickers hardness tester. The results of alloy-free specimens (No. 1 and No. 4) are shown in Fig. 4.74 for 16% Cr and Fig. 4.77 for 26% Cr specimens.
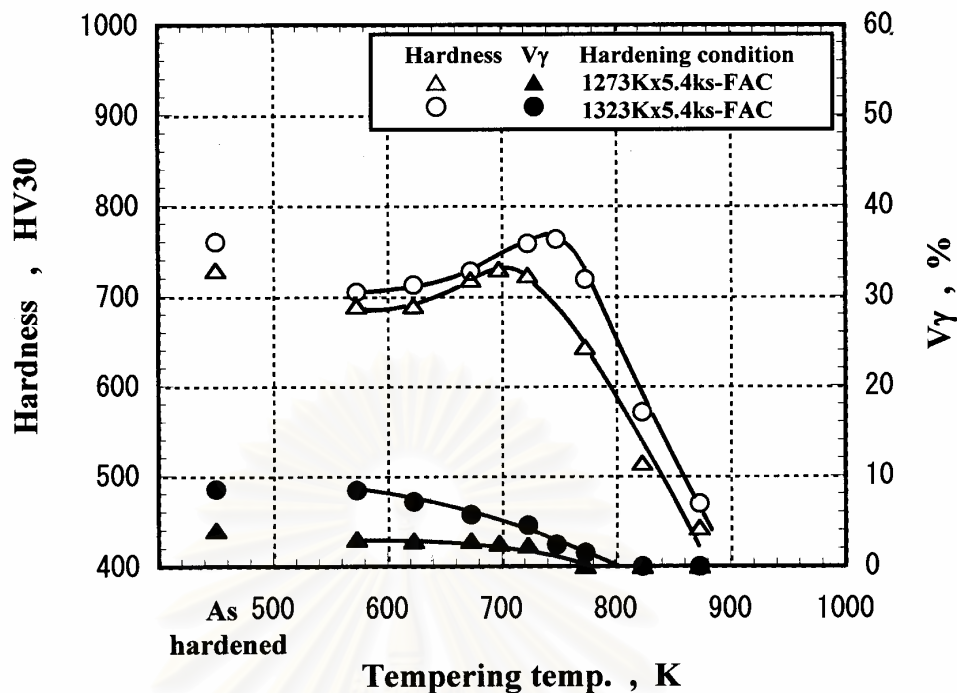
Fig. 4.85 Relationship between macro-hardness, volume fraction of retained austenite (Vγ) and tempering temperature of 26%Cr cast iron with 1% Cu. (Specimen No. 5)
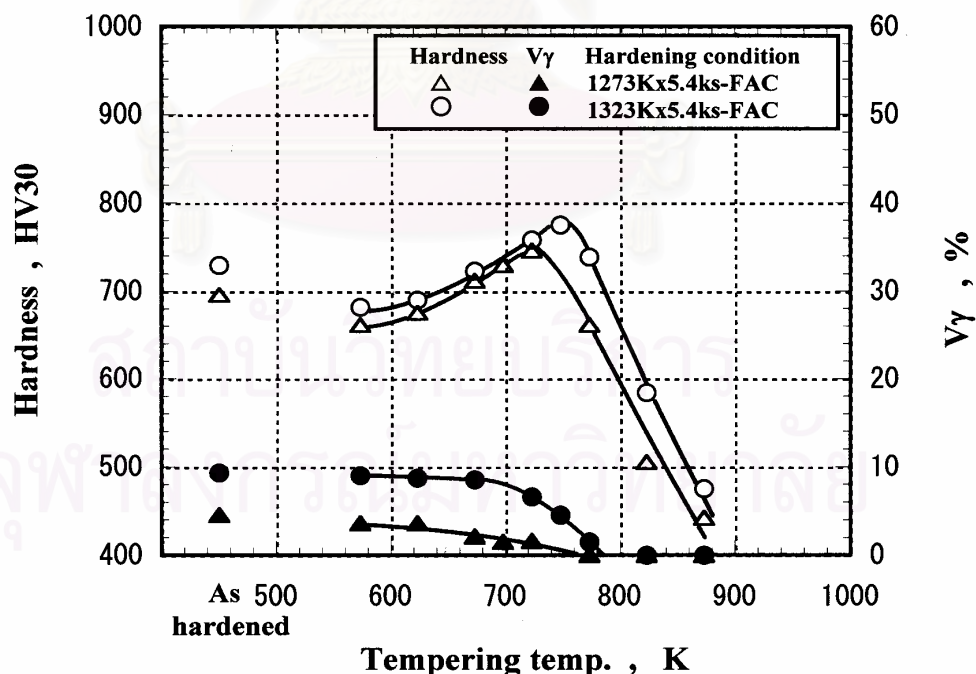

Fig. 4.86 Relationship between macro-hardness, volume fraction of retained austenite (Vγ) and tempering temperature of 26% Cr cast iron with 2% Cu. (Specimen No. 6)

The comparison of micro-hardness in the matrix with macro-hardness is shown in Fig. 4.87 for 16% Cr with 1% Cu and Fig. 4.88 for 16% Cr with 2% Cu specimen, and Fig. 4.89 for 26% Cr with 1% Cu and Fig. 4.90 for 26% Cr with 2% Cu specimens, respectively. In every specimen, the micro-hardness shows a quite same behavior as macro-harness and it is overall lower than macro-hardness. This suggests that the macro-hardness displays the total hardness of matrix and eutectic carbides. The peaks of micro-hardness are high in the case of high austenitization of 1323 K and the tempering temperatures at the peaks are almost same as those of macro-hardness. The micro-hardness curves also display the secondary hardening. The degrees and the maximum micro-hardness are summarized in Table 4.33 and Table. 4.34, respectively. It is found that the degrees are increased by increasing Cu content and the austenitizing temperature. In 16% Cr specimens, they vary from 25 HV0.1 at 0% Cu to 83 HV0.1 at 2% Cu in 1273 K and 55 HV0.1 at 0% Cu to 148 HV0.1 at 2% Cu in 1323 K austenitization. In 26% Cr specimens, they increase from 22 HV0.1 at 0% Cu to 73 HV0.1 at 2% Cu in 1273 K and 92 HV0.1 at 0% Cu to 52 HV0.1 at 2% Cu in 1323 K austenitization.

In the both Cr specimens, the maximum micro-hardness of Cu specimens are lower than Cu-free specimen. They are around 680 HV0.1 irrespective of Cu content and austenitizing temperature in 16% Cr specimens. In 26% Cr specimens, however, they show a little difference, 544 to 567 HV0.1 in 1273 K and 605 to 610 HV0.1 in 1323 K austenitization. The differences between macro-hardness and micro-hardness at the H_{Tmax} are 80 to 90 HV0.1 in 1273 K and 100 HV0.1 in 1323 K austenitization in 16% Cr specimens, and 160 to 180 HV0.1 in 1273 K and 180 to 200 HV0.1 in 1323 K in 26% Cr specimens, respectively.
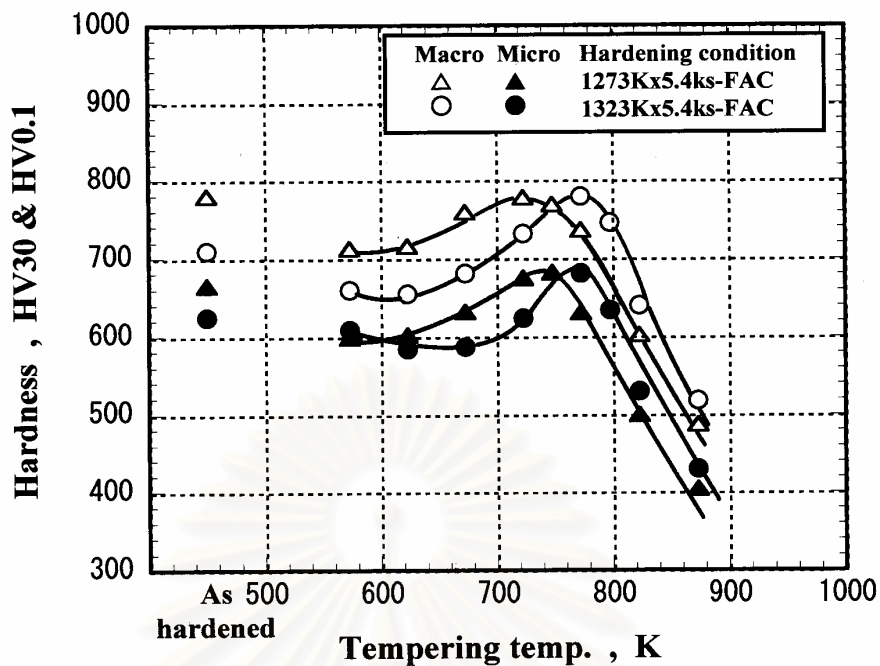
Fig. 4.87 Relationship between micro-hardness of matrix and tempering temperature of 16% Cr cast iron with 1% Cu. (Specimen No. 2)
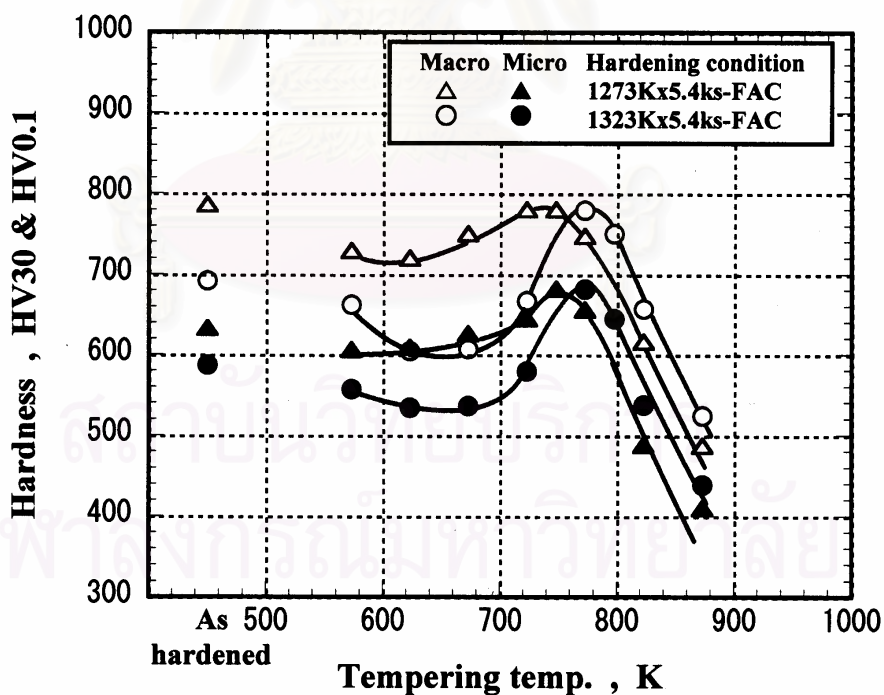

Fig. 4.88 Relationship between micro-hardness of matrix and tempering temperature of 16% Cr cast iron with 2% Cu. (Specimen No. 3)

Table 4.33 Degree of secondary hardening of micro-hardness.

Specimen	Cr (mass%)	Cu (mass%)	Degree of secondary hardening (HV0.1)	
			1273 K austenitization	1323 K austenitization
No.1	16	-	25	55
No.2		1	81	95
No.3		2	83	148
No.4	26	-	22	52
No.5		1	33	60
No.6		2	73	92

Table 4.34 Maximum micro-hardness of matrix.

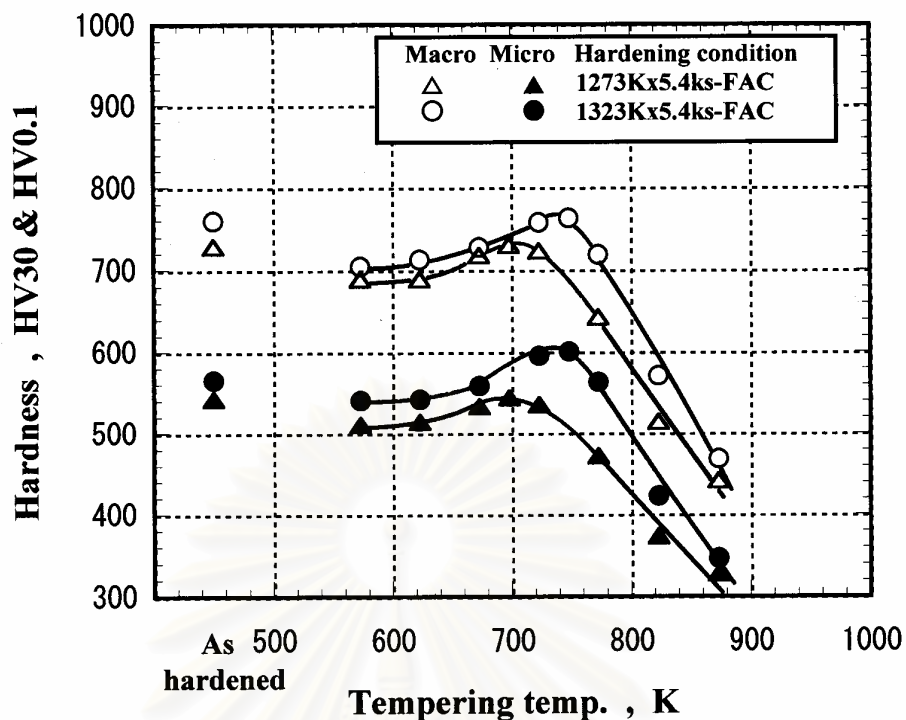| Specimen	Cr (mass%)	Cu (mass%)	Maximum micro-hardness (HV0.1)	
			1273 K austenitization	1323 K austenitization
No.1	16	-	697	706
No.2		1	680	682
No.3		2	682	682
No.4	26	-	683	703
No.5		1	544	605
No.6		2	567	610

Fig. 4.89 Relationship between micro-hardness of matrix and tempering temperature of 26% Cr cast iron with 1% Cu. (Specimen No. 5)
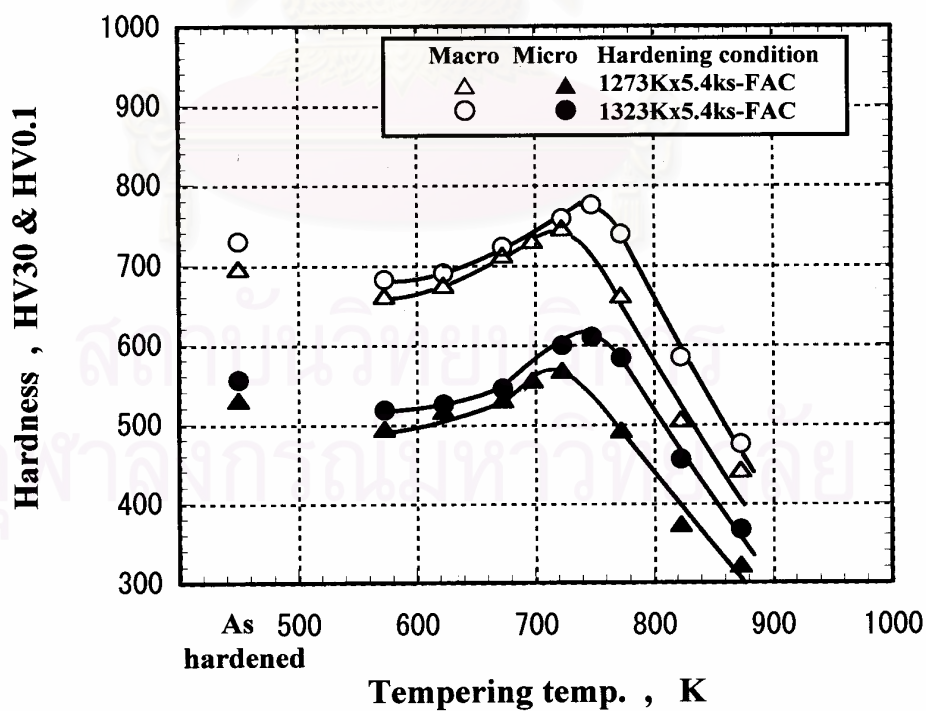

Fig. 4.90 Relationship between micro-hardness of matrix and tempering temperature of 26% Cr cast iron with 2% Cu. (Specimen No. 6)

4.2.3.3 Effect of molybdenum (Mo)

(a) Test specimens in as-cast state

Chemical compositions of the test specimens are listed in Table 4.35. Molybdenum is added up to 3% to the 16% Cr and 26% Cr specimens. The as-cast microstructures of alloy-free and Mo specimens are illustrated in Fig. 4.91. Mo is a strong carbide forming element and it combines with C to form eutectic Mo_2C (M_2C) carbide during solidification. The morphology of ($\gamma+M_7C_3$) eutectic structure is similar in the same chromium specimens but the sizes of eutectic colony and eutectic carbide particle are coarse in 16% Cr and fine in 26% Cr specimens. It is also found from particular observation that the carbide size seems to be even enlarged with an increase in Mo content. Mo is also distributed into matrix and affects the matrix structure. The matrices of the alloy-free specimens are pearlitic in 16%Cr specimen and austenitic in 26%Cr specimen. However, the matrix structures of Mo specimens are all austenititic and there some martensite could exist. This is explained by that Mo delays pearlite transformation and lowers the Ms temperature in as-cast state. In the study of 15% Cr cast iron with 1% Mo, Dupin and Schissler[33] mentioned that the M_2C carbide was not found. However, Laird [15] observed the M_2C carbides at the boundary in 20% Cr cast iron with 2% Mo. In this experiment, the M_2C carbide may precipitate from the melt in the specimens with Mo more than 2% but it can not be distinguished from the microphotographs taken by low magnification (Fig. 4.87). As shown in Fig.4.93, however, the M_2C carbides in eutectic morphology are clearly detected in the microphotographs with high magnification in of microphotographs of 3% Mo specimen.

Macro-hardness and Vγ of as-cast specimens are shown in Table 4.36. The hardness decreases from 572 HV0 to 503 HV30 in 16% Cr and 547 HV30 to 519 HV30 in 26% Cr specimens as Mo content increases in the both series of the specimens. When Mo content increases, the Vγ does not change so much in 16% Cr specimens, ranging from 87.7% to 90.8%,

but increases from 46.8% to 67.8% in 26% Cr specimens. At the same Mo content, the hardness is lower and the Vγ is higher in 16% Cr specimens compared with those in 26% Cr specimens.

Table 4.35 Chemical compositions of test specimens.

Specimen	Element (mass%)							
	C	Cr	Si	Mn	Ni	Cu	Mo	V
No. 1	3.01	16.48	0.62	0.78	-	-	-	-
No. 2	2.97	16.12	0.52	0.50	-	-	0.96	-
No. 3	2.97	15.93	0.51	0.51	-	-	2.03	
No. 4	3.05	15.82	0.55	0.51	-	-	3.05	-
No. 5	2.65	25.56	0.37	0.51	-	-	-	-
No. 6	2.66	25.84	0.48	0.50	-	-	0.98	-
No. 7	2.61	25.90	0.50	0.50	-	-	1.95	
No. 8	2.64	26.40	0.49	0.47	-	-	2.96	-

*S and P are less than 0.06 mass%

Table 4.36 Macro-hardness and volume fraction of retained austenite (Vγ) of as-cast specimens.

Specimen	Element (mass%)		Hardness (HV30)	Vγ (%)
	Cr	Mo		
No. 1		-	572	0
No.2	16	1	516	87.7
N0.3		2	507	88.4
No.4		3	503	90.8
No.5		-	547	46.8
No.6	26	1	539	59.3
No.7		2	520	65.8
No.8		3	519	67.8

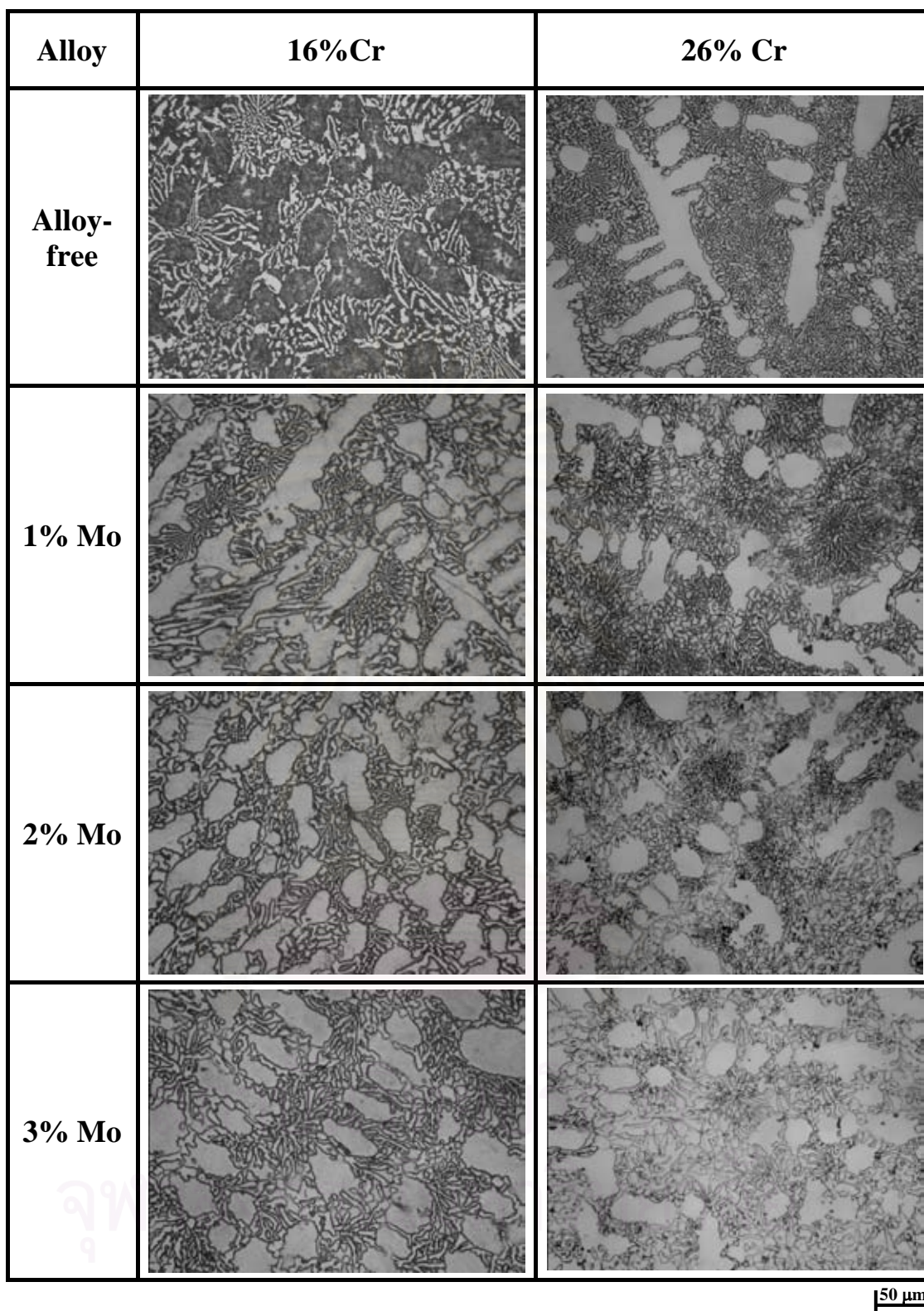| Alloy	16%Cr	26% Cr
Alloy-free		
1% Mo		
2% Mo		
3% Mo		

50 μm

Fig. 4.91 As-cast microstructures of 16% Cr and 26% Cr hypoeutectic cast irons without and with Mo. Matrices of all 16% Cr cast irons with Mo and alloy-free 26% Cr cast iron are austenitic possibly with martensite. Size of eutectic carbides seems to be enlarged by Mo addition.

(b) Effect of Mo content on macro-hardness and volume fraction of retained austenite (Vγ) during heat treatment

-As-hardened state

Macro-hardness and Vγ of as-hardened specimens are summarized in Table 4.37 and the relationship between hardness, the Vγ and Mo content are shown in Fig. 4.92 (a) and (b). As shown, an increase in Mo content raises the hardness of 16% Cr specimens from 775 HV30 at 0% Mo to 848 HV30 at 3% Mo in 1273 K and 730 HV30 to 777 HV30 in 1323 K austenitization. The hardness of 26% Cr specimens increases from 763 HV30 to 824 HV30 in 1273 K and 777 HV30 to 850 HV30 in 1323 K austenitization, as Mo content increases up to 3%. As for the influence of austenitizing temperature, the hardness are low in 16% Cr specimens but high in 26% Cr specimens when the austenitizing temperature is high. The highest hardness is obtained in the specimen containing 3% Mo regardless of austenitizing temperature. At the same Mo content, the hardness is high by the order of 26% Cr in 1323 K, 16% Cr in 1273 K, 26% Cr in 1273 K and 16% Cr specimens in 1323 K austenitization.

As shown in Fig. 4.92 (b), the Vγ is relatively high in 16% Cr specimens compared with 26% Cr specimens. In 16% Cr specimens, the Vγ increases from 18.1% at 0% Mo to 28.3% at 3% Mo in 1273 K and 31.8% to 51.5% in 1323 K austenitization. In 26% Cr specimens, the Vγ increases from 4.1% at 0% Mo to 14.0% at 3% Mo in 1273 K and 11.5% to 19.6% in 1323 K austenitization. It is found that the Vγ values in 1323 K austenitization are about twice as much as those in the case of 1273 K austenitization. This is because the more C, Cr and Mo dissolved in austenite in the case of high austenitizing temperature and they stabilized the austenite.

The as-hardened microstructures are shown in Fig. 4.93. The matrix structure consists of secondary carbides, martensite and austenite.

Table 4.37 Macro-hardness and volume fraction of retained austenite (Vγ) of as-hardened specimens.

Specimen	Element (mass%)		Austenitizing Temperature (K)			
	Cr	Mo	1273		1323	
			Hardness (HV30)	Vγ (%)	Hardness (HV30)	Vγ (%)
No. 1	16	-	775	18.1	730	31.8
No. 2		1	800	24.4	740	42.0
No. 3		2	820	25.0	750	45.9
No. 4		3	848	28.3	777	51.5
No. 5	26	-	763	4.1	777	11.5
No. 6		1	778	7.5	805	14.9
No. 7		2	817	13.0	832	17.5
No. 8		3	824	14.0	850	19.6

G. Powell [27] reported that the secondary carbides which precipitated in the matrix are mostly $M_{23}C_6$ carbides co-existing with small amount of M_7C_3 carbides. In the case of 16% Cr specimens, the pearlitic matrix in as-cast state is replaced by the secondary carbide, martensite and austenite. The matrix structure of 26% Cr specimens is similar to 16%Cr specimens. The retained austenite which existed much more in as-cast state is destabilized and the fine secondary carbides and martensite are produced. When the size of secondary carbides is compared, it can be said that the size is smaller in the specimens with Mo.

- Tempered state

To clarify the effect of Mo on the behavior of hardness and Vγ during heat treatment, the curve of tempered hardness is generally conducted. When the martensite is tempered, the hardness increase because the special carbides with high hardness which is formed by alloying element precipitate from martensite and this make the matrix hardness increase. At the same time, the Vγ remaining in the tempered

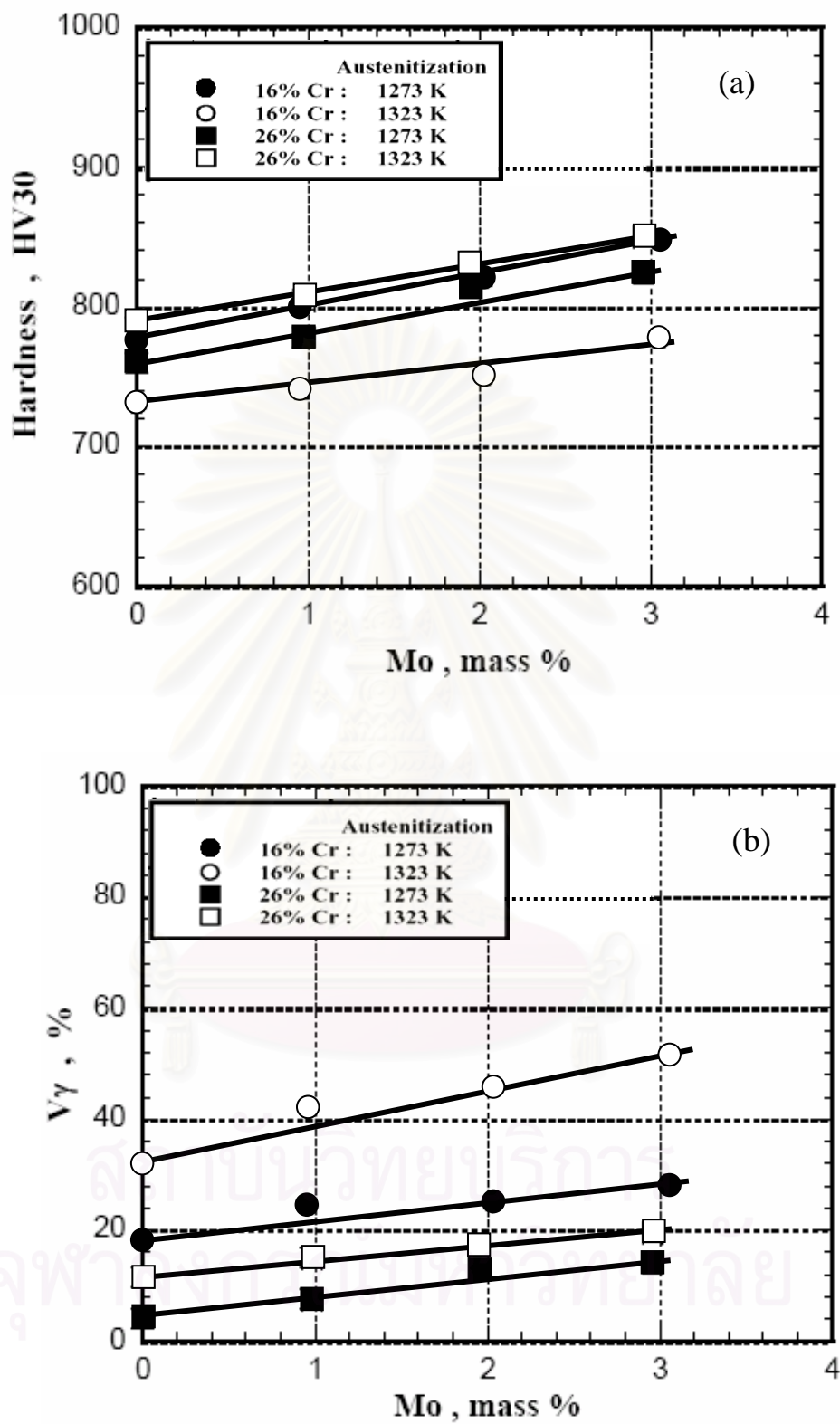Fig. 4.92 Effect of Mo content on macro-hardness (a) and Vγ (b) in as-hardened state.

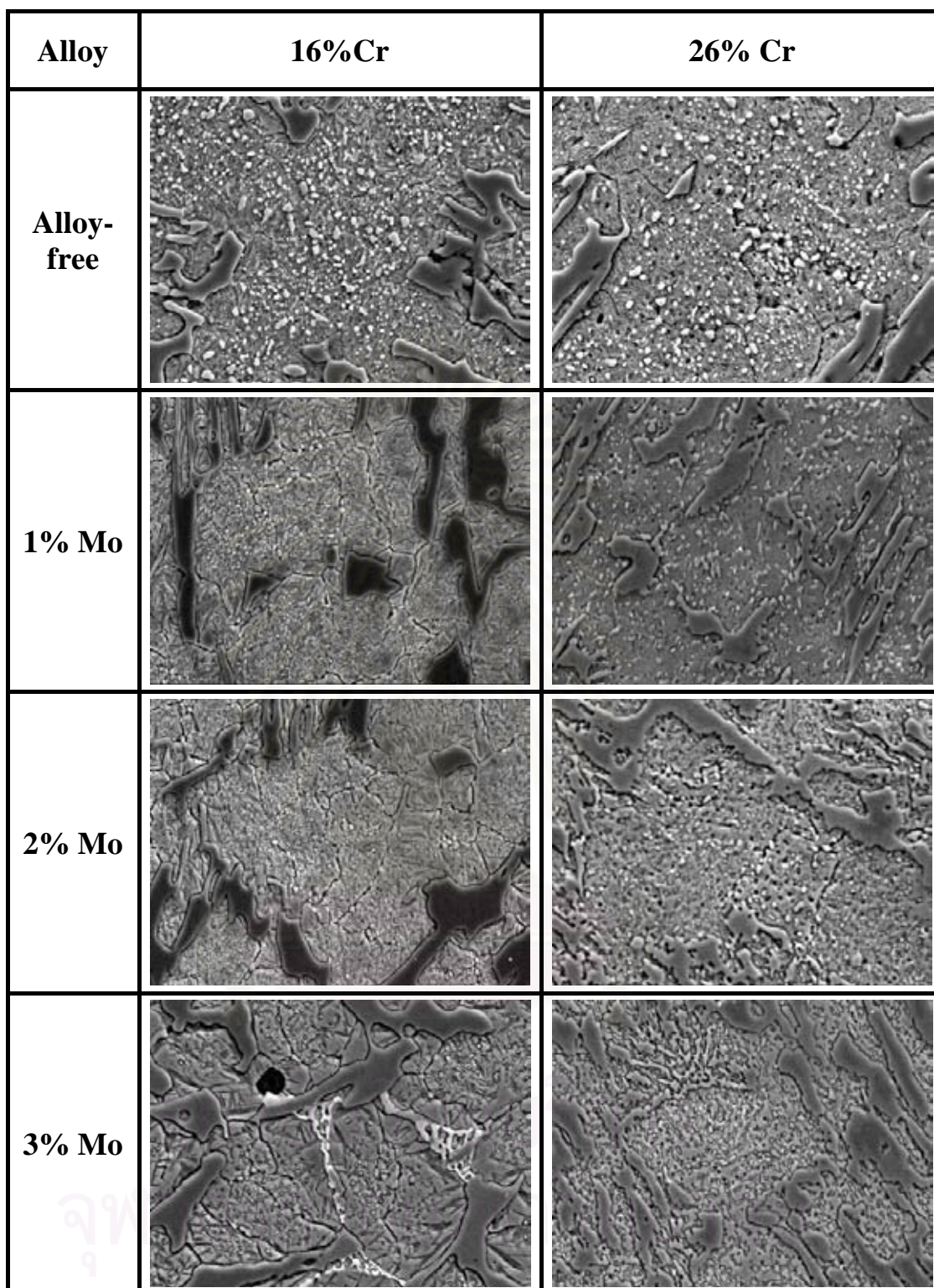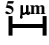| Alloy	16%Cr	26% Cr
Alloy-free		
1% Mo		
2% Mo		
3% Mo		

Fig.4.93 SEM microphotographs in as-hardened state of 16%Cr and 26% Cr hypoeutectic cast irons with and without Mo. Matrix of all cast irons consist of secondary carbides, martensite and austenite. (γ+Mo$_2$C) eutectic carbides can be seen in 16% Cr and 26% Cr cast irons with 3% Mo.

Table 4.38 Degree of the secondary hardening of tempered specimens.

Specimen	Element (mass%)		Degree of the secondary hardening (HV30)	
	Cr	Mo	1273 K austenitization	1323 K austenitization
No. 1	16	-	33	83
No. 2		1	44	135
No. 3		2	70	158
No. 4		3	83	185
No. 5	26	-	20	34
No. 6		1	30	71
No. 7		2	61	69
No. 8		3	57	75

state transforms into martensite during cooling and this also makes the hardness rise.

The relationships between macro-hardness, $V\gamma$ and tempering temperature are shown in Fig. 4.94 to 4.96 for 16% Cr and Fig. 4.97 to Fig. 4.99 for 26% Cr specimens, respectively. The tempered hardness curves of Mo specimens show more secondary hardening than those in alloy-free specimens which were shown in Fig. 4.68. and Fig. 4.71. The degrees of secondary hardening are listed in Table. 4.38.

(i) 16%Cr cast iron

The relationship between hardness, $V\gamma$ and tempering temperature of 1% Mo specimen (No. 2) is shown in Fig. 4.94. The hardness curve shows similar behavior to alloy-free specimen (Fig. 4.68). The hardness of specimens hardened from 1273 K are higher than those hardened from 1323 K in the range of tempering temperature lower than 773 K and over 773 K, it is reversed. The degrees of secondary hardening are much larger in Mo specimen compared with alloy-free specimen. Within Mo specimens, the degree increases with an increase in Mo content. The degrees in 1273 K are smaller than those in 1323 K austenitization,
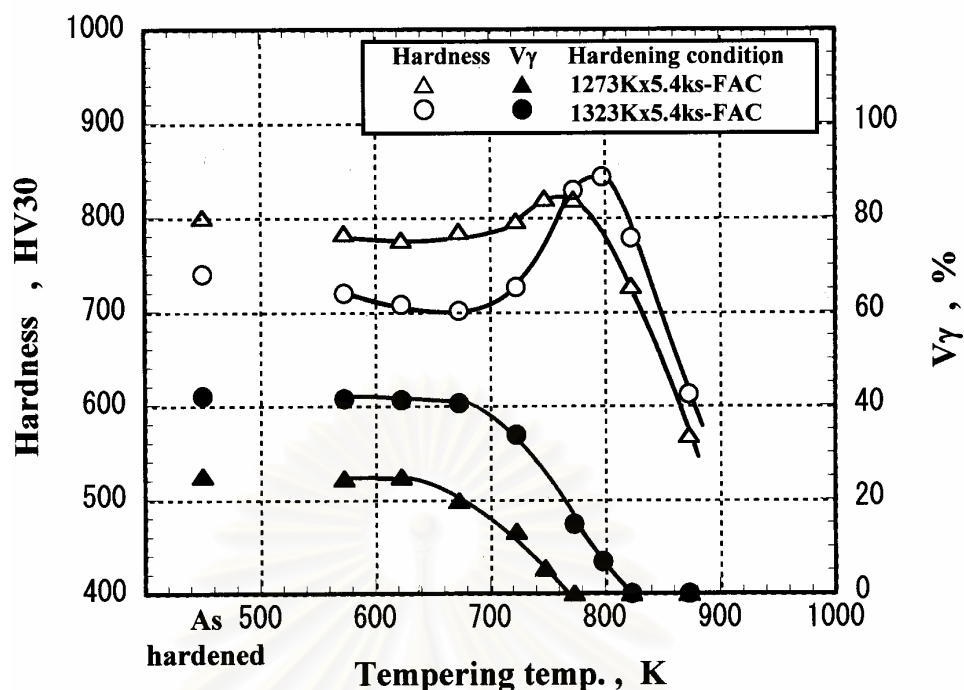
Fig. 4.94 Relationship between macro-hardness, volume fraction of retained austenite (Vγ) and tempering temperature of 16%Cr cast iron with 1% Mo. (Specimen No. 2)

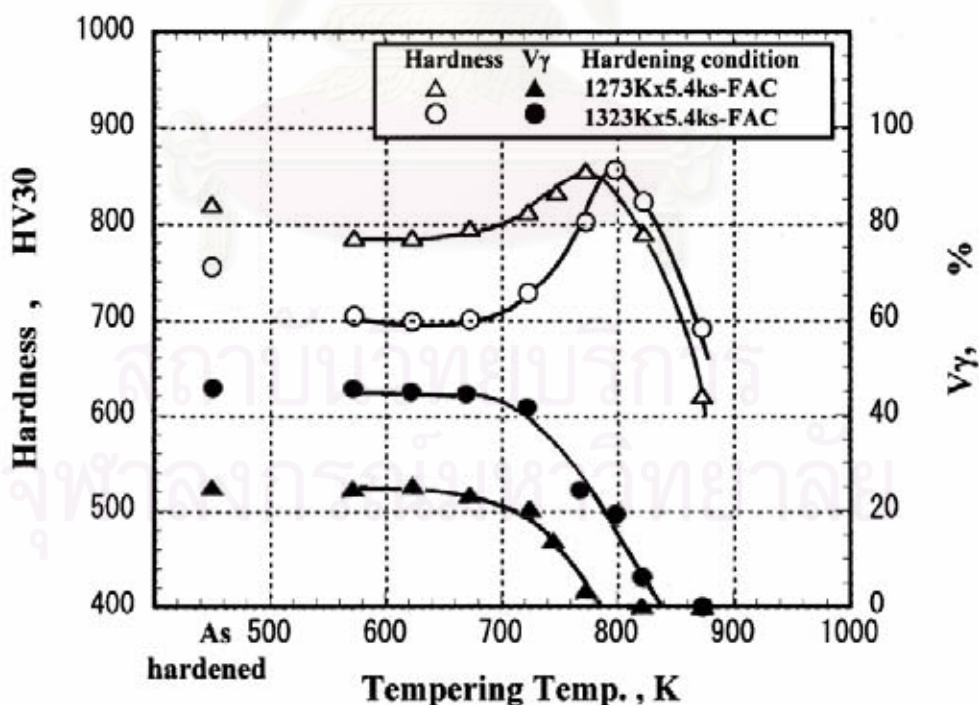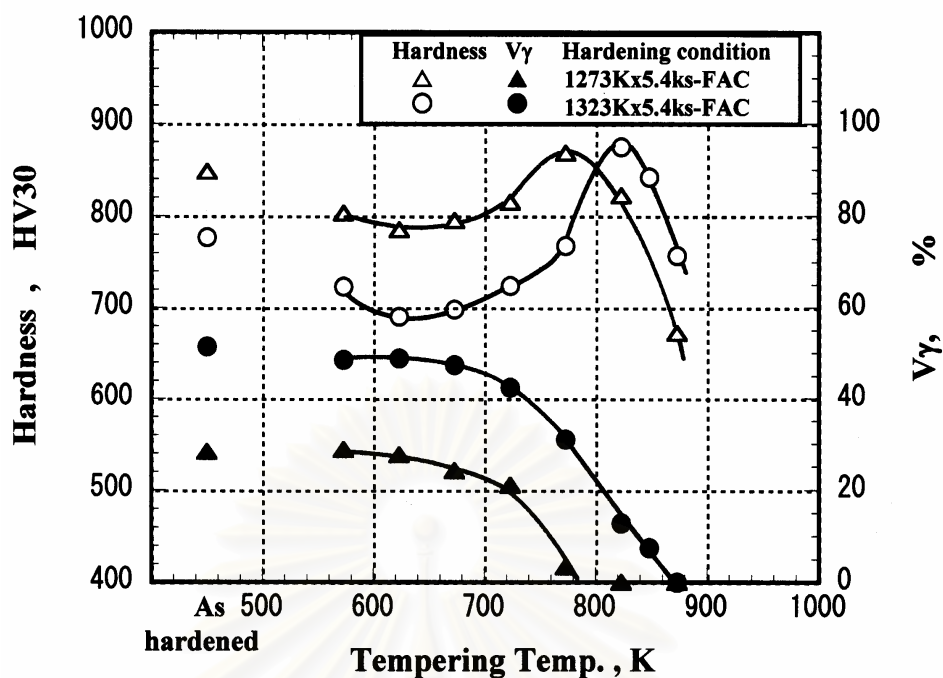Fig. 4.95 Relationship between macro-hardness, volume fraction of retained austenite (Vγ) and tempering temperature of 16%Cr cast iron with 2% Mo. (Specimen No. 3)

Fig. 4.96 Relationship between macro-hardness, volume fraction of retained austenite (Vγ) and tempering temperature of 16%Cr cast iron with 3%Mo. (Specimen No. 4)

44 HV30 in 1273 K and 135 HV30 in 1323 K austenitization. The H_{Tmax} is 820 HV30 at 773 K in 1273 K and 845 HV30 at 798 K tempering in 1323 K austenitization. It is clear from this result that the H_{Tmax} is high in the specimen hardened from high austenitizing temperature. This is because the more alloy concentration in the austenite due to high austenitization produced more precipitation of secondary carbides during tempering and more martensite during cooling.

The Vγ values of 24.4% and 42.0% in the specimens hardened from 1273 K and 1323 K, begin to reduce remarkably when the tempering temperature rises over 623 K in the case of 1273 K austenitization and 673 K in the case of 1323 K austenitization. The tempering temperatures at which the Vγ becomes 0% are 773 K and 823 K in 1273 K and 1323 K austenitization, respectively. The Vγ values at the H_{Tmax} are 5% in 1273 K and 7% in 1323 K austenitization.

In 2% Mo specimen (No. 3) shown in Fig. 4.95, the remarkable degrees of secondary hardening are obtained, 70 HV30 and 158 HV30 in 1273 K and 1323 K austenitization. The H_{Tmax} value obtained in the specimen hardened from 1323 K is 870 HV30 and it is higher than 855 HV30 of the specimen hardened from 1273 K. The tempering temperatures at the H_{Tmax} are 773 K in 1273 K and 798 K in 1323 K austenitization.

The 25% and 45.9% $V\gamma$ in as-hardened state begin to decrease at 673 K that agrees with the tempering temperature at which the secondary hardening starts. The $V\gamma$ values become 0% at 780 K in 1273 K and 840 K in 1323 K austenitization, and the $V\gamma$ values at the H_{Tmax} are 5% in 1273 K and 18% in 1323 K austenitization.

The results of 3% Mo specimen (No.4) are shown in Fig. 4.96. The tempered hardness curve shows quite similar behavior to other 16% Cr specimens. The degree of the secondary hardening is greatest in the Mo specimens and it is larger in the case of 1323 K austenitization. They are 83 HV30 in 1273 K and 185 HV30 in 1323 K austenitization. The H_{Tmax} values are 868 HV30 at 773 K in 1273 K and 875 HV30 at 823 K tempering in 1323 K austenitization. Both values are highest in the family of 16% Cr specimens.

The 28.3% $V\gamma$ value in as-hardened state in 1273 K austenitization reduces gradually from 623 K and gets to 0% at 780 K. In the case of 1323 K austenitization, 51.5% $V\gamma$ value begins to decrease from 673 K and reaches 0% at 873 K tempering. The $V\gamma$ values at the H_{Tmax} are 4% in 1273 K and 13% in 1323 K austenitization. It is clear that the high tempering temperature is needed to decompose most of the retained austenite and resultantly the H_{Tmax} shifts to the high temperature side.

(ii) 26%Cr cast iron

Fig. 4.97 shows the results of 1% Mo specimen (No. 6). The tempered hardness curve shows the similar behavior to alloy-free

specimen (Fig. 4.71) but the curves show clearly different shape from those of 16% Cr specimen. The hardness in the specimen hardened from 1323 K are overall larger than those hardened from 1273 K. However, the degree of secondary hardening is greater in the case of 1323 K austenitization and the tempering temperature to obtain the H_{Tmax} shifts to the higher temperature side. The degrees of secondary hardening are 30 HV30 in 1273 K and 71 HV30 in 1323 K austenitization. The H_{Tmax} values are 780 HV30 at 710 K in 1273 K and 830 HV30 at 748 K in 1323 K austenitization.

The $V\gamma$ values in as-hardened state are 7% in 1273 K and 15% in 1323 K austenitization. They decrease gradually as the tempring temperature increases and get to 0% at 773 K and 810 K in 1273 K and 1323 K austenitization. The $V\gamma$ values at the H_{Tmax} are 3% in 1273 K and 5% in 1323 K austenitization.

The results of 2% Mo specimen (No. 7) are shown in Fig. 4.98. The tempered hardness curves are almost similar to the alloy-free and 1% Mo specimens except for the hardness at tempering temperature of 673 K. The degree of secondary hardening does not make much difference between the austenitizing temperatures, that is, 61 HV30 in 1273 K and 69 HV30 in 1323 K austenitization. However, the degree is greater than that in alloy-free specimen. The H_{Tmax} values of 836 HV30 at 723 K in 1273 K and 856 HV30 at 748 K tempering in 1323 K austenitization are obtained.

The $V\gamma$ values in as-hardened state are 13% in 1273 K and 18 % in 1323 K austenitization, respectively. They decrease gradually as the tempering temperature increases and the $V\gamma$ disappears at 850 K in 1273 K and 873 K tempering in 1323 K austenitization. The $V\gamma$ values at the H_{Tmax} are 7% in 1273 K and 11% in 1323 K austenitization.

Fig. 4.99 shows the result of 3% Mo specimen (No. 8). The tempered hardness curves show similar behavior to alloy-free and 1% Mo specimens, that is, the hardness is overall higher in the specimen hardened from 1323 K. The tempered hardness curves show the
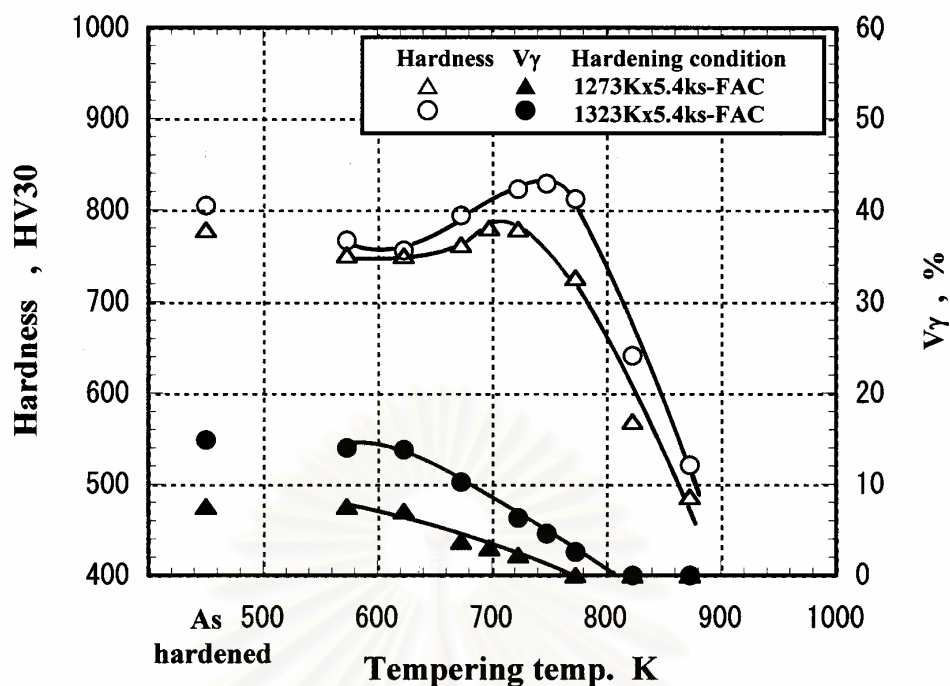
Fig. 4.97 Relationship between macro-hardness, volume fraction of retained austenite (Vγ) and tempering temperature of 26%Cr cast iron with 1%Mo. (Specimen No. 6)
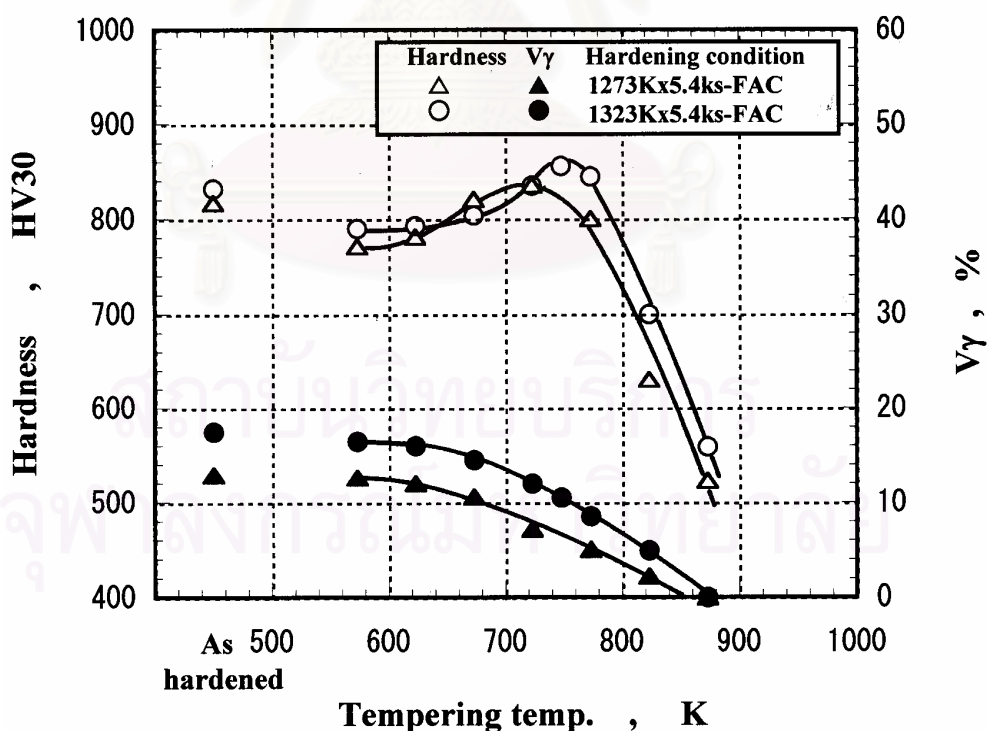

Fig. 4.98 Relationship between macro-hardness, volume fraction of retained austenite (Vγ) and tempering temperature of 26%Cr cast iron with 2%Mo. (Specimen No. 7)
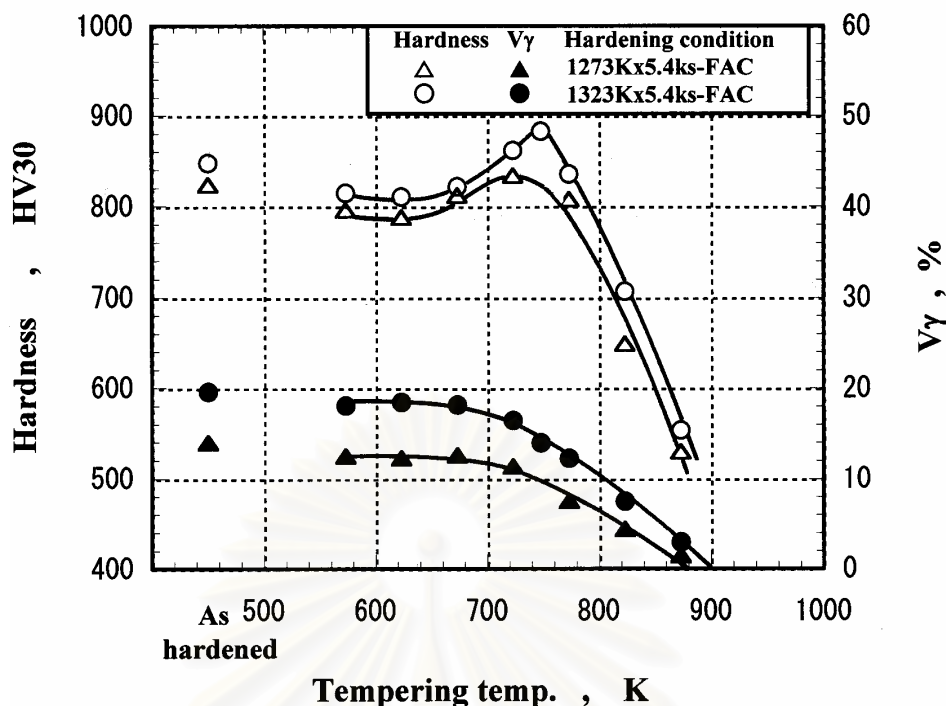
Fig. 4.99 Relationship between macro-hardness, volume fraction of retained austenite (Vγ) and tempering temperature of 26%Cr cast iron with 3%Mo. (Specimen No. 8)

secondary hardening in the same manner as other specimens and the degrees are 57 HV30 in 1273 K and 75 HV30 in 1323 K austenitization. The H_{Tmax} values are 840 HV30 at 723 K in 1273 K and 883 HV30 at 748 K tempering in 1323 K austenitization, respectively.

The 14% and 20% Vγ values in as hardened state are decreased by tempering from 723 K and get to 0% at 880 K in 1273 K and 900 K in 1323 K austenitization. The Vγ values at the H_{Tmax} are 11% in 1273 K and 14% in 1323 K austenitization, respectively.

(c) **Relationship between micro-hardness of matrix and tempering temperature**

In order to clarify the effect of Mo on the tempering behavior of matrix, the matrix hardness or micro-hardness has usually measured associated with the condition of heat treatment. The micro-hardness is the sum of the hardness of matrix phases and that secondary carbides

precipitated during tempering. On the other hand, the macro-hardness is the total of the matrix hardness and the hardness of eutectic carbides. Therefore, it can be said that the difference between macro-hardness and micro-hardness causes by the existence of eutectic carbides.

The comparisons of micro-hardness with macro-hardness are shown in Fig. 4.100 to Fig. 4.102 for 16% Cr and Fig. 4.103 to Fig. 4.105 for 26% Cr specimens. The degrees of secondary hardening in the micro-hardness curves and the maximum micro-hardness are listed up in Table 4.39 and Table 4.40, respectively. The profiles of the micro-hardness curves are in good accordance with those of macro-hardness curves. When compared with alloy-free specimen, the degrees are high in Mo specimen and they increase with increasing Mo content except for 26% Cr specimens with Mo in the case of 1273 K austenitization. The degrees increase from 25 HV0.1 at 0% Mo to 60 HV0.1 at 3% Mo in 1273 K and 55 HV0.1 to 167 HV0.1 in 1323 K austenitization for 16% Cr specimens. In the case of 26% Cr specimens in 1273 K austenitization, the degree changes little even if Mo is contained ranging from 61 HV30 at 1% Mo to 62 HV30 at 3% Mo. However, the degrees of specimens hardened from 1323 K increase greatly from 52 HV30 in 0% Mo, 71 HV30 at 1% Mo and 109 HV30 at 3% Mo. The maximum micro-hardness of 16% Cr specimens with Mo do not change so much ranging from 698 HV0.1 at 1% Mo to 710 HV0.1 at 3% Mo in 1273 K and 706 HV0.1 to 715 HV0.1 in 1323 K austenitization and those of 26% Cr specimens with Mo range from 618 HV0.1 at 1% Mo to 672 HV0.1 at 3% Mo in1273 K and 630 HV0.1 to 732 HV0.1 in 1323 K austenitization, respectively. The difference between macro-hardness and micro–hardness at the H_{Tmax} is larger in 26% Cr specimens ranging from 120 HV to 155 HV in 1273 K and 145 HV to 170 HV in 1323 K austenitization for 16% Cr specimens, and for 26% Cr specimens ranging from 160 HV to 180 HV in 1273 K and 140 HV to 200 HV in 1323 K austenitization.

Table 4.39 Degree of secondary hardening of micro-hardness.

Specimen	Cr (mass%)	Mo (mass%)	Degree of secondary hardening (HV0.1)	
			1273 K austenitization	1323 K austenitization
No. 1	16	-	25	55
No. 2		1	50	110
No. 3		2	53	115
No. 4		3	60	167
No. 5	26	-	22	52
No. 6		1	61	71
No. 7		2	59	86
No. 8		3	62	109

Table 4.40 Maximum micro-hardness of matrix.

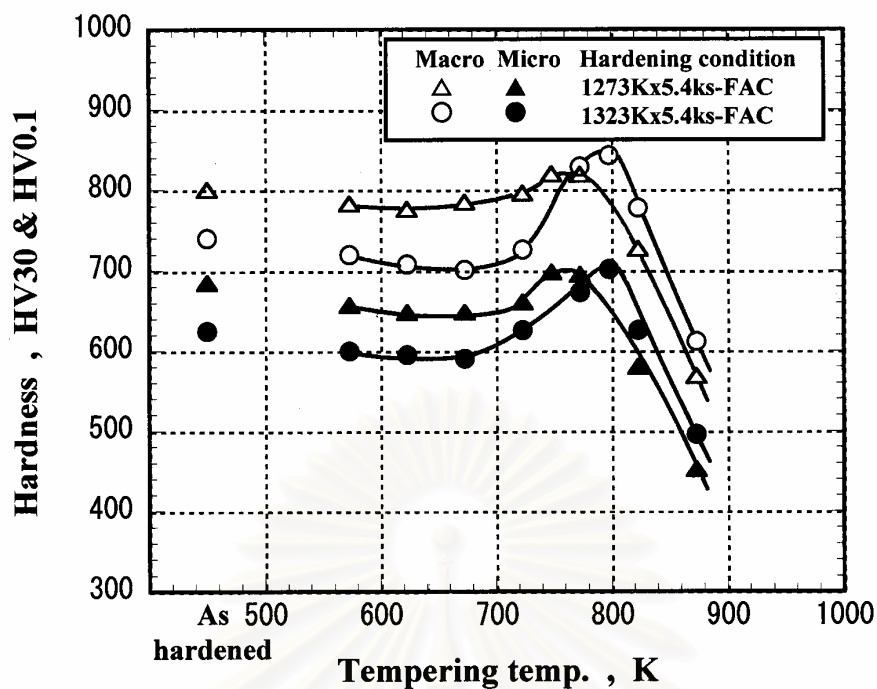| Specimen	Cr (mass%)	Cu (mass%)	Maximum micro-hardness (HV0.1)	
			1273 K austenitization	1323 K austenitization
No. 1	16	-	697	706
No. 2		1	698	705
No. 3		2	699	702
No. 4		3	710	715
No. 5	26	-	683	703
No. 6		1	618	630
No. 7		2	672	720
No. 8		3	672	732

Fig. 4.100 Relationship between micro-hardness of matrix and tempering temperature of 16% Cr cast iron with 1% Mo. (Specimen No. 2)
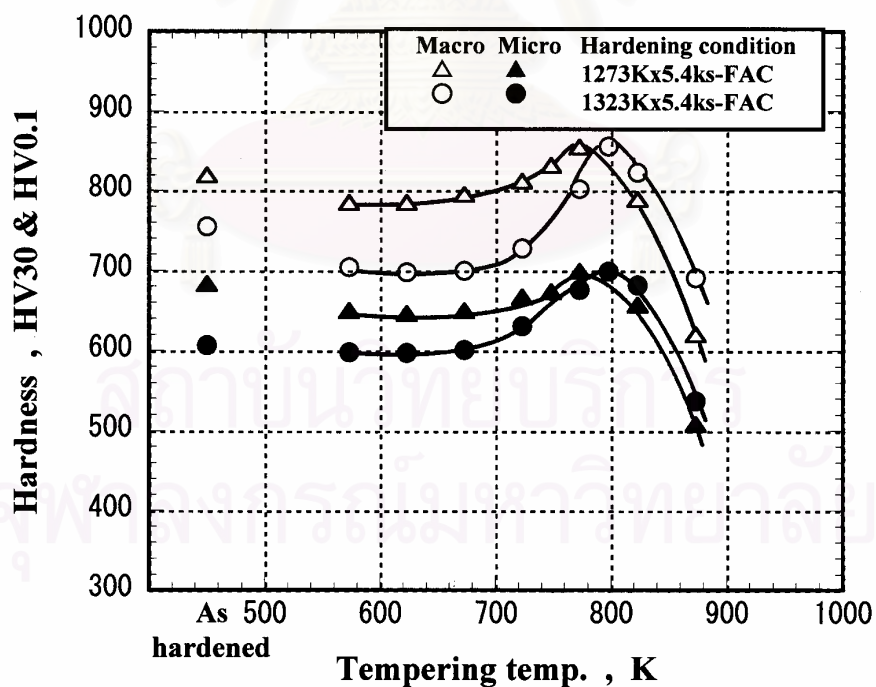

Fig. 4.101 Relationship between micro-hardness of matrix and tempering temperature of 16% Cr cast iron with 2% Mo. (Specimen No. 3)
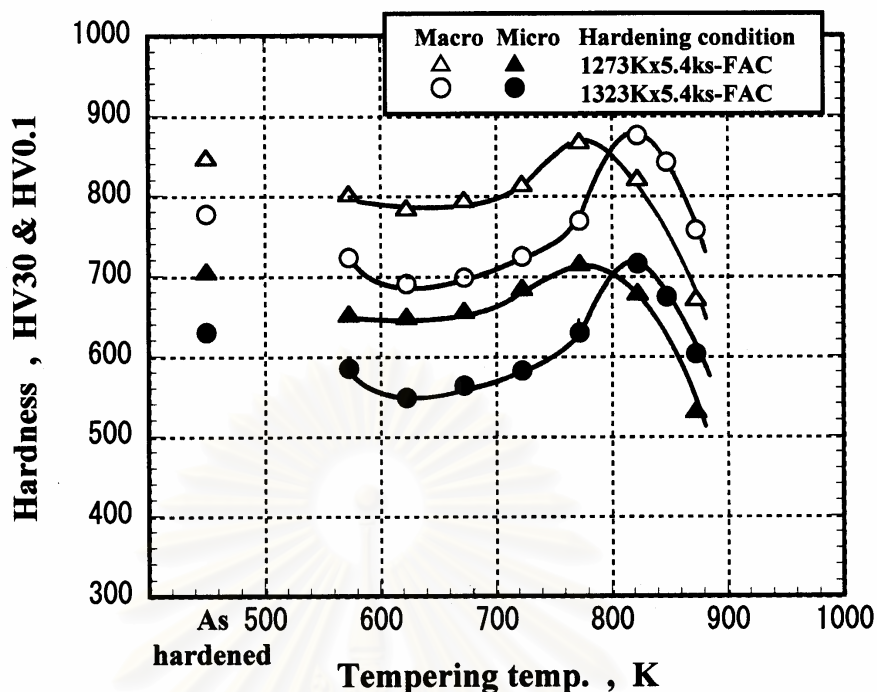
Fig. 4.102 Relationship between micro-hardness of matrix and tempering temperature of 16% Cr cast iron with 3% Mo. (Specimen No.4)
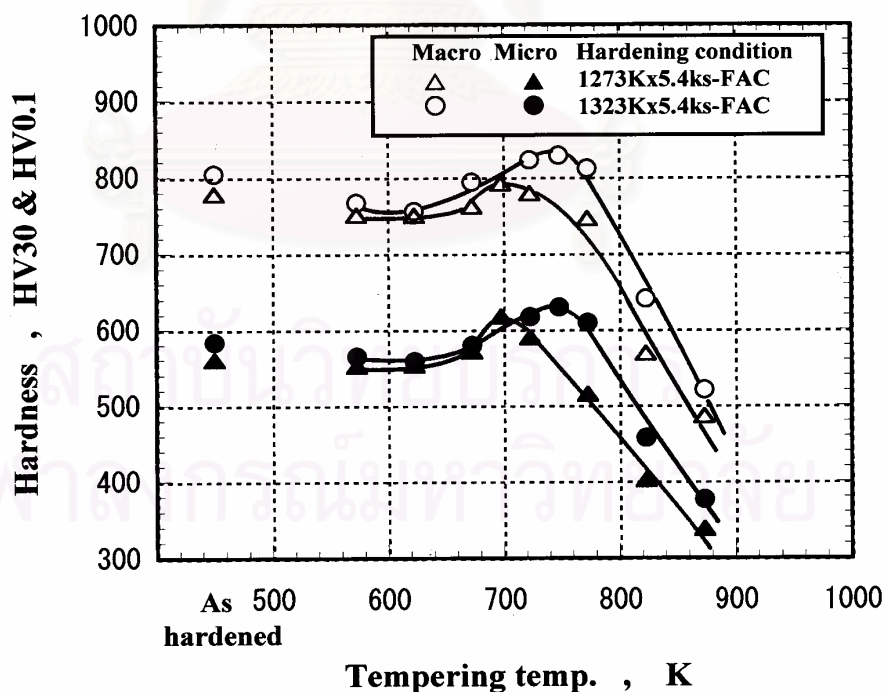

Fig. 4.103 Relationship between micro-hardness of matrix and tempering temperature of 26% Cr cast iron with 1% Mo. (Specimen No.6)
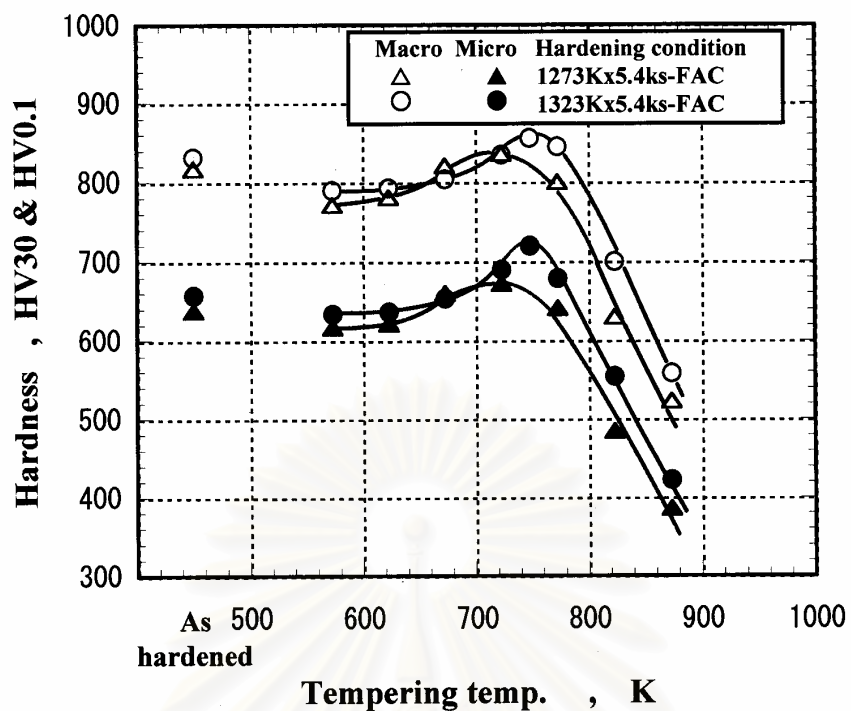
Fig. 4.104 Relationship between micro-hardness of matrix and tempering temperature of 26% Cr cast iron with 2% Mo. (Specimen No.7)
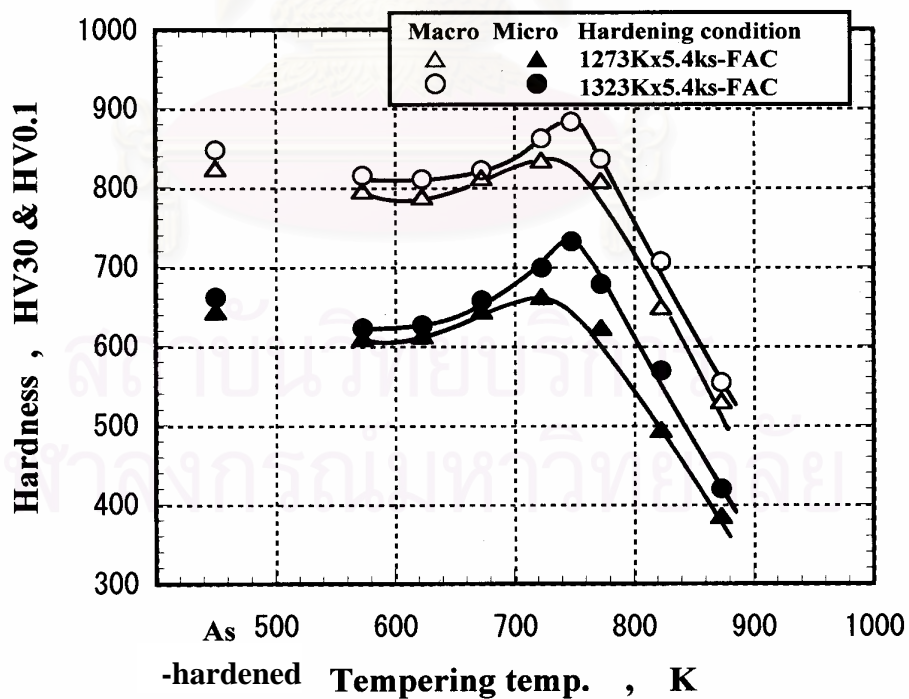

Fig. 4.105 Relationship between micro-hardness of matrix and tempering temperature of 26% Cr cast iron with 3% Mo. (Specimen No.8)

4.2.3.4 Effect of vanadium (V)

(a) Test specimen in as-cast state

      The chemical compositions of test specimens are shown in Table 4.41. Vanadium was added up to 3% in the both 16% Cr and 26% Cr specimens. Typical as-cast microstructures are shown in Fig. 4.106. In 16% Cr specimens, the microstructures of all specimens consist of pearlitic matrix and (γ+M$_7$C$_3$) eutectic structure. It is clear that the size of primary dendrite and eutectic colony in the specimens with V is smaller than that in alloy-free specimen. This results support that V refines the eutectic structure.[51] In 26%Cr specimens, the microstructures consist of austenitic matrix in dendritic morphology where martensite is possibly mixing and very fine (γ+M$_7$C$_3$) eutectic. V is a strong carbide former and it combines with C to form MC carbide. However, the eutectic MC carbides can be seen clearly in these specimens though Radulovic reported that eutectic MC carbides precipitated only when the V content is more than 3%.[52]

      Hardness and volume fraction of retained austenite (Vγ) are shown in Table 4.42. As V content increases from 0% to 3%, the hardness decreases from 572 HV30 to 547 HV30 in 16% Cr specimen but increases from 547 HV30 to 663 HV30 in 26% Cr specimen. The Vγ values in 16% Cr specimens are zero regardless of V content. In the case of 26% Cr specimens, the Vγ is greatly influenced by the V content, that is, the Vγ reduces from 46.8% at 0% V to 10.6% at 3% V.

(b) Effect of V content on variation of macro-hardness and volume fraction of retained austenite (Vγ) during heat treatment

-   **As-hardened state**

      The hardness and Vγ of as-hardened specimens are summarized in Table 4.43. It is found that the hardness and Vγ are varied by V content

Table 4.41 Chemical compositions of test specimens.

Specimen	Element (mass%)							
	C	Cr	Si	Mn	Ni	Cu	Mo	V
No. 1	3.01	16.48	0.62	0.78	-	-	-	-
No. 2	2.96	16.13	0.50	0.51	-	-	-	1.00
No. 3	3.13	16.08	0.53	0.53	-	-	-	2.10
No. 4	3.06	16.06	0.47	0.50	-	-	-	3.05
No. 5	2.65	25.56	0.37	0.51	-	-	-	-
No. 6	2.61	25.97	0.51	0.50	-	-	-	1.05
No. 7	2.64	25.91	0.51	0.51	-	-	-	2.02
No. 8	2.71	26.46	0.52	0.51	-	-	-	3.02

*S and P are less than 0.06 mass%

Table 4.42 Macro-hardness and volume fraction of retained austenite ($V\gamma$) of as-cast specimens.

Specimen	Element (mass%)		Hardness (HV30)	$V\gamma$ (%)
	Cr	V		
No.1	16%	-	572	0
No.2		1%	570	0
N0.3		2%	564	0
No.4		3%	547	0
No.5	26%	-	547	46.8
No.6		1%	607	37.4
No.7		2%	651	22.8
No.8		3%	663	10.6

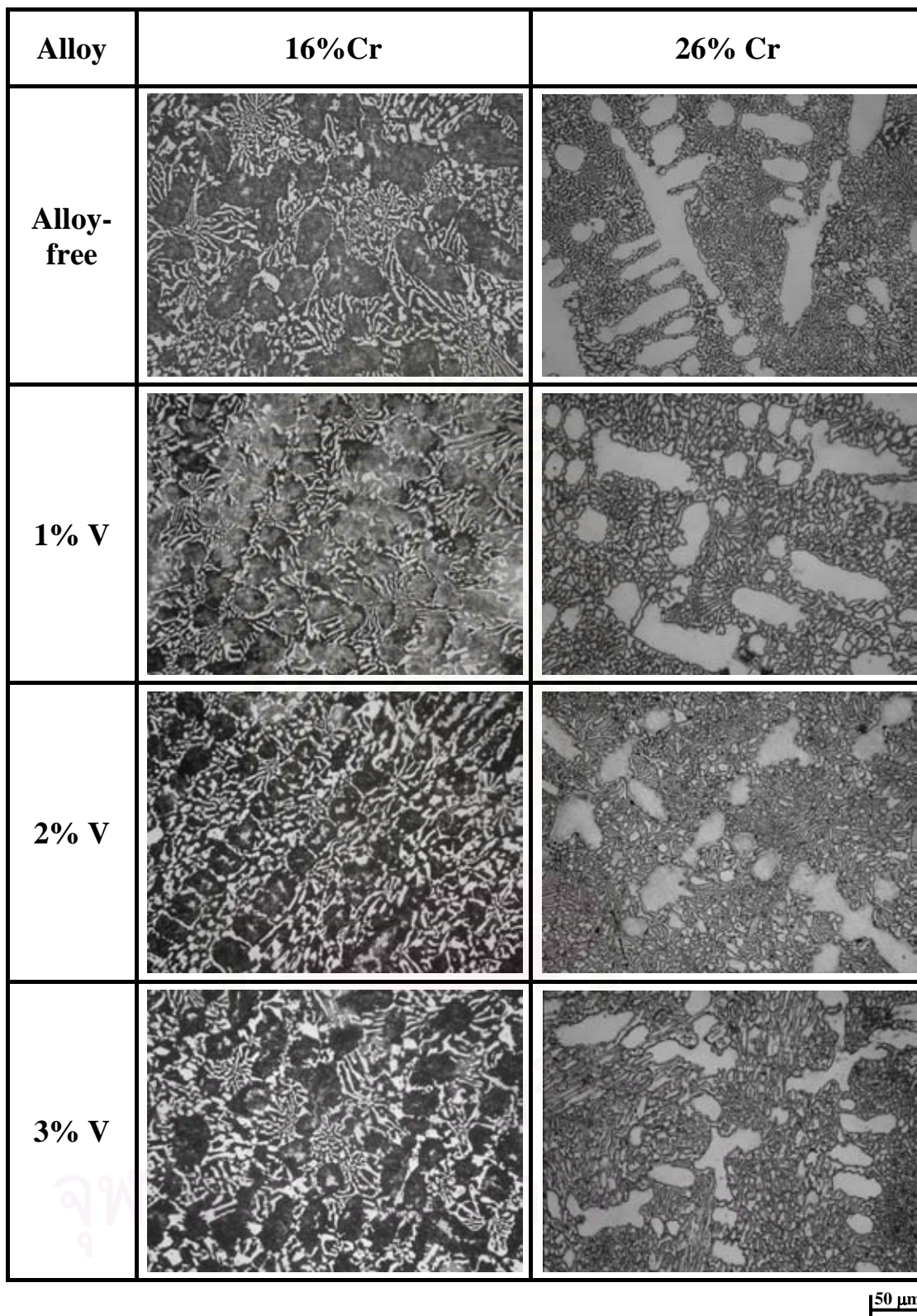| Alloy	16%Cr	26% Cr
Alloy-free		
1% V		
2% V		
3% V		

50 μm

Fig. 4.106 As-cast microstructures of 16% Cr and 26% Cr hypoeutectic cast irons with and without V. Matrices are mostly pearlitic in 16% Cr cast irons and are austenitic possibly with some martensite in 26% Cr cast rons. Size of eutectic colony seems to become smaller by V addition.

and austenitizing temperature. The effect of V content on the hardness and Vγ is shown in Fig. 4.107 (a) and (b). In 16% Cr specimens, the hardness increases with increasing V content, from 775 HV30 at 0% V to 863 HV30 at 3% V in 1273 K and 730 HV30 to 839 HV30 in 1323 K austenitization. In 26%Cr specimens, on the other hand, the harness decreases from 763 HV30 at 0% V to 626 HV30 at 3% V in 1273 K and 777 HV30 to 697 HV30 in 1323 K austenitization with an increase in V content. When the austenitizing temperature increases from 1273 K to 1323 K, the hardness becomes high in 16% Cr specimens but low in 26%Cr specimens.

As for the Vγ shown in Fig 4.107 (b), it decreases gradually from 18.1% at 0% V to 8.2% at 3% V in 1273 K and 31.8% to 14.6% in 1323 K austenitization with an increase in V content in the both 16% Cr specimens. In 26% Cr specimens that have essentially small amount of Vγ, however, the decrease in Vγ is very small. The Vγ decreases gradually from 4.1% at 0% V to 2.1% at 3% V in 1273 K and 11% to 3% in 1323 K austenitization as V content increases. In both Cr specimens, the Vγ is overall more in the case of 1323 K austenitizatization.

SEM observation was carried out to investigate the detailed matrix structure. The typical SEM micrographs of 16% Cr and 26% Cr specimens without and with V are shown in Fig. 4.108. In 16% Cr specimens, the matrix structure consists of a larger number of secondary carbides, martensite and austenite. This suggests that the pearlite in which existed much more in as-cast state dissolves back to the matrix and make alloy concentration in austenite increase by the austenitization. In the 26% Cr specimens that had mostly austenitic matrix, on the other side, the matrix structures are similar to those 16%Cr specimens. It is found from these observations that the austenitic matrix in as-cast state was destabilized and it allowed the fine secondary carbides to precipitate and the retained austenite to transform into martensite. It seems that the secondary carbides precipitated more at the central region of dendrite.

Table 4.43 Macro-hardness and volume fraction of retained austenite (Vγ)
of as-hardened specimens.

| Specimen | Element (mass%) | | Austenitizing Temperature (K) | | | |
| | Cr | V | 1273 | | 1323 | |
			Hardness (HV30)	Vγ (%)	Hardness (HV30)	Vγ (%)
No. 1	16	-	775	18.1	730	31.8
No. 2		1	822	18.4	770	34.4
No. 3		2	849	14.6	826	23.0
No. 4		3	863	8.2	839	14.6
No. 5	26	-	763	4.1	777	11.5
No. 6		1	720	2.8	742	4.3
No. 7		2	687	2.0	730	3.5
No. 8		3	626	2.1	697	3.0

- Tempered state

The as-hardened specimens were tempered at several temperatures
from 573 K to 873 K. The relationship between macro-hardness, Vγ and
tempering temperature are shown in Fig. 4.109 to Fig. 4.111 for 16% Cr
specimens and Fig 4.112 to Fig. 4.114 for 26%Cr specimens. In each
specimen, the secondary hardening occurs clearly and the degree is
summarized in Table. 4.44. When it is compared with alloy-free
specimen, the degrees are low in 16% Cr specimens but high in 26% Cr
specimens.

(i) 16%Cr cast iron

In 1% V specimens (No.2) shown in Fig. 4.109, the tempered
hardness curve shows similar behavior to alloy-free specimen (No.1)
shown in Fig. 4.68. In the range of tempering temperature less than 730 K,
the hardness of the specimens hardened from 1323 K are lower than those
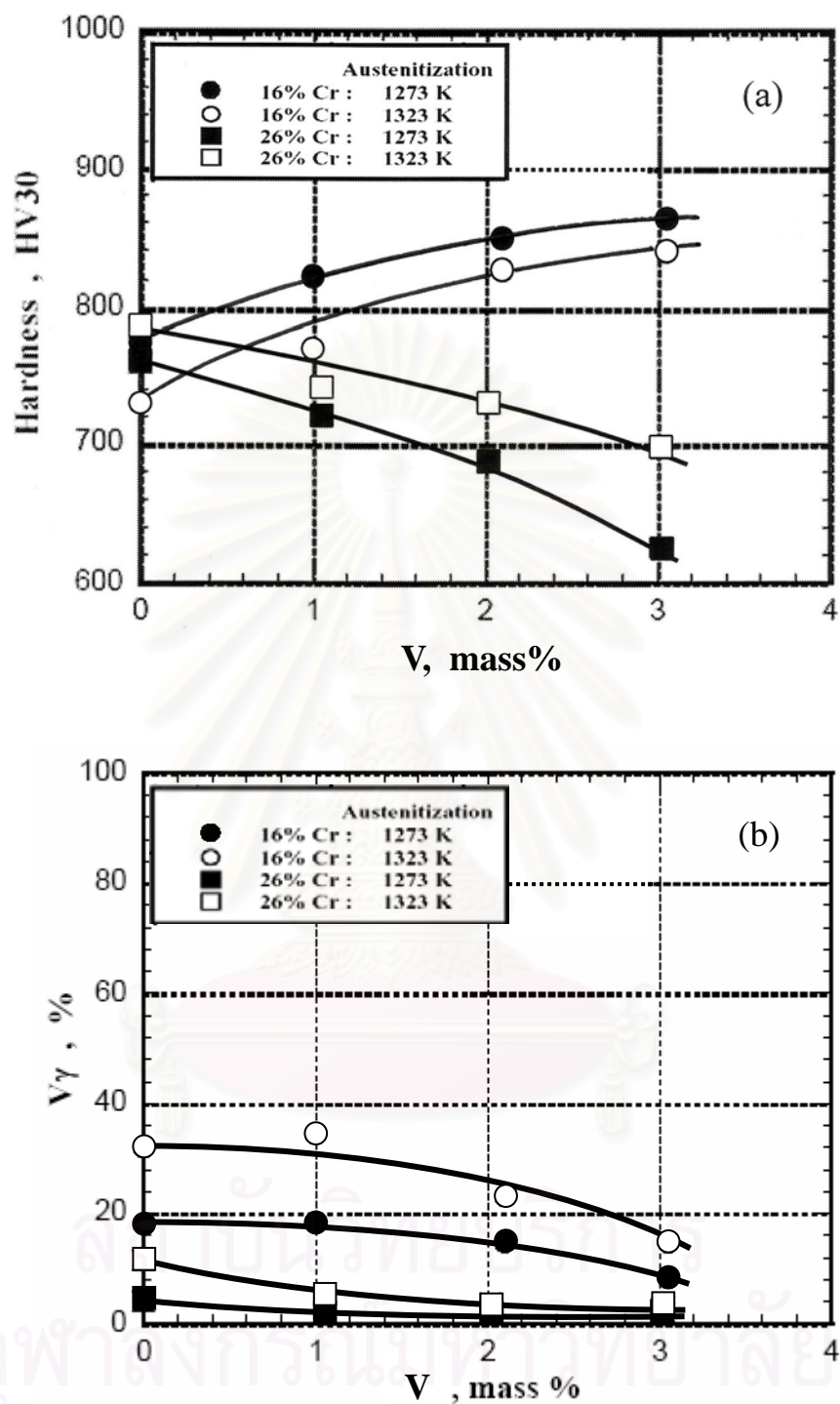
Fig. 4.107 Effect of V content on macro-hardness (a) and Vγ (b) in as-hardened state.

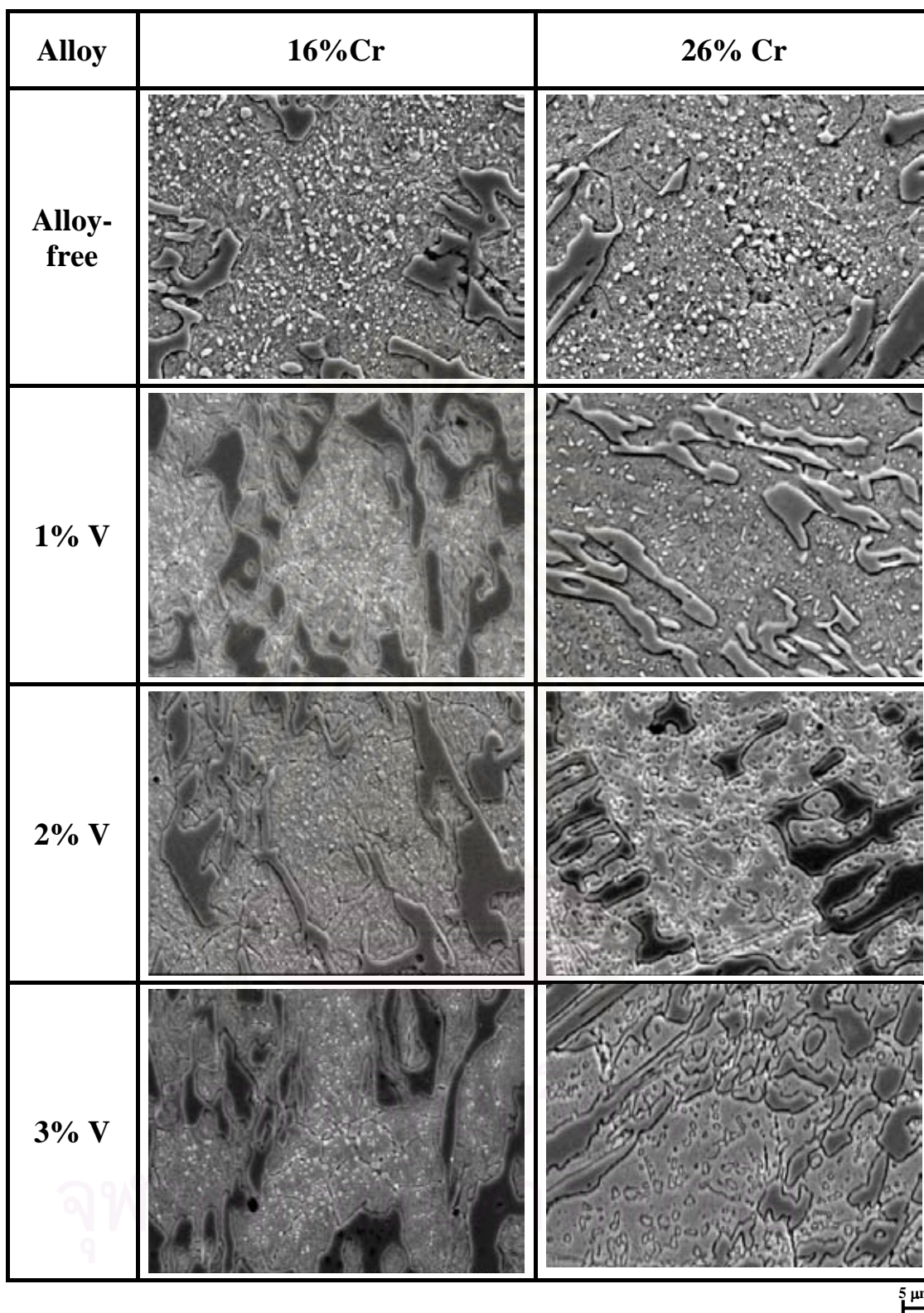| Alloy	16%Cr	26% Cr
Alloy-free		
1% V		
2% V		
3% V		

5 μm

Fig. 4.108 SEM microphotographs in as-hardened state of 16%Cr and 26% Cr hypoeutectic cast irons with and without V. Fine secondary carbides precipitated in matrix of austenite and martensite.

Table 4.44 Degree of the secondary hardening of test specimens.

Specimen	Element (mass%)		Degree of the secondary hardening (HV30)	
	Cr	V	1273 K austenitization	1323 K austenitization
No. 1	16	-	33	83
No. 2		1	17	77
No. 3		2	13	36
No. 4		3	21	33
No. 5	26	-	20	34
No. 6		1	39	50
No. 7		2	44	48
No. 8		3	38	52

those hardened from 1273 K. Over 730 K, it is reversed. The degree of secondary hardening is high in the case of 1323 K austenitization. However, the degrees are smaller compared with alloy-free specimen. The degrees are 17 HV30 in 1273 K and 77 HV30 in 1323 K austenitization. The H_{Tmax} values are 810 HV30 in 1273 K and 820 HV30 in 1323 K austenitization.

The 18% and 34% $V\gamma$ existing in as-hardened begin start to decrease from 623 K in 1273 K and 673 K in 1323 K austenitization and they become 0% at 740 K in 1273 K and 773 K in 1323 K austenitization. The temperature at which the retained austenite disappears is high in the case of high austenitizing temperature which contains larger amount of $V\gamma$ in as-hardened state. This behavior corresponds well with that H_{Tmax} shifts to a high temperature side. In 1323 K austentization, the $V\gamma$ values at the H_{Tmax} are 4% at 723 K in 1273 K and 7% at 748 K tempering.

As for 2% V specimen (No.3) shown in Fig. 4.110, the shapes of tempered hardness curves are similar to the alloy-free and 1% V specimens. However, the difference in the tempered hardness due to an increase in the austenitizing temperature and the degree of secondary hardening are small. The degrees are 13 HV30 in 1273 K and 36 HV30 in
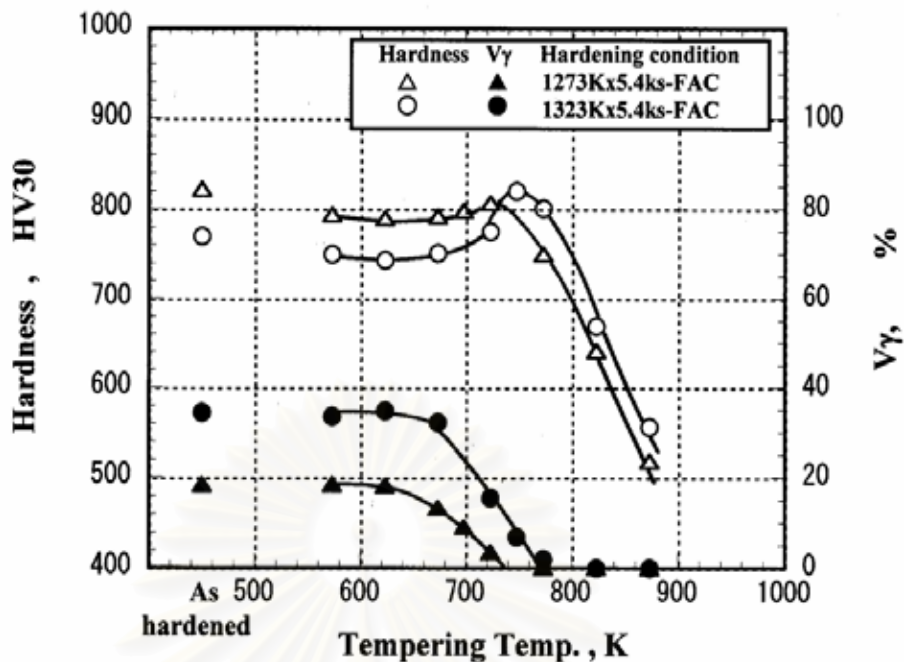
Fig. 4.109 Relationship between macro-hardness, volume fraction of retained austenite (Vγ) and tempering temperature of 16% Cr cast iron with 1%V. (Specimen No. 2)

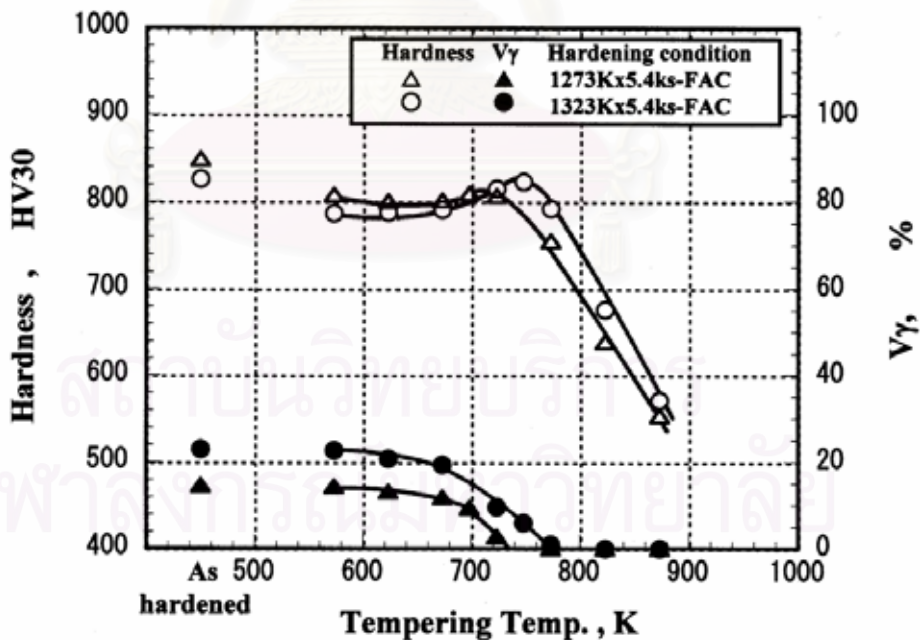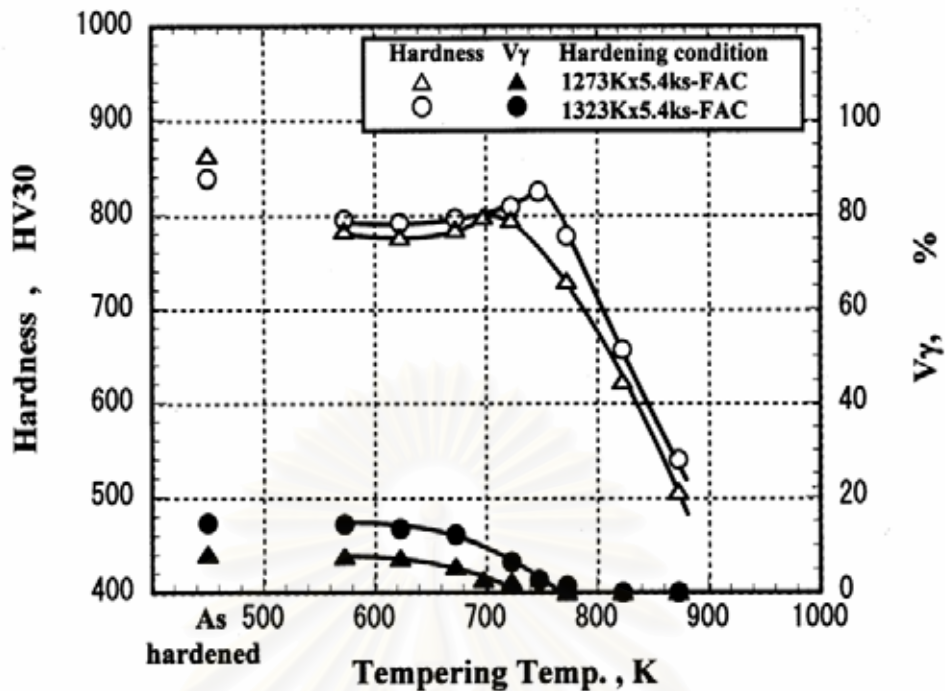Fig. 4.110 Relationship between macro-hardness, volume fraction of retained austenite (Vγ) and tempering temperature of 16% Cr cast iron with 2%V. (Specimen No. 3)

Fig. 4.111 Relationship between macro-hardness, volume fraction of retained austenite (Vγ) and tempering temperature of 16% Cr cast iron with 3% V. (Specimen No.4)

1323 K austenitization. The H_{Tmax} are 807 HV30 in 1273 K and 823 HV30 in 1323 K.

As the tempering temperature is raised, the Vγ values in as-hardened state of 15% in 1273 K and 23% in 1323 K austenitization decrease gradually from 623 K and get to 0% at 730 K in 1273 K and 773 K in 1373 K austenitization. The Vγ values at the H_{Tmax} are 9% at 698 K and 6% at 748 K tempering in 1273 K and 1323 K austenitization, respectively.

As shown in Fig. 4.111 for the results of 3% V specimens (No.4), the tempered hardness show different tendency in the group of 16% Cr specimens. The hardness of the specimen hardened from 1323 K is overall more than that hardened from 1273 K. However, the difference in the hardness between the austenitizing temperatures of 1273 K and 1323 K is small. The hardness curves show the smallest degrees of secondary hardening in a group of 16% Cr specimens, 21 HV30 in 1273 K and 33

HV30 in 1323 K austenitization. The H_{Tmax} values of 798 HV30 at 698 K tempering in 1273 K austenitization and 825 HV30 at 748 K in 1323 K are obtained, respectively.

The $V\gamma$ in the specimen hardened from 1273 K is 8% and that hardened from 1323 K is 15%. Such $V\gamma$ values decrease gradually as the tempering increases and they disappear all at 723 K in 1273 K and 773 K in 1323 K austenitization.

(ii) 26%Cr cast iron

In 1% V specimen (No.6) shown by Fig. 4.112, the hardness curve shows similar behavior to alloy-free specimen shown in Fig. 4.71, that is, the hardness is overall higher in the specimen hardened from high austenitization of 1323 K. Both hardness curves display the secondary hardening and the degrees are greater than that in alloy-free specimen. They are 39 HV30 in 1273 K and 50 HV30 in 1323 K austenitization. The H_{Tmax} values of 726 HV30 and 753 HV30 are obtained at 723 K in 1273 K and 748 K in 1323 K austenitization, respectively. It can be said that the higher degree and the higher H_{Tmax} are obtained in the specimen hardened from higher austenitization.

The $V\gamma$ within 3% in the specimen hardened from 1273 K disappears all at 723 K tempering. The 4% $V\gamma$ existed in as-hardened specimen hardened from 1323 K austenitization lowers as the tempering temperature rises up to 673 K and then it becomes 0% at 773 K. The $V\gamma$ values at the H_{Tmax} are 2% in 1273 K and 3% in 1323 K austenitization.

In 2% V specimen (No.7) by Fig. 4.113, the tempered hardness curve is similar to that of alloy-free and 1% V specimens, that is, two hardness curves are on parallel. The degrees of secondary hardening are greater than the alloy-free and 1% V specimens and they are 44 HV30 in 1273 K and 48 HV30 in 1323 K austenitization. The H_{Tmax} values are 717 HV30 at 723 K in 1273 K and 760 HV30 at 748 K tempering in 1323 K austenitization.

Though the Vγ values in as-hardened state are less than 5%, the secondary hardening appears. One of the reasons why secondary hardening occurs is precipitation of secondary carbides from martensite. It may be enough that 2% V addition precipitates special V carbides from martensite by the carbide reaction. The tempering temperature at which Vγ gets to 0% is 723 K in 1273 K and 773 K in 1323 K austenitization. The Vγ values at the H_{Tmax} are 2% in the both case of austenitization.

Fig. 4.114 shows the results of 3% V specimen (No.6). The tempered hardness curves behave in similar manner to those in the family of 26% Cr specimens. However, the difference in the hardness between 1273 K and 1323 K austenitization is largest in the V containing specimens. The secondary hardening is also seen and the degrees are 38 HV30 in 1273 K and 52 HV30 in 1323 K austenitization. The H_{Tmax} values are lowest, 651 HV30 in 1273 K and 725 HV30 in 1323 K austenitization. The tempering temperatures at H_{Tmax} are 723 K in 1273 K and 748 K in 1323 K austenitization.

The Vγ values in as-hardened state are 2% to 3%. The tempering temperatures at which the Vγ disappears are 723 K in 1273 K and 773 K in 1323 K austenitization. The Vγ values at the H_{Tmax} are also less than 2%.

Even if the Vγ in as-hardened state of V specimen is very less, the fairly amount of the secondary hardening occurred. This can be due to the special V carbides precipitated from martensite by carbide reaction. However, the H_{Tmax} are very low. This reason is considered that the Vγ in as-hardened state was in a small amount and resultantly the retained austenite after tempering, which is supported to transform into martensite, was much less.
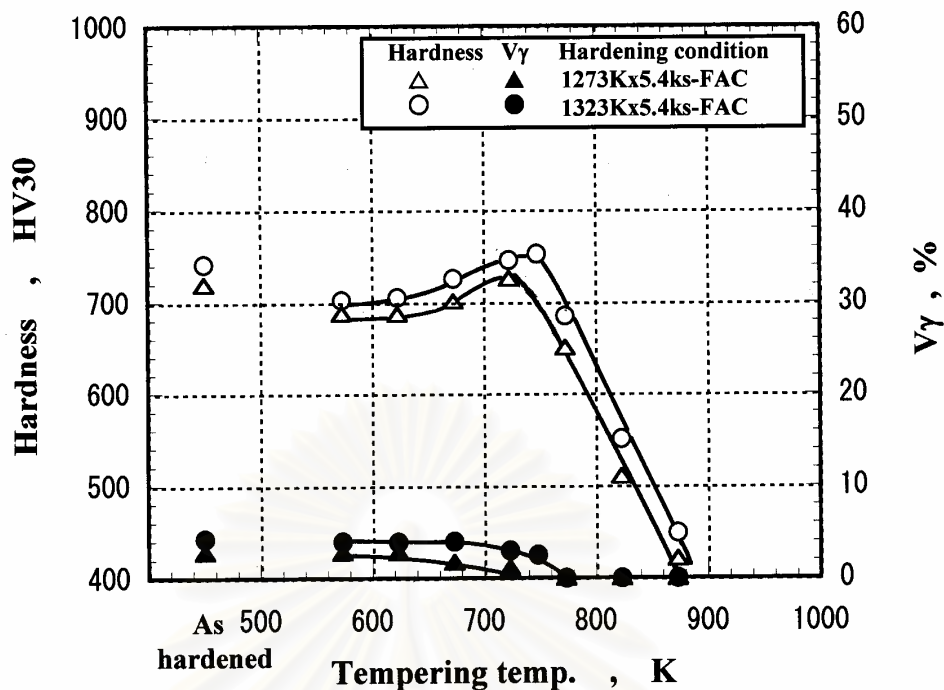
Fig. 4.112 Relationship between macro-hardness, volume fraction of retained austenite (Vγ) and tempering temperature of 26% Cr cast iron with 1%V. (Specimen No. 6)
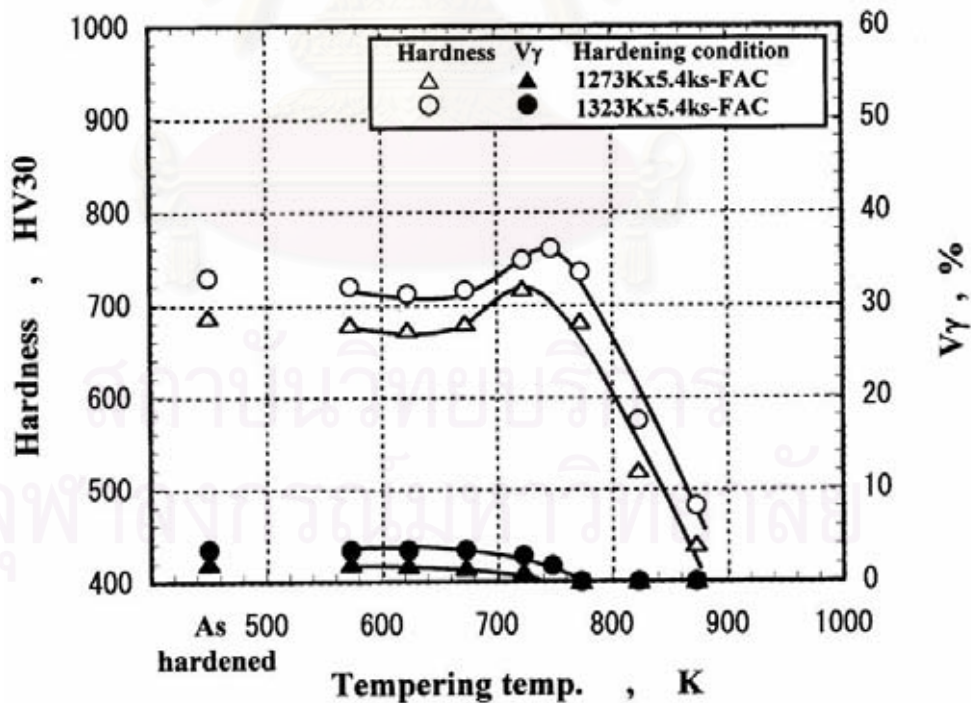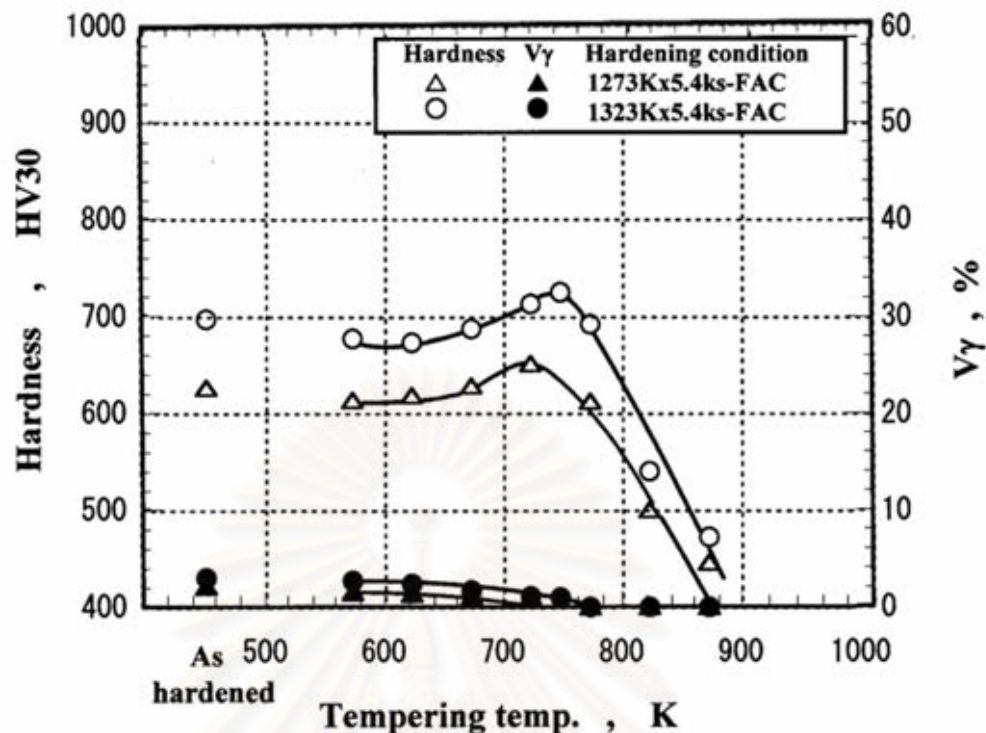

Fig. 4.113 Relationship between macro-hardness, volume fraction of retained austenite (Vγ) and tempering temperature of 26% Cr cast iron with 2% V. (Specimen No.7)

Fig. 4.114 Relationship between macro-hardness, volume fraction of retained austenite (Vγ) and tempering temperature of 26% Cr cast iron with 3% V. (Specimen No.8)

(c) Relationship between micro-hardness of matrix and tempering temperature

The relationship between micro-hardness of the matrix and tempering temperature is shown in Fig. 4.115 to Fig. 4.117 for 16% Cr specimens and Fig. 4.118 to Fig. 4.120 for 26% Cr specimens, respectively. In each diagram, the macro-hardness curves are plotted for comparisons. In each specimen, the micro-hardness curves show the similar behavior to those of macro-hardness curves. The micro-hardness curves show the secondary hardening in the same manner as macro-hardness and the tempering temperature at the peak of micro-hardness curve agrees almost with that of macro-hardness curve. The degrees of secondary hardening and the maximum micro-hardness are listed in Table 4.45 and Table 4.46. In 16% Cr specimens, the degree of V specimens gradually increases from 16 HV0.1 at 0% V to 29 HV0.1 at 3% V in 1273

K but decreases from 103 HV0.1 to 35 HV0.1 in 1323 K austenitization. In 26% Cr specimens, it ranges from 38 HV0.1 to 29 HV0.1 in 1273 K and increases from 44 HV0.1 to 74 HV0.1 in 1323 K austenitization. It is found that the maximum micro-hardness decreases as V content increases regardless of chromium content and austenitizing temperature. The maximum micro-hardness value decreases from 697 HV0.1 at 0% V to 647 HV0.1 at 3% V in 1273 K and 706 HV0.1 to 662 HV0.1 in 1323 K for 16% Cr specimens, and 683 HV0.1 to 536 HV0.1 in 1273 K and 703 HV0.1 to 616 HV0.1 in 1323 K austenitization for 26% Cr specimens, respectively. The differences between macro-hardness and micro-hardness at the peak are larger in 16% Cr specimens, 140 HV to 160 HV in 1273 K and 135 HV to 165 HV in 1323 K austenitization for 16% Cr specimens, and 115 HV to 140 HV in 1273 K and 110 HV to 135 HV in 1323 K austenitization for 26% Cr specimens.

Table 4.45 Degree of secondary hardening of micro-hardness.

Specimen	Cr (mass%)	V (mass%)	Degree of secondary hardening (HV0.1)	
			1273 K austenitization	1323 K austenitization
No. 1	16	-	25	55
No. 2		1	16	103
No. 3		2	18	40
No. 4		3	29	35
No. 5	26	-	22	52
No. 6		1	38	44
No. 7		2	52	66
No. 8		3	29	74

Table 4.46 Maximum micro-hardness of matrix.

Specimen	Cr (mass%)	V (mass%)	Maximum micro-hardness (HV0.1)	
			1273 K austenitization	1323 K austenitization
No. 1	16	-	697	706
No. 2		1	673	686
No. 3		2	645	659
No. 4		3	647	662
No. 5	26	-	683	703
No. 6		1	602	635
No. 7		2	577	626
No. 8		3	536	616
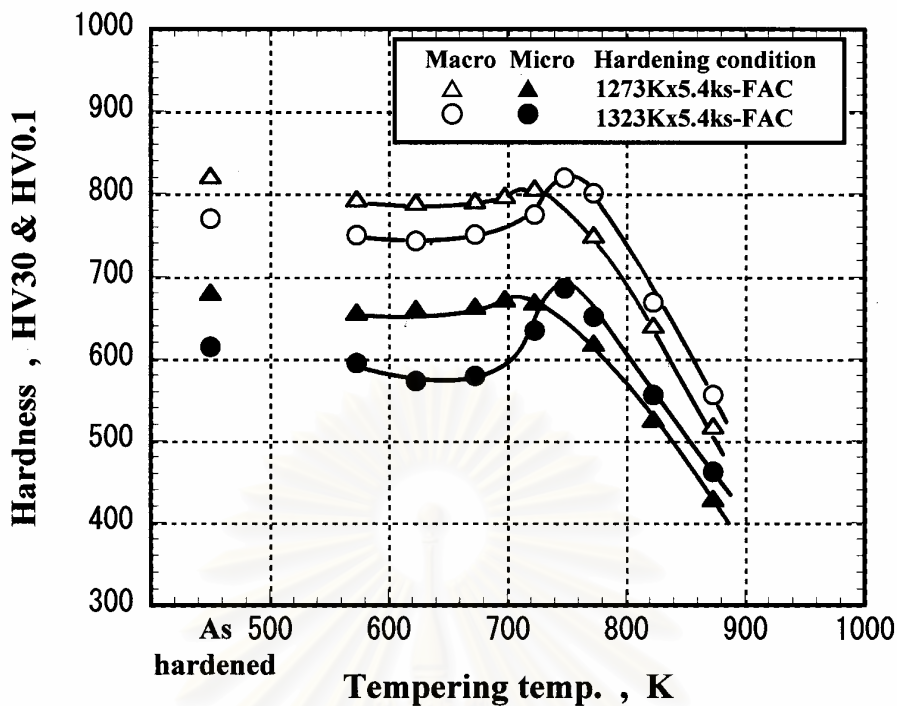
Fig. 4.115 Relationship between micro-hardness of matrix and tempering temperature of 16%Cr cast iron with 1% V. (Specimen No. 2)
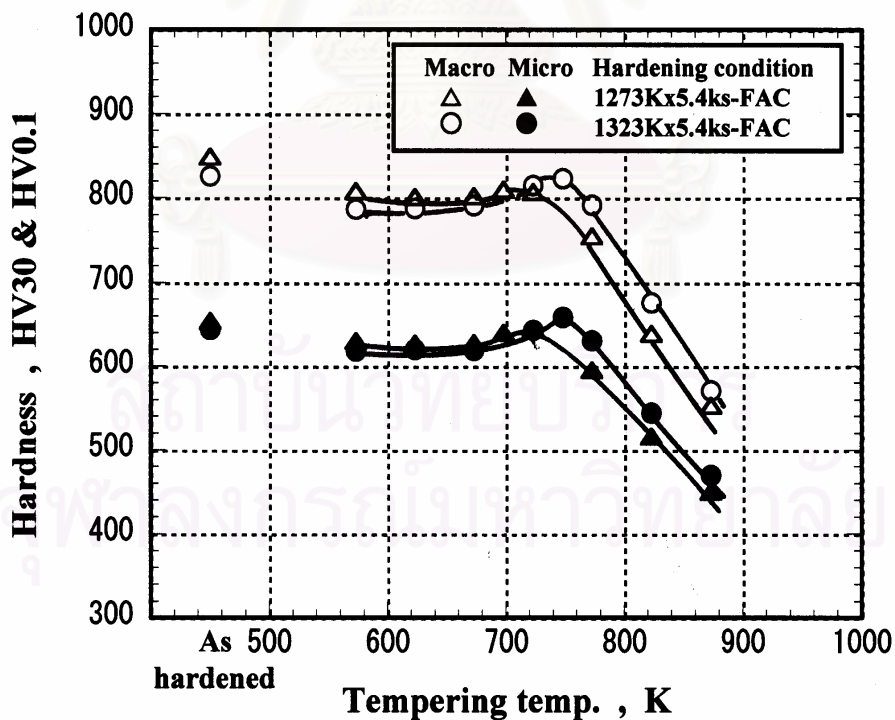

Fig. 4.116 Relationship between micro-hardness of matrix and tempering temperature of 16%Cr cast iron with 2% V. (Specimen No. 3)
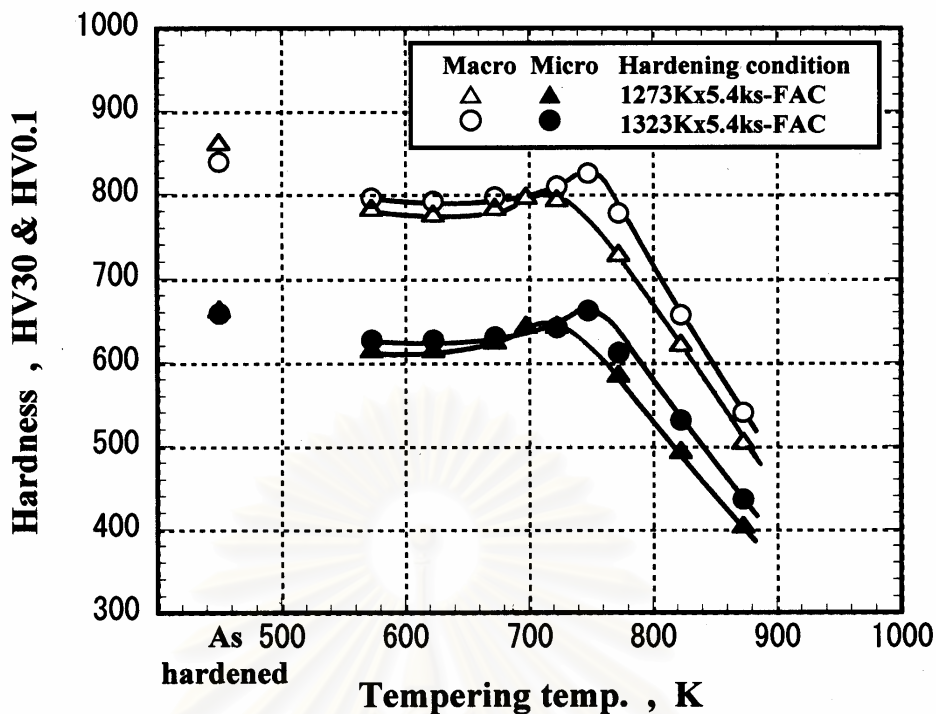
Fig. 4.117 Relationship between micro-hardness of matrix and tempering temperature of 16%Cr cast iron with 3% V. (Specimen No. 4)
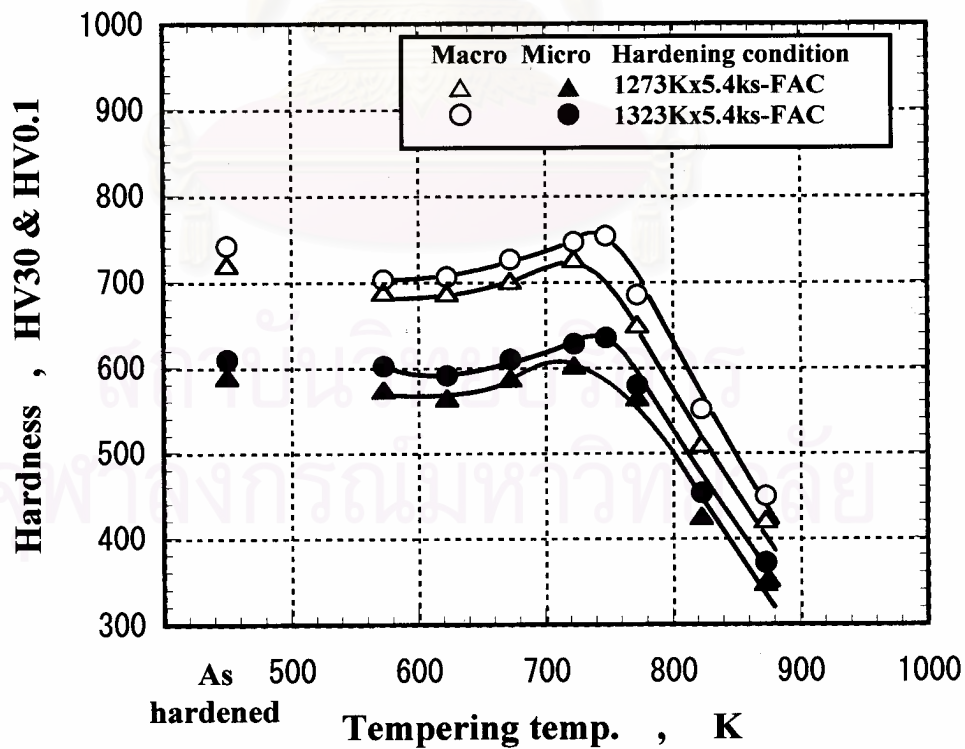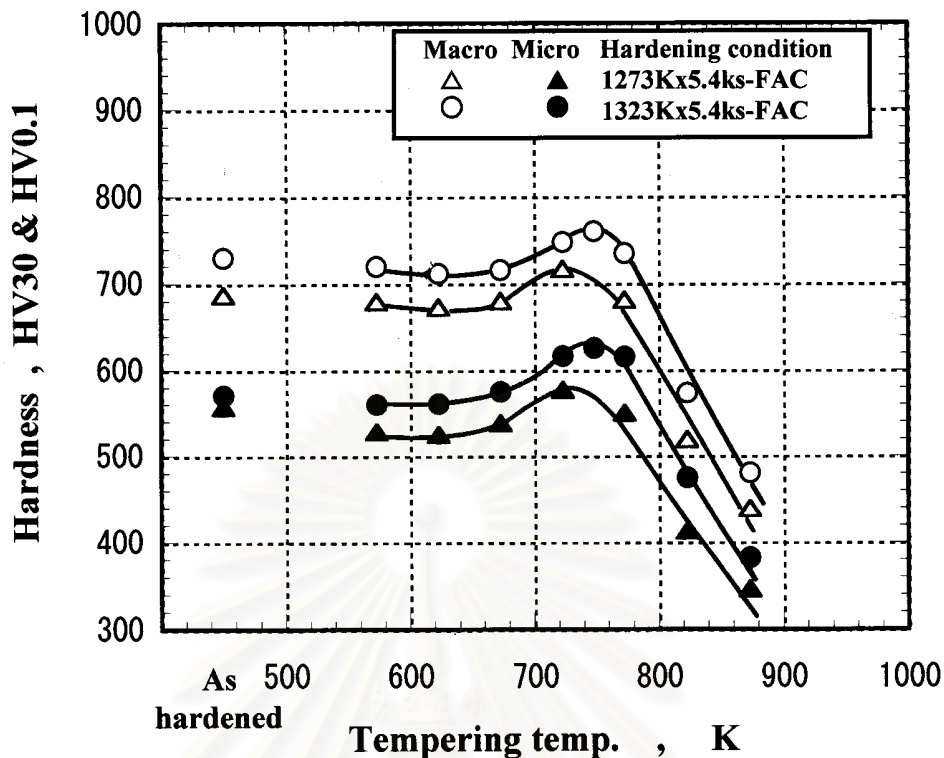

Fig. 4.118 Relationship between micro-hardness of matrix and tempering temperature of 26%Cr cast iron with 1% V. (Specimen No.6)

Fig. 4.119 Relationship between micro-hardness of matrix and tempering temperature of 26%Cr cast iron with 2% V. (Specimen No.7)
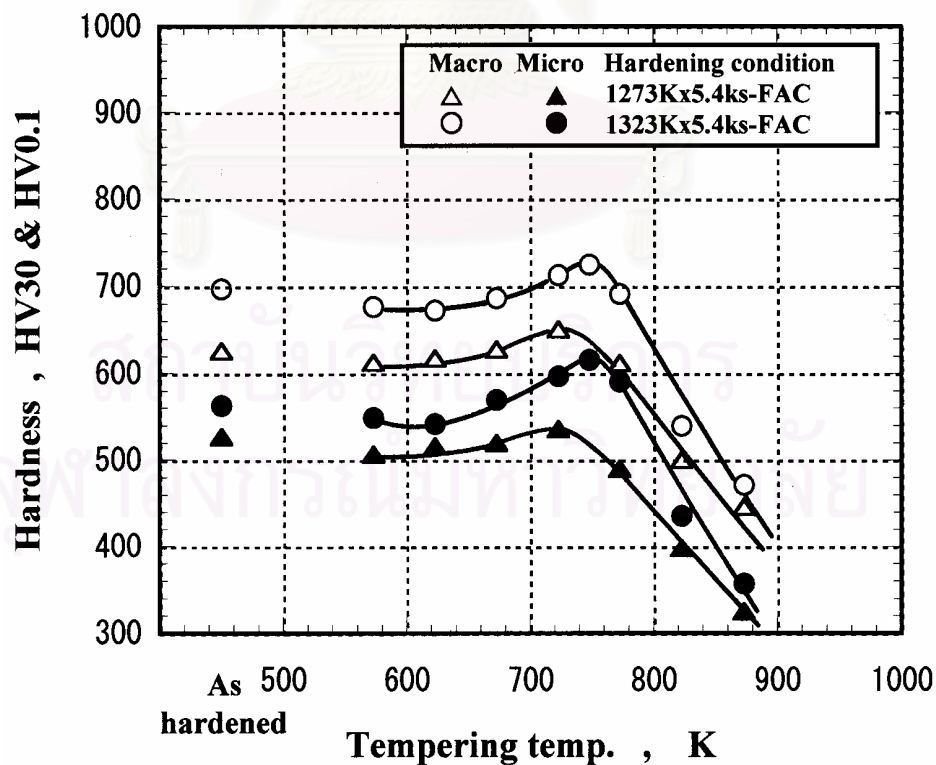

Fig. 4.120 Relationship between micro-hardness of matrix and tempering temperature of 26%Cr cast iron with 3% V. (Specimen No.8)

CHAPTER V

DISCUSSIONS

5.1 Effects of C and Cr Contents on Macro-hardness and Vγ of Heat-treated Plain High Chromium Cast Iron

5.1.1 As-hardened state

5.1.1.1 Relationship between macro-hardness and Cr/C value

Macro- and micro-hardness in as-hardened state are closely related to the amount of retained austenite. As shown Table 4.3, the macro-hardness is higher in the specimens austenitized at higher temperature. By increasing the austenitizing temperature, the solubility of C and Cr in austenite is increased. Therefore, it is possibly because the hardness of martensite itself increases due to the enrichment of C in martensite. Maratray and Poulalion [18] reported that the highest hardness of some high chromium cast irons were obtained under the existence of some retained austenite. The other reasons why the hardness goes up when the austenitizing or hardening temperature rises is that the pearlite and banite transformations are delayed and then hardenability is improved. In order to understand the mutual effect of C and Cr on the macro-hardness, the hardness are connected to the Cr/C values. The relation is shown in Fig. 5.1. Regardless of austenitizing temperature, it shows roughly uniform behavior. The hardness decreases as the Cr/C value increases up to about 4. This reason could be due to an increase in Vγ and a decrease in the amount of eutectic carbide. In the case of Cr/C value over 4, the hardness rises to the maximum of 800 HV30 at about Cr/C value of 7 and then decreases with an increase in the Cr/C value. Such behaviors can be explained by that in the range of Cr/C value from 4 to 11, the hardness depends on the Vγ which varies according to the

amount of C and Cr contents. When the C content is sufficient to depress the martensite transformation or Ms point near or below the room temperature, the Vγ increases with increasing the C content.   Resultantly, when Cr/C value is less than 7, an increase in the Cr/C value, in other words, a decrease in Vγ, makes the hardness up. When the Cr/C value exceeds 7, a decrease in hardness of martensite itself may rather or strongly make the hardness down.

5.1.1.2 Relationship between Vγ and Cr/C value

It is known that the amount of martensite transformation depends on how much percentage of temperature between Ms and Mf temperatures the specimen is cooled down. In high chromium cast iron, the Ms temperature is changed by C and Cr contents. C gives a much more influence on Ms temperature than other alloying element, the more the C content, the lower the Ms temperature. When austenitizing temperature increases, C and Cr dissolve more in austenite matrix and resultantly the Ms temperature gets down. As a result, a large volume fraction of austenite is retained in the matrix. In this experiment, a parameter of Cr/C value that was used in the literatures [14,18] can be introduced to understand the simultaneous effect of C and Cr on transformation behavior. As for the Cr/C parameter, it is shown that Cr content increases and instead C content decreases in the matrix when the Cr/C value increases.[35]

Here, the relationship between the Vγ value and the Cr/C value were obtained for all the as-hardened specimens and it is shown in Fig. 5.2. The relationship is separated into two parts at the Cr/C value of around 4.0, one is an increase in the Vγ from 4% to 26% in 1273 K and 22% to 42% in 1323 K austenitization and another is a decrease in the Vγ from 30% to 2% in 1273 K and 42% to 10% in 1323 K austenitization, as the Cr/C value increases. From a viewpoint of phase transformation, the specimens in the former case participate in the pearlite transformation and those in
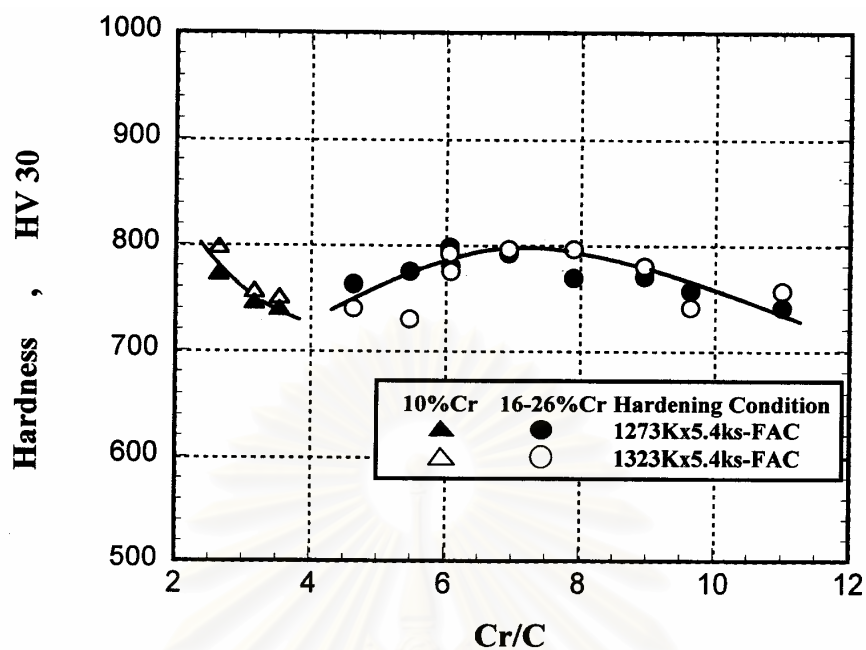
Fig. 5.1   Relationship between macro-hardness and Cr/C value
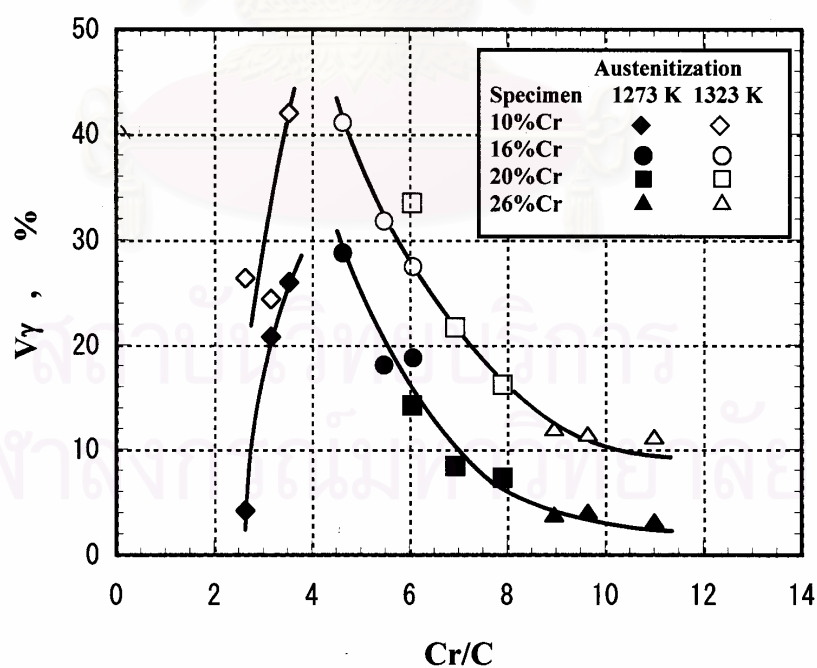of as-hardened specimens.

Fig. 5.2 Relationship between volume fraction of retained austenite (Vγ)
and Cr/C value of as-hardened specimens.

the latter case are free from it, supposing that the specimens are hardened by almost the same cooling rate. In the case of Cr/C value less than 4, when the Cr/C value increases or C content reduces, pearlite transformation delays and therefore the amount of pearlite phase decreases, that is to say, the Vγ increases. In the range of Cr/C value over 4, the matrix consists of martensite and austenite because all the specimens were cooled away from the pearlite transformation or the nose of pearlite transformation. Therefore, the Vγ is determined only by Ms temperature, the more Cr/C value, the higher Ms temperature and results in a decrease in Vγ. It is found from this results that the Vγ decreases roughly in proportion to the Cr/C value. With respect to the austenitizing temperature, the Vγ at the same Cr/C value of specimen austenitized at 1323 K is about 10% more in comparison with those austenitized at 1273 K. This is because more retained austenite formed due to more dissolution of C and Cr in austenite by elevating the austenitizing temperature from 1273 K to 1323 K.

5.1.1.3 Effect of Vγ on macro-hardness in as-hardened state

Effect of Vγ on the macro-hardness is shown in Fig. 5.3. Though this relation is a little scattered, the hardness changes in a uniform manner irrespective of austenitizing temperature, except for the data of 10% Cr specimens containing both of M_7C_3 and M_3C carbides. As the Vγ increases, the hardness rises first and then decreases when the Vγ value is over 20%. It is found that the hardness is closely related to the Vγ besides the amount of martensite. While the hardness increases in the range of low Vγ, soft pearlite phase decreases and simultaneously martensite increases. This condition continues until the hardness reaches the maximum at about 20 %Vγ where the quantities of Vγ and martensite could be well balanced. Over 20% Vγ, the hardness continues to lower due to both of an increase in Vγ and a decrease in martensite. This tendency agrees with the results of 15% Cr cast iron with molybdenum reported by Maratray.[18] The

hardness of 10% Cr specimens shown by triangle symbols in Fig. 5.3 are lower than those of 16% Cr to 26% Cr specimens at the same $V\gamma$ values. This will be understood from two reasons that a certain quantity of eutectic M_3C carbide with lower hardness coexists in the solidification structure and some pearlite phases precipitate in the matrix even by fan air cooling.
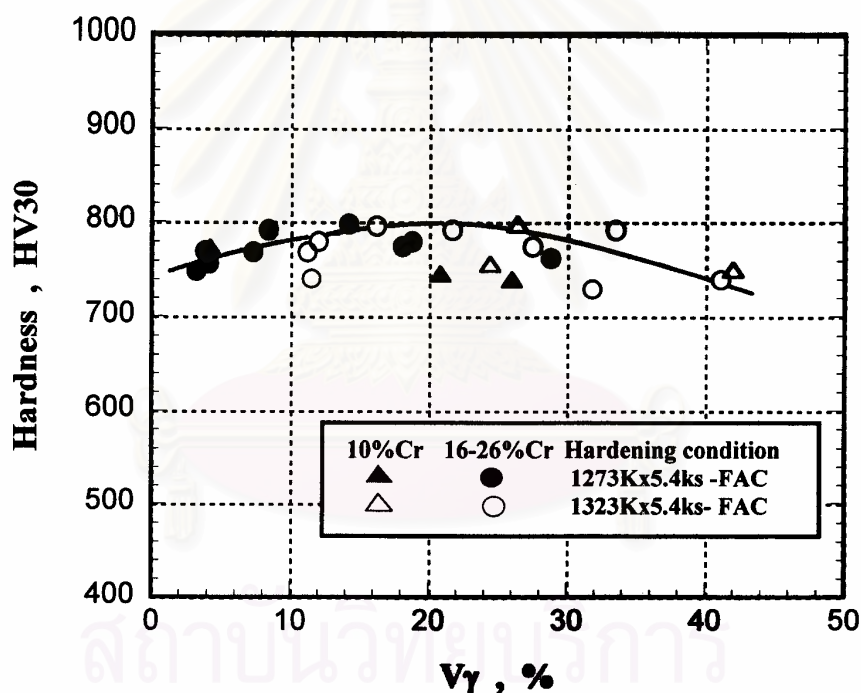

Fig. 5.3   Influence of volume fraction of retained austenite($V\gamma$) on macro-hardness in as-hardened state.

5.1.2 Tempered state

5.1.2.1 Relationship between macro-hardness and Vγ

Macro-hardness of specimens is sum of the hardness of eutectic carbides and matrix, and therefore the Vγ in the tempered matrix can also affect the macro-hardness greatly. In steels, it is known that subcritical heat treatment or tempering varies the hardness and reduces the quantity of retained austenite, and that the hardness in tempered state increases in the case of alloyed steel due to the precipitation of fine hard carbides by carbide reaction. The relation of macro-hardness vs. Vγ is obtained for all tempered specimens, and it is shown in Fig. 5.4 for the specimens hardened from 1273 K and Fig. 5.5 for those hardened from 1323 K.

In the case of 1273 K austenitization, the hardness of specimens with 0% Vγ ranges widely from 420 HV30 to 645 HV30 in 10% Cr, 440 HV30 to 690 HV30 in 16%Cr, 430 HV30 to 710 HV30 in 20%Cr and 425 HV30 to 610 HV30 in 26% Cr specimens, respectively. It is considered that in the specimens with high hardness, the retained austenite has fully decomposed to martensite and in the specimens with low hardness, the specimens are over-tempered. Therefore, the large difference in hardness at 0% Vγ is due to the difference in the matrix structure. The maximum hardness of 780 HV30 to 800 HV30 are obtained at around 4% to 10% Vγ. It is found that the hardness of 10% Cr specimens are especially low compared with other chromium specimens. This is because the M_3C carbide with lower hardness than M_7C_3 carbide coexists in the specimen. After the hardness of 16% Cr, 20% Cr and 26% Cr specimens reach the maximum values they decrease roughly in proportion to an increase in Vγ, and the relationship between the macro-hardness and Vγ is expressed by the following equation,

$$\text{Macro-hardness (HV30)} = -1.92 \times \% V\gamma + 784.4 \qquad (5.1)$$

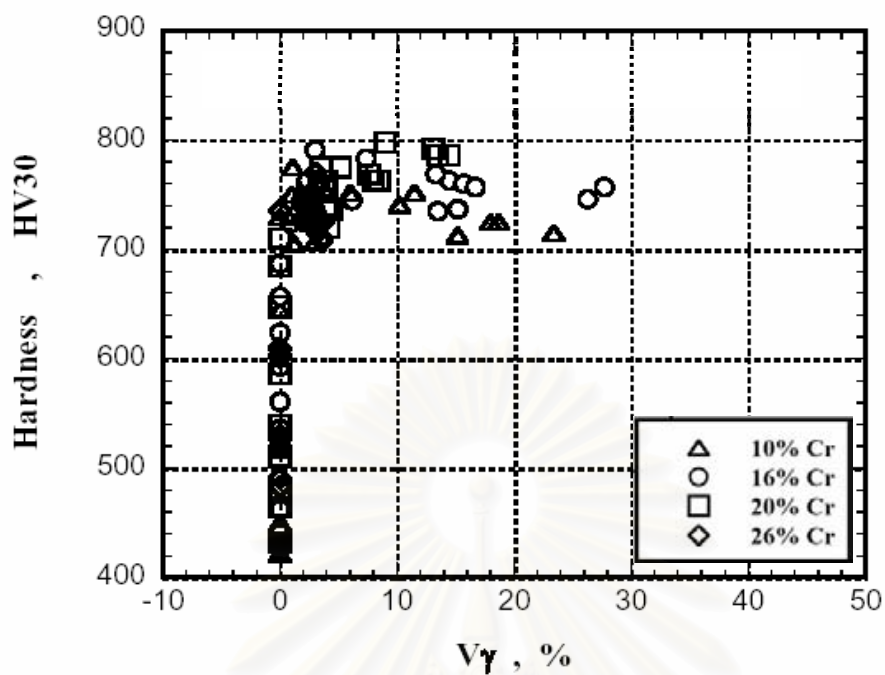Fig. 5.4 Relationship between macro-hardness and volume fraction of
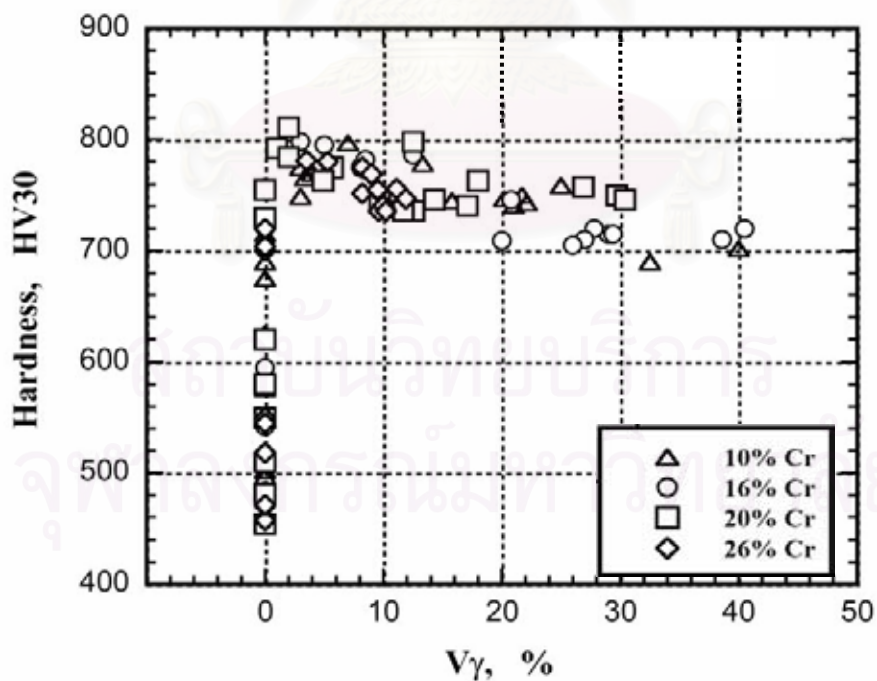retained austenite (Vγ) of tempered alloy-free specimens.
(Austenitized at 1273 K)

Fig. 5.5 Relationship between macro-hardness and volume fraction of
retained austenite (Vγ) of tempered alloy-free specimens.
(Austenitized at 1323 K)

In the case of specimens austenitized at 1323 K, the hardness shows a similar manner to the case of 1273 K austenitization. The hardness at 0% Vγ ranges from 497 HV30 to 715 HV30 in 10%Cr, 484 HV30 to 757 HV30 in 16%Cr, 455 HV30 to 755 HV30 in 20% Cr and 471 to 700 HV30 in 26% Cr specimens. After the hardness reaches the maximum value of 780 HV30 to 800 HV30 at 2% to 8% Vγ, much better relation is obtained between the hardness and Vγ; it decreases proportionally as the Vγ increases, and the relationship between macro-hardness and Vγ is given by the next equation,

$$\text{Macro-hardness (HV30)} = -1.69 \times \%V\gamma + 779.1 \qquad (5.2)$$

From the relationship between tempered macro-hardness and Vγ shown by Fig. 5.4 and Fig. 5.5, it is found that the hardness in tempered state is closely related to the Vγ value which is determined by the C and Cr contents and that the behaviors of a decrease in hardness against the Vγ are similar regardless of austenitizing temperature.

5.1.2.2 Relationship between maximum tempered hardness (H$_{Tmax}$) and Cr/C value

In applications of high chromium cast iron for abrasive wear resistance, the heat treatment so as to get very high hardness or maximum hardness is usually given to the cast iron. It is meaningful that the relationships between H$_{Tmax}$ and parameters that affect the H$_{Tmax}$ are obtained. The effect of Cr/C value on the H$_{Tmax}$ is shown in Fig. 5.6. The H$_{Tmax}$ had a tendency to decrease slightly as the Cr/C value increases and the decreasing rate is a little different between 10% Cr iron and 16% Cr to 26% Cr specimens. At the same Cr/C value, the H$_{Tmax}$ are a little high in the specimens hardened from high austenitizing temperature. The H$_{Tmax}$ are ranged from 770 HV30 to 750 HV30 in 1273 K and 800 HV30 to 750 HV30 in 1323 K austenitizing temperature for 10% Cr cast iron, and 780

HV30 to 740 HV30 in 1273 K and 800 HV30 to 760 HV30 in 1323 K austenitizing temperature for 16% to 26% Cr specimens. In Fig. 5.6, the graphs are separated into two parts at the Cr/C value of 4.0 of which behavior is similar to the relationship between hardness and Cr/C value in as-hardened state (Fig. 5.2). The reason is considered to be same as discussed on Fig. 5.2. In the case of Cr/ C value less than 4.0, the H_{Tmax} decreases gradually with an increase in Cr/C value. This is due to a decrease in amount of eutectic carbides. In the case of Cr/C value over 4.0, on the other hand, the H_{Tmax} values are almost same in the low Cr/C value ranging from 4.5 to 6.1. When the Cr/C value rises over 6.1, the H_{Tmax} decreases gradually regardless of the austenitizing temperature as the Cr/C value increases. This decrease in hardness can be explained from the facts that an increase in Cr/C value raises Ms temperature and at the same time shifts the pearlite and banite transformation to the short time side, and resultantly, the Vγ in as-hardened state which works upon the increase of tempered hardness is reduced. The H_{Tmax} values of low Cr/C region are a little higher than those in high Cr/C region. This is because a large volume fraction of retained austenite contributes to increase the precipitation of carbides and C dissolved more in martensite also contributes to increase the hardness of martensite itself.

5.1.2.3 Relationship between maximum tempered hardness (H_{Tmax}) and Vγ

Since the Vγ in as-hardened state is directly connected to the H_{Tmax} under the same tempering condition, the effect of Vγ value on the H_{Tmax} was obtained and it is shown in Fig. 5.7. Regardless of the austenitizing temperature, the H_{Tmax} goes up uniformly to 800 HV30 as the Vγ increases up to 20%. Over 20% Vγ, however, the H_{Tmax} is kept constant at approximately same value. It is evident that the cast irons retaining the Vγ up to 40% can provide the highest hardness by tempering.

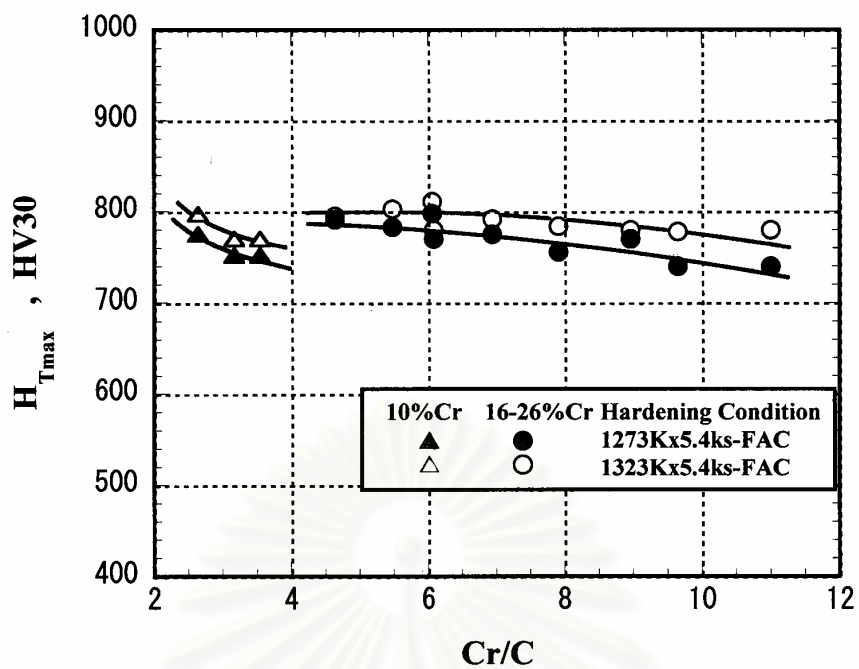In practical uses of high chromium cast iron, the hardness of 16%

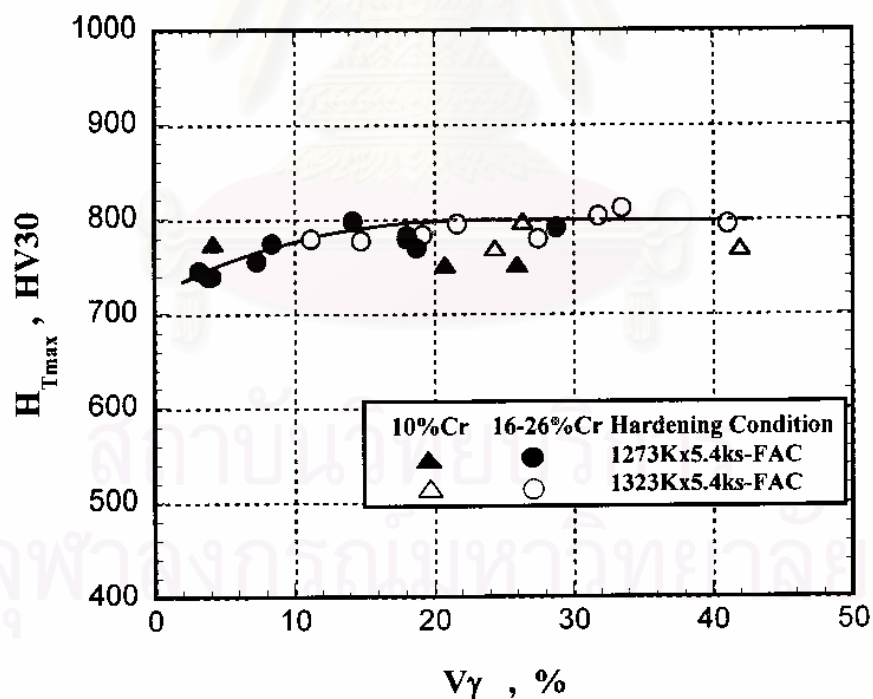Fig. 5.6 Relationship between maximum tempered macro-hardness (H_{Tmax}) and Cr/C value.

Fig. 5.7 Effect of volume fraction of retained austenite $(V\gamma)$ in as-hardness state on maximum tempered hardness (H_{Tmax}).

Cr cast iron used for hot working mill roll is 640 to 750 HV and that of 26% Cr cast iron for the mineral pulverizing mill roll and table is 700 to 880 HV. When much higher hardness is required to the parts of mineral pulverizing mills in severe abrasion wear condition, the other alloying elements which improve the hardenability and simultaneously promote the secondary hardening by forming the specials carbides with much higher hardness than chromium carbides should be added to the cast iron. In general, the high chromium cast iron with heavy section contains alloying elements such as Ni, Cu, Mo and V.

5.1.3 Observation of transformed matrix by SEM

Heat-treated matrix hardness is closely related to the transformation behavior of matrix. In order to discuss the change in the macro-hardness, SEM observation is employed and the transformed microstructure of matrix was investigated in detail.

SEM microphotographs of 16% Cr hypoeutectic specimen (No.5), which were hardened from 1323 K and tempered at 673 K, 748 K, 773 K and 823 K, are shown in Fig. 5.8. At 2500 magnifications, the matrix structure can be revealed in detail. In the matrix of as-hardened specimen, a large amount of carbides exist mixing with martensite and retained austenite. Large particles of carbides could be indissoluble carbides already existed in annealed state. It is found that the appearance of secondary carbides changes depending on the tempering temperature. At 673 K tempering, the austenite still remains but morphology of secondary carbides is similar to that in as-hardened matrix. When the tempering temperature is increased to 773 K, however, more secondary carbides exist in the matrix but very fine carbides are newly seen. The carbides in the matrix of specimens tempered at 823 K decrease in number and increase in size. In this point, either martensite or retained austenite can not be distinguished. This tempering condition that the coarsening of carbides took place can be called as "over tempering".
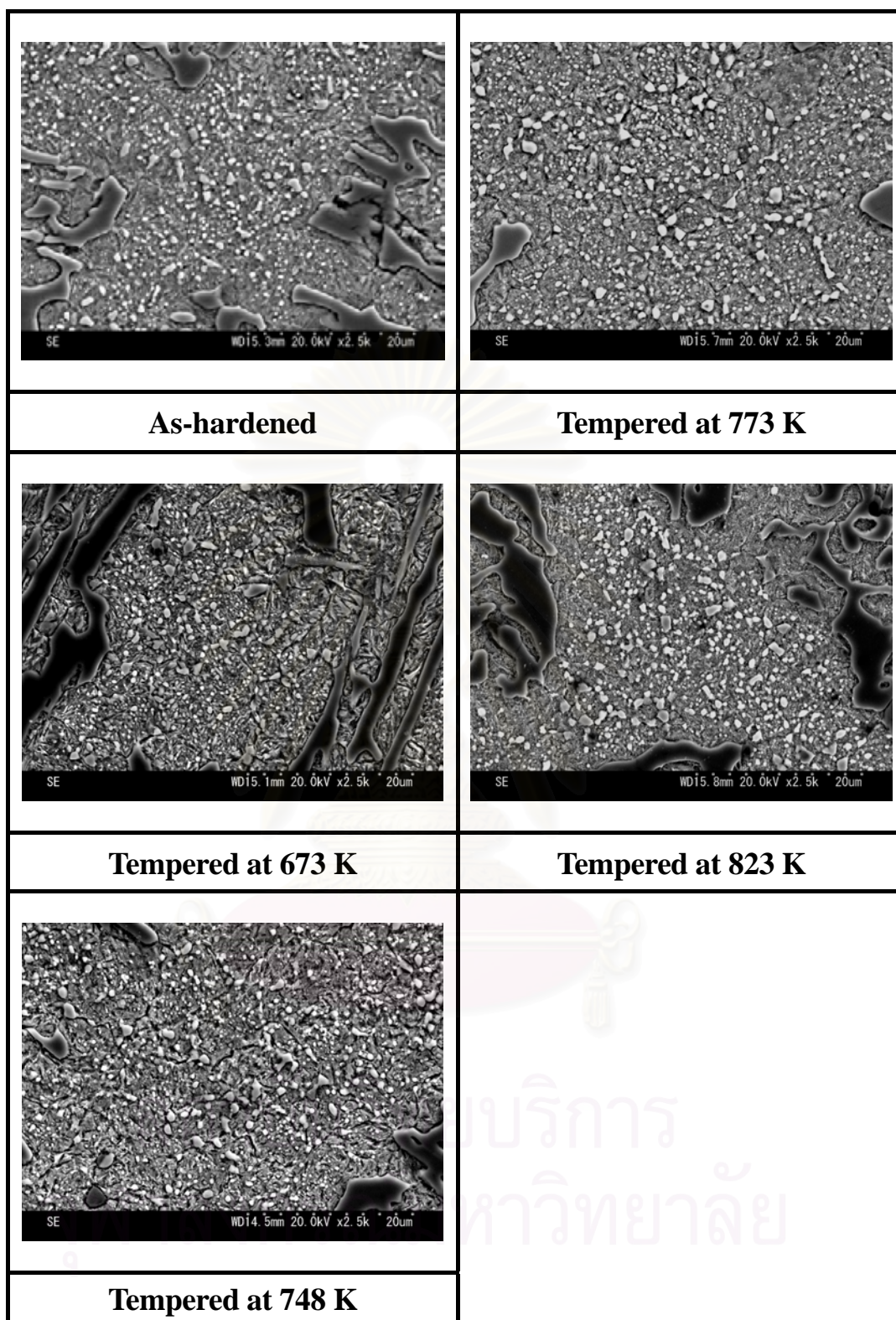
Fig. 5.8 SEM micrographs of 16%Cr cast iron (No.2) hardened from 1323 K and then tempered at four different temperatures. Size and amount of secondary carbides precipitated in matrix vary depending on the tempering temperature. In this case, precipitated carbides in specimen tempered at 748 K are smallest in size and in large amount.

The matrix structure tempered at 748 K corresponds to that of the specimen with H_{Tmax}, and the hardness of the other three specimens are all low. Though it can not be confirmed, the difference in hardness among them must be mostly due to the matrix microstructure filling up the spaces around the carbide particles, say, matrices could consist of a tempered martensite and/or transformed martensite from retained austenite. It is sure that these matrix structures can contribute to obtain the highest hardness in the tempered state.

SEM microphotographs in the case of 26% Cr specimen (No.11) hardened from 1323 K and tempered at different temperatures are shown in Fig. 5.9. The detailed phases in matrix such as martensite and retained austenite can be seen little from these microphotographs with 2500 magnifications. However, the behavior of secondary carbides is evident, and the transition of carbide structure associated with tempering temperature is quite similar to that of 16% Cr cast iron. The amount of carbide is increased by tempering and the carbides are most and finest in the specimen tempered at 748 K. This specimen shows the H_{Tmax}. It is clear that these carbides are coarsened and decrease in number as the tempering temperature gets over 723 K. Here, one question is left, why is the H_{Tmax} value of 16%Cr cast iron higher than that of 26%Cr cast iron?, whereas the amount of secondary chromium carbides is more and the hardness of chromium carbide containing more Cr in 26% Cr specimen is higher.[26] According to the relationship between micro-hardness of matrix and tempering temperature shown in Fig.4.22 (16% Cr specimen) and in Fig. 4.26 (26% Cr specimen), the H_{Tmax} values of micro-hardness of both specimens are close each other. This means that the difference in macro-hardness between 16% Cr and 26% Cr specimens arises from the difference in the hardness of eutectic carbides between 16% Cr and 26% Cr specimens. In the case of specimens with eutectic composition (No.4 and No.10), for example, the volume fractions of eutectic carbide calculated from the equation 2.3 [14] are 36.2% in 16% Cr and 36.4% in 26% Cr specimens, respectively. In the specimens with hypoeutectic

composition, therefore, the volume fractions of eutectic carbide may be approximately same if the specimens have similar eutectic ratio. Resultantly, the influence of the amount of eutectic carbide on the macro-hardness is considered to be less between the 16% Cr and 26% Cr specimens. From above discussions, it is concluded that the higher macro-hardness in 16% Cr specimen is due to the difference in morphology of eutectic chromium carbide; the carbide morphology of 16% Cr specimen is thicker and more interconnected in comparison with that of 26% Cr specimen which is thin or fine and more discontinuous.[1,6] In order to prove this consideration, the three dimensional microstructures of eutectic chromium carbide are investigated by SEM using deep-etched specimen. As an example, the SEM microphotographs of eutectic chromium carbides are shown in Fig. 5.10 (a) for 16% Cr and (b) for 26% Cr specimens. By dissolving matrix of the specimen using deep etching method, the eutectic carbides are three-dimensionally revealed. It is observed that eutectic carbides in 16% Cr specimen are more connected or more continuous. It is no exaggeration to say that such a difference in morphology of eutectic chromium carbide may produce the difference in hardness of 16% Cr and 26% Cr specimens.

As-hardened

Tempered at 773 K

Tempered at 673 K

Tempered at 823 K
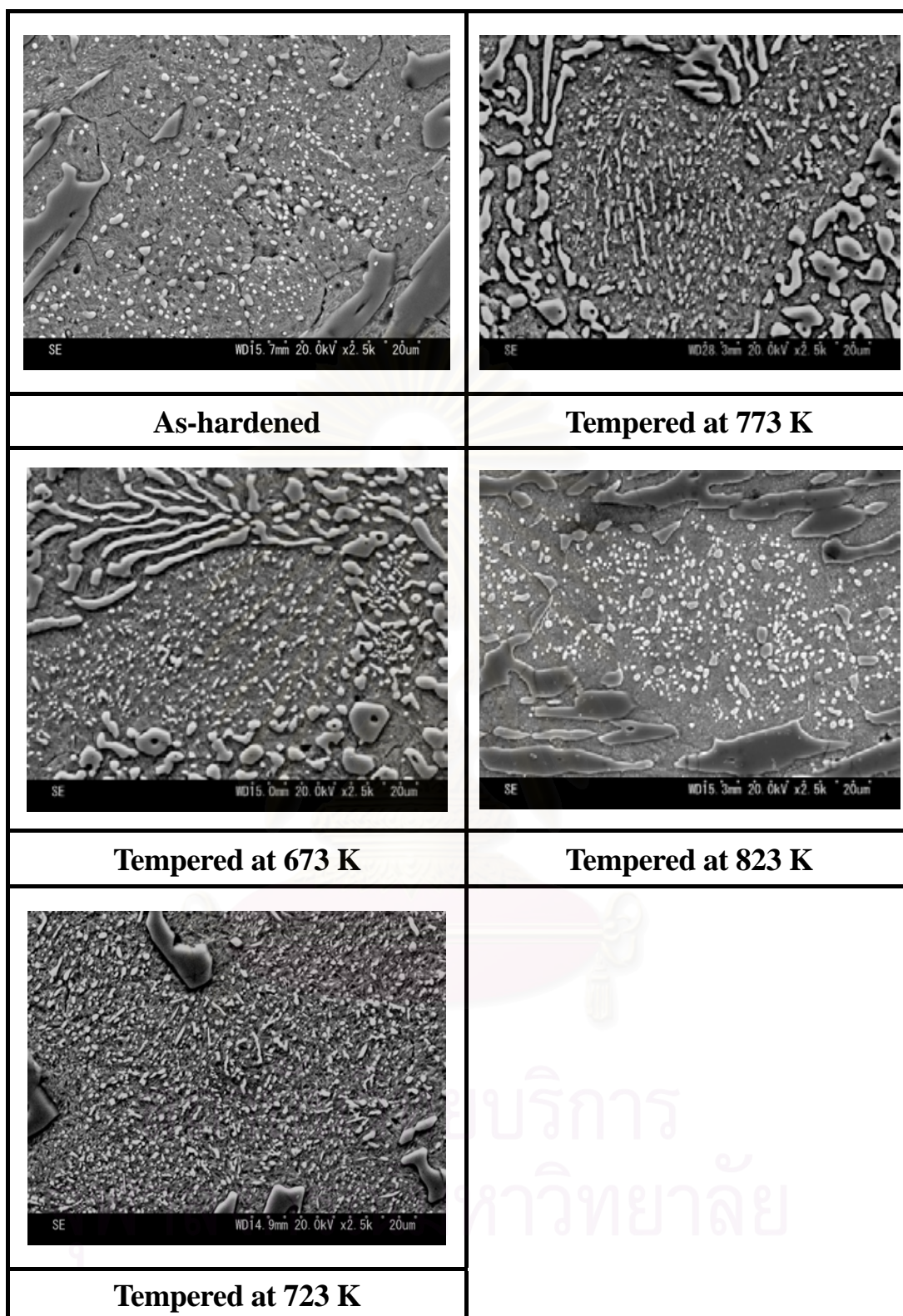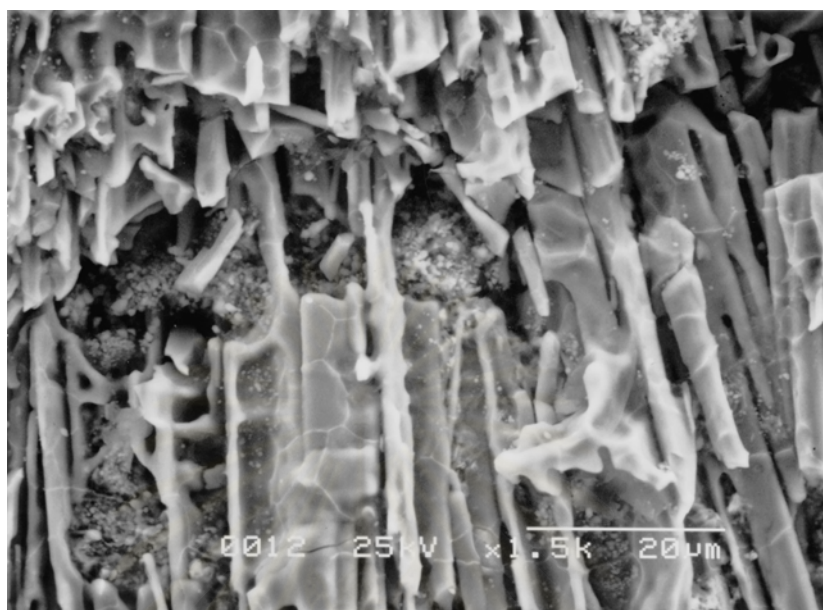
Tempered at 723 K

Fig. 5.9 SEM microphotographs of 26% Cr cast iron (No.5) hardened from 1323 K and then tempered at four different temperatures. Large amount of secondary carbides in finer size precipitate in matrix tempered at 723 K. Coarsening of precipitated carbides or over-tempering occurs at high tempering temperature of 823 K.

(a)

(b)

Fig. 5.10 SEM microphotographs of eutectic M_7C_3 carbides, (a) 16% Cr and (b) 26% Cr cast irons. Morphology of M_7C_3 eutectic carbides is thicker and more interconnected in 16% Cr cast iron than that in 26% Cr cast iron which is thinner or finer and discontinuous.

5.2 Effects of Alloying Elements on Macro-hardness and Vγ of Heat-treated Eutectic 16% Cr and 26% Cr Cast Irons

5.2.1 As-hardened state

5.2.1.1 Effects of alloying elements on macro-hardness

Effect of alloying elements on the hardness in as-hardened state is shown in Fig. 5.11 and Fig. 5.12 for 16% Cr and Fig. 5.13 and Fig. 5.14 for 26% Cr specimens. In the case of 16% Cr specimens, in comparison with alloy-free cast iron, the hardness unexpectedly decreases with an increase in Ni and Cu contents, and the addition of Mo or V raises the hardness in each chromium specimen. The decreasing rate by Ni and Cu addition is much more in the case of 1323 K austenitization. In 26% Cr specimens, the hardness increases with increasing Mo content whereas Ni, Cu and V decrease it. With respect to the effect of austenitizing temperature, the hardness is substantially low in 16% Cr specimen and high in 26% Cr specimen when the austenitizing temperature is high. The highest hardness is obtained in the specimens containing V in 16% Cr and Mo in 26% Cr specimens, respectively.

5.2.1.2 Effects of alloying elements on Vγ

Effect of alloying elements on the Vγ is shown in Fig. 5.15 for 1273 K and Fig. 5.16 for 1323 K austenitization in 16% Cr specimens and Fig. 5.17 for 1273 K and Fig. 5.18 for 1323 K austenitization in 26% Cr specimens, respectively. The Vγ in 16% Cr specimens increases in proportion to Ni, Cu and Mo contents, however, it decreases gradually by increasing the V content. At the same alloy content, the Vγ values in 16% Cr specimens are higher than those in 26% Cr specimens. Ni shows the strongest effect on the increase of retained austenite, and followed by Cu in 16% Cr and Mo in 26% Cr specimens, respectively. This is because Ni
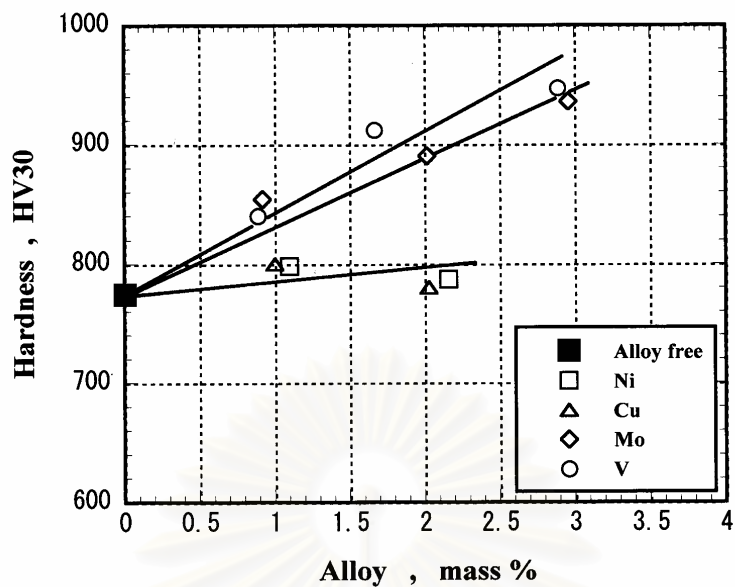
Fig. 5.11 Effect of alloying elements on macro-hardness of eutectic 16% Cr specimens in as-hardened state. (Austenitized at 1273 K)
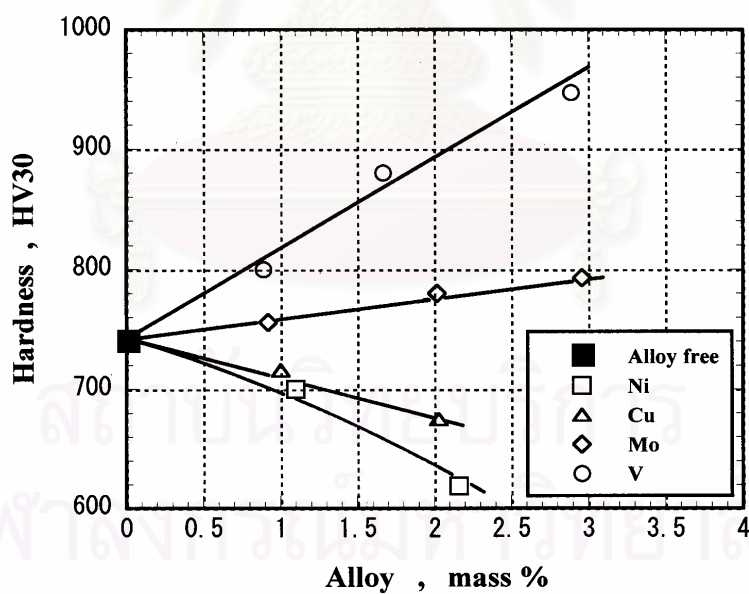

Fig. 5.12   Effect of alloying elements on macro-hardness of eutectic 16% Cr specimens in as-hardened state. (Austenitized at 1323 K)
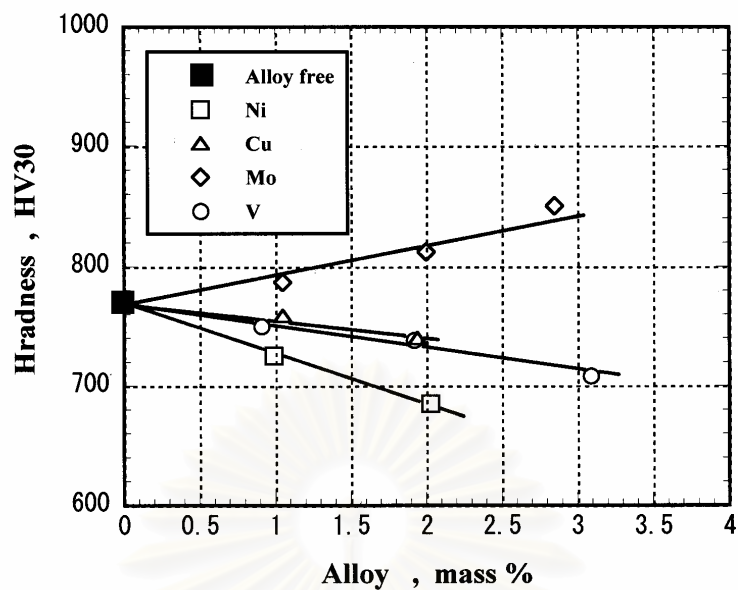
Fig. 5.13 Effect of alloying elements on macro-hardness of eutectic 26% Cr specimens in as-hardened state. (Austenitized at 1273 K)
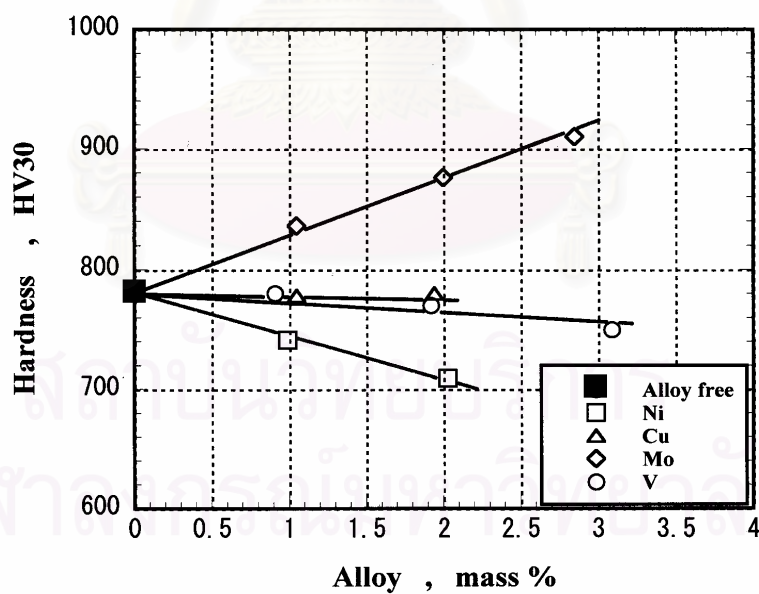

Fig. 5.14 Effect of alloying elements on macro-hardness of eutectic 26% Cr specimens in as-hardened state. (Austenitized at 1323 K)
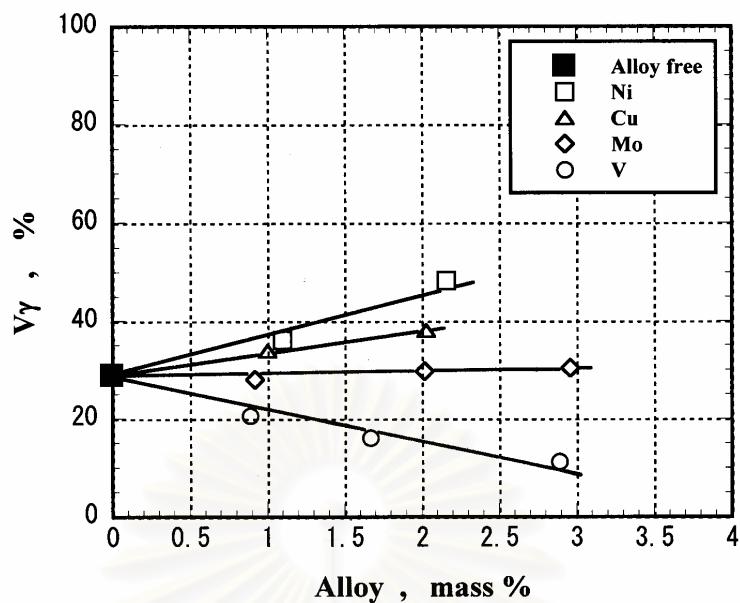
Fig. 5.15 Effect of alloying elements on the volume fraction of retained austenite (Vγ) of eutectic 16% Cr specimens in as-hardened state. (Austenitized at 1273 K)

Fig. 5.16 Effect of alloying elements on the volume fraction of retained austenite (Vγ) of eutectic 16% Cr specimens in as-hardened state. (Austenitized at 1323 K)

Fig. 5.17 Effect of alloying elements on the volume fraction of retained austenite (Vγ) of eutectic 26% Cr specimens in as-hardened state. (Austenitized at 1273 K)

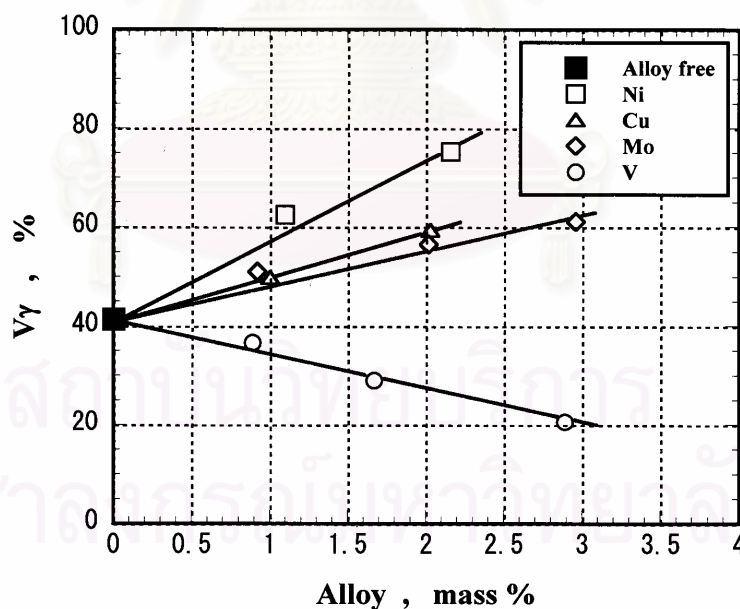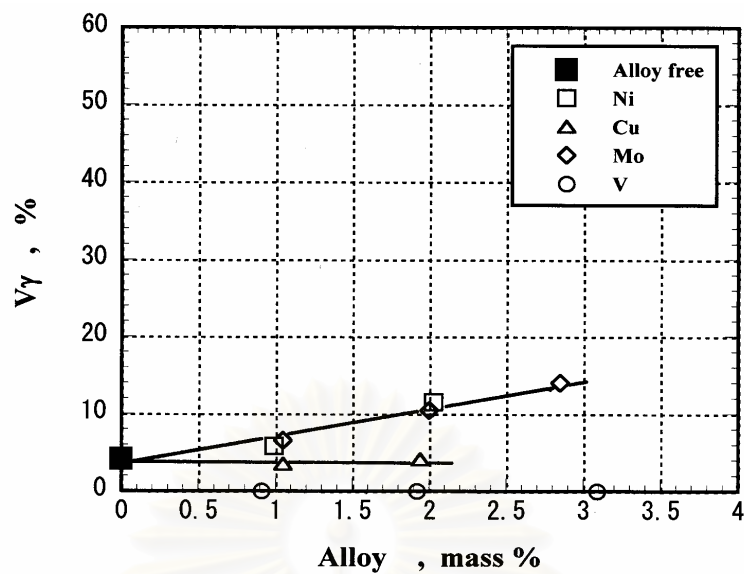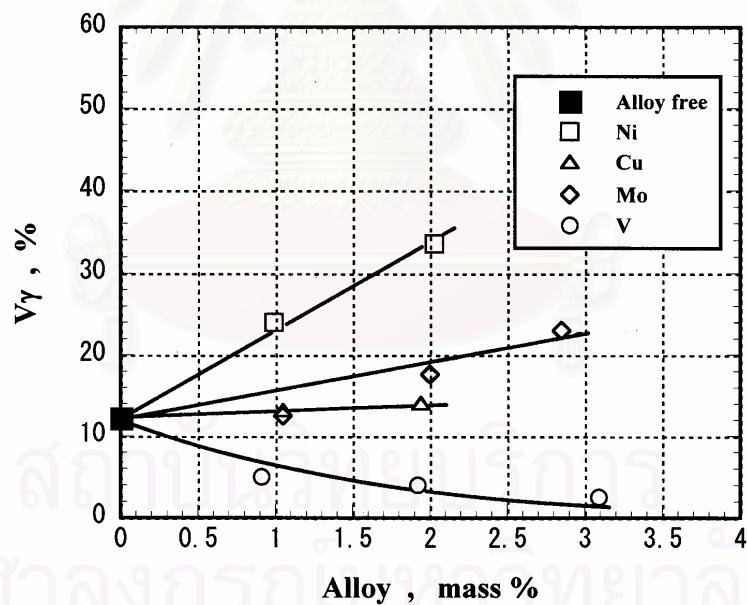Fig. 5.18 Effect of alloying elements on the volume fraction of retained austenite (Vγ) of eutectic 26% Cr specimens in as-hardened state. (Austenitized at 1323 K)

and Cu mostly dissolving in matrix could stabilize the austenite.

5.2.1.3 Correlation between hardness and Vγ

Here, the hardness in as-hardened state is discussed for the effect of V and Mo by referring to the retained austenite in as-hardened state. The 16% Cr specimens with V show the highest hardness in the case of both austenitization because as-hardened matrix consists of large portion of martensite and the smallest amount of Vγ. However, the 26% Cr specimens containing V show much lower hardness than the specimens with Mo, rather they decrease in the hardness. This reason can be explained by that since the as-hardened matrix shows martensite and very small quantity of Vγ, 0 to 5% Vγ, some pearlite phases could exist in the matrix. The increase in V content reduces the C content in austenite and promotes the pearlite transformation, and therefore it decreases the hardness.

On the other side, the hardness of specimen with Mo depends mainly on the Vγ value. When the hardness was connected to the Vγ values, the Vγ value which gives the highest hardness was 20% to 30% and this value is near the result reported by Maratray.[18]

5.2.2 Tempered state

It was reported that multi-component white cast iron, which contains plural kinds and large amount of carbide forming elements of Cr, Mo, W and V, showed the remarkable secondary hardening during tempering.[23] In the high chromium cast irons with low content of the third alloying element, such a secondary hardening can be expected to appear, if strong carbide forming element is added.

From the tempering curves, the tempered hardness was connected to the Vγ for all specimens and the relation is shown in Fig. 5.19 for 1273 K and Fig. 5.20 for 1323 K austenitization. It is noted that the relationship

is expressed as one uniform line in the case of low austenitizing temperature, 1273 K and the hardness decreases from the maximum value in proportion to the Vγ value regardless of Cr content and the kind and the amount of the third alloying element. In the case of 1323 K austenitization, however, it is also noted that as the Vγ increases, the hardness decreases in two ways regarding to Cr content of the specimens and the decreasing rates are roughly same. This suggests that effect of Cr content on the tempered hardness appears strongly in higher austenitization. At the same Vγ value, the hardness of 16% Cr specimen is higher than that of 26% Cr specimen. Since not only C and Cr but the alloying element dissolves more in the matrix at high austenitizing temperature, the tempered hardness becomes high because more secondary carbides including special carbides precipitate from martensite and more martensite transformed from destabilized retained austenite is obtained during tempering.

Effect of alloying elements on the H_{Tmax} is shown in Fig. 5.21 and Fig. 5.22 for 16% Cr and Fig. 5.23 and Fig. 5.24 for 26% Cr specimens. It is found that the H_{Tmax} is influenced by the kind and the amount of alloying elements and austenitizing temperature. At the same alloy content, the H_{Tmax} values are a little high in the specimens hardened from high austenitizing temperature. In 16% Cr specimens, the H_{Tmax} values are mostly high in the specimens with alloying elements compared with that of alloy-free specimen. The H_{Tmax} goes up gradually as alloy content increases, and the increasing rate is largest in Mo specimen and smallest in Ni specimen. In 26% Cr specimens, the H_{Tmax} increases largely with an increase in Mo content but the increasing rates of Ni and Cu specimens are smaller than that of Mo specimen. However, V lowers the H_{Tmax} gradually. The highest values of H_{Tmax}, 890 HV30 in 16% Cr and 920 HV30 in 26% Cr specimens, were obtained in the specimen with Mo.

The high H_{Tmax} are not obtained in the specimens with Ni or Cu even if they show very high degree of precipitation hardening, because the secondary carbides that precipitate in the matrix are only chromium

carbide as same as those in the alloy-free specimen. On the other hand, the highest H_{Tmax} is obtained in the specimen with Mo because the large amount of retained austenite in as-hardened state contributed largely to the secondary hardening. In this case, molybdenum carbides precipitate as secondary carbide that is much higher in hardness than chromium carbides, and they give rise to the secondary hardening. In spite of the fact that V is strong carbide former and vanadium carbide has extremely high hardness, the high hardness can not be obtained in the V specimens by this heat treatment, and V shows even bad effect in 26% Cr specimen. This reason is explained as follows,

The specimen with V produces less retained austenite in as-hardened state because V combines with C, in other words, V shifts the pearlite transformation to the short time side [23], or V rises the temperature of eutectoid transformation and increases a critical cooling rate of martensite transformation.[11] Consequently, V in austenite is consumed to form pearlite and then less austenite with low V content is retained after hardening. In order for V to display its full effect in tempering, that is, the increase in tempered hardness, higher austenitizing temperature will be introduced to make V dissolve more and more in the austenite.

Fig. 5.19 Relationship between macro-hardness and volume fraction of retained austenite (Vγ) of tempered eutectic specimens with alloying elements. (Austenitized at 1273 K)
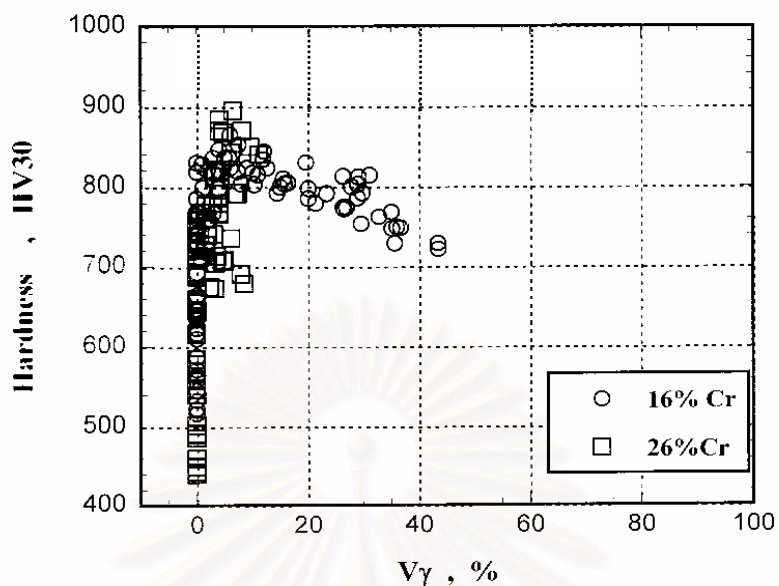

Fig. 5.20 Relationship between macro-hardness and volume fraction of retained austenite (Vγ) of tempered eutectic specimens with alloying elements. (Austenitized at 1323 K)

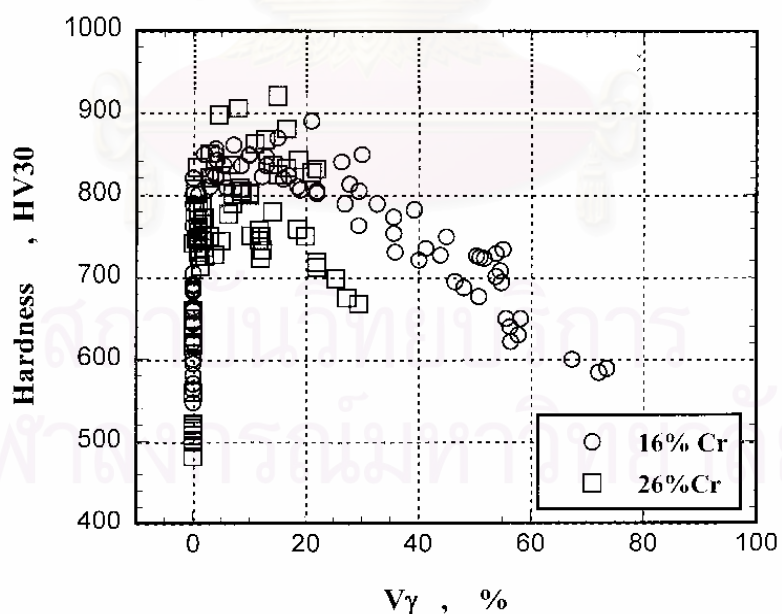Fig. 5.21 Effect of alloying elements on maximum tempered hardness (H$_{Tmax}$) of 16% Cr specimens. (Austenitized at 1273 K)

Fig. 5.22 Effect of alloying elements on maximum tempered hardness (H$_{Tmax}$) of 16% Cr specimens. (Austenitized at 1323 K)
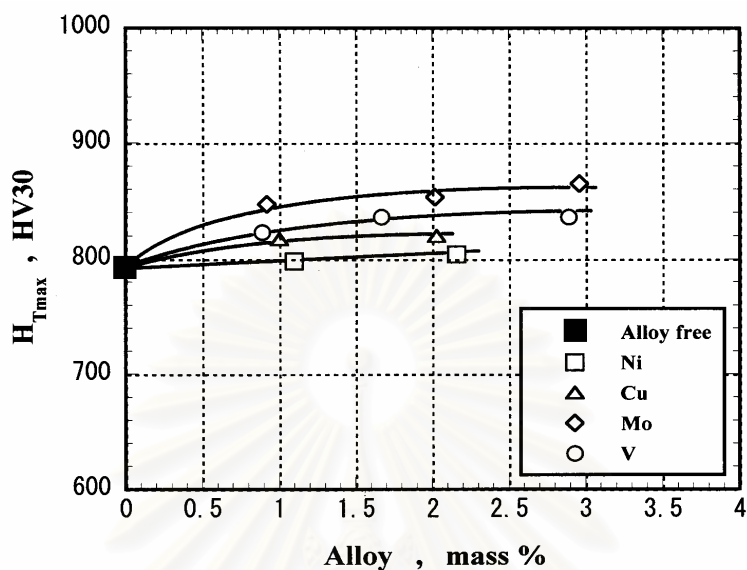
Fig. 5.23 Effect of alloying elements on maximum tempered hardness
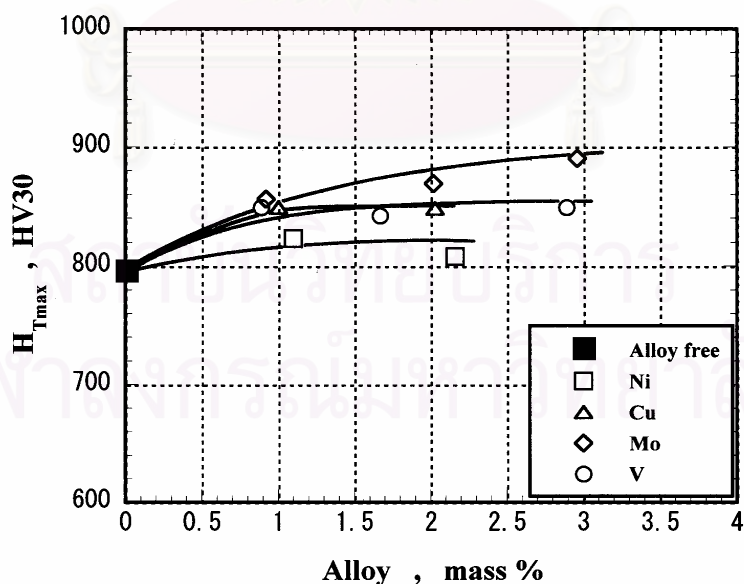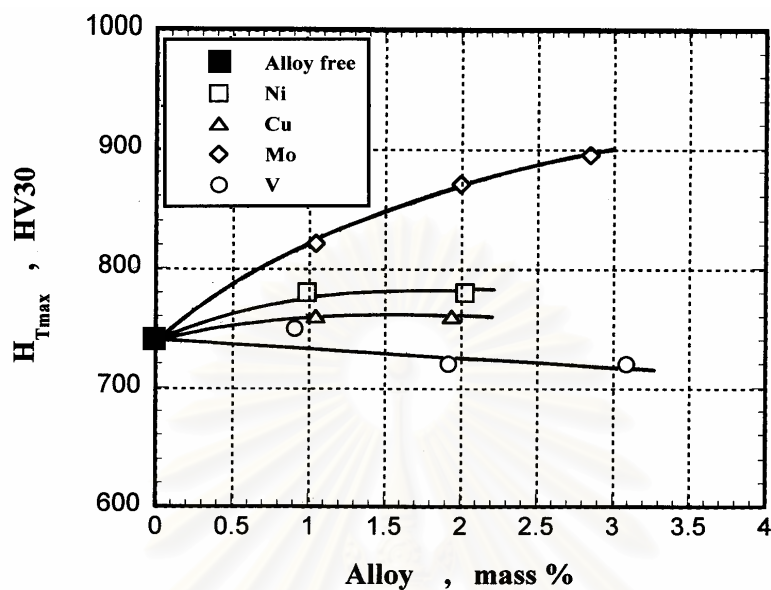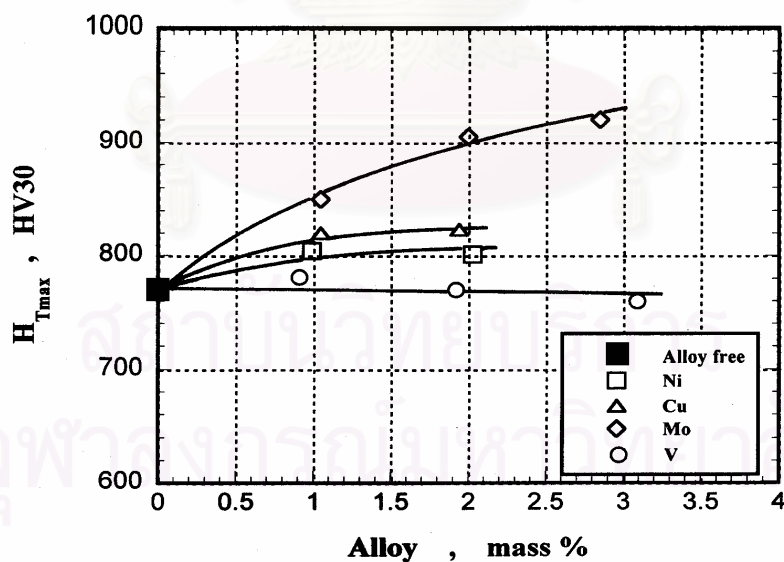(H_{Tmax}) of 26% Cr specimens. (Austenitized at 1273 K)

Fig. 5.24 Effect of alloying elements on maximum tempered hardness
(H_{Tmax}) of 26% Cr specimens. (Austenitized at 1323 K)

5.3 Effects of Alloying Elements on Macro-hardness and Vγ of Heat-treated Hypoeutectic 16%Cr and 26%Cr Cast Irons

5.3.1 As-hardened state

5.3.1.1 Effects of alloying elements on macro-hardness

Macro-hardness depends on the type and the volume fraction of carbide and matrix structure. Particularly in hypoeutectic cast iron, the matrix hardness is closely related to the Vγ and greatly influenced by the hardness of martensite itself besides the Vγ value. Generally, greater amounts of carbide and martensite lead to an increase in hardness but the greater amount of retained austenite, which is dependent on the type and amount of third alloying element added, produces a decrease in hardness. The relationship between alloying elements and macro-hardness for the specimen hardened from the austenitizing temperatures of 1273 K and 1323 K are shown in Fig. 5.25 to Fig. 5.26 for 16% Cr and Fig. 5.27 to Fig. 5.28 for 26%Cr specimens, respectively. The relations have same tendency regardless of austenitizing temperatures.

As for the 16% Cr specimens hardened from 1273 K (Fig. 5.25), the hardness increases as Mo and V content increases but it decreases with an increases in Ni content. Cu changes little the hardness. The increasing rates of the hardness are summarized in Table 5.1. The largest increasing rate is obtained by V addition followed by Mo, Cu and the smallest rate is obtained by Ni addition. The increasing rates of Ni and Cu specimens are determined by how much both elements postpone the pearlite transformation, how much martensite is formed and how much austenite is stabilized. Cu acts rather to decrease martensite and Ni rather does to stabilize austenite because the stabilizing ability of Ni is stronger than that of Cu.

Mo delays the pearlite transformation greatly but the decreasing rate of Ms temperature is rather small. The reason why Mo increases the

Table 5.1 Increasing rate of macro-hardness by alloying element.

Alloying element	Increasing rate (HV30 /alloy)	
	1273 K austenitization	1323 K austenitization
Ni	-23.5	-40.0
Cu	4.5	-19.0
Mo	23.7	15.7
V	28.7	36.4

hardness is an increase in martensite and the precipitation of hard molybdenum carbides in matrix during austenitizing. Mo and V form their special carbides of M_2C or M_6C and MC with higher hardness. It is reported that the hardness of carbide and matrix increase with an increase in Mo content.[5] On the other side, the hardness of V specimens is largest in spite of lower Vγ. This is because V, the strongest carbide former in the third alloying elements, promotes the perecipitation of vanadium carbides with much higher hardness than the molybdenum carbide during destabilization and increases the amount of martensite by decreasing the carbon concentration in austenite.

Even when the austenitizing temperature is elevated to 1323 K, the order of the hardness increasing rate for alloying element does not change, and the effects of alloying elements can be explained by the same reasons.

As for 26% Cr specimens, the order of the increasing rate for the third alloying element is different from that of 16% Cr specimens. The largest hardness is obtained in Mo specimen followed by Ni, Cu and V specimens. However, this order does not change according to the austenitizing temperature. The reason that the increasing rate of the hardness for Mo is greatest is the same explained in the case of 16% Cr

Fig. 5.25 Effect of alloying elements on macro-hardness of hypoeutectic
16%Cr specimens in as-hardened state. (Austenitized at 1273 K)

Fig. 5.26 Effect of alloying elements on macro-hardness of hypoeutectic
16% Cr specimens in as-hardened state. (Austenitized at 1323 K)
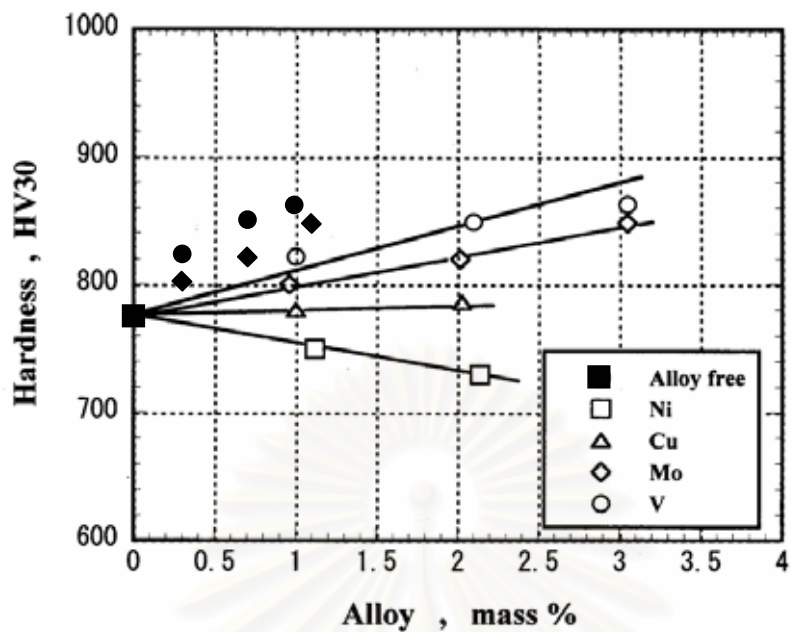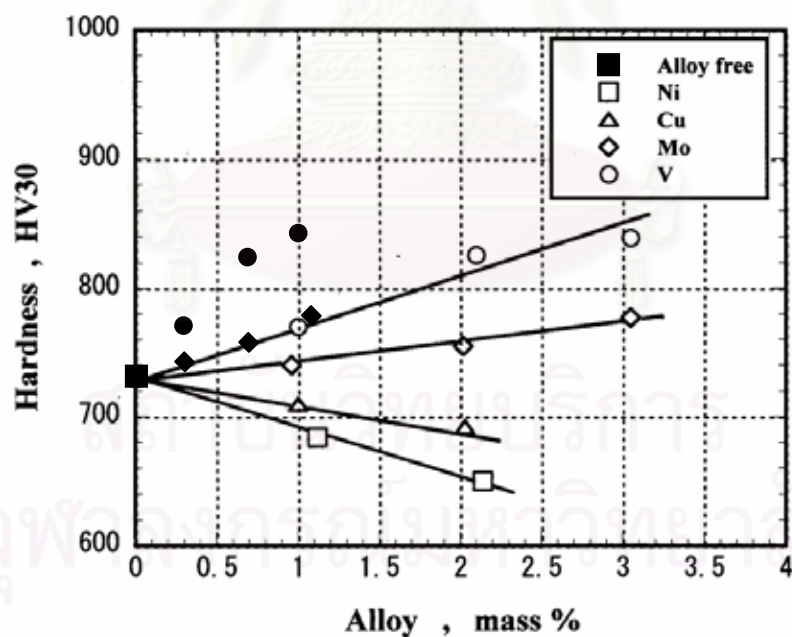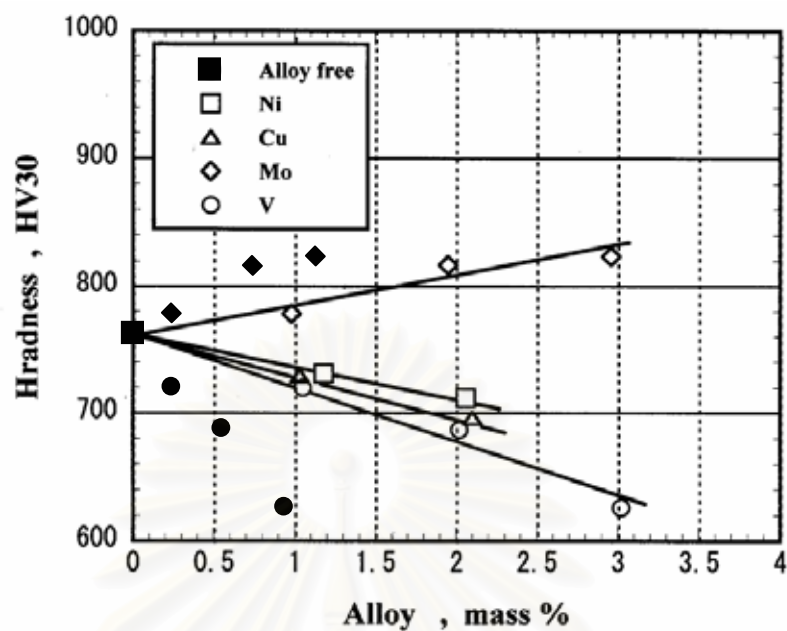
Fig. 5.27 Effect of alloying elements on macro-hardness of hypoeutectic
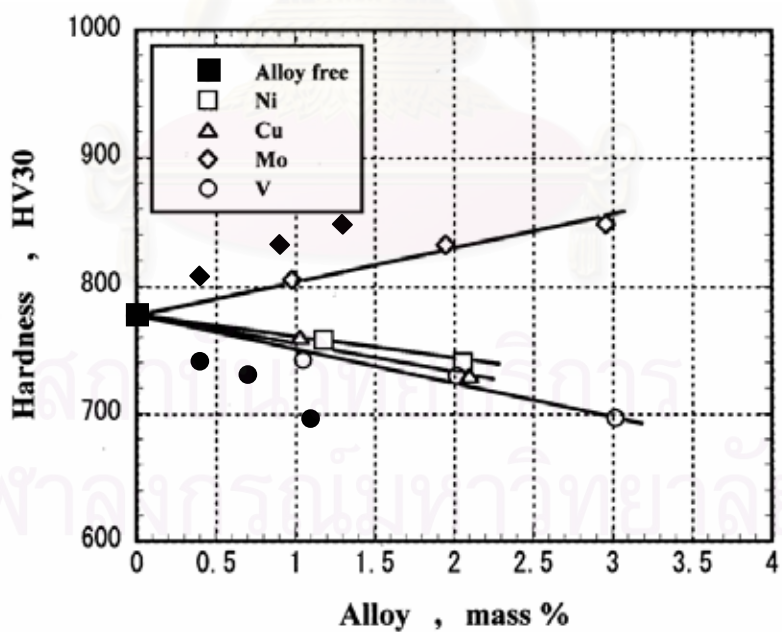26% Cr specimens in as-hardened state. (Austenitized at 1273 K)

Fig. 5.28 Effect of alloying elements on macro-hardness of hypoeutectic
26% Cr specimens in as-hardened state. (Austenitized at 1323 K)

specimens. The effects of Ni and Cu on the increasing rate are also explained by the same reasons. As for the V specimens which shows the smallest increasing rate, it can be explained that since most of retained austenite transform into pearlite and martensite is in small amount, the hardness lowers greatly. Also in 26% Cr specimens, the effect of alloying elements on the increasing rate of the hardness, in other words, the order of alloying element does not change by the austenitizing temperature.

In stead of alloy content of specimens, the alloy concentration in austenite is calculated for Mo and V from its partition coefficient (K_x^γ) and the relation of the hardness vs. alloy content in austenite is displayed by solid symbols in each figure. In the relationship between the hardness and the alloy content in austenite, the increasing rates for Mo and V are increased in 16% Cr specimens but in 26% Cr specimens, that for Mo is increased whereas that for V is decreased. The order of the increasing rate for each alloying element was found to be same.

It is clarified from the results that the hardness is decreased with an increase in Ni content regardless of the austenitizing temperatures. Cu shows same effect except for the 16% Cr specimen austenitized at 1273 K. An addition of Mo leads to an increase in the hardness in all specimens. As V content increases, the hardness rises in 16% Cr specimens but unexpectedly reduces in 26% Cr specimens. The highest hardness is obtained in the 16% Cr specimen containing V and 26% Cr specimen with Mo.

5.3.1.2 Effects of alloying elements on Vγ

Effects of Ni, Cu, Mo and V on the Vγ of the specimens hardnened from 1273 K and 1323 K are shown in Fig. 5.29 and Fig. 5.30 for 16% Cr and Fig. 5.31 and Fig. 5.32 for 26% Cr specimens, respectively.

In 16% Cr specimens, the Vγ increases in proportion to Ni, Cu and Mo contents but gradually decreases with an increase in V content. The

increasing rates are summarized in Table 5.2. The absolute values of Vγ are much greater in 1323 K austenitization. The increasing rate by Ni is largest followed by the order of Cu, Mo and V. As the austenitizing temperature is increased, the increasing rates for Ni, Cu and Mo increased and that of V is decreased.

The increasing rates of Vγ by alloying elements for 26% Cr specimens are shown in Table 5.3. From Fig. 5.31 for 1273 K and Fig 5.32 for 1323 K austenitization, it is found that the Vγ values are much lower but the relation of Vγ vs. alloy content is similar to the case of 16% Cr specimens. However, the orders of increasing rates are Mo→Ni →Cu→V in 1273 K, and Ni→Mo→Cu→V in 1323 K austenitization, respectively.

When an element is added as a third alloy to a certain steel, the amount of the element that dissolves in austenite held at austenitizing temperature participate the transformation according to its amount. In the case of steel, the effect of alloying elements on Ms temperature has been expressed by the nest equation supposing that all the alloying element has dissolved in matrix. [36]

$$Ms\ (^{o}C) = 550 - 350 \times \%C - 35 \times \%V - 20 \times \%Cr - 17 \times \%Ni$$
$$-10 \times \%Cu - 10 \times \%Mo \qquad\qquad (5.3)$$

In the alloying elements added in this experiment, V is largest in the lowering rate of Ms temperature followed by Ni, Cu and Mo. When it is considered that this lowering rate should correspond to the increasing rate of Vγ, Ni and Cu agree well even in high chromium cast iron. This is because both elements dissolve almost all in the matrix of austenite. However, the behavior of Mo and V is quite different from that in the case of steel. This reason can be explained as follows.

Since Mo and V are strong carbide forming elements, both prefer to dissolve in their eutectic carbides during solidification. The rest of elements consumed in carbide formation dissolve in austenite and it participates the solid state transformation and affects Ms temperature.

Table 5.2 Increasing rate of Vγ by alloying element in 16% Cr cast irons.

Alloying element	Increasing rate (% / alloy)	
	1273 K austenitization	1323 K austenitization
Ni	7.8	12.6
Cu	6.0	9.1
Mo	3.4	6.6
V	-3.3	-5.7

Table 5.3 Increasing rate of Vγ by alloying element in 26% Cr cast irons.

Alloying element	Increasing rate (% / alloy)	
	1273 K austenitization	1323 K austenitization
Ni	1.2	5.2
Cu	0.2	-1.1
Mo	3.3	2.7
V	-0.7	-2.8

Fig. 5.29 Effect of alloying elements on the volume fraction of retained austenite (Vγ) of hypoeutectic 16% Cr specimens in as-hardened state. (Austenitized at 1273 K)

Fig. 5.30 Effect of alloying elements on the volume fraction of retained austenite (Vγ) of hypoeutectic 16% Cr specimens in as-hardened state. (Austenitized at 1323 K)

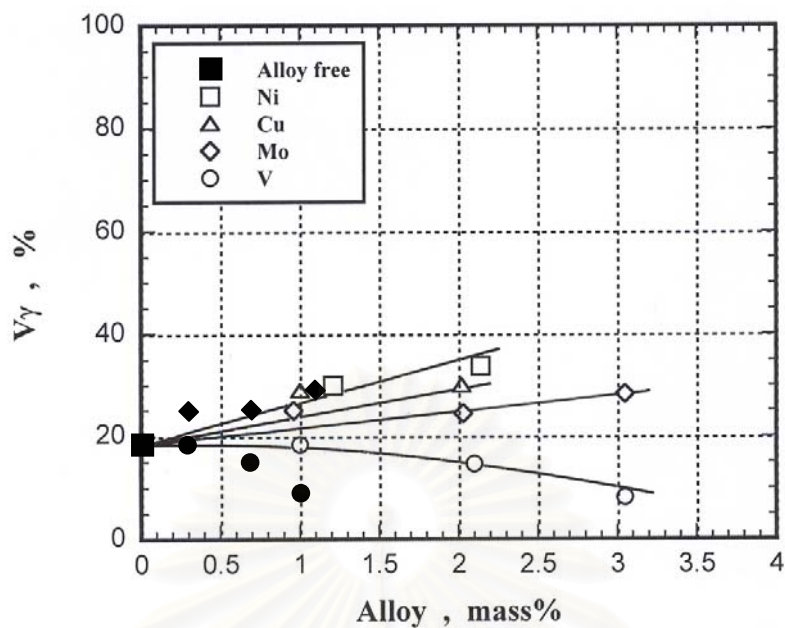Fig. 5.31 Effect of alloying elements on the volume fraction of retained austenite (Vγ) of hypoeutectic 26% Cr specimens in as-hardened state. (Austenitized at 1273 K)

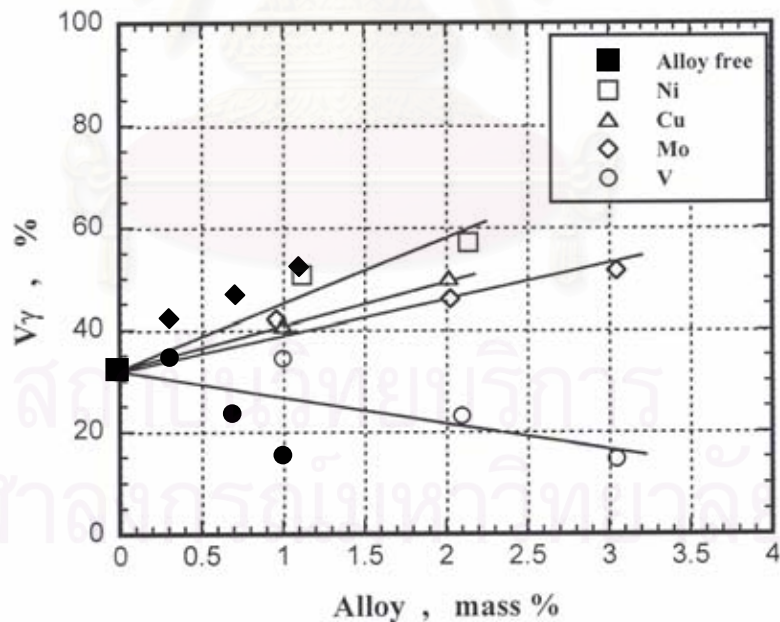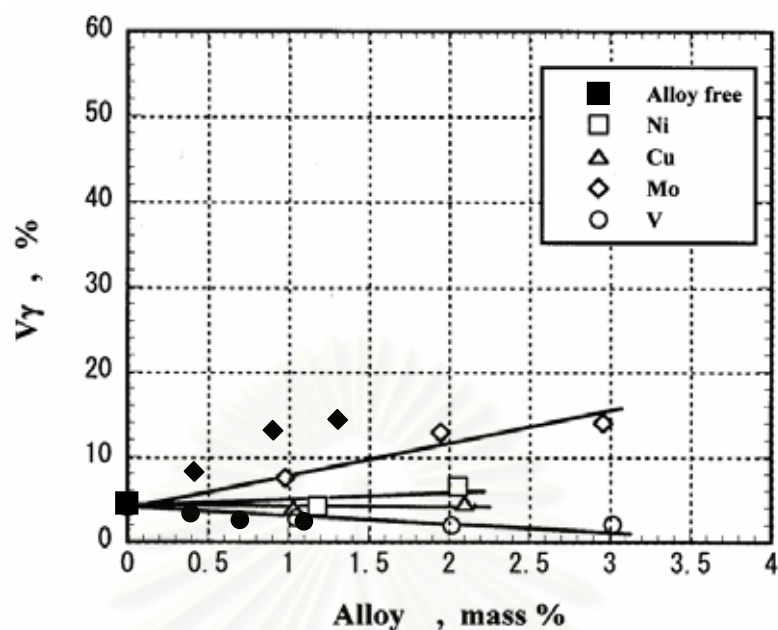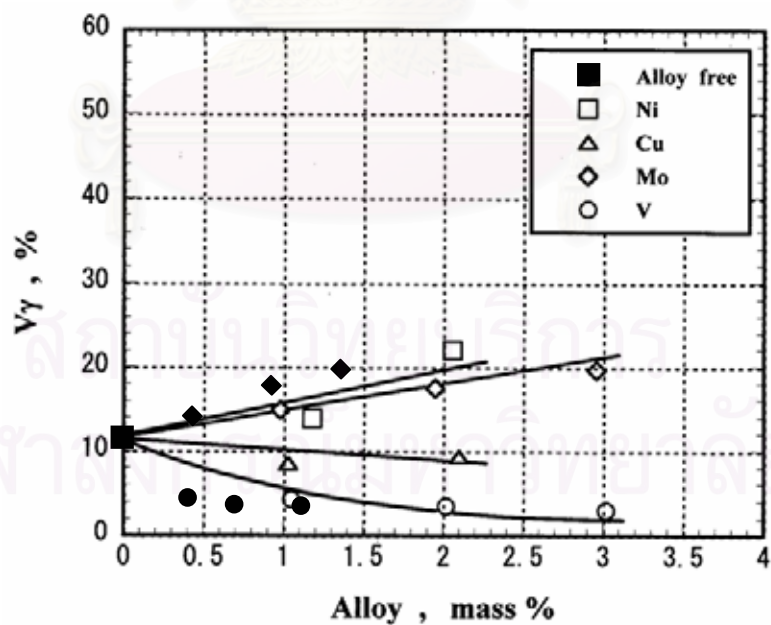Fig. 5.32 Effect of alloying elements on the volume fraction of retained austenite (Vγ) of hypoeutectic 26% Cr specimens in as-hardened state. (Austenitized at 1323 K)

The amount of dissolution of element in the matrix or austenite is determined by the partition coefficient (k_x^γ). The k_{Mo}^γ is 0.36 for 15% Cr and 0.45 for 30% Cr cast irons, and k_V^γ is 0.32 for 15% Cr and 0.35 for 30% Cr cast irons.[37] The k_{Mo}^γ values are larger than k_V^γ values regardless of Cr content of cast iron, and the k_{Mo}^γ and k_V^γ are higher in the cast irons with high Cr content.

Here, the alloy concentration in austenite were obtained by using the partition coefficient to austenite of Mo and V, and then the relationship between Vγ and Mo and V concentration in austenite were illustrated in the figures from 5.29 to 5.32 by solid symbols. The increasing degree of Vγ in the case of relationship between Vγ and alloy percent in austenite are summarized in Table 5.4.

When the alloy content in austenite is taken into account, it is clear that the increasing degree of Vγ becomes smaller in order of Mo, Ni, Cu, V regardless of Cr content in the specimen and the austenitizing temperature. This order is different from the order of the lowering degree in Ms temperature, that is, V, Ni, Cu, Mo. Moreover, Mo increases the Vγ whereas V decreases it reversely. This reason can be considered as follows.

Table 5.4 Order of increasing degree of Vγ per alloying element.

Specimen	Austenitization (K)	Alloy content in specimen	Alloy content in austenite
16% Cr	1273	Ni→Cu→Mo→V	Mo (Ni)→Cu→V
	1323	Ni→Cu→Mo→V	Mo→Ni→Cu→V
26% Cr	1273	Mo→Ni→Cu→V	Mo→Ni→Cu→V
	1323	Ni→Mo→Cu→V	Mo→Ni→Cu→V

Both of Mo and V are strong carbide formers but the ability of V is much larger than that of Mo. Therefore, V can form its carbide even in the austenite and simultaneously C concentration in austenite is decreased greatly. This causes the rise of Ms temperature and makes the Vγ decrease.

5.3.2 Tempered state

It was found that in as-hardened state, the hardness was related to the Vγ. Therefore, the tempered hardness must be also influenced by the Vγ existing in as-hardened state and being still left after tempering. The relationship between the macro-hardness and Vγ value in tempered state is shown in Fig. 5.33 for 1273 K and Fig. 5.34 for 1323 K austenitization.

The tempered hardness decrease after maximum values which are 5% to 15% Vγ in the case of 1273 K and 10% to 20% Vγ in 1323 K austenitization, regardless of the kind and amount of third alloying element. In 1273 K austenitization, there is no difference in the decreasing rate of hardness between chromium content of the specimens. In 1323 K austenitization, the decreasing tendency is separated into two groups, 16% Cr and 26% Cr specimens but the decreasing rates are almost same. At the same Vγ value, the hardness of 16 %Cr specimens is higher than that of 26 % Cr specimens.

In the case of both austenitizing temperatures, the hardness of the specimens free of Vγ ranges widely from 420 HV30 to 800 HV30 and it seems to be lower in the specimens with 26% Cr. The high hardness are in the case that the retained austenite was fully transformed into martensite and the low hardness are in the case that the specimens were over-tempered. Therefore, the large difference in hardness at 0% Vγ is due to the difference of the kind, size and amount of precipitated carbides in addition to the matrix structure. The specimens distributed with exceptionally high hardness contain Mo and there some molybdenum carbides could precipitate secondarily in the matrix.

Here, the H_{Tmax} was connected to the Vγ in as-hardened state and it
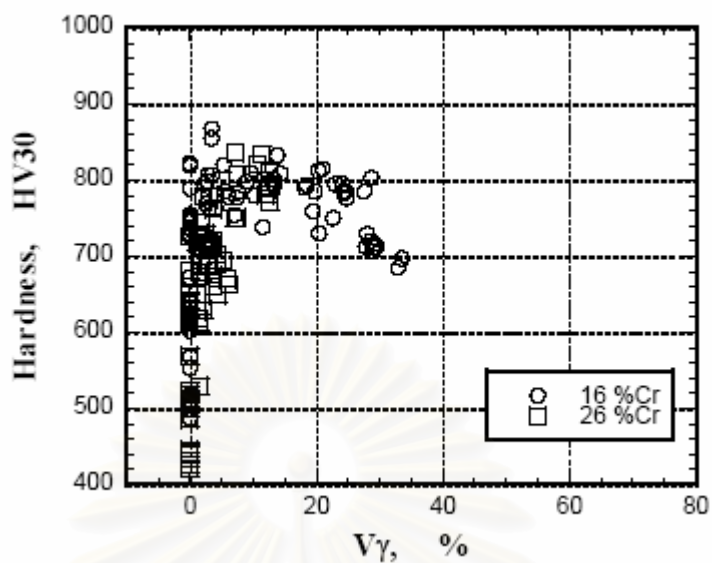
Fig. 5.33 Relationship between macro-hardness and volume fraction of retained austenite ($V\gamma$) of tempered hypoeutectic specimens with alloying elements. (Austenitized at 1273 K)
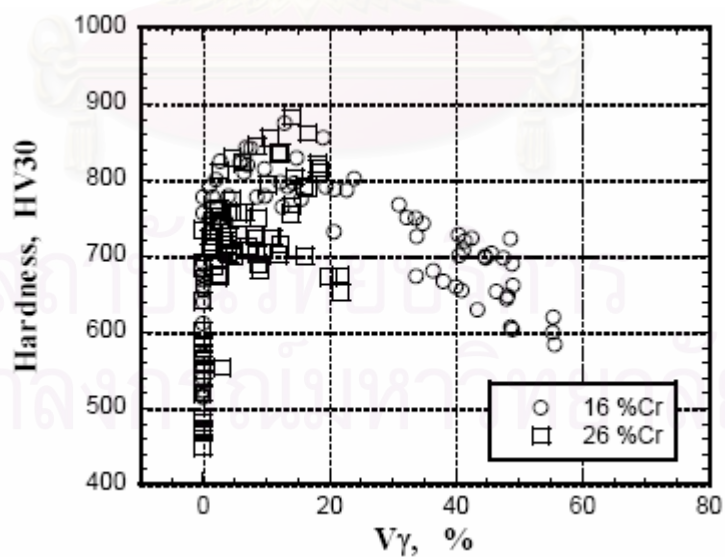

Fig. 5.34 Relationship between macro-hardness and volume fraction of retained austenite ($V\gamma$) of tempered hypoeutectic specimens with alloying elements. (Austenitized at 1323 K)

is shown in Fig. 5.35 for 16% Cr and Fig. 5.36 for 26% Cr specimens. In 16 % specimens, even when the $V\gamma$ increases, the H_{Tmax} does not change in the specimens with Ni and Cu but it increases in the Mo and V specimens. In 26% Cr specimens, the H_{Tmax} of Cu, Mo and V specimens increase with an increase in the $V\gamma$ whereas Ni specimen varies little. The H_{Tmax} of V specimens increases in the small range of $V\gamma$ from 2% to 5%. This reason may be that V in austenite, even it is a small amount, can promote its secondary carbides and this contributes to the increase of hardness much more. As shown in Fig. 5.36, the H_{Tmax} of 26% Cr specimens with Cu rises in the range less than 10% $V\gamma$. In this range, the hardness could be increased by not only the decrease in $V\gamma$ but also by the precipitated carbides formed from martensite during tempering. Over 10% $V\gamma$, the effect of $V\gamma$ on the H_{Tmax} is same significant in the specimens with Mo and V. This is due to an increase in amount of the precipitated special carbides and martensite transformed from destabilized austenite as the $V\gamma$ in as-hardened state increases.

The effects of alloying elements on H_{Tmax} in 16% Cr specimens are shown in Fig. 5.37 for 1273 K and Fig. 5.38 for 1323 K austenitization. The relations of H_{Tmax} vs. Mo and V contents in the austenite are also plotted in both of figures. At the same alloy content, the H_{Tmax} value of each alloy specimen does not make much difference by the austenitizing temperature. The H_{Tmax} increases remarkably as Mo content rises and it keeps constant at a little high hardness to an increase in V content. In 26% Cr specimens shown by Fig. 5.39 and Fig. 5.40, it is same manner as the 16% Cr specimens that Mo increases the H_{Tmax} in both the austenitizing temperatures. However, it is different manner from the 16% Cr specimens that V decreases the H_{Tmax}. This behavior can be seen more clearly when V contents in the austenite are plotted. It is also similar manner to the 16% Cr specimens that Ni, Cu and V make the H_{Tmax} decrease slightly. However, the degree of decrease for Ni and V are more than that for Cu.

When the degree of an increase in the H_{Tmax} shown by the order of a large figure, it is Mo, V, Cu and Ni irrespectively of the austenitizing

temperature. Here, Cu and Ni decrease the H_{Tmax}. In 26% Cr specimens, on the other hand, the degree decreases by the order of Mo, Cu, Ni, V in the case of 1273 K and Mo, Cu, V, Ni in 1323 K austenitization, respectively. However, the difference in the degree among Cu, Ni and V sense is made clearer because the solubility of each element in austenite is expanded by elevating the austenitizing temperature.

The highest values of H_{Tmax}, 875 HV30 in 16% Cr and 885 HV30 in 26% Cr specimens, were obtained in the cast irons with 3% Mo. It is because the large amount of retained austenite in as-hardened state contributed greatly to the secondary precipitation of molybdenum carbides with extremely high hardness than chromium carbides, and as a result, the matrix hardness is much more increased. Ni and Cu do not contribute to the increase of H_{Tmax}, and therefore, such elements should be added for the improvement of hardenability. In spite of the fact that V is strong carbide former and the vanadium carbide has higher hardness than molybdenum carbide, the high hardness could not be obtained by the addition of V in the heat treatment, and that V rather lowered the H_{Tmax} in 26% Cr specimens. As an increase of Cr content raises the eutectoid temperature and decreases the solubility of C and V [23], and that V promotes pearlite transformation.[11] Consequently, the cast iron with V produces less retained austenite in as-hardened state.

In order to make V display its full effect on an increase in hardness, much higher austenitizing temperature must be taken for a great degree of V dissolution in the austenite.
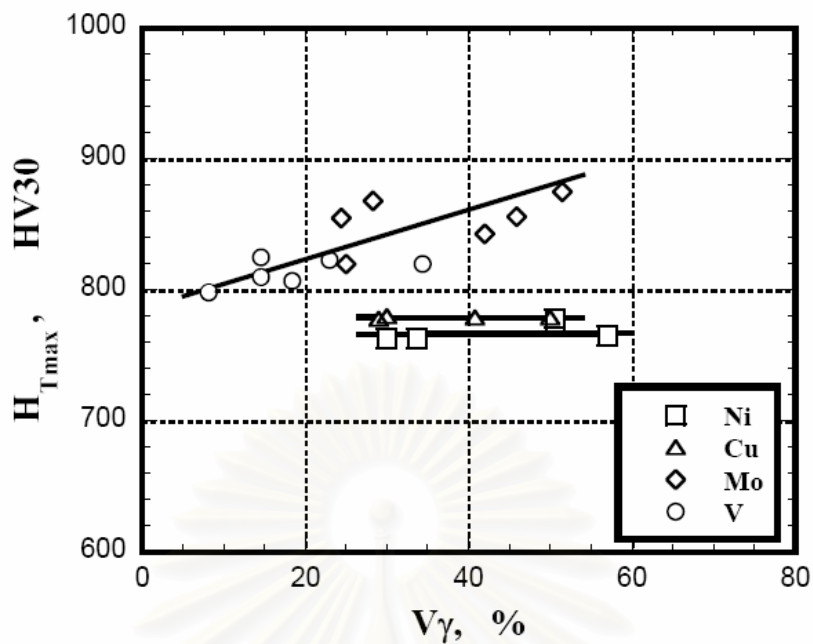
Fig. 5.35 Relationship between maximum tempered hardness (H_{Tmax}) and volume fraction of retained austenite ($V\gamma$) in the as-hardened state for hypoeutectic 16% Cr specimens with alloying elements.
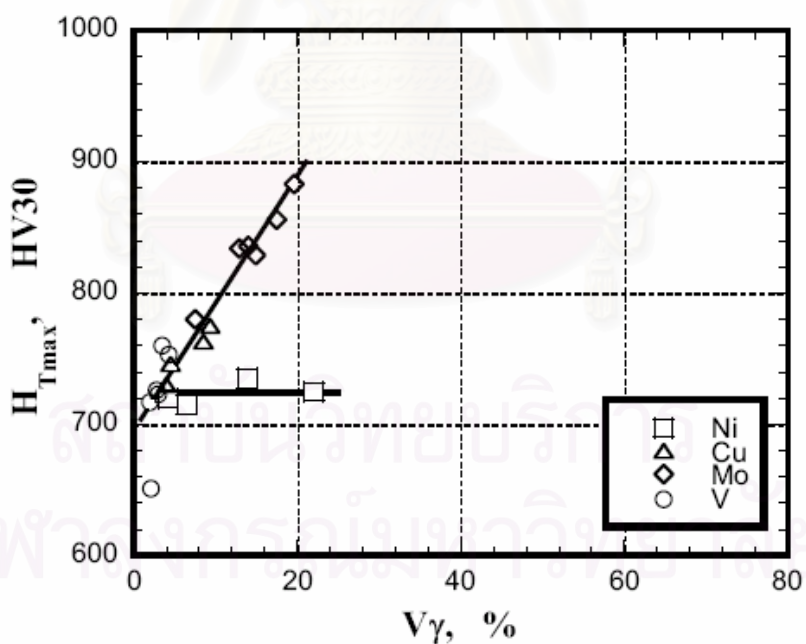
Fig. 5.36 Relationship between maximum tempered hardness (H_{Tmax}) and volume fraction of retained austenite ($V\gamma$) in the as-hardened state for hypoeutectic 26% Cr specimens with alloying elements.
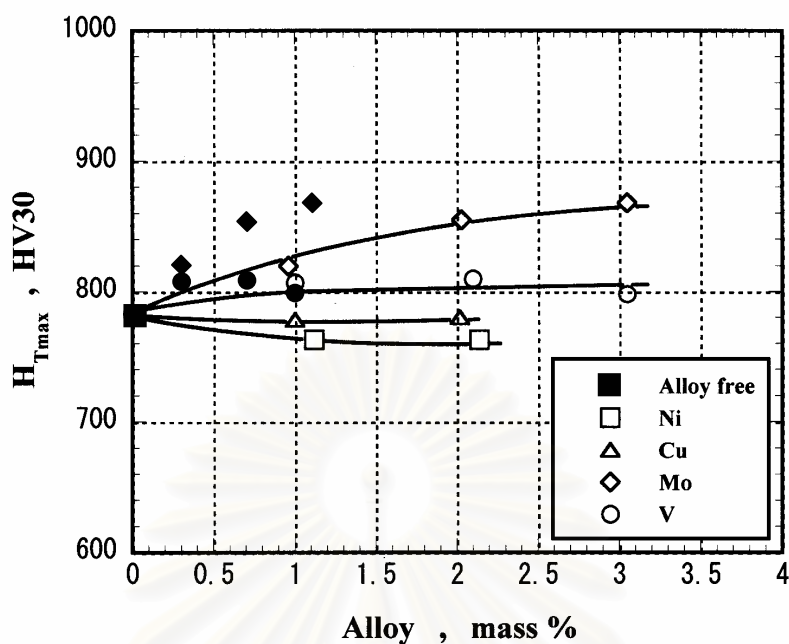
Fig. 5.37 Effects of alloying elements on maximum tempered hardness (H_{Tmax}) of hypoeutectic 16% Cr specimens with alloying elements. (Austenitized at 1273 K)
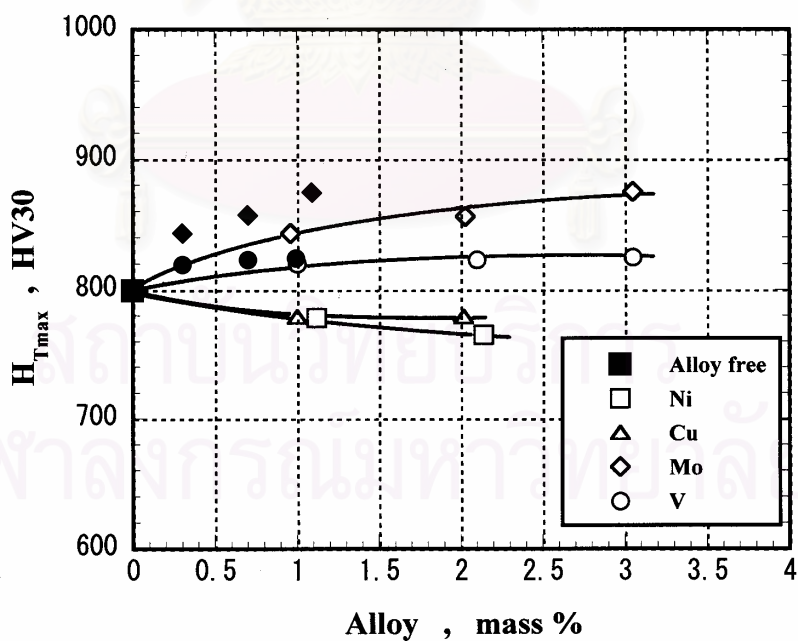
Fig. 5.38 Effects of alloying elements on maximum tempered hardness (H_{Tmax}) of hypoeutectic 16% Cr specimens with alloying elements. (Austenitized at 1323 K)
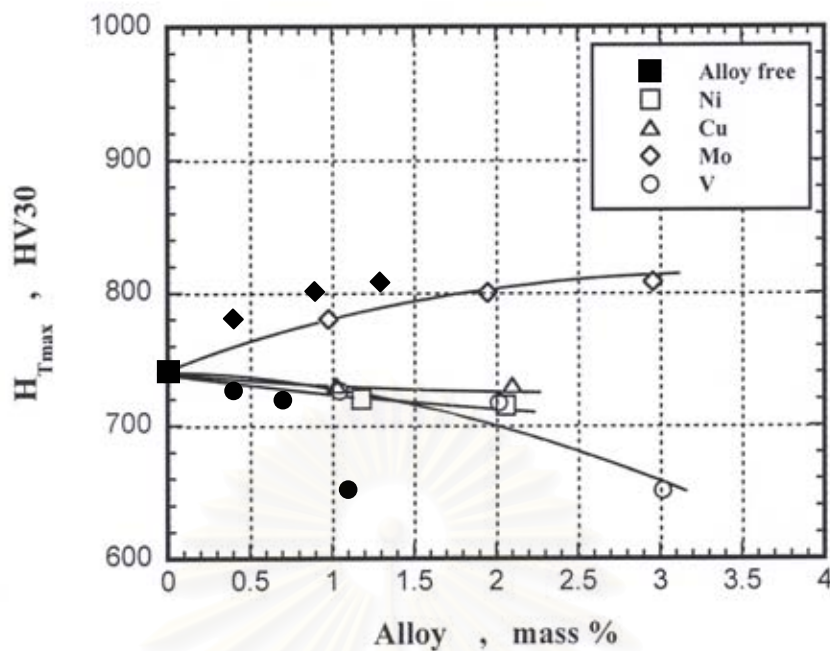
Fig. 5.39 Effects of alloying elements on maximum tempered hardness (H_{Tmax}) of hypoeutectic 26% Cr specimens with alloying elements. (Austenitized at 1273 K)
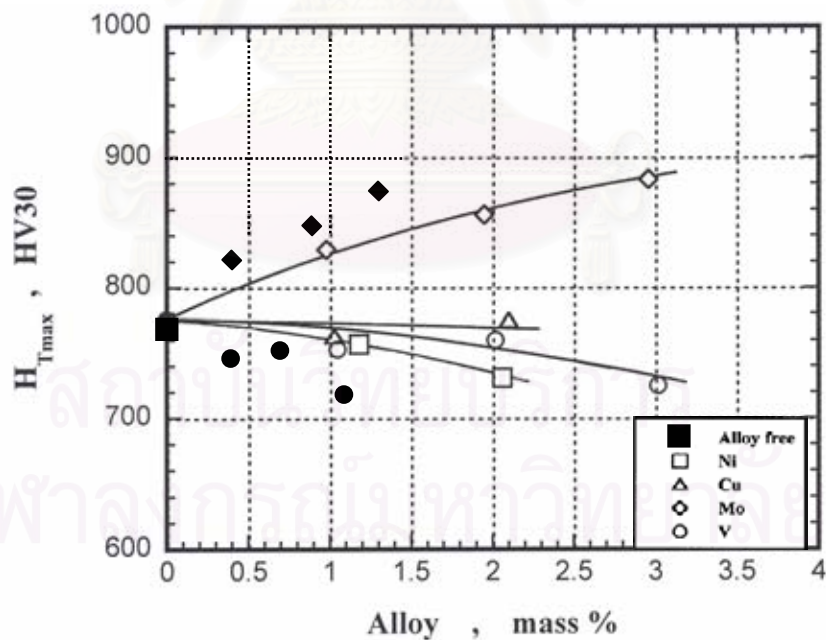
Fig. 5.40 Effects of alloying elements on maximum tempered hardness (H_{Tmax}) of hypoeutectic 26% Cr specimens with alloying elements. (Austenitized at 1323 K)

5.4 Mechanism of Secondary Hardening

Though high chromium cast iron is sometimes applied in as-cast or as-hardened conditions, it is generally used in hardened and tempered states so that the necessary hardness and toughness can be given to the cast iron.

The solidified microstructure of high chromium cast iron consists of primary and/or eutectic carbide and matrix. The macro-hardness is the total sum of their hardness that may be obtained using the composite law. As for the micro-hardness of main M_7C_3 carbide in high chromium cast iron, there is a relationship between the micro-hardness and Cr concentration in the carbide and it is expressed by the following equation; [38]

Hardness of M_7C_3 Carbide (HV0.15) = 7.03 x % Cr in M_7C_3 carbide

$$+1288.9 \qquad (R= 0.998) \qquad (5.4)$$

Since the micro-hardness of carbide itself increases in proportion to Cr concentration in carbide, it is considered that the macro-hardness must be increased if the Cr content in cast iron increases. However, the macro-hardness does not always correspond to the Cr content in the specimen. In this experiment, the macro-hardness were often lower in the specimens with high Cr content. This tells that the matrix structure affects greatly the macro-hardness. From this point of view, it is considered that the variation of macro-hardness should be connected to the transformation of matrix. In this section, therefore, the mechanism of the secondary hardening near the maximum tempered hardness (H_{Tmax}) is discussed.

In this experimental results, it seems that the retained austenite has been closely related to the hardness in hardened and tempered states, and besides the behavior of secondary hardening.

The secondary hardening in tempering is considered to occur by the following reactions;

(1) Precipitation of secondary carbides from martensite.

(2) Precipitation of carbides from retained austenite in as-hardened state.

(3) Transformation of retained austenite destabilized by tempering into martensite.

Each reaction acts the part of an increase in hardness. However, the increasing degree of hardness could be greater in the reactions (1) and (3), but the effect of reaction (2) is maybe small.

Here, the discussion is focused on the mechanism of the secondary hardening from the viewpoints of the reactions (1) and (3) using 16% Cr specimens containing much more $V\gamma$ in as-hardened state. The degree of secondary hardening (ΔH_D, HV30) is introduced as a parameter defined as the difference between the highest hardness (H_{Tmax}) and the hardness at which the tempered hardness curve begins to rise. Fig. 5.41 shows the effect of $V\gamma$ in as-hardened state on the ΔH_D. It can be understood that the ΔH_D is closely related to the $V\gamma$ and it increases in proportion to the $V\gamma$. When the regression analysis is carried out, the relationship is expressed by the following equation;

$$\Delta H_D \text{ (HV30)} = 3.86 \text{ x } \% V\gamma - 38.69 \quad (R = 0.96) \tag{5.5}$$

The data of hypoeutectic specimens displayed by solid circles were picked up because they have larger portion of matrix where the effect of precipitation hardening can be caused and seen remarkably. It has been clarified from all the experiments that the $V\gamma$ is determined by not only C and Cr contents but also the kind and the amount of third alloying element and the austenitizing temperature. It is said from Fig. 5.41 that the more $V\gamma$ in as-hardened state contributed more to the secondary hardening.

Here, the relationship between ΔH_D and H_{Tmax} was obtained and it is shown in Fig. 5.42. Even if the ΔH_D varies, the H_{Tmax} values in the alloy-free, Ni and Cu specimens do not make much difference ranging

from 770 HV30 to 790 HV30. The Δ H_D values in the V specimens also do not change but the H_{Tmax} values are in higher position than those in the alloy-free, Ni and Cu specimens. However, the H_{Tmax} values of Mo specimens increases proportionally with an increase in the ΔH_D. The reason why Ni and Cu did not show a significant effect on H_{Tmax} can be explained as follows;

The H_{Tmax} of these specimens are obtained mainly due to the reaction (1) and (3). As for reaction (1), since Ni and Cu do not form their special carbides, the tempering behaviors of Ni and Cu specimens must be same as that in alloy-free specimen, that is, the precipitation of chromium carbides ($M_{23}C_6$ and/or M_7C_3) could contribute to the secondary hardening. Biss [20] reported that $M_{23}C_6$ carbides were produced in the tempering of 17% to 20% Cr cast irons at 723 K to 823 K. Here, the hardness and Vγ value at which the tempered hardness begins to increase must be paid attention. The hardness and the Vγ values are 640 HV30 and 45% Vγ in 1% Ni, 580 HV30 and 55% Vγ in 2% Ni specimens, and 650 HV30 and 42% Vγ in 1% Cu and 590 HV30 and 50% Vγ in 2% Cu specimens, respectively. Even if the specimens with more Vγ in as-hardened state have larger ΔH_D, the H_{Tmax} values did not show dominant difference because the hardness at the datum points are lower when the ΔH_D is greater.

In the case of Mo and V specimens, the higher H_{Tmax} are obtained. It is considered that the hardness were increased due to the precipitation of special carbides from martensite by tempering or carbide reaction at high temperature, which are molybdenum M_6C carbide (~1650 HV) in Mo specimen and vanadium MC carbide (2500 - 3000 HV) in V specimen in addition to the precipitation of chromium $M_{23}C_6$ carbide (1000 - 1520 HV).[39] The martensite transformed from destabilized retained austenite also raised the hardness in the same manner as alloy-free specimen. Therefore, the increase in H_{Tmax} of Mo specimen must be due to the precipitation of special molybdenum carbides.
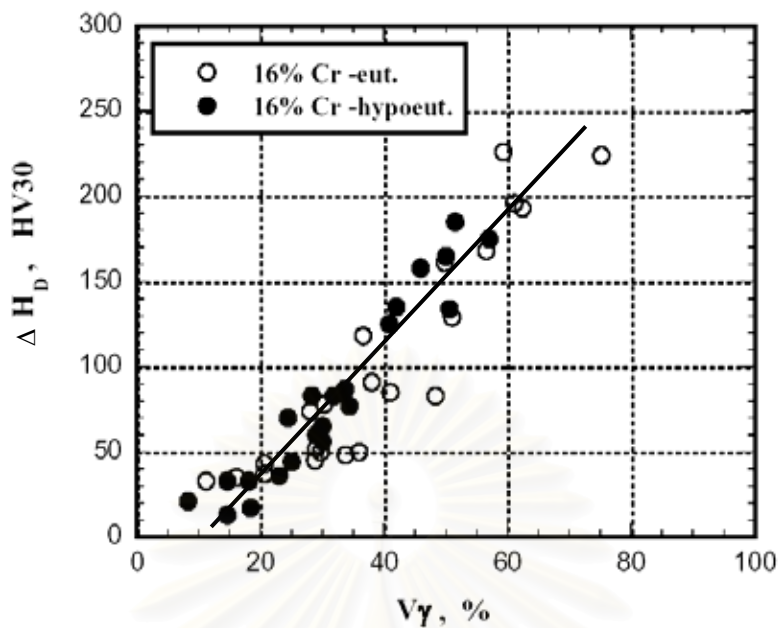
In the case of V specimens, the hardness and Vγ at which the

Fig. 5.41 Effect of Vγ in as-hardened state on the degree of the secondary hardening (Δ H_D) in 16% Cr cast irons with alloying element.
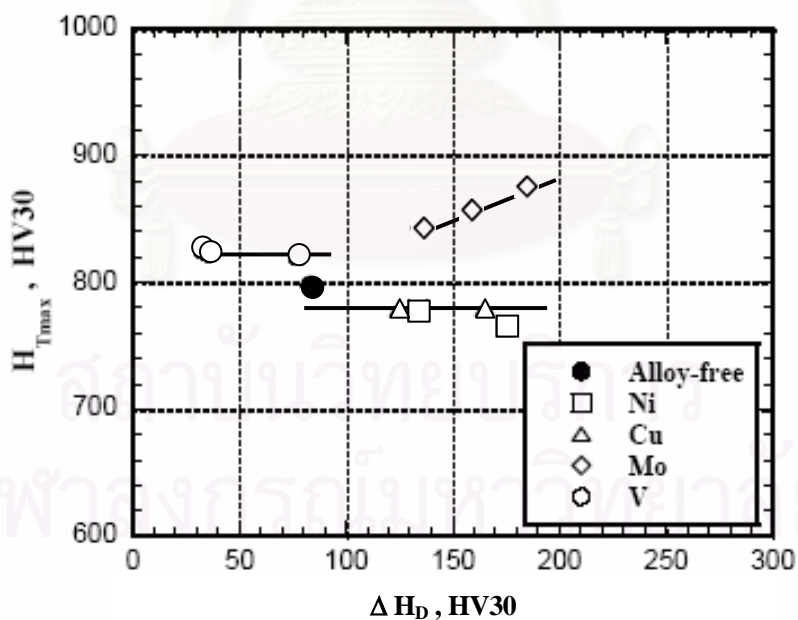

Fig. 5.42 Relationship between H_{Tmax} and Δ H_D of 16% Cr cast irons with alloying element. (1323 K austenitization)

secondary hardening starts are 740 HV30 and 35% Vγ in 1% V, 790 HV30 and 21% Vγ in 2% V and 795 HV30 and 15% Vγ in 3% V specimens, respectively. Jacudine [40] reported that 2% V added to 17% Cr cast iron mostly dissolved into eutectic carbides, and the hardness of eutectic carbide was increased. This suggests that even a small amount of V can dissolve into chromium carbide and increase the hardness and that the H$_{Tmax}$ of specimens used in this experiment should increase with increasing V content. As V dissolves into carbides preferentially, the dissolution of V in the austenite is decreased and inevitably V content in martensite is reduced. As a result, a small amount of V carbide precipitates from martensite.

Even if the ΔH$_D$ is increased by V addition, the hardness of martensite itself transformed from destabilized retained austenite is low because C content is reduced by increasing V content. Resultantly, these factors of an increase and a decrease in hardness are considered to be compensated.

Fig. 5.43 shows the effect of Vγ in as-hardened state on the H$_{Tmax}$. This diagram is similar to that in Fig. 5.42. The H$_{Tmax}$ values do not change in Ni, Cu and V specimens but it increases gradually in Mo specimens as the Vγ increases. These reasons are mostly same as the discussions described up to now.

Another discussion can be proposed for the effect of Vγ on the secondary hardening. Since the Vγ at the H$_{Tmax}$ is shown in the diagram for tempering, the amount of austenite reduced by tempering, which is the difference between the Vγ in as-hardened state and that at the H$_{Tmax}$. Supposing that the amount of the difference is consumed for the precipitation of carbide (Vcp) and the transformation of martensite (M), the (Vcp+M) value can be also connected to the secondary hardening. The relationship between the maximum micro-hardness of matrix and (Vcp+M) of 16% Cr hypoeutectic specimens is shown in Fig. 5.44. This relation is similar to that of the Vγ vs. the macro-hardness in as-hardened state of plain high chromium specimens (Fig. 5.3). These results support

that the Vγ controlled the matrix hardness which in turn contributed the macro-hardness of specimen.

From the discussions mentioned above, it is clear that the austenite plays very important role in the heat treatment. Austenite dissolving alloying elements makes their carbides precipitate during austenitization and the retained austenite transforms into martensite. Both of them took an active part in increasing the hardness. In order to get higher H$_{Tmax}$, high Vγ value in as-hardened state is required, especially, in Mo specimens.

Here, it can be concluded that the alloying element which shows highest effect on the H$_{Tmax}$ is Mo followed by V. In order to get the high hardness after tempering, the high Vγ value in as-hardened state is necessary to increase the secondary hardening, say, by employing high austenitizing temperature like 1323 K. In the case of Ni and Cu, they do not show dominant effect on the H$_{Tmax}$, and therefore, such alloying elements should be added to improve the hardenability.

It is presumed that the secondary hardening of 26% Cr cast iron can be caused by the similar mechanism to the case of 16% Cr cast iron even if the Vγ value is less.

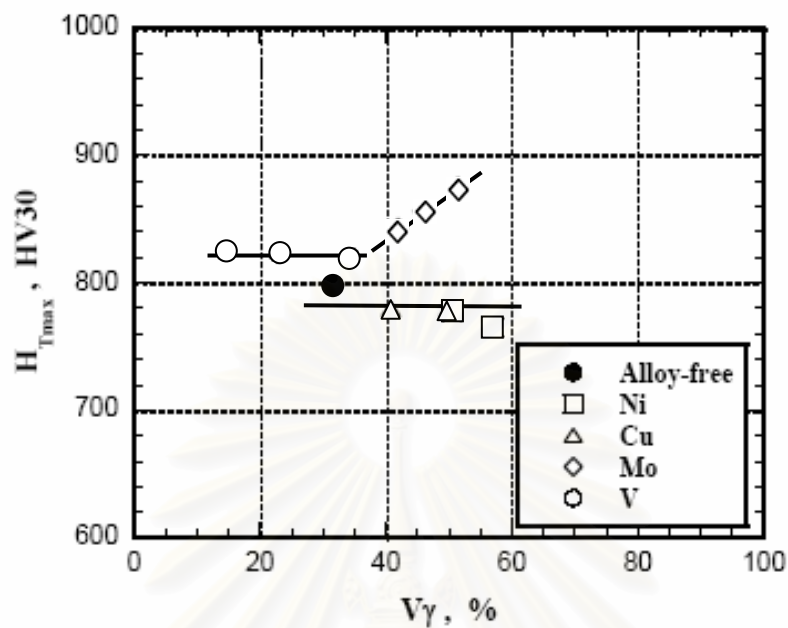Fig. 5.43 Effect Vγ in as-hardened state on H_{Tmax} of 16% Cr cast irons
with alloying element. (1323 K austenitization)
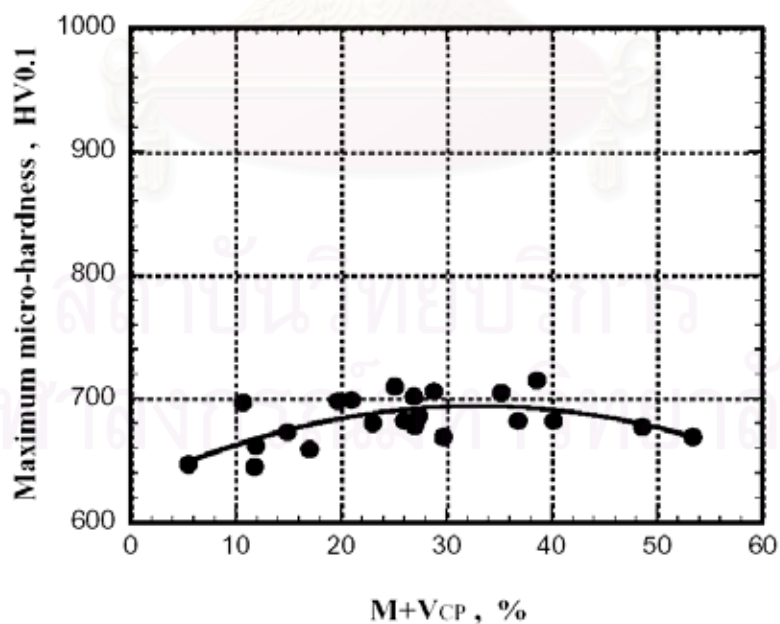
Fig. 5.44 Effect of M+Vcp on maximum micro-hardness of 16%
Cr cast irons with alloying element.

CHAPTER VI

CONCLUSIONS

The heat treatment behavior of plain high chromium cast irons containing 10% Cr, 16% Cr, 20% Cr and 26% Cr, and 16% Cr and 26% Cr cast irons with single addition of Ni, Cu, Mo and V were systematically investigated. After annealing, the alloys were hardened and tempered, and the effects of heat treatment condition and chemical composition on the hardness and volume fraction of retained austenite (Vγ) were clarified. The following conclusions have been drawn from the experimental results and discussions.

As-hardened State

< Macro-hardness >

(1) The macro-hardness and Vγ change widely depending on the combination of C and Cr contents and the kind and the amount of third alloying element.

(2) In a family of the alloy-free cast irons or plain high chromium cast irons with same Cr contents, however, the macro-hardness does not change much even when C content varies within the range of chemical composition in this experiment, and so the clear relationship between macro-hardness and C content is not discovered.

(3) In alloy-free cast irons, the hardness decreases as the Cr/C value increases up to about 4.0. Over 4.0, the hardness rises to the maximum value of 800 HV30 at about Cr/C value of 7.0 and then decreases with an increase in Cr/C value.

(4) In alloyed cast irons, the hardness is changed remarkably by Vγ which is generated depending on the kind and the amount of alloying element.

(5) In alloyed cast irons, the hardness does not increase with an increase in Ni or Cu content, but addition of Mo increases the hardness in both

the 16% and 26% Cr cast irons. V increases the hardness in 16 % Cr iron but reduces it in 26 % Cr iron. This is because the matrix of 16% Cr cast iron consists of large portion of martensite and some retained austenite but that in 26% Cr cast iron consists of pearlite, some martensite and small amount of retained austenite.

(6) When the austenitizing temperature increases, the hardness does not change so much in alloy-free cast iron. In alloyed cast irons, on the other hand, the hardness decreases in 16% Cr cast irons and increases in 26% Cr cast irons regardless of the kind and the amount of alloying element.

(7) In alloyed cast irons, the highest hardness is obtained in the iron with V in 16% Cr cast irons and that with Mo in 26% Cr cast irons. The lowest hardness is obtained in the cast iron with Ni except for hypoeutectic 26% Cr cast irons in which the lowest hardness is obtained by V addition.

(8) The largest increasing rate of hardness is obtained by V followed by Mo, Cu and Ni in 16% Cr cast irons. In 26% Cr cast irons, it is obtained by Mo followed by Cu, V and Ni in eutectic cast irons, and in hypoeutectic cast irons it is by Mo followed by Ni, Cu and V regardless of austenitizing temperature.

< Retained austenite ($V\gamma$) >

(9) In alloy-free cast irons, the $V\gamma$ is always more at the same C content when the austenitizing temperature is 1323 K.

(10) In alloy-free cast irons, the $V\gamma$ increases gradually as the Cr/C value increases to 4.0, and after that the $V\gamma$ decreases roughly in proportion to the Cr/C value.

(11) In alloyed cast irons, the $V\gamma$ increases with an increase in alloying element except for V.

(12) In alloyed cast irons, the largest increasing rate of $V\gamma$ is obtained by Ni followed by the order of Cu, Mo and V in 16% Cr cast irons regardless of austenitizing temperature. In 26% Cr cast irons, the

order of increasing rate is Ni, Mo, Cu and V except for hypoeutectic 26% Cr cast iron austenitized at 1273 K of which order is Mo, Ni, Cu and V.

(13) In alloyed cast irons, an increase in austenitizing temperature increases the Vγ overall.

Tempered State

< Macro-hardness >

(1) In alloy-free cast irons, the tempered macro-hardness curve shows a secondary hardening due to the precipitation of chromium carbides in matrix and the reduction of Vγ.

(2) In alloyed-cast irons, the curve of tempered hardness shows a remarkable secondary hardening due to the precipitation of special carbides formed by carbide forming elements of Mo and V and the transformation of destabilized austenite into martensite.

(3) Micro-hardness of the tempered matrix shows a quite similar behavior to the macro-hardness in all hypoeutectic cast irons.

<Maximum tempered hardness (H_{Tmax})>

(4) The peak of the hardness which is expressed as H_{Tmax} (maximum tempered hardness) is obtained mostly when the cast iron is tempered at 723 K to 730 K in alloy-free cast irons and at 748 K to 823 K in alloyed cast irons.

(5) The H_{Tmax} value is higher in the case of 1323 K austenitization, and the H_{Tmax} appears at higher temperature side as the austenitizing temperature is increased.

(6) Mo increases the H_{Tmax} in both 16% Cr and 26% Cr cast irons. V increases it slightly in 16% Cr cast irons but decreases it in 26% Cr cast irons. Ni and Cu did not show a significant effect on the H_{Tmax} even if they show the high degree of the secondary hardening.

(7) The reason why Ni and Cu do not increase the H_{Tmax} even if they show the high degree of secondary hardening is due to the secondary

carbide that precipitated in the matrix is chromium carbide as same as in alloy-free cast iron. The high H_{Tmax} is obtained in the cast irons with Mo and V because the precipitation of their special carbides increases the hardness much more.

(8) V shows the poor effect on H_{Tmax} in 26% Cr cast irons due to the matrix containing less $V\gamma$ in as-hardened state.

(9) The highest values of H_{Tmax} are obtained in the cast irons containing 3% Mo, 890 HV30 in 16% Cr and 920 HV30 in 26% Cr eutectic cast irons and 875 HV30 in 16% Cr and 885 HV30 in 26% Cr hypoeutectic cast irons, respectively.

< Corelation of $V\gamma$, secondary hardening, hardness and H_{Tmax} >

(10) The degree of secondary hardening is closely related to the $V\gamma$ in as-hardened state, the more $V\gamma$, the more the secondary hardening because more secondary carbides precipitate and more martansites transform from destabilized retained austenite during tempering.

(11) In alloyed cast irons, except for the cast iron containing V, the degrees of secondary hardening are much larger in cast irons with the third alloying element than those in the alloy-free cast irons, and the degree is greater in the order of cast irons with Ni, Cu and Mo. In addition, it is larger in the cast irons hardened from higher austenitizing temperature.

(12) High tempered hardness is obtained in the cast irons with high $V\gamma$ in as-hardened state which is obtained by the addition of some alloying elements and by high austenitizing temperatures.

(13) The tempered hardness decreases in proportion to the $V\gamma$ from the maximum value at 5% to 10 % $V\gamma$ in alloy-free and 10% to 20% $V\gamma$ in alloyed cast irons.

(14) In alloyed cast irons, Cr shows a remarakable effect on the tempered hardness in the case of 1323 K austenitization. The tempered hardness decreases in two ways regarding to Cr content of the cast iron as the $V\gamma$ increases and the decreasing rates are roughly same. At the same

Vγ value, the hardness of 16% Cr cast irons is higher than that in 26% Cr cast irons.

(15) The H_{Tmax} is obtained at certain tempering temperatures at which the Vγ decreases to less than 10% in alloy-free and less than 20% in alloyed cast irons.

(16) In alloy-free cast irons, the H_{Tmax} rises to the highest value of about 800 HV30 as the Vγ in as-hardened state increases up to 20% and over 20% Vγ, it settles at the same hardness as the H_{Tmax}. The cast irons with Vγ values from 20% to 40% in as-hardened state provide the maximum hardness (H_{Tmax}) after tempering.

(17) In alloyed cast irons, the H_{Tmax} closely related to the Vγ in as-hardend state which is also closely related to the kind and the amount of alloying element. The H_{Tmax} values of the cast irons with Mo and V increase with an increase in the Vγ in as-hardend state but they do not change in the cast irons with Ni and Cu.

(18) In alloy-free cast iron, it is found from SEM observations that the specimens of which matrix contains large amount of fine carbides provide the maximum tempered hardness.

(19) In alloy-free cast iron, the reason why the macro-hardness of 16% Cr irons are higher than that of 26% Cr cast iron under the same matrix hardness is considered to be due to the difference in the morphology of eutectic chromium carbides, thicker and more interconnected in 16% Cr, and thinner or finer and discontinouse in 26% Cr cast irons.

<Secondary Hardening>

(1) The macro-hardness is closely related to the matrix hardness depending on the kind and the amount of secondary carbide, amount of martensite and retained austenite in the matrix.

(2) The secondary hardening occurs mainly by the following mechanism,

(a) the precipitation of secondary carbide from martensite at high temperature.

(b) the transformation of destabilized as-hardened retained austenite

into martensite during cooling.

(3) The formation of special molybdenum carbides in the secondary precipitation of Mo cast iron and special vanadium carbides in the secondary precipitation of V cast iron provide the higher hardness than only formation of secondary chromium carbides in alloy-free cast iron.

REFERENCES

1. G.L.F Powell.   Morphology of Eutectic M_3C and M_7C_3 in White Iron Castings.   Metals Forum 3 (1980): 37-46.

2. Y. Matsubara, K. Ogi, and K Matsuda.   Eutectic Solidification of High Chromium Cast Iron-Eutectic Structures and Their Quantitative Analysis.   AFS Transaction 89 (1981): 183-196.

3. S.K. Yu, N. Sasaguri, and Y. Matsubara.   Effect of retained austenite on abrasion wear resistance and hardness of hypoeutectic high Cr white cast iron.   Int. J. Cast Metals Res 11 (1999): 561-566.

4. I.R. Sare, and B.K. Arnold.   The Effect of Heat Treatment on Gouging Abrasion Resistance of Alloy White Cast Iron.   Metallurgical Transactions A 26A (1995): 359-370.

5. Y. Matsubara, et al.   Basic Study on Multi-component White Cast Iron and It Practical Use for Rolling and Pulverizing Mills. Proc.of the International Conference on the Science of casting and solidification, pp. 377-386. Romania, 2001.

6. Y. Matsubara, K. Ogi, and K Matsuda.   Eutectic Structures of High Chromium Cast Iron.   J. JFS 48 (1976): 706-711.

7. K. Ogi, Y. Matsubara, and K. Matsuda. Eutectic Solidification of High Chromium Cast Iron – Mechanism of Eutectic Growth. AFS Trans., 89 (1981): 197-204.

8. K Ogi, K. Nagasawa, Y. Matsubara, and K. Matsuda. Reddistribution of alloying element during eutectic growth of high chromium cast iron. International Colloquium on Wear Resistance Materials-Frame 18 (1983): 1-12.

9. G.Y. Liang, and J.Y. Su.   The Effect of Rare Earth Elements on the Growth of Eutectic Carbides in White Cast Irons Containing Chromium.   Cast Metals 4 (1991): 83-88.

10. O.N. Dogan, J.A. Hawk, and G. Laird II.   Solidification Structure and

Abrasive Resistance of High Chromium White Irons.   <u>Metallurgical Transactions A</u> 28A (1997): 1315-1328.

11. M. Kuwano, et al.   Influence of Destabilization Heat Treatment on Martensitic Transformation of High Chromium Cast Iron.   <u>J. JFS</u> 54 (1982): 586-592.

12. Trope, W.R., and Chicco, B.   The Fe-Rich Corner of the Metastable C-Cr-Fe Liquidus surface.   <u>Metallurgical Transactions A</u> 16A (1981): 11-19.

13. Thong, C.P., Suzuki, T., and Umeda, T.   Eutectic solidification of High-Chromium Cast Irons.   <u>Physical Metallurgy of Cast Iron IV</u>, G.Ohira, T. Kusakawa, E. Niyama, Editors, Materials Research Society, Pittsburgh, PA, (1989): 403-410.

14. Maratray, F.,and Usseglio-Nanot R.   Factors Affecting the structure of Chromium and Chromium-Molybdenum White Irons.   <u>Climax Molybdenum S.A.</u>, Paris, France, (1971): 32.

15. Laird II, G., Microstructure of Ni-hard I, Ni-hard IV and High-Cr White cast irons.   <u>AFS Transactions</u> 99 (1991): 339-357.

16. Rickard, J.   Some Experiments Concerning the As-cast Grain Size in 30% Chromium Cast Irons.   <u>BCIRA Journal</u> 8 (1960): 200-216.

17. Y. Matsubara, K. Ogi, and K. Matsuda.   Influence of Alloying Elements on the eutectic Structures of high Chromium Cast Iron.   <u>J.JFS(IMONO)</u> 51 (1979): 545-550.

18. Maratray, F.,and Poulalion, A.   Austenite Retention in High-Chromium White Iron.   <u>AFS Transactions</u> 90 (1982): 795-804.

19. Andrew, K.W.   Empirical Formulae for the Calculation of Some Transformation Temperatures.   <u>JISI</u> 203 (1988): 678-685.

20. .Biss, V.   unpublished research, Climax Molybdenum Co. (1981).

21. I.R. Sare, and B.K. Arnold.   The Influence of Heat Treatment on the High-Stress Abrasion Resistance and Fracture Toughness of Alloy White Cast Irons.   <u>Metallurgical Transactions A</u> 26A (1995):

1785-1793.

22. Y. Matsubara, unpublished report, Kurume National College of Technology,(1988).

23. W. Khanitnantharak, N. Sasaguri, K. Nanjo, P. Sricharoenchai , and Y. Matsubara.   Heat Treatment Behavior of Low Carbon Multi-component Cast Alloy.   Proceeding of the 7 th Asian Foundry Congress-Taipei, pp. 63-72. Taiwan, 2000.

24. C. Kim.   X-Ray Method of Measuring Retained Austenite in Heat Treat White Cast Irons.   J. Heat treating ASM 1 (1979): 43-51.

25. Y. Matsubara, Y. Yokomizo, N. Sasaguri, and M. Hashimoto.   Effect of Carbon Content and Heat-treating Condition on Retained Austenite and Hardness of Multi-component White Cast Iron.   J. JFS 74 (2000): 471-477.

26. Y. Matsubara, and N. Sasaguri.   Improvement of Toughness of Alloyed White Cast Iron for Wear Resistance by Hot Rolling.   J. JFS 68 (1996): 1099-1105.

27. G.L.F. Powell, and V. Randle.   The Morphology and Microtexture of M_7C_3 in Fe-Cr-C and Fe-Cr-C-Si Alloys of Near Eutectic Composition.   J. Mater.Sci.Lett 29 (1977): 4889-4896.

28. G. laird, and G.L.F. Powell.   Solidification and Solid-state Transformation Mechanisms in Si Alloyed High-Chromium White Cast Irons.   Mat. Trans 24A (1993): 981-988.

29. J. Shen, and Q.D Zhou.   Cast Met 1 (1988): 79.

30. N. Ma, Q. Rao, and Q. Zhou.   AFS Trans 98 (1990): 775.

31. H.Q. Wu, N. Sasaguri, Y. Matsubara, and M. Hashimoto.   Solidification of multialloyed white cast irons.   AFS Trans 104 (1996): 103-108.

32. H.K. Baik, and C.R. Loper Jr.   The influence of niobium on the solidification structure of Fe-C-Cr alloys.   AFS Trans 96 (1988): 405-411.

33. P. Dupin, J. Saverna, and J.M. Schissler.   A structural study of

chromium white cast iron. $\underline{\text{AFS Trans}}$ 90 (1982): 711-718.

34. Jackson, R.S.   The austenite liquidus surface and constitutional diagram for the Fe-Cr-C metastable system. $\underline{\text{JISI}}$ 208 (1970): 163-167.

35. C.P. Tong, T. Suzuki, and T. Umeda.   The influence of chemical composition and destabilization on transformation characteristics of high chromium cast irons. $\underline{\text{J. JFS (Imono)}}$ 62 (1990): 344-351.

36. Netsushori Guide Book, $\underline{\text{The Japan society for Heat Treatment}}$, (2002)

37. Y. Ono, N. Murai, and K. Ogi.   Partition Coefficients of Alloying Elements to Primary Austenite and Eutectic Phases of Chromium Irons for Rolls**.** $\underline{\text{ISIJ}}$ 32 (1992): 1150-1156.

38. Y. Matsubara. $\underline{\text{Heat treatment of high chromium cast iron : Text for seminar for graduate students}}$. Chulalongkorn University Thailand, (2005).

39. G. Laird, R. Gundlace, and Rohing. $\underline{\text{Abrasion-Resistance Cast Iron Handbook.}}$: American Foundry Society, 2000.

40. Arnoldo Bedolla-Jacudine.   Microstructure of vanadium-, niobium,-and titanium-alloyed high-chromium white cast irons. $\underline{\text{Int. J. Cast Metals Res.}}$ 13 (2001): 343-361.

41. Rivlin, V.G..   Critical review of construction of carbon-chromium-iron and carbon-iron-manganese systems. $\underline{\text{Int. Mat.}}$ 29 (1988): 143-156.

42. R. Benz, J.F. Elliott, and J. Chipman.   Thermodynamic s of the carbides in the system of Fe-Cr-C. $\underline{\text{Metall. Trans.}}$ 5 (1974): 2235-2240.

43. R.L. Pattyn.   Heat treatment of high-Cr white irons. $\underline{\text{AFS Trans}}$. 1 (1993): 161-167.

44. C.P. Ta brett, I.R. Sare, and M.R. Ghomashchi.   Microstructure-property relationships in high chromium white irons, Int. $\underline{\text{Mater. Rev.}}$ 41 (1996): 59-82.

45. G. Laird, R. Gundlach, and K. Rohring. $\underline{\text{Abrasion-Resistance Cast Iron Handbook.}}$ USA: American Foundry Society, (n.d.).

46. G.L.F. Powell, and G. Laird II.   Structure, nucleation, growth and morphology of secondary carbide formation in 25% Cr high chromium irons.   Cast Metals 8 (1995): 123-127.

47. K.A. Kibble, and J.T.H.   Pearce, Influence of heat treatment on the microstructure and hardness of 19% high-chromium cast irons. Cast Metals 6 (1993): 9-15.

48. H.N. Liu, M. Sakamoto, M. Nomura, and K. Ogi.   Abrasion resistance of high Cr cast irons at an elevalted temperature. Wear 250 (2001): 71-75.

49. J.T.H. Pearce.   Structural characterization of high chromium cast irons, Solidification Science &Processing: Outlook for the 21st Century, February 18-21, Bangalore, India, (2001): 241-247.

50. J.T.H., Pearce.   High chromium irons to resist wear, Proceeding of the 6th Asian Foundry Congress, Jan 23-26, Calcutta India,(1998): 120-134.

51. Y. matsubara, et al.   Eutectic structures of high chromium cast iron. J.JFS 48 (1976): 706-711.

52. M. Radovic, M. Fiset, K. Peev, and M. Tomovic.   The influence of vanadium on fracture and abrasion wear resistance in high chromium cast irons.   Journal of Materials Science 29 (1994):5085-5094.

Appendix

Appendix

Wear Resistance of High Chromium Cast Iron

Introduction

The commercial plain high chromium cast irons have eutectic and hypoeutectic compositions containing chromium from 15% to 30% and they are widely used for wear parts in many kinds of industries. For the applications, the heat treatment used to be given to provide the optimum wear resistance combining suitable toughness. In order to evaluate the effect of matrix structure on the abrasion wear resistance, plain hypoeutectic 16%, 20% and 26% Cr cast irons, which will display the effect of matrix on the wear resistance more remarkably, were employed, and the relationship between the wear loss and the duration of wear test was obtained using Suga Wear Testing Machine.[3]

Wear test results

The chemical compositions of test specimens are shown in Table A1. The test specimens in as-hardened and tempered states by three different temperatures were employed. One specimen was tempered at H_{Tmax} temperature in which the retained austenite was in low level, and for two other specimens, one was tempered at lower temperature than that of H_{Tmax} where more amount of retained austenite was left and another was tempered at higher temperature than that of H_{Tmax} where martensite has over-tempered and little retained austenite. The relationships between wear loss and testing time are shown in Fig. A1 for 16% Cr, Fig. A2 for 20 % Cr and Fig. A3 for 26% Cr specimens, respectively. In each specimen, a linear relationship between wear loss and testing time was obtained regardless of heat treatment conditions. The wear rate (Rw: mg/s), which is expressed by a slope of each straight line, was calculated as an index and the Rw values of the specimens are summarized in Table A2.

It is found that in each chromium specimen, the wear rate of

specimen with H_{Tmax} is smallest, that is, it shows the highest wear resistance followed by as-hardened specimen with largest Vγ, that with relative amount of Vγ, and the largest Rw or the lowest wear resistance is obtained in the specimen overed-tempered in which the Vγ was almost disappeared and even the coarsening of secondary carbides occurred.

From these results, it was found that the control of retained austenite is a very important factors for the abrasion wear resistance.

Table A1 Chemical compositions and Cr/C values of test specimens.

Specimen	Element (mass%)				Cr/C
	C	Cr	Si	Mn	
No.2 (Hypo)	3.01	16.48	0.62	0.78	5.48
No.4 (Hypo)	2.90	20.12	0.60	0.53	6.94
No.6(Hypo)	2.65	25.56	0.37	0.51	9.65

Table A2 Wear rate of test specimens.

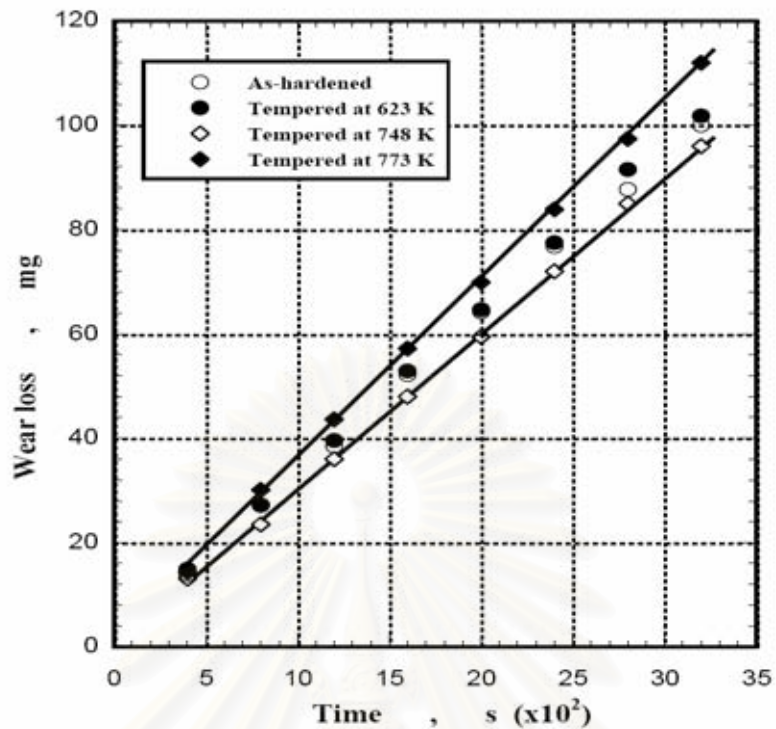| Specimens	Element (mass%)		Wear rate (Rw), (x 10^{-2} mg/s)				
	C	Cr	As-hardened (1323 K)	Tempering temperature (K)			
				623	723 (H_{Tmax})	748 (H_{Tmax})	773
No. 1	2.62	15.93	3.07	3.14	-	3.00	3.44
No. 2	2.57	20.34	3.14	3.20	-	2.86	3.40
No. 3	2.32	25.53	2.75	3.00	2.52	-	2.67

Fig. A1   Influence of tempering temperature on relationship between wear loss and testing time of 16% Cr hypoeutectic high chromium cast irons.
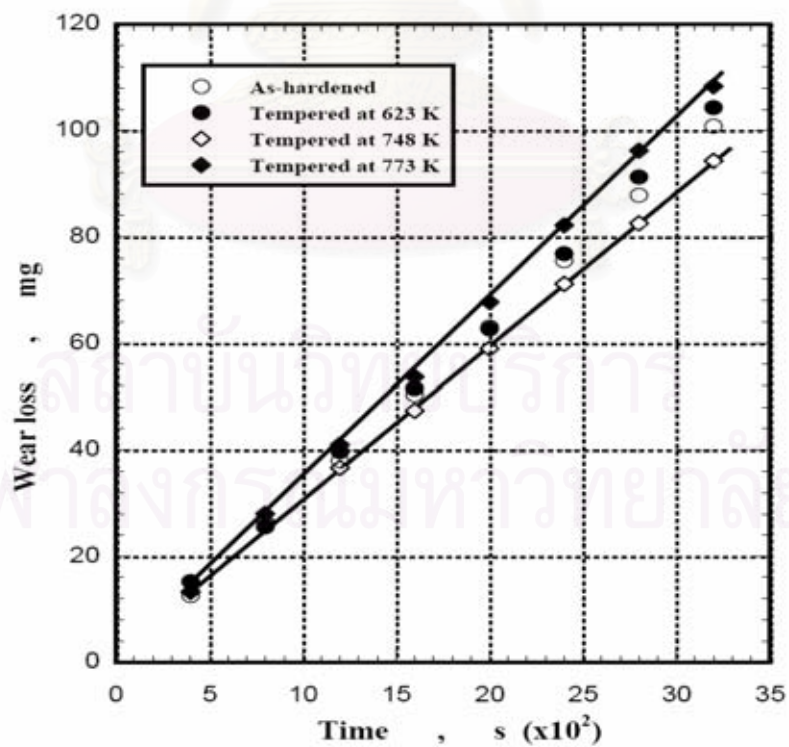

Fig. A2   Influence of tempering temperature on relationship between wear loss and testing time of 20% Cr hypoeutectic high
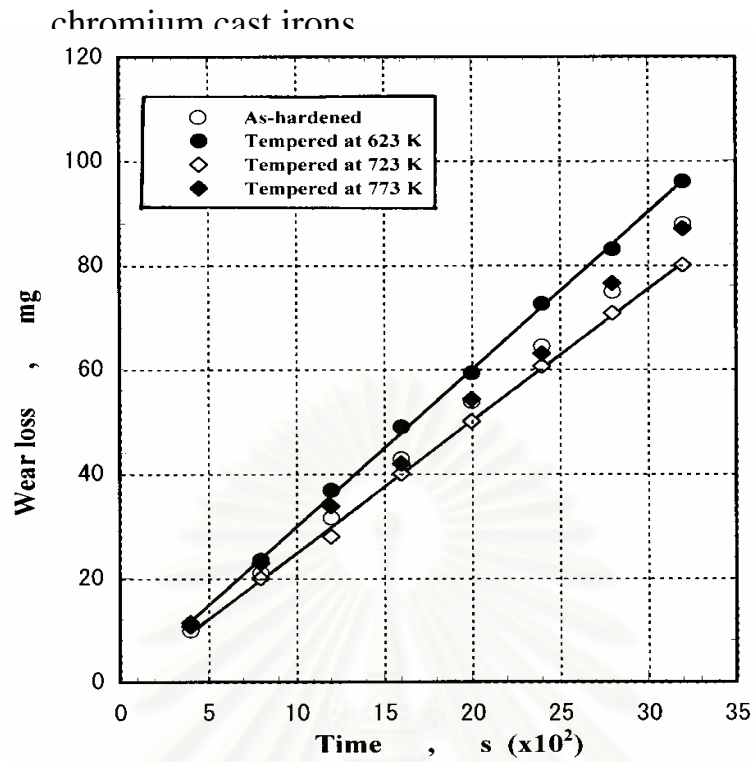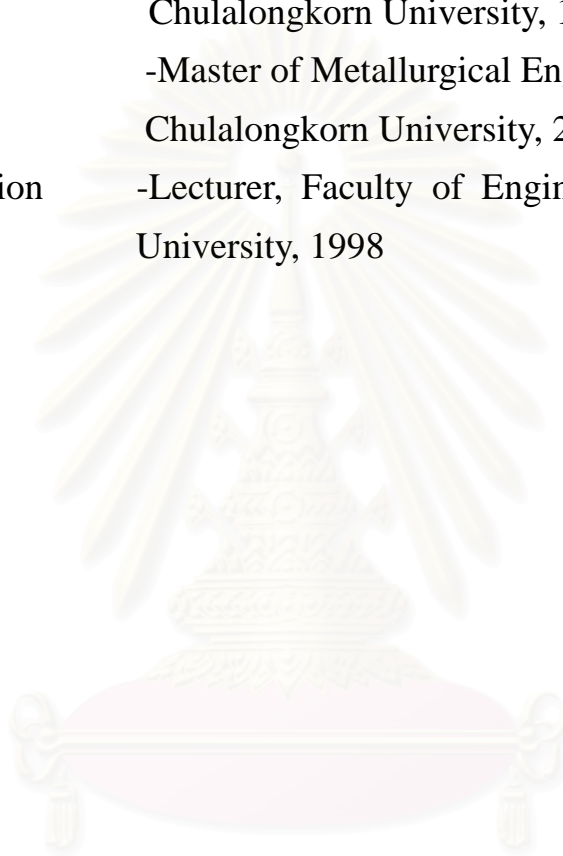
Fig. A3   Influence of tempering temperature on relationship between wear loss and testing time of 26% Cr hypoeutectic high chromium cast irons.

BIOGRAPHY

Name   Mr. Sudsakorn Inthidech

Birthday   25 December 1976

Education   -Bachelor of Metallurgical Engineering,
                                Chulalongkorn University, 1998
                                -Master of Metallurgical Engineering,
                                Chulalongkorn University, 2002

Present Position   -Lecturer, Faculty of Engineering, Mahasarakam
                                University, 1998